

Some pages of this thesis may have been removed for copyright restrictions.

If you have discovered material in Aston Research Explorer which is unlawful e.g. breaches copyright, (either yours or that of a third party) or any other law, including but not limited to those relating to patent, trademark, confidentiality, data protection, obscenity, defamation, libel, then please read our [Takedown policy](#) and contact the service immediately (openaccess@aston.ac.uk)

PRODUCTION OF RENEWABLE FUELS AND CHEMICALS FROM BIO-OIL USING FLUIDS NEAR THE CRITICAL POINT

SAINAB OMAR
Doctor of Philosophy

ASTON UNIVERSITY
October 2019

© Sainab Omar, 2019

Sainab Omar asserts her moral right to be identified as the author of this thesis

This copy of the thesis has been supplied on condition that anyone who consults it is understood to recognise that its copyright belongs to its author and that no quotation from the thesis and no information derived from it may be published without appropriate permission or acknowledgement.

Aston University

PRODUCTION OF RENEWABLE FUELS AND CHEMICALS FROM BIO-OIL USING
FLUIDS NEAR THE CRITICAL POINT

Sainab Omar

Doctor of Philosophy

October 2019

Thesis Summary

The production of energy and chemicals using dwindling fossil feedstock reserves (oil, gas and coal) has generated global environmental and energy security concerns. This has motivated research into alternative energy technologies and sustainable products and processes. Over the past few decades, research and interest in biomass as a renewable feedstock has exponentially grown. Bio-oil from biomass is particularly interesting as it can be used for energy, chemicals, or as an energy carrier. However, crude bio-oil possesses certain physical and chemical properties which prevent its direct application and integration into existing fuel infrastructures. For example, the high acidity of untreated bio-oil can cause corrosion of vessels and pipework.

Therefore, a detailed study which aimed to improve the properties of bio-oil using methanol, ethanol and isopropanol for bio-oil blending and supercritical upgrading was conducted. The results showed supercritical methanol treatment eliminated the acids and improved the pH of the bio-oil. However, the crude bio-oil contained 37.03 % phenols which did not transform after blending with alcohols or after supercritical upgrading. Therefore, the research aimed to convert phenol to less reactive compounds such as cyclohexanol in order to improve the bio-oil properties. A process of in situ catalytic hydrogenation of phenol using aqueous phase reforming of methanol for the hydrogen source achieved high cyclohexanol yield (93.35 %) and selectivity (94.23 %).

A new process of producing industrially desirable and valuable chemicals including methyl isovalerate and a mixture of monoterpenes (p-Mentha-1,4(8)-diene, D-Limonene, and γ -Terpinene) from a bio-oil based compound (geranyl isovalerate) was reported in Chapter 6. No catalyst was used, and subcritical water performed the role of catalyst and co-solvent with supercritical methanol. Very high geranyl isovalerate conversions was achieved as less than 3 % of it was detected in the products and methyl isovalerate and the monoterpenes accounted for 97 %.

Keywords: bio-oil, upgrading, subcritical, supercritical, phenol, monoterpenes,

Dedication

This thesis is dedicated to my family and friends, most importantly my mother Fatimo Salad Adan and father Omar Mohamoud Roble.

Acknowledgements

Firstly, I would like to thank my supervisor Dr Jiawei Wang for the research opportunity, and for sharing his knowledge and expertise over the course of this research.

I would also like to thank Professor Brian Tighe for imparting his knowledge and insight into the research.

I am very thankful to Dr Khalid Doudin for continuously and patiently providing guidance and knowledge.

I gratefully acknowledge the financial support from Aston University, the School of Engineering and Applied Science.

Contents

Thesis Summary	2
Dedication	3
Acknowledgements	4
List of Tables.....	9
List of Figures.....	10
List of Abbreviations	12
List of Schemes.....	13
List of Equations.....	14
1. Introduction	15
1.1. Objectives	16
1.2. Structure of the thesis	16
2. Overview of Supercritical Fluids in Biomass and Bio-oil Related Processes.....	17
2.1. Supercritical Fluids (SCFs).....	17
2.2. SCFs in Biomass-related Process.....	18
2.3. The Effects of SCFs on Bio-oil Upgrading	19
3. Catalytic & Non-Catalytic Bio-oil Upgrading in SCFs: A Literature Review	22
3.1. Introduction	22
3.2. Catalytic Bio-oil Upgrading in SCF	23
3.2.1. Precious metals catalysts - Palladium	24
3.2.2. Precious metals catalysts - Ruthenium.....	25
3.2.3. Precious metals catalysts - Platinum.....	26
3.2.4. Non-precious metal catalysts	28
3.3. Non-catalytic Bio-oil Upgrading in SCF	31
3.3.1. Non-catalytic bio-oil upgrading in supercritical ethanol	31
3.3.2. Non-catalytic bio-oil upgrading in supercritical methanol	33
3.3.3. Non-catalytic bio-oil upgrading in supercritical water	34
3.3.4. Non-catalytic bio-oil upgrading in other SCFs.....	36
3.4. Conclusion	46

4. Production of Renewable Fuels by Blending Bio-oil with Alcohols and Upgrading under Supercritical Conditions.....	47
4.1. Introduction	47
4.2. Materials and Methods.....	50
4.2.1. Materials	50
4.2.2. Bio-oil blending and upgrading reactions.....	50
4.2.3. Product analysis and characterisation	51
4.3. Results and Discussions	53
4.3.1. Reproducibility	53
4.3.2. Product yields	54
4.3.3. Physicochemical properties of bio-oil and treated bio-oils	55
4.3.4. Characterisation of bio-oil and treated bio-oils.....	57
4.3.4.1. GC-MS analysis	57
4.3.4.2. FT-IR analysis.....	60
4.3.4.3. ¹³ C NMR analysis.....	65
4.3.4.4. TGA analysis.....	67
4.4. Conclusion	70
5. In situ Catalytic Hydrogenation of Phenol using Raney-Ni Catalyst and Near-Critical Water-Methanol Mixtures	72
5.1. Introduction	72
5.2. Materials and Method.....	75
5.2.1. Materials	75
5.2.2. Experimental procedure	75
5.2.3. Analytical methods	76
5.3. Results and Discussions	77
5.3.1. Reproducibility	77
5.3.2. Effect of varying Raney-Ni catalyst loading	78
5.3.3. Effect of varying reaction time	80
5.3.4. Effect of varying reaction temperature.....	82
5.3.5. Effect of varying reaction starting material ratios	84

5.3.6.	Comparing the experimental reaction temperatures and pressures and the critical properties calculated by ASPEN HYSYS simulator	86
5.4.	Conclusion	88
6.	A One-pot Synthesis of Monoterpenes by Transforming a Bio-oil Compound using Near-Critical Water-Methanol Mixtures as Solvent and Catalyst.....	90
6.1.	Introduction	90
6.1.1.	Catalytic production of terpenes	91
6.1.2.	Non-catalytic terpene production using supercritical alcohol solvents and supercritical water as acid catalyst	92
6.1.3.	Transesterification.....	94
6.1.4.	Summary	97
6.2.	Materials and Method.....	98
6.2.1.	Materials	98
6.2.2.	Experimental procedure	98
6.2.3.	Analytical methods.....	99
6.3.	Results and Discussions	99
6.3.1.	Transformation of the bio-oil compound geranyl isovalerate to methyl isovalerate and a mixture of monoterpenes.....	99
6.3.2.	Reproducibility	104
6.3.3.	Various molar ratio of water, methanol, and geraniol.....	105
6.3.4.	Various molar ratio of water, methanol, and nerol	114
6.3.5.	Effect of various reaction time - Geraniol.....	121
6.3.6.	Effect of various reaction time- Nerol	123
6.3.7.	Effect of various reaction temperature- Geraniol	128
6.3.8.	Effect of various reaction temperature- Nerol	132
6.3.9.	Comparing the experimental reaction temperatures and pressures and the critical properties calculated by ASPEN HYSYS simulator	134
6.4.	Conclusion	136
7.	Thesis Conclusion and Recommendations.....	138
	References.....	141
	Appendix 1. GCMS results of bio-oil blending and reactions	148

Appendix 2. Detailed results of in situ catalytic hydrogenation of phenol	166
Appendix 3. GCMS results of monoterpene production	178

List of Tables

Table 2.1 Comparing the properties of liquid, gas and SCFs. Data from [7]	17
Table 2.2 Advantages of using SCFs as reaction media for chemical synthesis [6]	18
Table 2.3 Commonly used SCFs [17]	19
Table 3.1 Summary of SCF bio-oil upgrading methods reported in literature	37
Table 4.1 Analysis of mass balance reproducibility	53
Table 4.2 Mass balance of bio-oil reactions	54
Table 4.3 Physicochemical properties of liquid products of bio-oil reactions with methanol, ethanol and isopropanol.	56
Table 4.4. Distribution of chemical composition in bio-oil samples	58
Table 4.5 Classes of compounds identified in the bio-oil and treated bio-oils using FTIR analysis.	61
Table 4.6 Boiling point distribution of bio-oil and treated bio-oils.	70
Table 5.1 Bond Dissociation Energies [64]	73
Table 5.2 Reproducibility analysis of phenol conversion experiments	78
Table 5.3 Comparing the critical properties of phenol experiments and ASPEN HYSYS.	87
Table 6.1 Summary of the GCMS analysis results of the geranyl isovalerate reaction products.	103
Table 6.2 Summary of GCMS analysis results of the geraniol reaction products at various starting material ratios.	106
Table 6.3 Summary of GCMS analysis results of the nerol reaction products at various starting material ratios.	115
Table 6.4 Summary of GCMS analysis results of the geraniol reaction products at various reaction times.	121
Table 6.5 Summary of GCMS analysis results of the nerol reaction products at various reaction times.	125
Table 6.6 Summary of GCMS analysis results of the geraniol reaction products at various reaction temperatures.	128
Table 6.7 Summary of GCMS analysis results of the nerol reaction products at various reaction temperatures.	133
Table 6.8 Comparing the critical properties from experiments and ASPEN HYSYS.	135

List of Figures

Figure 3.1 Comparison of wood-derived crude bio-oil and heavy petroleum fuel oil [1,33–36].	22
Figure 3.2 Schematic diagram of bio-oil upgrading in SCF experiments. (1) heater, (2) autoclave, (3) stirrer, T, temperature detector, P, pressure gauge.....	23
Figure 4.1 Schematic diagram of bio-oil blending and supercritical reaction.....	49
Figure 4.2 The 50 mL stainless steel autoclave used for the bio-oil-alcohol reactions.	51
Figure 4.3 FTIR spectra of (a) bio-oil, (b) bio-oil-methanol blend, and (c) bio-oil-methanol reaction products.....	62
Figure 4.4 FTIR spectra of (a) bio-oil, (b) bio-oil-ethanol blend, and (c) bio-oil-ethanol reaction products.	63
Figure 4.5 FTIR spectra of (a) bio-oil, (b) bio-oil-isopropanol blend, and (c) bio-oil-isopropanol reaction products.....	64
Figure 4.6 Quantitative ¹³ C NMR characterisation of bio-oil and treated bio-oils.....	66
Figure 4.7 TGA and DTG profiles of (a) bio-oil, (b) bio-oil-methanol blend, and (c) bio-oil-methanol reaction products.	68
Figure 4.8 TGA and DTG profiles of (a) bio-oil, (b) bio-oil-ethanol blend, and (c) bio-oil-ethanol reaction products.....	69
Figure 4.9 TGA and DTG profiles of (a) bio-oil, (b) bio-oil-isopropanol blend, and (c) bio-oil-isopropanol reaction products.	69
Figure 5.1 The 70 mL stainless steel autoclave used for the experiments.	76
Figure 5.2 Phenol conversion and product selectivity at various catalyst loading.	79
Figure 5.3 Product yield at various catalyst loading.....	79
Figure 5.4 Conversion and selectivity at various reaction times.....	81
Figure 5.5 Product yield at various at various reaction times.....	81
Figure 5.6 Conversion and selectivity at various reaction temperatures.	83
Figure 5.7 Product yield at various reaction temperatures.....	83
Figure 5.8 Product selectivity at various starting material ratios.	85
Figure 5.9 Product yield at various at various starting material ratios.	85
Figure 5.10 Changes in the critical properties of the reaction mixture at different concentration of H ₂ O.	87
Figure 6.1 Major compounds in the geraniol reaction products at various starting material ratios.....	112
Figure 6.2 Major compounds in the nerol (4) reaction products at various starting material ratios.....	119
Figure 6.3 Major compounds in the geraniol reaction products at various reaction temperatures.....	129

Figure 6.4 Major compounds in the nerol reaction products at various reaction temperatures.
..... 134

Figure 6.5 Changes in the critical properties of the solvent mixture at different concentration of
H₂O. 135

List of Abbreviations

SCF; Supercritical fluids

SCW; Supercritical water

TAN; Total acid number

HHV; Higher heating value

FFA; Free fatty acids

GCMS; Gas chromatography mass spectrometry

FTIR; Fourier-transform infrared spectroscopy

¹³C NMR; Carbon-13 nuclear magnetic resonance

TGA; Thermogravimetric analysis

HDO; Hydrodeoxygenation

List of Schemes

Scheme 6.1 Transesterification of geranyl isovalerate.....	101
Scheme 6.2 Dehydration and cyclisation of geraniol and nerol.....	102
Scheme 6.3. Geraniol conversion to (2E)-1-Methoxy-3,7-dimethylocta-2,6,diene (12)	111
Scheme 6.4 Geraniol conversion to alpha-Terpineol (13).....	111
Scheme 6.5 Geraniol conversion to o-Cymene (14) and p-Cymene (15).....	112

List of Equations

Equation 4.1 Liquid yield	52
Equation 4.2 Solid yield	52
Equation 4.3 Gas yield	52
Equation 5.1 Methanol reforming.....	73
Equation 5.2 Water-gas shift reaction.....	73
Equation 5.3 Aqueous phase reforming.....	73
Equation 5.4 The hydrogenation of phenol (1) to cyclohexanone (2)	73
Equation 5.5 The hydrogenation of phenol (1) to cyclohexanol (3)	74
Equation 5.6 Aqueous phase reforming of methanol and hydrogenation of phenol to cyclohexanone	74
Equation 5.7 Aqueous phase reforming of methanol and hydrogenation of phenol to cyclohexanol	74
Equation 5.8 Conversion	77
Equation 5.9 Selectivity	77
Equation 5.10 Yield.....	77
Equation 5.11 Methanation.....	80
Equation 6.1 General equation for transesterification [106]	94

1. Introduction

In recent years, the world has been facing an energy crisis due to a combination of several factors including the depletion of fossil fuels, accelerated population growth, increase in global energy demand, and crude oil price fluctuations. Furthermore, the extensive use of fossil fuels has led to climate change and global warming. These global issues have motivated research into alternative energy technologies, renewable resources, and more sustainable techniques for energy generation.

Biomass can be utilised as a renewable feed for conversion into gaseous, liquid, and solid bio-fuels [1]. Biomass is any biodegradable material of biological origin excluding fossilized material or peat [2]. Fast pyrolysis is a thermal conversion technique which decomposes biomass in the absence of oxygen [1]. Pyrolysis liquid (bio-oil) is produced under moderate temperature (~500 °C) and short vapour residence times (~1 s) [1]. Fast pyrolysis for liquid production is especially interesting as the process directly converts biomass to high yield liquid of up to 75 wt.% on a dry feed basis, whilst keeping gas and char by-products at low yields of 12 wt.% and 13 wt.% yields [3]. Common feedstocks for pyrolysis oil production include wood, bagasse, rice straw, switchgrass and wheat straw [4]. The liquid biofuel, commonly known as crude bio-oil, has generated growing interest as it can be used for energy, chemicals, or as an energy carrier [1]. However, the properties of crude pyrolysis oil such as high acidity and viscosity and high oxygen and water contents lead to detrimental effects during application including corrosion to metal components, instability during storage and reduced heating value [1]. This affects the direct use of crude bio-oil and its assimilation into existing liquid fuel infrastructures.

Consequently, the key aim and motivation of this research is to investigate and improve the properties of a sample of crude bio-oil. Studies have shown supercritical fluids provide unique benefits in bio-oil upgrading processes. Therefore, methanol, ethanol, and isopropanol under supercritical conditions were utilised to upgrade crude bio-oil. An extensive literature review (Chapter 3) was conducted to guide the bio-oil upgrading research. From the experiments, crude bio-oil was found to contain 37.03 % phenols. These compounds are notably undesirable in bio-oil because the high oxygen content causes unfavourable properties such as; low energy density, instability, high viscosity, corrosion, and tendency to polymerize [5]. Therefore, Chapter 5 reports on a detailed study on phenol conversion to cyclohexanol (**3**) and cyclohexanone (**2**) which have a lower concentration of oxygen and are more stable than phenol as they do not behave like aromatic acids.

The PhD research also discusses a novel route for producing valuable monoterpene compounds which are highly desirable in the chemicals industry as intermediates for bulk/fine chemicals production. The main process involves a non-catalytic sub/supercritical aqueous-

alcohol reaction to convert the reactant geranyl isovalerate (a bio-oil based compound) to monoterpenes. Subcritical water was used as a catalyst and co-solvent with supercritical methanol. High proportions of cyclic monoterpenes particularly p-Mentha-1,4(8)-diene (**7**), D-Limonene (**8**), and γ -Terpinene (**9**) were identified.

1.1. Objectives

The objectives of the PhD research can be summarised as follows:

- To search, evaluate and survey the research conducted on catalytic and non-catalytic bio-oil upgrading in supercritical fluids.
- To utilise the main findings from the literature review to guide the bio-oil blending and upgrading research (Chapter 4).
- To provide a detailed account of the findings of the bio-oil blending and upgrading study.
- To investigate phenol conversion using Raney-Ni catalyst and the aqueous phase reforming of methanol to in situ generate hydrogen.
- To convert geranyl isovalerate (a bio-oil based compound) using subcritical water as catalyst and co-solvent with supercritical methanol.
- To examine the effects of varying the reaction operating parameters during dehydration of the intermediates geraniol (**3**) and nerol (**4**).
- To present a general strategy for future work.

1.2. Structure of the thesis

The remaining chapters of the report are organised as follows:

Chapter 2 provides an overview of supercritical fluids in biomass and bio-oil related processes and includes a definition of supercritical fluids and discussions of the unique properties of supercritical fluids.

Chapter 3 evaluates and compares the principal literature on catalytic and non-catalytic bio-oil upgrading in supercritical fluids.

Chapter 4 provides a detailed account of the bio-oil blending and upgrading work.

Chapter 5 reports the investigation on conversion of phenol by in situ catalytic hydrogenation.

Chapter 6 details a novel one-pot process to produce valuable compounds including methyl isovalerate and a mixture of monoterpenes from geranyl isovalerate (a bio-oil based compound).

Chapter 7 provides recommendations for future research and concludes the thesis.

2. Overview of Supercritical Fluids in Biomass and Bio-oil Related Processes

2.1. Supercritical Fluids (SCFs)

A supercritical fluid (SCF) is defined as the state of a compound, mixture, or element above its critical temperature (T_c) and critical pressure (P_c) but lower than the pressure necessary to condense it into a solid [6]. The critical point marks the end of the liquid-vapour coexistence and only a single homogenous fluid phase can exist in the supercritical region [6]. Thus, the properties of SCFs are frequently described as an intermediate between those of a liquid and a gas, as shown in Table 2.1 [6,7].

Table 2.1 Comparing the properties of liquid, gas and SCFs. Data from [7]

Physical Property	Liquid (ambient conditions)	Supercritical fluid	Gas (ambient conditions)
Density (kg m^{-3})	600-1600	200-500	0.6-2
Dynamic viscosity (mPa s)	0.2-3	0.01-0.03	0.01-0.3
Diffusion coefficient ($10^6 \text{ m}^2 \text{ s}^{-1}$)	0.0002-0.002	0.07	10-40

Table 2.1 compares selected physical properties of liquid, gas, and supercritical fluid [7]. The density of a supercritical fluid approximates to that of a liquid while the viscosity and diffusivity is close to that of a gas. The liquid-like density of SCFs allows many materials to be solubilized to a level significantly greater than that predicted by ideal gas considerations [6]. Due to the high compressibility of fluids near the critical point, their density is highly sensitive to small changes in pressure and temperature [6,7]. Many solvent properties such as dissolving power and dielectric constant are directly related to bulk density, and therefore exhibit a similar pressure dependence [6]. These characteristics are unique to SCFs and enables the opportunity to tune the reaction environment to optimise the reaction rate and selectivity [6]. The tunable solvent properties is one of the many interesting features associated with SCFs and forms the basis for its application in modern chemical synthesis.

The diffusivity of solutes in SCFs is higher and the viscosity is lower, compared with liquid solvents [6,7]. This means that a faster rate of diffusion of a species through a SCF medium can be achieved, than in a liquid solvent. Hence, a solid would dissolve more rapidly in a SCF. Additionally, SCFs can more effectively penetrate a microporous solid material [6]. These

favourable transport properties enhance the rates of mass transfer in SCFs and is one of the main features which differentiate SCFs from liquid solvents. Although perhaps the most notable advantage of SCFs, is the absence of residual solvent after the release of pressure [6].

The advantages of using SCFs as reaction media for chemical synthesis rather than liquids have been broadly organised into four categories by Jessop and Leitner and summarised in Table 2.2.

Table 2.2 Advantages of using SCFs as reaction media for chemical synthesis [6]

Category	Advantage	SCF type
Environment	do not contribute to smog	most
	do not damage ozone layer	most
	no acute ecotoxicity	CO ₂ , H ₂ O
	no liquid wastes	CO ₂ and other volatile SCFs
Health and safety	noncarcinogenic	most (but not C ₆ H ₆)
	nontoxic	most (but not HCl, HBr, HI, NH ₃)
	non-flammable	CO ₂ , N ₂ O, H ₂ O, Xe, Kr, CHF ₃
Process	no solvent residues	CO ₂ and other volatile SCFs
	facile separation of products	CO ₂ and other volatile SCFs
	high diffusion rates	all
	low viscosity	all
	adjustable solvent power	all
	adjustable density	all
	inexpensive	CO ₂ , H ₂ O, NH ₃ , Ar, hydrocarbons
Chemical	high miscibility with gases	all
	variable dielectric constant	the polar SCFs
	high compressibility	all
	high diffusion rates	all

2.2. SCFs in Biomass-related Process

In biomass-related processes, SCFs have been applied in transesterification, liquefaction and gasification of biomass. Supercritical transesterification is a non-catalytic transesterification process for biodiesel production. Supercritical alcohols can be used as an alternative technology to produce biodiesel via transesterification without catalyst addition [8,9]. In this process, the reaction mixture is heated to the critical temperature and pressure of the alcohol. Researchers have used supercritical transesterification for a catalyst-free, highly efficient biodiesel production process to overcome the problems of homogenous/heterogenous catalytic processes [8,9].

In hydrothermal liquefaction (HTL), water functions as a reactant and catalyst. Several studies have used water at supercritical conditions to enhance its effects in HTL [10–12]. At sub- and supercritical conditions, water acquires unique properties such as low viscosity and high solubility of organic compounds [11]. Therefore, water at conditions above the critical point is

a good medium for fast, homogenous and efficient reactions [11]. Furthermore, the dielectric constant of water is reduced under supercritical conditions, this increases the solubility of hydrophobic organic compounds such as free fatty acids [11].

Conventional biomass gasification processes require feed pre-treatment to reduce its water content. To overcome this economically and energy-intensive step, researchers have focused on using sub- and supercritical water (SCW) as both reaction media and reactant during biomass gasification [13–15]. In supercritical reaction conditions the mass transfer barrier between the different phases is removed. Consequently, the permanent gases and the organic compounds are highly soluble in SCW during SCW biomass gasification [15]. At temperatures 550-700°C SCW biomass gasification promotes high reaction rates, thus complete gasification can be achieved without catalyst addition [15].

2.3. The Effects of SCFs on Bio-oil Upgrading

Due to the high oxygen content of bio-oil, it is immiscible with hydrocarbons but miscible with polar solvents such as acetone, ethanol and methanol [1]. Polar solvents have been used for over a decade to stabilize the viscosity of bio-oil [1]. Solvent addition, particularly methanol, proved to increase bio-oil homogeneity, reduce viscosity, and improve stability [1,5,16]. There are numerous advantages associated with the use of SCF solvents in bio-oil treatment processes compared to conventional organic solvents; all of which are based on the unique properties of the supercritical state. For example, the adjustable solvent strength and the favourable transport properties of SCFs may be exploited to separate products from by-products or to recover homogenous catalysts [6]. Table 2.3 lists the most frequently used organic and inorganic compounds as SCFs in bio-oil upgrading processes. Carbon dioxide is the most widely used SCF due to its favourably low critical parameters. This section aims to briefly examine the reported influence of these fluids on supercritical bio-oil upgrading.

Table 2.3 Commonly used SCFs [17]

Solvent	Critical temperature (K)	Critical pressure (MPa)	Critical density (kg m ³)
Carbon dioxide	304.21	7.383	468.2
Methanol	512.5	8.084	273.8
Ethanol	514	6.137	274.2
1-butanol	563.1	4.414	271.5
Water	647.096	22.064	322.0

Crude bio-oil contains reactive intermediates which can participate in polymerisation reactions to produce larger molecules and eventually form coke [1,18]. Supercritical alcohols and

supercritical water (SCW) possess unique hydrogen-donating ability [12,19–21]. The hydrogen produced can be used to prevent repolymerisation of reactive intermediates and subsequent formation of coke [12,19,22]. Furthermore, the complete miscibility of SCFs with hydrogen leads to significantly higher hydrogenation rates compared with conventional liquid solvents which have limited hydrogen solubility [6,7].

SCFs can suppress coke formation during bio-oil upgrading by unique solvation and dispersion techniques not ordinarily found in liquid reactions. The low-molecular-weight reactive intermediates can be surrounded by solvent molecules or dispersed in the supercritical fluid medium, this prevents repolymerisation and coke production [19]. The high alcoholysis ability associated with supercritical ethanol and methanol can further suppress coke formation during bio-oil upgrading [21,23]. Likewise, SCW can facilitate hydrolysis reactions to inhibit repolymerisation of reactive species [20]. Moreover, near the critical point, SCW behaves like a moderately polar organic liquid [6]. This is because, its dielectric constant is reduced to the extent that organic materials are readily soluble, and the solubility of inorganic species is significantly reduced [6]. These unique solvation characteristics make SCW an ideal medium for dissolving low polar organic compounds in bio-oil; which are usually insoluble in polar solvents during bio-oil upgrading processes [6].

Supercritical alcohols (namely methanol and ethanol) and SCW have shown to reduce oxygen concentration by hydrodeoxygenation, decarboxylation and decarbonylation reactions [19,20,24]. Bio-oil upgraded in supercritical ethanol, methanol or water exhibits decreased oxygen concentration and O/C ratios relative to the original bio-oil [19,24–26]. For example, Prajitno et al. reported an upgraded bio-oil with oxygen content of 12.6 wt% after supercritical ethanol treatment; a significant decrease compared to the original fast pyrolysis bio-oil (26.8 wt%) [19]. Reduced O/C ratio has several advantages including increased bio-oil stability, decreased acidity (and ultimately corrosiveness), enhances the heating value and inhibits repolymerisation and tar formation [1,19,24]. Moreover, using supercritical fluids increases carbon and hydrogen content and H/C ratio in the upgraded bio-oil compared to the untreated bio-oil [19,24]. High hydrocarbon content improves the co-processing of bio-oil with hydrocarbon fuels. SCW or supercritical methanol treatment alone (i.e. catalyst free) can effectively decrease the sulphur content in the crude bio-oil to non-detectable levels [18,19,24,26]. Moreover, SCW as a reaction medium promotes denitrogenation of the crude bio-oil by extracting nitrogen during the upgrading process [18,26].

SCFs can effectively reduce the high content of oxygenated organics in the bio-oil and improve its chemical and physical properties. Bio-oil upgraded in supercritical alcohols (ethanol, methanol or 1-butanol) exhibit improved properties due to decreased undesirable compounds such as acids, aldehydes, ketones, phenols (highly reactive, corrosive, and high oxygen

content compounds) and resulting increased concentration of stable compounds such as alcohols, esters, and ethers [19,27–29].

Moreover, SCFs reduce the levels of acidity in the crude bio-oil by functioning as reactants in esterification. For instance, supercritical ethanol and methanol can participate in esterification of organic acids in the bio-oil which leads to the formation of non-corrosive, less reactive species e.g. ethyl esters and methyl esters [28,30]. Similarly, Cui et al. found supercritical CO₂ removed up to 86.78% of total acids in crude bio-oil [31]. Consequently, supercritical CO₂ treatment increases the pH value of bio-oil and ultimately the storage stability of upgraded bio-oil.

Thus, due to the various desirable reactions promoted by supercritical fluids during bio-oil upgrading, a corresponding increase in bio-oil yield can be obtained. One study reported 40.0 wt % oil yield in biocrude which increased to 59.6 wt% in supercritical water upgraded oil [19]. Moreover, bio-oil upgraded in supercritical water, ethanol, methanol, 1-butanol and CO₂ exhibit higher heating value compared to the original bio-oil [26,28,29,31,32]. This is due to the reduction or removal of unfavourable components (such as high oxygen content). Supercritical CO₂ (SCCO₂) is particularly effective for increasing the heating value of crude bio-oil. This is because SCCO₂ can be used to extract the water from the crude bio-oil to produce an upgraded bio-oil with higher heating value. Cui et al. reported an 83% increase in heating value when crude bio-oil underwent supercritical CO₂ upgrading [31].

3. Catalytic & Non-Catalytic Bio-oil Upgrading in SCFs: A Literature Review

3.1. Introduction

Figure 3.1 compares select characteristics of wood-derived crude bio-oil and heavy petroleum fuel oil [1,33,34]. The properties of crude bio-oil such as low heating value, high moisture, and oxygen content lead to unfavourable effects during application including poor stability and immiscibility with hydrocarbons [1]. This inhibits the direct use of crude bio-oil and its assimilation into existing fuel infrastructures. Thus, upgrading the crude bio-oil is necessary. This involves reducing or eliminating one or more of its undesirable properties, ultimately improving its quality before practical application [1]. Among the various upgrading technologies, the use of supercritical fluids (SCF) has proved promising for bio-oil upgrading.

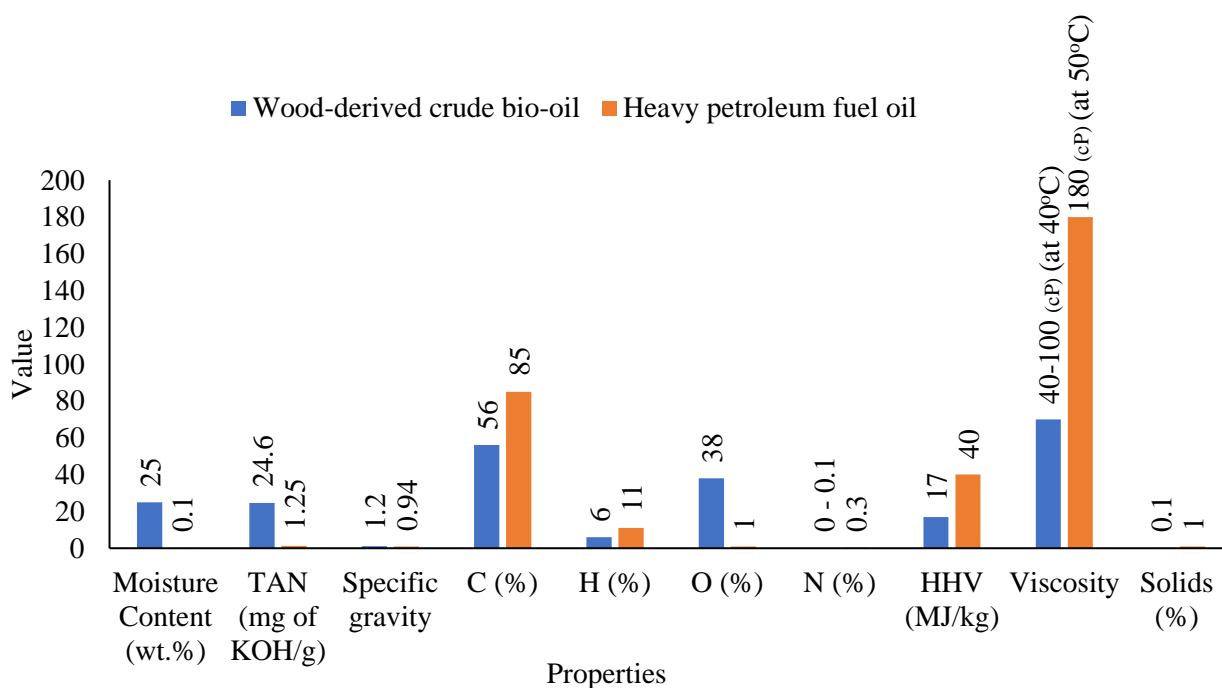


Figure 3.1 Comparison of wood-derived crude bio-oil and heavy petroleum fuel oil [1,33–36].

Figure 3.2. demonstrates a typical process of bio-oil upgrading in supercritical solvents reported in literature. In the past decade, extensive research has been conducted on bio-oil upgrading in SCFs. However, although several reviews have been done on the topic of bio-oil upgrading; there are no reviews to date, summarising the research on supercritical fluid upgrading of bio-oil. The key words; bio-oil, upgrading, review, were used to identify a total of 19 research papers. When the search terms bio-oil, upgrading, supercritical fluids, review,

were used 0 records were identified. This work aims to review the conducted research and current progress on catalytic and non-catalytic bio-oil upgrading in SCFs.

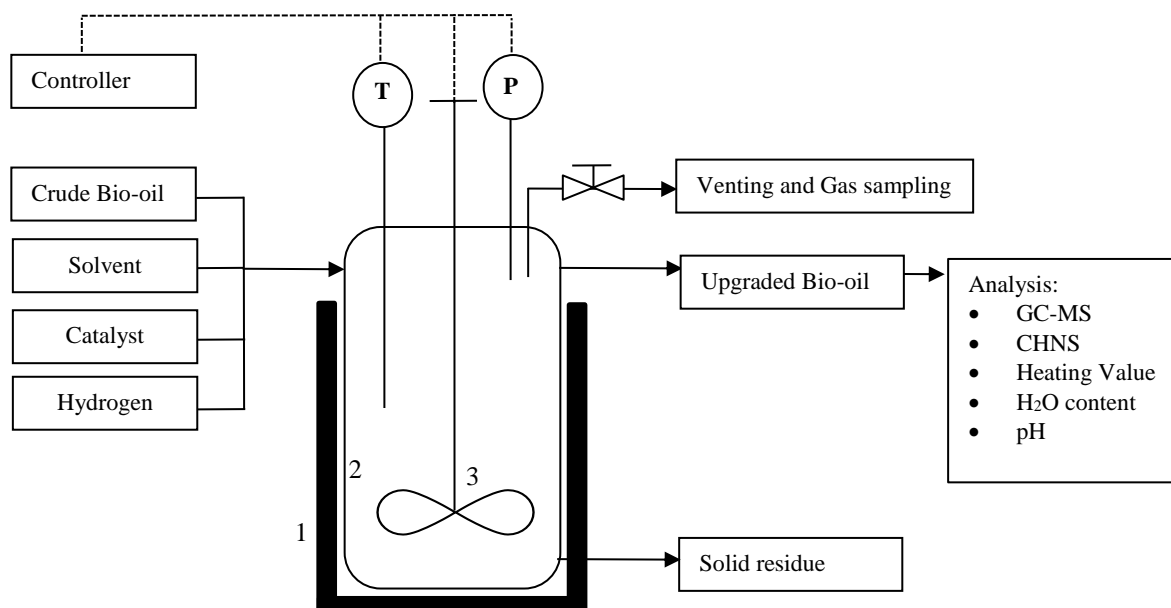


Figure 3.2 Schematic diagram of bio-oil upgrading in SCF experiments. (1) heater, (2) autoclave, (3) stirrer, T, temperature detector, P, pressure gauge.

3.2. Catalytic Bio-oil Upgrading in SCF

The application of catalysts during bio-oil treatment processes improves the reaction rates and bio-oil yield. However, homogenous catalytic reactions lead to expensive and energy-intensive separation processes [8]. Likewise, concerns for heterogenous catalytic reactions include long reaction times and expensive catalyst [8]. Thus, researchers have developed alternative methods such as addition of SCFs to overcome the limitations of catalytic bio-oil upgrading processes. Table 3.1. summarises the key data reported by researchers on bio-oil upgrading in supercritical fluids.

The ideal catalyst for bio-oil upgrading is highly active, eliminates the oxygen in the bio-oil, promotes high yield, and forms no coke deposits [37]. Studies of bio-oil upgrading by hydrodeoxygenation have used sulfided NiMo and CoMo catalysts [37]. However, these catalysts lead to sulfur contamination in the bio-oil and rapid catalyst deactivation [38]. Thus, precious metal catalysts such as supported Pd, Pt, and Ru have been utilised for catalytic upgrading experiments [37,38]. These catalysts promote increased hydrodeoxygenation and higher yields compared to traditional hydrotreatment catalysts [37].

3.2.1. Precious metals catalysts - Palladium

Palladium (Pd) is one of the most frequently used active metal catalysts for bio-oil upgrading due to its high hydrotreating capability [39]. Among the catalysts used for bio-oil upgrading, Pd is highly active during the deoxygenation and hydrogenation of unsaturated carbon-carbon bonds [38]. Pd is also recognised for its effectiveness in converting fatty acids to alkanes, this improves the storage stability of the bio-oil and enhances its energy density [40].

Chen et al. compared and studied the stability of various catalysts (Ru/C, Pd/C, Pt/C, Ru/HZSM-5) in bio-oil upgrading with supercritical ethanol [27]. The results showed the highest heating value, pH value and lowest water content of upgraded bio-oil in supercritical ethanol was achieved over Pd/C. The improvement of these properties in the bio-oil increases its potential for application as an alternative fuel. Similarly, Tang et al. used Pd based catalysts for bio-oil upgrading in supercritical ethanol. In this study, upgrading crude bio-oil in supercritical ethanol using Pd/SO₄²⁻/ZrO₂/SBA-15 (PdSZr) generated trace amount of tar or coke while with SO₄²⁻/ZrO₂/SBA-15 (SZr) catalyst, or upgrading without any catalyst, significant amount of tar and coke was formed [39]. Hence, PdSZr effectively performed as a hydrotreating catalyst and inhibited polymerisation and condensation reactions. In addition, the highest heating value, oil yield and the lowest water content was obtained with PdSZr catalyst [39].

J. Zhang et al. investigated bio-oil upgrading over supported Pt and Pd catalysts in supercritical methanol/ethanol [23]. Like Tang et al., the findings showed Pd, with more dissolved active hydrogen, had a higher hydrogenation activity for large molecular-weight compounds, thus inhibited unstable polymers to form solid products. Moreover, although both Pt and Pd upgraded bio-oils exhibited complete absence of acids, the Pd/HZSM-5 treated oil contained higher esters compared to the Pt/HZSM-5 oil, which may indicate higher esterification was achieved with the former catalyst.

Bai et al. examined the activity of various catalysts on processing of pre-treated algal oil in supercritical water [41]. In this study, Pd/C generated higher oil yield and lower coke yield than Pt/C. Similarly, C. Zhang et al. examined the effects of several different commercially available catalysts on biocrude in subcritical water [42]. The results showed Pd/C produced bio-oil had a higher H/C content, lower sulfur and water content than Pt/C as well as lower ash content than both Ru/C and Pt/C. Reduced sulfur, water and ash content in bio-oil are desirable as these components can lead to catalyst poisoning, reduced heating value, and a phase-separated oil, respectively. However, Duan et al. suggested Pd/C (5%) and Pt/C (5%) have similar catalytic activity towards upgrading of algal bio-oil in SCW despite their different metal dispersion, specific surface area and micropore volume [40].

3.2.2. Precious metals catalysts - Ruthenium

Ruthenium (Ru) is a commonly used active metal catalyst for bio-oil upgrading due to its high hydrocracking capabilities [43]. This has several advantages including increasing the oil yield, and heating value whilst limiting solid production. Tang et al. found bio-oil upgraded in supercritical ethanol and Ru catalyst obtained significantly lower solid residue, and higher oil yield and heating value than with ZrO₂/SBA-15, SO₄²⁻/ZrO₂/SBA-15, or supercritical ethanol alone (i.e. catalyst free conditions) [43]. Ru based catalysts also provide higher hydrocracking than other commonly used precious metal catalysts. Chen et al. found Ru/C and Ru/HZSM-5 generated an upgraded bio-oil with higher oil content than Pd/C and Pt/C treated oils [27]. Likewise, Bai et al. found among all the single component and precious metal catalysts, Ru/C upgraded oil exhibited the highest oil yield and the highest heating value (45.1 MJ/kg); slightly higher than that of petroleum diesel (44.8 MJ/kg) [41]. Yao et al. found introducing Ru into acidic catalysts promoted pyrolytic lignin hydrocracking and inhibited polymerization and condensation, this caused the oil yield to increase significantly[44]. Similarly, Duan et al. reported the presence of Ru/C during bio-oil upgrading in SCW led to reduced coke formation due to the catalyst promoting hydrogenation of the coke precursor, and inhibiting polymerisation and condensation reactions [45]. Finally, Ahmadi et al. compared the effects of CoMo and Ru/C catalyst and reported the latter produced the highest oil yield and negligible coke formation (<1 wt%) [25].

Ru based catalysts are also recognised for improving the elemental properties of bio-oil through hydrogenation, deoxygenation and denitrogenation reactions. C. Zhang et al. found Ru/C was the most active catalyst for the upgrading of biocrude compared to 11 different catalysts including Pt/C and Pd/C [42]. Moreover, contrary to findings from Bai et al., C. Zhang et al. reported Ru/C was the only catalyst capable of promoting denitrogenation [41,42]. Additionally, the oil produced with this catalyst exhibited the lowest sulfur content, highest hydrocarbon content, and the highest heating value. The catalyst screening study by Bai et al. also found Ru/C showed the best performance for deoxygenation by generating an upgraded oil with the lowest O/C molar ratio compared to 15 different catalysts including Pd and Pt [41]. Additionally, the Ru/C produced upgraded oil contained the highest carbon content.

Duan et al. reported on the high performance of Ru/C in hydrogenation reactions, as a result Ru/C upgraded bio-oil had the lowest unsaturated hydrocarbon content and highest aromatic content [45]. Similarly, Chen et al. found the highest relative content of desired products was achieved over Ru/C and Ru exhibited higher hydrogenation ability than Pd and Pt which might be the reason for the better upgrading performance of Ru/C [27].

Oh et al. investigated the effects of Ru/C and Pt/C catalysts on the hydrodeoxygenation of bio-oil [46]. Although both Ru/C and Pt/C treated oils obtained complete removal of acid content,

the total acid number (TAN) of the Ru/C upgraded oil decreased by 59% of the original bio-oil whilst Pt/C decreased the TAN by 54%. Similarly, Bai et al. found Ru/C upgraded oil had the lowest TAN compared to several catalysts including Pt/C and Pd/C [41]. The TAN measures the acidity of the bio-oil based on the milligrams of potassium hydroxide (KOH) required to neutralise one gram of bio-oil. Bio-oil with TAN above the ASTM specification (0.50mg KOH/g according to the ASTM D 6751-07a) may lead to operational problems and cause corrosion during storage [26]. Thus, reducing the acidity of bio-oil is essential to enable storage and transportation of bio-oil.

Interestingly, Bai et al. found a combination of Ru/C and Raney Ni performed better during bio-oil upgrading than either catalyst alone [41]. Likewise, Xu et al. examined the effect of two-component catalyst mixtures, with Ru/C as the baseline catalysts, on upgrading of pre-treated algal oil in SCW [18]. The authors reported the catalyst mixture provided favourable advantages to bio-oil upgrading such as higher hydrogenation. However, the catalyst mixtures were less effective for deoxygenation compared to Ru/C alone. In addition, ruthenium is very expensive and difficult for regeneration, thus not a viable catalyst for bio-oil upgrading on a large scale.

3.2.3. Precious metals catalysts - Platinum

Among the noble metal catalysts commonly used in bio-oil upgrading, platinum (Pt) is one of the most active catalysts [47]. Pt is a frequently selected catalyst due to its hydrotreating capability, effectiveness for decarboxylation of fatty acids, enhancing the oil stability, and its high durability and thermal resistance [26,46]. Bio-oils upgraded in Pt based catalysts have been shown to exhibit a high abundance of hydrocarbons, and lead to a free flowing liquid product oil [26,47].

As previously mentioned, J. Zhang et al. conducted bio-oil upgrading studies using Pt and Pd catalysts and found Pd/HZSM-5 treated oil contained higher esters compared to the Pt/HZSM-5 oil under supercritical methanol [23]. However, bio-oil upgraded in Pt/SZr and supercritical methanol/ethanol and bio-oil upgraded in Pt/HZSM-5 and supercritical ethanol all exhibited higher ester content than with Pd based catalyst. Similarly, the catalyst screening study by Chen et al. showed bio-oil upgraded over Pt/C exhibited the highest relative content of esters compared to various catalysts including Pd/C and Ru/C [27]. The high presence of esters in upgraded bio-oil is favourable as it corresponds to the reduction in acids due to esterification reactions which leads to less corrosive and more stable bio-oil.

Moreover, the changes in the TAN and pH of the bio-oil can be used to examine the catalysts ability to promote acid decreasing reactions such as esterification during upgrading processes. Bai et al. showed Pt/C upgraded oil had a lower TAN than Pd/C upgraded oil. Hence, the former catalysts proved more effective for reducing the acidity of biocrude oil [41]. However,

Chen et al. showed Pd/C upgraded oil exhibited a higher pH than Pt/C treated oil due to the higher relative content of acids in the latter [27]. Nevertheless, Pt based catalysts have been shown to increase the pH of crude bio-oil in many studies. For example, Dang et al. demonstrated Pt/SZr catalyst can increase the pH of crude pyrolysis oil by up to 83% under supercritical ethanol [32]. Likewise, Li et al. demonstrated bio-oil upgraded over PtNi/MgO in supercritical methanol increased in pH value from 2.9 to 6.7 [21]. Overall, these findings may be an indication to Pt based catalysts ability to catalyse esterification reactions, hence decrease the acidity of crude bio-oil during supercritical upgrading processes.

Several studies have shown Pt catalysts effectiveness for increasing the oil yield. The bio-oil HDO study by Oh et al. found the highest oil yield can be obtained with Pt based catalyst compared to the Ru based catalyst [46]. Similarly, Chen et al. showed bio-oil upgrading with supercritical ethanol in Pt/C produced higher oil content (28.15%) than Pd/C treatment (27.66%) [27]. Moreover, both Bai et al. and C. Zhang et al. showed sulfided Pt/C upgraded oil in supercritical and subcritical water respectively generated higher oil yield than with Pd/C [41,42]. Whereas non-sulfided Pt/C treated oil obtained comparatively lower oil yield. These findings indicated the sulfide form of this catalyst is favourable for realising higher upgraded oil yields [18,41,42]. However, the results from both Bai et al. and C. Zhang et al., showed the carbon and hydrogen content, and HHV of the sulfided Pt/C upgraded oil were lower than that of the Pt/C upgraded oil [41,42]. Hence, the authors concluded pre-sulfiding the Pt/C does not cause any significant variations in the characteristics of the upgraded oil [41,42,48].

C. Zhang et al. also reported that Pt/C showed the best performance for hydrodeoxygenation and biocrude treated with this catalyst exhibited higher heating value, carbon content, and lower nitrogen content than with Pd/C catalyst [42]. Similarly, Bai et al. found Pt/C upgraded oil had lower O/C ratio, nitrogen content, higher H/C ratio and heating value than several catalysts including Pd/C [41]. Interestingly, Oh et al. found the Pt active sites might accelerate hydrogenation, deoxygenation as well as further decomposition, while hydrogenation and deoxygenation were separated active sites on the Ru catalyst [46]. Moreover, Oh et al. carried out several hydrodeoxygenation reaction runs with various reaction temperatures and time [46]. The findings showed compared to the Ru/C upgraded oils, the Pt/C upgraded oils exhibited the lowest water, nitrogen, sulfur, and oxygen content, as well as the lowest viscosity, and the highest heating value. However, the studies by Chen et al., C. Zhang et al., and Bai et al. showed Ru/C upgraded oil exhibited more improvement in properties compared to Pt/C treated oil (e.g. higher heating value) [27,41,42]. Ultimately, the findings from Oh et al. indicate under certain reaction conditions Pt/C can perform better than Ru/C during bio-oil upgrading in supercritical ethanol.

3.2.4. Non-precious metal catalysts

Although precious metal catalysts have been predominantly used for bio-oil upgrading in SCFs, non-precious metal catalysts have also been tested and proven effective for improving the quality of crude bio-oil. In two different studies, Peng et al. showed aluminium silicate and HZSM-5 catalyst played an essential role in upgrading crude bio-oil in supercritical ethanol [49,50]. The acidic aluminium silicate facilitated esterification and cracking reactions and the produced bio-oil exhibited higher pH, heating value, and lower viscosity compared to the crude bio-oil, and the catalyst free upgraded bio-oil. In the second study, Peng et al. showed acidic HZSM-5 also promoted esterification reactions, and stronger acidic HZSM-5 effectively facilitated cracking of heavy components of crude bio-oil. Q. Zhang et al. similarly reported the complete transformation of acetic acid in the supercritical ethanol and HZSM-5 system [51]. Likewise, in the catalytic bio-oil upgrading investigation by X. Zhang et al., the results showed complete removal of acids in the crude bio-oil after treatment with HZSM-5 supported Ni and supercritical ethanol [22]. However, Chen et al. found at a low ethanol to bio-oil ratio less acid was esterified over HZSM-5 supported Ru compared to Ru/C [27]. The authors concluded for non-acidic catalyst should be used at lower mass ratio of ethanol to bio-oil for higher acid conversion.

Bio-oil treatment with zeolites has been shown to lead to high coke yield and low upgraded oil yield. Both catalyst screening studies by Bai et al. and C. Zhang et al. reported that HZSM-5 and zeolite treatments led to the highest coke production lowest upgraded oil yield [41,42]. Barreiro et al. also reported a significant increase in the production of solid residue and decrease in upgraded oil yield with HZSM-5 catalyst compared to Pt/Al₂O₃ [48]. Duan et al. carried out a series of catalytic hydrothermal upgrading experiments of pre-treated algal bio-oil over nine different zeolites [52]. All the zeolite catalysts reduced the production of upgraded bio-oil, and most promoted more coke formation relative to the noncatalytic treatment. The results from Cheng et al.'s bio-oil upgrading study in supercritical methanol also demonstrated bio-oil upgrading with HZSM-5 led to the lowest biofuel yield and highest coke yield out of the six varied catalytic conditions [53]. X. Zhang et al. compared catalytic bio-oil upgrading in supercritical ethanol over various Ni supported catalyst and found the highest coke yield was obtained with Ni/HZSM-5 [22]. Duan et al. suggested the ease of coking and cracking of the zeolites are possible reasons for the reduced production of upgraded bio-oil [52]. In addition, despite the low oil yield, Cheng et al. reported that the content of desirable hydrocarbons in biofuel produced by HZSM-5 based catalysts increased compared to the raw bio-oil [53].

J. Zhang et al. found processing over HZSM-5-supported catalysts results in less high-molecular-weight components with aromatic groups [23]. Cheng et al. found similar results as HZSM-5 and supercritical methanol upgraded oil exhibited reduced content of phenols compared to raw bio-oil [53]. Similarly, Duan et al. found the presence of HZSM-5 effectively

promotes the cracking of macromolecules in the bio-oil and conversion to materials with low-boiling-point fractions [52].

In some cases, zeolite catalysts can provide similar or higher improvement in the elemental composition of bio-oil relative to precious metal catalysts. For example, C. Zhang et al. showed zeolite upgraded oil had lower nitrogen content than Pt/C and Pd/C upgraded oils [42]. Likewise, Bai et al. found HZSM-5 upgraded oil had lower nitrogen content than all the precious metal catalyst treated oils [41]. Duan et al. also reported HZSM-5 with a low Si/Al molar ratio provided a good performance for denitrogenation [52]. Moreover, Barreiro et al. reported HZSM-5 and SCW upgraded biocrude from *Scenedesmus almeriensis* algae obtained the lowest O/C ratios compared to Pt/Al₂O₃ [48].

The studies by C. Zhang et al. and Bai et al. found using activated carbon for upgrading biocrude in subcritical and supercritical water, respectively, produced an upgraded bio-oil with lower nitrogen and oxygen content than the uncatalyzed upgraded oil [41,42]. The authors suggested the carbon might be responsible for denitrogenation (by adsorption rather than catalytic reaction) and deoxygenation. Additionally, both studies showed activated carbon generated an upgraded oil yield comparable to that of Pt/C upgraded oil. Likewise, the results from Xu et al. showed similar upgraded oil yields was achieved with bio-oil upgraded in Ru mixed with Pt/C and Ru mixed with activated carbon [18]. C Zhang et al. also found the activated carbon led to lower coke yield relative to the coke yield with precious metal catalyst treatments [42]. Duan et al. compared the performance of several activated carbons and Ru/C during catalytic bio-oil upgrading in supercritical water [45]. All the activated carbons exhibited higher desulfurization capability compared to Ru/C, which was confirmed by the lower sulfur content in all the activated carbon upgraded bio-oils relative to the Ru/C upgraded oil. Additionally, four out of the six activated carbons facilitated greater nitrogen removal than Ru/C. Interestingly, the bio-oil upgraded with bamboo stem derived activated carbon obtained a higher heating value and hydrogen content and lower nitrogen and sulfur content than the Ru/C upgraded oil. This demonstrates that activated carbons can be used as an inexpensive alternative to Ru/C to generate a liquid fuel that has similar properties to those of hydro-carbon fuels derived from fossil fuel resources.

Nickel based catalysts are one of the most commonly used non-precious metal catalysts in the bio-oil upgrading studies reviewed in this report. Shi et al. investigated bio-oil upgrading over Ni/ZrO₂ in supercritical cyclohexane and reported the catalysts stability and effectiveness in catalysing several reactions including hydrogenation, and decarbonylation [54]. Similarly, X. Zhang et al. utilised Ni/SiO₂-ZrO₂ catalyst and supercritical ethanol to upgrade bio-oil and reported the catalysts ability to facilitate complete removal of acids and aldehydes and increase the esters, higher heating value, and pH value [22]. In another study by X. Zhang et

al. Ni based catalyst demonstrated excellent resistance to coking and the Ni/MgO catalyst generated an upgraded oil yield over 80% [55]. The author also found the complete removal of organic acids over the 20Ni/MgO catalyst. The results from Bai et al. also showed Ni/SiO₂-Al₂O₃ generated the second-largest upgraded oil yield and the lowest coke yield out of the fifteen catalytic conditions examined [41].

Many studies have incorporated cobalt into catalytic bio-oil upgrading in supercritical fluids [18,25,41,42,56,57]. Cheng et al. used non-sulfided Fe-Co/SiO₂ and supercritical methanol to upgrade raw bio-oil and reported that the bimetallic Fe-Co/SiO₂ catalysts resulted in better hydrodeoxygenation performance than monometallic Fe/SiO₂ or Co/SiO₂ catalysts due to the synergistic effect of Fe and Co on the SiO₂ support [56]. In another study, Cheng et al. used bifunctional Co-Zn/HZSM-5 to upgrade bio-oil and found the bimetallic catalyst increased biofuel yields and hydrocarbons contents in biofuels compared to monometallic Co/HZSM-5 and Zn/HZSM-5 catalysts [57]. Xu et al. reported the Ru/C + Co-Mo/Al₂O₃ catalyst produced the lowest coke yield compared to eleven other catalytic conditions [18]. Moreover, the combination of Ru/C with the Co-Mo based catalyst produced higher yields of upgraded oil compared to that obtained with Ru/C alone. Likewise, C. Zhang et al. found of all the catalysts examined in the catalyst screening study, the Co-Mo/ γ -Al₂O₃ catalyst generated the highest upgraded oil yield, and lower coke yield than C based Ru, Pd and Pt [42]. Similarly, Bai et al. showed the upgraded oil yield with CoMo/ γ -Al₂O₃ exceeded that with Pt/C and Pd/C catalysts and the second-lowest coke yield was observed with this catalyst [41]. Ahmadi et al. investigated the effects of CoMo catalysts on HDO of bio-oil in supercritical ethanol [25]. The results showed CoMo/MCM-41 catalyst produced a high oil fraction which was comparable to Ru/C treatment. Additionally, the composition of the light oil produced from the CoMo catalysts where reportedly comparable to that of the light oil obtained with the Ru/C catalyst.

The catalyst screening studies by C. Zhang et al. and Bai et al. effectively demonstrate the comparable results of bio-oil upgrading with precious metals and less commonly used ordinary catalysts in sub- and supercritical water, respectively [41,42]. C. Zhang et al. showed Mo₂C upgraded oils exhibited higher oil yields than all the precious metal catalysts, and MoS₂ upgraded bio-oil had higher oil yield than Pt/C and Pd/C [42]. In addition, both catalysts generated lower coke yields than C supported Ru, Pd and Pt. Likewise, Bai et al. demonstrated Mo₂C upgraded oils obtained higher oil yield than Pt/C and Pd/C treated oils and lower coke yield than all the precious metal catalysts [41]. Xu et al. showed mixing Ru/C with Mo₂C led to highest oil yield compared to mixing with any other catalyst including various precious metal catalysts [18].

Another less frequently utilised catalyst for bio-oil upgrading in SCFs is alumina. As an active metal catalyst, alumina has repeatedly shown good deoxygenation activity. Bai et al. found

alumina upgraded oil exhibited lower oxygen content than Pd/C and Pt/C upgraded oils [41]. Similarly Xu et al. showed mixing Ru/C with alumina led to deoxygenation and denitrogenation activities equivalent to Ru/C mixed with carbon-supported noble metal catalysts [18]. The authors in this study suggested that carbon or alumina is primarily responsible for the denitrogenation and deoxygenation, whereas noble metals play a smaller role, possibly by adsorption rather than catalytic reaction.

Overall, non-precious metal catalysts have shown activities comparable to that of the precious metal catalysts and they are promising inexpensive catalytic materials for upgrading bio-oils. However, these ordinary catalysts provide a limited improvement in the quality of the bio-oil when compared to precious metal catalysts. For example, Tang et al. examined upgrading of bio-oil and pyrolytic lignin through cracking and hydrotreatment in supercritical ethanol using various catalytic conditions [39,43]. The findings highlighted that although ordinary catalysts such as ZrO₂/SBA-15 (Zr) and SO₄²⁻/ZrO₂/SBA-15 (SZr) exhibit high cracking capabilities, these catalysts are prone to promote polymerisation reactions, while the Ru catalysts could promote hydrocracking and inhibit polymerisation [43]. Thus, as stated by Bridgwater, when approaching bio-oil upgrading, it is important to identify which characteristic or characteristics require modification [1]. Consequently, the relevant catalyst can be appropriately selected to meet the product bio-oil specification.

3.3. Non-catalytic Bio-oil Upgrading in SCF

Non-catalytic bio-oil upgrading using SCFs has been extensively researched and proved to be a promising alternative to catalytic bio-oil upgrading processes. The challenges associated with catalytic bio-oil upgrading processes (i.e. expensive precious metal catalyst and external H₂ addition, possibility of catalyst deactivation due to contaminants in crude bio-oil and coking on active sites) are not encountered with SCF upgrading [8,19,25]. Thus, SCFs can be effectively used to upgrade crude bio-oil without a catalyst.

3.3.1. Non-catalytic bio-oil upgrading in supercritical ethanol

Prajitno et al. carried out non-catalytic, non-external H₂ bio-oil upgrading in supercritical ethanol [19]. The unique reactivity associated with supercritical ethanol such as hydrogen donation, esterification, alcoholysis, cracking and alkylation, effectively decreased the TAN, water, oxygen contents and increased the bio-oil yield, carbon, hydrogen contents and HHV. The authors concluded, the bio-oil upgraded at 400°C demonstrated comparable performance to heavy fuel oil in terms of the gas temperature distribution and heat flux produced. Thus, can be considered for utilisation as boiler combustion fuel.

Supercritical ethanol performs the role of solvent and reactant during bio-oil upgrading. Dang et al. found the distribution of ethers in the product indicated to the participation of supercritical

ethanol in aldolization and etherification reactions [32]. Similarly, Chen et al. reported that the increase in pH value after upgrading was mainly due to the esterification of acetic acid and ethanol [27]. Similarly, studies by Peng et al. and Kim et al. found supercritical ethanol functioned as both a reaction medium and reactant; as esterification occurred without a catalyst in the supercritical conditions [37,49,50]. Yang et al. also reported on the esterification between acids and ethanol during HDO of bio-oil in supercritical ethanol [58]. Moreover, Peng et al. identified a high relative content of ethanol related compounds in the produced bio-oil, such as 18.53% of 1,1-diethoxy ethane, which suggests ethanol participated in further reactions besides esterification [50]. However, the authors established that although the quality (i.e. higher pH and heating value) of the catalyst-free upgraded bio-oil was higher than that of crude bio-oil, the catalytically upgraded bio-oil generally performed best [49]. X. Zhang et al. also showed the role of the supercritical ethanol solvent was extended to reactant [55]. This was confirmed when a part of ethanol was transferred into the upgraded oil via esterification and alkylation. The results also showed that bio-oil esterification with supercritical ethanol is more efficient than with subcritical conditions.

Furthermore, X. Zhang et al. investigated bio-oil upgrading with supercritical ethanol and found an 11.93% decrease in acid content and 6.45% increase in ester content after the upgrading process without catalyst addition [22]. These results suggested that organic acids in the bio-oil can be converted into esters via esterification without any catalyst in supercritical ethanol. It should be noted that with the addition of catalysts the esterification reaction was further enhanced and with 20Ni/HZSM-5 catalyst, the acids were completely removed. Moreover, the authors compared upgrading bio-oil without ethanol and found the yield of solid residues and the acids content significantly decreased with the addition of supercritical ethanol. X. Zhang et al. explained that the coke formation was suppressed due to the excellent dissolubility of supercritical ethanol [22]. J. Zhang et al. also reported that ethanol has a long alkyl chain which can dissolve higher molecular-weight products, this led to less solid products after bio-oil upgrading [23]. Moreover, ethanol acts as a capping agent which can prevent the re-polymerisation which led to the reduced coke yield [22]. Furthermore, the esterification of bio-oil under supercritical conditions proved more efficient than with liquid or subcritical ethanol. Like X. Zhang et al., Q. Zhang et al. showed carboxylic acids in crude bio-oil can be esterified with supercritical ethanol and 100% conversion of acetic acid was found after 30 minutes[22,51].

Tang et al. reported bio-oil upgraded with supercritical ethanol alone exhibited the highest pH value [39]. However, it also possessed higher water content, lower oil yield and heating value compared to PdSZr and SZr upgraded oil in supercritical ethanol [39]. A further study by Tang et al. achieved similar findings [43]. The supercritical ethanol upgraded oil exhibited improved qualities e.g. higher oil yield, heating value and lower solid yield than Zr and SZr catalyst

treated bio-oils, as well as, lower water content than RuSZr and SZr catalyst treated bio-oils [43]. However, the Ru based catalysts effectively converted the pyrolytic lignin to stable monomers such as esters relative to non-catalytic, Zr or SZr catalytic conditions. In another bio-oil upgrading study the authors showed similar results, where uncatalyzed upgraded oil exhibited higher oil yield, and lower solid and water yield than SZr upgraded oil [44]. These results indicate that although supercritical ethanol can provide elements of upgrading, the combination of supercritical ethanol and catalyst further enhances the upgrading process. Moreover, precious metal catalysts significantly enhance the bio-oil upgrading in supercritical ethanol whereas ordinary catalysts provide limited advantage compared supercritical ethanol alone.

3.3.2. Non-catalytic bio-oil upgrading in supercritical methanol

Cheng et al. found supercritical methanol promoted hydrogenation and esterification reactions over Fe-Co/SiO₂ catalyst during the bio-oil hydrodeoxygenation process [56]. This improved the contents of desirable hydrocarbons and esters in the product bio-oil. Moreover, supercritical methanol functioned as a hydrogen donor and promoted the hydrodeoxygenation of unsaturated compounds during the upgrading process. In another bio-oil upgrading study by Cheng et al., the results showed a significant reduction in acids in the product oil, the authors predicted the acidic compounds were converted to esters through esterification reactions with alcohols in the supercritical methanol [53].

Li et al. upgraded the low-boiling fraction (LBF) of bio-oil in supercritical methanol and reported that after 6 h reaction time the acids were converted into esters without catalyst addition [28]. supercritical methanol functioned as a reaction medium and reactant by providing an acidic environment for the system and facilitating esterification of LBF of bio-oil without catalyst addition. Moreover, the esterification of LBF in supercritical methanol proceeded under the same reaction mechanism as that of catalytic esterification of LBF using liquid methanol. In another study Li et al. examined the effects of upgrading the high boiling fraction (HBF) of bio-oil under different supercritical media [21]. The findings showed as the polarity of the supercritical media increased (tetrahydrofuran < ethanol < methanol), a corresponding increase in the yield and decrease in the coke formation were observed. Li et al. explained that methanol has the strongest polarity of all monohydric alcohols and in the supercritical phase the polarity of C-O and O-H bonds increase, thus the apparent polarity and acidity are enhanced. This enables supercritical methanol to chemically break acid molecules into methyl esters [28]. The alcoholysis ability, and esterification activity of supercritical methanol made it a promising medium for breaking chemical bonds of molecules in HBF and promoting the esterification of high boiling carboxylic acids in HBF.

However, catalytic upgrading with supercritical methanol also demonstrated zero acid content and proved more advantageous for reducing aldehyde and phenol content [21,28]. This is ideal as aldehyde and phenol can form carbonaceous deposits [28]. Likewise, Cheng et al. concluded that the bio-oil quality improvement after upgrading in supercritical methanol and Co-Zn/HZSM-5 catalyst was partly due to the long contact time of methanol solvent and bio-oil [57]. However, the incorporation of the HZSM-5 based catalysts further promoted the improvement of upgraded bio-oil quality.

Jo et al. investigated the effect of supercritical alcohols (methanol, ethanol, and isopropyl alcohol) on non-catalytic bio-oil upgrading [59]. Despite the absence of a catalyst, the yields of upgraded bio-oil were in the range of 77-85wt.% and the solid residue yield was in the range of 0.3-0.7wt.%. Acetic acid esters were the dominant chemical species in the upgraded light-fraction bio-oil. These were predicted to be from esterification reactions between acetic acid in the LBF bio-oil and the corresponding supercritical alcohols. However, the authors recognised that although the supercritical methanol upgrading process at 400°C resulted in a significant increase in the HHV and decrease in the TAN, there was a high consumption of methanol at this high temperature. Chen et al. carried out solvent recovery and reutilisation as part of the bio-oil upgrading process in order to reduce the solvent consumption and costs [27]. The relative content of acids remained stable with the reutilisation of ethanol and relative content of esters increased gradually. The authors concluded that the recovery and reutilisation of ethanol was an effective method for decreasing the ratio of ethanol to bio-oil.

3.3.3. Non-catalytic bio-oil upgrading in supercritical water

Duan et al. found supercritical water (SCW) upgraded bio-oil exhibited lower O/C and N/C molar ratio than bio-oil upgraded in SCW over Pt/C catalyst [26]. Moreover, no sulphur content was detected in SCW-only treated upgraded oil [26]. Thus, deoxygenation, denitrogenation and desulphurization reactions effectively proceeded without catalyst addition. This phenomenon was also observed in the catalyst screening study by Bai et al. [41]. In this study, bio-oil upgraded in SCW alone exhibited improvement in quality in terms of higher H/C ratio than activated carbon, Mo₂C, Ni/SiO₂-Al₂O₃, and alumina catalysts, as well as, lower O/C ratio and higher heating value than activated carbon catalyst [41]. However, the study by Duan et al. showed the total acid number (TAN) of the uncatalyzed upgraded oil was almost double the Pt/C upgraded oil [26]. This is unfavourable as high acid levels lead to corrosion and hinders consideration for practical application of the oil. In a further report, Duan et al. showed that bio-oil upgraded in SCW without a catalyst exhibited higher TAN, nitrogen and sulphur content, and lower carbon, hydrogen, and HHV than bio-oils treated with various activated carbon catalysts and SCW [45]. Moreover, the bio-oil upgraded with bamboo activated carbon exhibited higher heating value than Ru/C. Hence, bamboo activated carbon may be considered

as an inexpensive alternative which overcomes both challenges of SCF-only upgrading and precious-metal catalyst upgrading.

Isa et al. investigated upgrading bio-oil to bio-fuel using sub- and supercritical water [20]. The supercritical water conditions gave the highest bio-oil plus water yield and the lowest char yield. Moreover, the non-catalytic SCW treatment reduced the oxygen contents of the bio-oil.

In another study by Duan et al., the treated oil and coke yields with the non-catalytic upgrading process was comparable to the catalytic upgrading process [47]. SCW demonstrated effective coke control due to its ability to extract and transport potential coke precursors from the catalyst pores [47]. Moreover, minimal differences were noted in the H/C ratio between bio-oil upgraded in SCW over Pt/ γ -Al₂O₃ and bio-oil upgraded in SCW alone [47]. Thus, SCW alone was capable of promoting hydrogenation of the crude bio-oil. However, significantly higher levels of deoxygenation, denitrogenation and heating value were achieved with Pt/ γ -Al₂O₃ upgraded oil in SCW [47]. Likewise, in a further study Duan et al. found SCW suppresses coke formation due to its solvation and dilution characteristics, but further reduced coke formation was observed with Ru/C [45]. Another study by Duan et al. showed uncatalyzed bio-oil in SCW generated the highest bio-oil yield and one of the lowest coke yields relative to several different zeolite catalysts [52]. However, bio-oil treated with zeolite catalysts in SCW provided higher levels of hydrogenation, deoxygenation, denitrogenation, desulphurisation and ultimately higher heating value than SCW upgraded oil alone. Similarly, Remon et al. found the presence of SCW can partially reduce solid formation and/or favour its removal [60]. The results showed 0% coke yield and the highest liquid yield was obtained without catalyst addition. Moreover, the carboxylic acids were eliminated without catalyst addition at conditions of 450°C 260bar. However, the HHV without catalyst addition was lower than with the incorporation of Ni-Co/Al-Mg catalyst.

C. Zhang et al. reported that non-catalytically treated biocrude in subcritical water showed higher oil yield, carbon content, and lower coke yield and water content compared to treatment with several different catalysts [42]. The subcritical water appeared to incorporate into the products fraction and demonstrated some denitrogenation of the biocrude by dissolving the nitrogen-containing compounds [42]. However, uncatalyzed upgraded oil exhibited the lowest HHV and H/C molar ratio; this is unfavourable for considering the fuel for further applications.

In the algal oil upgrading study by Xu et al., the SCW physically decreased the nitrogen content in the upgraded bio-oil [18]. This was indicated by the large amount of nitrogen compounds detected in the water-soluble side product. Moreover, the sulphur content was reported as undetectable using a common elemental analyser but was quantified using a coulometric titration method [18]. However, catalytic bio-oil upgrading in SCW achieved higher H/C ratio, heating value and significantly lower N/C and O/C ratio compared to uncatalyzed upgraded oil

[18]. Likewise, Remon et al. found the level of sulphur in the SCW-only treated liquid was the same as the catalytically treated bio-oil [24]. In addition, SCW-only upgraded oil exhibited higher heating value, H/C ratio and lower O/C ratio than NiCo/CNF_r-900 catalysed bio-oil in SCW. However, NiCo/CNF_r and NiCo/CNF_r-600 catalysts further enhanced the heating value and hydrocarbon content and reduced the carboxylic acids in the bio-oil.

3.3.4. Non-catalytic bio-oil upgrading in other SCFs

SCFs are recognised for the unique dissolving power which is highly effective during bio-oil upgrading for increasing yield and improving the characteristics of the bio-oil. Shi et al. investigated upgrading bio-oil using supercritical cyclohexane and noted the excellent solubility of hydrogen in the SCF which led to the improvement in yield and quality of liquid hydrocarbons [54]. This was confirmed by the lower liquid hydrocarbon yield and the content of C₈-C₂₂ hydrocarbons with non-supercritical cyclohexane, relative to supercritical cyclohexane.

Xu et al. examined bio-oil upgrading using supercritical 1-butanol over Ru/C [29]. The highest hydrogen and carbon content, HHV, pH and the lowest viscosity, moisture and oxygen content was achieved under these conditions relative to subcritical 1-butanol or without solvent addition. More significantly, the solid product decreased from 2.5% without solvent to 0.2% with supercritical 1-butanol which indicated to reduced coke formation in the presence of the supercritical solvent. The study demonstrated that the use of supercritical solvent particularly enhances the quality of bio-oil. Moreover, like many studies of bio-oil upgrading in supercritical alcohol, Xu et al. reported the carboxylic acids were converted into their corresponding esters via esterification with 1-butanol.

Likewise, Cui et al. examined the effect of scCO₂ on the esterification of acids in bio-oil and found the conversion of the acids was higher under the scCO₂ conditions compared to atmospheric which indicated the promoting effect of scCO₂ [31]. Moreover, scCO₂ was used to upgrade the bio-oil by extraction and the scCO₂ extract fraction contained higher amounts of esters and lower amounts of water and acids. Additionally, the volatile compounds were enriched into the extract fraction and this oil exhibited improved pH, heating value and stability, thus demonstrated to be a promising fuel for further application.

Table 3.1 Summary of SCF bio-oil upgrading methods reported in literature

Feed	Crude Bio-oil Properties		Reaction Conditions		H ₂ (MPa); Catalyst	Upgraded Bio-oil Properties		Ref.
	Organic components (relative content %); Elemental Analysis (wt%); HHV (MJ kg ⁻¹); H ₂ O (wt%); pH/TAN(mg KOH/g);		T (°C); P (MPa); t (min); Solvent; Feed: Solvent, Reactor			Organic components (relative content %); Oil yield (wt.); Elemental Analysis (wt%); HHV (MJ kg ⁻¹); H ₂ O (wt%); pH/TAN(mg KOH/g);		
Fast pyrolysis of rice husk	Acids; Phenols; Esters; Ketones; Aldehydes: C; H; O; N: HHV: H ₂ O: pH:	33.17; 16.06; 6.85; 17.82; 4.45 N/A 19.70 N/A 2.91	T: P: t: Solvents: Feed: Solvent Reactor	260 7.8 180 Ethanol N/A 100mL autoclave	H ₂ : N/A Catalyst: Aluminium silicate (Al ₂ O ₃ SiO ₂)	Acids; Phenols; Esters; Ketones; Aldehydes: Oil yield: C; H; O; N: HHV: H ₂ O: pH:	1.76; 3.05; 69.57; 1.95; 0.17.12; 13.66; 21.94; 10.98; 3.92 (no catalyst) N/A N/A 20.79; 20.08(no catalyst) N/A 5.81; 3.92(no catalyst)	Peng et al., 2008 [49]
Fast pyrolysis of rice husk	Acids; Phenols; Esters; Ketones; Aldehydes: C; H; O; N: HHV: H ₂ O: pH:	33.17; 16.06; 6.85; 17.82; 4.45 N/A N/A N/A N/A	T: P: t: Solvents: Feed: Solvent Reactor	100; 238; 260 N/A 180 Ethanol N/A 100mL autoclave	H ₂ : N/A Catalyst: HZSM-5 (Si/Al = 22)	Acids; Phenols; Esters; Ketones; Aldehydes: Oil yield: C; H; O; N: HHV: H ₂ O: pH:	6.29; 12.94; 33.65; 5.38; 2.5 N/A N/A N/A N/A	Peng et al., 2009 [50]
Flash pyrolysis of rice husk	Acids; Phenols; Esters; Ketones; Aldehydes: C; H; O; N: HHV: H ₂ O: pH:	14.8; 18.6; 1.3; 12.79; 10; N/A 17.4 ^a 30.0 3.2	T: P: t: Solvents: Feed: Solvent Reactor	280 8.5-10.5 180 Ethanol 33wt%:67wt % 150mL autoclave	H ₂ : 0-2 MPa Catalyst: Pd/SO ₄ ²⁻ /ZrO ₂ /SBA-15	Acids; Phenols; Esters; Ketones; Aldehydes: Oil yield: C; H; O; N: HHV: H ₂ O: pH:	1.5; 12.9; 27.4; 3.9; 0.2 18.0 (excluding water and ethanol); 6.6 (uncatalyzed) N/A 20.1 ^a ; 6.2 ^a (uncatalyzed) 16.2; 29.9(uncatalyzed) 4.7; 5.5(uncatalyzed)	Tang et al., 2009 [39]

Flash pyrolysis of pulverized corn stalk	Acids; Phenols; Esters; Ketones; Aldehydes; Alcohol: C; H; O; N: HHV: H ₂ O: pH:	26.24; 17.42; 0; 10.25; 3.87 N/A 13.95 N/A 3.78	T: P: t: Solvents: Feed: Solvent Reactor	80 28 180 CO ₂ 10g:20g 150mL autoclave	H ₂ : N/A Catalyst: p-toluene sulfonic acid	Acids; Phenols; Esters; Ketones; Aldehydes; Alcohol: Oil yield: C; H; O; N: HHV: H ₂ O: pH:	5.17; 23.62; 29.48; 16.08; 6.93; 0.69 N/A N/A 25.55 ^b N/A 5.11	Cui et al., 2010 [31]
Pyrolytic lignin from flash pyrolysis of rice husk	Acids; Phenols; Esters; Ketones; Aldehydes; Alcohol: C; H; O; N: HHV: H ₂ O: pH:	N/A 60.21; 6.42; 31.3; 2.07 23.56 N/A N/A	T: P: t: Solvents: Feed: Solvent Reactor	260 9.5 480 Ethanol 3g:33.3g 150mL autoclave	H ₂ : 2 MPa Catalyst: Ru/SO ₄ ²⁻ /ZrO ₂ /SBA-15 or Ru/ZrO ₂ /SB A-15	Acids; Phenols; Esters; Ketones; Aldehydes; Alcohol: Oil yield: C; H; O; N: HHV: H ₂ O: pH:	N/A; 28.59; 12.76; 2.23; 5; 11.41 (RuSZr) N/A; 38.22; 7.43; 0.82; N/A; 0(no catalyst) 99.51(RuZr); 51.28(uncatalyzed) N/A 34.94 ^b (RuSZr); 27.87(uncatalyzed) N/A N/A	Tang et al., 2010 [43]
Crude algal bio-oil from liquefaction of microalga paste	Acids; Phenols; Esters; Ketones; Aldehydes: C; H; O; N: HHV: H ₂ O: TAN:	N/A 77.32; 10.52; 6.52; 4.89 40.1 N/A 256.5	T: P: t: Solvents: Feed: Solvent Reactor	400 N/A 240 Water 0.6g:0.6mL 4mL batch	H ₂ : 3.4 MPa Catalyst: Pt/C	Acids; Phenols; Esters; Ketones; Aldehydes: Oil yield: C; H; O; N: HHV: H ₂ O: TAN:	N/A N/A 82.09; 11.21; 4.46; 2.24; 82.75; 10.76; 4.31; 2.17(uncatalyzed) 43.0; 42.6(uncatalyzed) N/A 25.3; 49.6(uncatalyzed)	Duan et al., 2011a [26]
Crude algal bio-oil from liquefaction of microalga paste	Acids; Phenols; Esters; Ketones; Aldehydes: C; H; O; N: HHV: H ₂ O: pH:	N/A 74.3; 9.71; 10.97; 4.46 37.07 N/A N/A	T: P: t: Solvents: Feed: Solvent Reactor	400 N/A 60 to 480 Water N/A:0.4mL N/A	H ₂ : 3.4 MPa Catalyst: Pd/C	Acids; Phenols; Esters; Ketones; Aldehydes: Oil yield: C; H; O; N: HHV: H ₂ O: pH:	N/A 83 81.73; 11.51; 3.08; 3.68 43.79 N/A N/A	Duan et al., 2011b [40]
Heavy residues of fast pyrolysis of rice husk (high boiling fraction)	Acids; Phenols; Esters; Ketones; Aldehydes: C; H; O; N: HHV: H ₂ O: pH:	N/A 46.55; 6.69; 46.03 ^c 0.73; 20.40 N/A 2.80	T: P: t: Solvents: Feed: Solvent Reactor	290 N/A 300 Methanol 5mL:40mL 100mL autoclave	H ₂ : 2MPa Catalysts: Pt, PtNi, PdNi Support: Al ₂ (SiO ₃) ₃ , SiO ₂ , MgO	Acids; Phenols; Esters; Ketones; Aldehydes; Alcohols: Oil yield: C; H; O; N: HHV: H ₂ O: pH:	0; 4.2; 30.1; 18.1; 0; 20.0 (PtNi/MgO) 72.4 (PtNi/MgO) 54.6; 8.74; 36.61 ^c ; 0.048 31.7 ^b N/A 6.7	Li et al., 2011 [21]

Light residues of fast pyrolysis of rice husk (low boiling fraction)	Acids; Phenols; Esters; Ketones; Aldehydes; Alcohol: C; H; O; N: HHV: H ₂ O: pH:	(21.0; 18.2; 12.2; 16.6; 9.0; 19.9) ^d N/A N/A N/A N/A	T: P: t: Solvents: Feed: Solvent Reactor	250 8.6-9.6 180-540 Methanol 4mL:40mL 100mL autoclave	H ₂ : 1.5MPa Catalysts: Pt Support: Al ₂ (SiO ₃) ₃ , C, MgO	Acids; Phenols; Esters; Ketones; Aldehydes; Alcohols: Oil yield: C; H; O; N: HHV: H ₂ O: pH:	0; 2.8; 70.6; 14.3; 0; 11.3 (Pt/MgO) 0; 3.4; 66.8; 15.7; 2.9; 9.4(uncatalyzed) N/A N/A N/A N/A N/A	Li et al., 2011 [28]
Pyrolysis of <i>P. sylvestris</i> L.	Acids; Phenols; Esters; Ketones; Aldehydes; Alcohol: C; H; O: HHV: H ₂ O: pH:	20.1; 34.26; 1.31; 19.34; 13.57; 5.13 39.0; 7.71; 53.29 20.8 31.3 N/A	T: P: t: Solvents: Feed: Solvent Reactor	260 7.5-11.5 180 Ethanol; Methanol 5g:50g 100mL autoclave	H ₂ : 2MPa Catalyst: Pd; Pt Support: HZSM-5; SO ₄ ²⁻ /ZrO ₂ /SBA-15	Acids; Phenols; Esters; Ketones; Aldehydes; Alcohols: Oil yield: C; H; O: HHV: H ₂ O: pH:	0; 13.3; 63.76; 3.50; 0; 2.72 (upgraded distillate residue, Pt/SZr in SCEtOH) N/A 58.48; 8.81; 32.71 29.20 ^b 28.70 N/A	J. Zhang et al., 2012 [23]
Fast pyrolysis of rice husk	Acids; Phenols; Esters; Ketones; Aldehydes; Alcohols: C; H; O; N: HHV: H ₂ O: pH:	10.52; 27.39; 4.85 25.29; 4.83; 20.29 N/A 21.89 ^b 41.84 3.22	T: P: t: Solvents: Feed: Solvent Reactor	260; 280; 300 7-11.8 180 Ethanol 1:5; 1:3; 1:2; 1:1 100mL autoclave	H ₂ : 0.5; 2MPa Catalysts: Pt/ SO ₄ ²⁻ /ZrO ₂ /SBA-15	Acids; Phenols; Esters; Ketones; Aldehydes; Alcohols: Oil yield: C; H; O; N: HHV: H ₂ O: pH:	2.12; 16.89; 34.1; 1.96; 2.84; 6 (Case 9) 92.21 N/A 29.56 ^b 8.92 5.88	Dang et al., 2013 [32]
Crude algal oil from liquefaction of <i>Chlorella p.</i> (Alga) powder	Acids; Phenols; Esters; Ketones; Aldehydes: C; H; O; N: HHV: H ₂ O: pH:	N/A 75.1; 9.9; 7.8; 7.3; 38.1 N/A N/A	T: P: t: Solvents: Feed: Solvent Reactor	400 N/A 60 Water 1g:0.43mL 17.2mL autoclave	H ₂ : 6MPa Catalysts: Pt/ γ -Al ₂ O ₃	Acids; Phenols; Esters; Ketones; Aldehydes: Oil yield: C; H; O; N: HHV: H ₂ O: pH:	N/A 71; 70.0 (no catalyst) 79.8; 9.8; 5.6; 4.7. 73.6; 9.0; 12.3; 5.1 (no catalyst) 40; 35.6 (no catalyst) N/A N/A	Duan et al., 2013 [47]
Bio-oil from fast pyrolysis of rice husk	Acids; Phenols; Esters; Ketones; Aldehydes; Alcohols: C; H; O; N: HHV: H ₂ O: pH:	12.48; 28.48; 28.22 17.56; 1.87; 13.09 N/A 21.45 ^b 46.60 3.13	T: P: t: Solvents: Feed: Solvent Reactor	300 N/A 300 Ethanol 40g:80g 300mL batch	H ₂ : 2MPa Catalysts: Pt/C; Pd/C; Ru/C; Ru/HZSM-5	Acids; Phenols; Esters; Ketones; Aldehydes; Alcohols: Oil yield: C; H; O; N: HHV: H ₂ O: pH:	1.99; 17.89; 49.42; 7.35; 0; 23.35 (Ru/C) 32.00 (Ru/HZSM-5) N/A 31.03 ^b (Pd/C) 21.63 (Pd/C) 5.80 (Pd/C)	Chen et al., 2014 [27]

Bio-oil from fast pyrolysis of <i>Miscanthus sinensis</i> biomass	Acids; Phenols; Esters; Ketones; Aldehydes; Alcohols: C; H; O; N: HHV: H ₂ O: pH:	4.1; 31.4; 0; 18.0; 10.6; 1.6 40.0; 7.5; 52.2; <1 17.3 18 3	T: P: t: Solvents: Feed: Solvent Reactor	250; 300; 350 N/A 30; 45; 60 Ethanol 4:1 (w/w) 200mL autoclave	H ₂ : 3MPa Catalysts: Pd/C	Acids; Phenols; Esters; Ketones; Aldehydes; Alcohols: Oil yield: C; H; O; N: HHV: H ₂ O: pH:	0; 73.9; 5.1; 17.2; 0; 0 60 63.3; 9.3; 27.2; <1 30.6 <1 5	Oh et al., 2014 [38]
Fast pyrolysis of pine sawdust	Acids; Phenols; Esters; Ketones; Aldehydes: C; H; O; N: HHV: H ₂ O: pH:	N/A 44.6; 6.9; 48.0; 0.5 17.9 21.20 2.60	T: P: t: Solvents: Feed: Solvent Reactor	250-300 8.8-11.5 180 1-butanol 50g:50g 500mL autoclave	H ₂ : 2MPa Catalysts: Ru/C;	Acids; Phenols; Esters; Ketones; Aldehydes: Oil yield: C; H; O; N: HHV: H ₂ O: pH:	N/A 56.3 72.4; 11.3; 14.5; 0.2 32.0 6.7 4.4	Xu et al., 2014 [29]
Bio-oil from fast pyrolysis of yellow poplar wood	Acids; Phenols; Esters; Ketones; Aldehydes; Alcohols: C; H; O; N: HHV: H ₂ O: pH:	N/A 47.5; 7.0; 45.1; 0.5 20.1 21.5 3.0	T: P: t: Solvents: Feed: Solvent Reactor	250-370 N/A 40-120min Ethanol 40g:10g 150mL autoclave	H ₂ : 3MPa Catalysts: Pd/C	Acids; Phenols; Esters; Ketones; Aldehydes; Alcohols: Oil yield: C; H; O; N: HHV: H ₂ O: pH:	N/A 51.8; 47.8 (uncatalyzed) 74.4; 8.2; 16.7; 0.7 72.7; 8.1; 18.6; 0.6(uncatalyzed) 34.5; 33.4(uncatalyzed) 0.6; 0.8(uncatalyzed) 4.7; 3.8(uncatalyzed)	Kim et al., 2014 [37]
Duckweed biocrude from liquefaction of duckweed powder	Acids; Phenols; Esters; Ketones; Aldehydes: C; H; O; N: HHV: H ₂ O: pH:	N/A 73.4; 7.9; 13.6; 4.7 33.5 1.0 N/A	T: P: t: Solvents: Feed: Solvent Reactor	350 18 240 SubCW 1.5g:3.5mL 17mL autoclave	H ₂ : 6MPa Several Catalysts: including Ru/C; Pt/C; Pd/C	Acids; Phenols; Esters; Ketones; Aldehydes: Oil yield: C; H; O; N: HHV: H ₂ O: pH:	N/A 73.1 (Co-Mo/y-Al ₂ O ₃); 70.3 (no catalyst) 83.5; 10.8; 0.1; 5.4 (Pt/C) 82.3; 7.30; 3.3; 6.8 (no catalyst) 42.6 (Ru/C); 36.9 (no catalyst) 0.9 (Ru/C); 0.7 (no catalyst) N/A	C. Zhang et al., 2014 [42]
Bio-oil from HTL of cornstalks	Acids; Phenols; Esters; Ketones; Aldehydes: C; H; O; N: HHV: H ₂ O: pH:	N/A 65.45; 6.74; 26.79; 1.02 26.96 <1.0 N/A	T: P: t: Solvents: Feed: Solvent Reactor	300 N/A 240 Cyclohexane 0.05g:4.0mL 10mL reactor	H ₂ : 5MPa Catalysts: Ni/ZrO ₂	Acids; Phenols; Esters; Ketones; Aldehydes: Hydrocarbon yield: C; H; O; N: HHV: H ₂ O: pH:	N/A 81.6 85.66; 12.67; 0.75; 0.92 46.86 0 N/A	Shi et al., 2014 [54]
Pre-treated algal biocrude from liquefaction of	Acids; Phenols; Esters;	N/A	T: P: t:	400 N/A 240	H ₂ : 6MPa Catalysts: Several	Acids; Phenols; Esters; Ketones; Aldehydes:	N/A	Bai et al., 2014 [41]

chlorella p. algae powder	Ketones; Aldehydes; Alcohols C; H; O; N: HHV: H ₂ O: TAN:	82.1; 10.2; 3.6; 4.1 41.7 1.4 103.9	Solvents: Feed: Solvent Reactor	Water 3g:1.5mL 58mL autoclave	including Ru/C; Pt/C; Pd/C	Oil yield: C; H; O; N: HHV: H ₂ O: TAN:	59.6(uncatalyzed); 77.2(Ru/C + Raney-Ni) 84.5; 11.8; 1.1; 2.6 (Ru/C); 79.7; 11.0; 5.1; 4.1(uncatalyzed) 45.3(Ru/C + Raney-Ni); 41.8(uncatalyzed) 0.3(Ru/C + Raney-Ni); 0.3(uncatalyzed) 30.4(Ru/C + Raney-Ni); 90.4(uncatalyzed)	
Bio-oil from fast pyrolysis of Miscanthus sinensis	Acids; Phenols; Esters; Ketones; Aldehydes: C; H; O; N: HHV: H ₂ O: TAN:	28.00; 11.90; 0; 0.90; 8.80 40.0;7.5;52.20; 0.2 17.30 17.70 164.80	T: P: t: Solvents: Feed: Solvent Reactor	250; 300; 350 N/A 30; 45; 60 Ethanol 4:1 (w/w) autoclave	H ₂ : 3MPa Catalysts: Pt/C; Ru/C;	Acids; Phenols; Esters; Ketones; Aldehydes: Oil yield: C; H; O; N: HHV: H ₂ O: TAN:	0; 14.50; 0.80; 0.8; 0 (Ru/C) 56.30 (Pt/C) 70.7; 9.0; 20.10; 0.2 (Pt/C) 27.80 (Pt/C) 0.50 (Pt/C) 67.20 (Ru/C)	Oh et al., 2015 [46]
Bio-oil from fast pyrolysis of rice husk	Acids; Phenols; Esters; Ketones; Aldehydes; Alcohols: C; H; O; N: HHV: H ₂ O: pH:	25.28; 30.65; 0; 14.51; 14.55; 3.75 N/A 13.1 51.4 2.38	T: P: t: Solvents: Feed: Solvent Reactor	280 N/A 300 Ethanol 15g:35g 250mL autoclave	H ₂ : 1.5MPa Catalysts: Ni/SiO ₂ - ZrO ₂	Acids; Phenols; Esters; Ketones; Aldehydes; Alcohols: Oil yield: C; H; O; N: HHV: H ₂ O: pH:	0; 40.11; 17.4; 8.93; 3.7; 8.51 (20Ni/HZSM-5). 11.93; 39.81; 6.45; 10.2; 2.1;4.66 (uncatalyzed) N/A N/A 24.4 15.6 5.24	X. Zhang et al., 2015 [22]
Fast pyrolysis of sawdust	Acids; Phenols; Esters; Ketones; Aldehydes; Alcohols: C; H; O; N: HHV: H ₂ O: pH:	42.19; 11.55; N/A; 23.24;11.11; 4.04 N/A N/A N/A N/A	T: P: t: Solvents: Feed: Solvent Reactor	200; 250 7 180 Ethanol 1:10; 1:5; 1:3; 1:1 100mL autoclave	H ₂ : N/A Catalysts: Zeolite	Acids; Phenols; Esters; Ketones; Aldehydes: Oil yield: C; H; O; N: HHV: H ₂ O: pH:	N/A N/A N/A N/A N/A N/A	Q. Zhang et al., 2015 [51]
Pre-treated crude bio-oil from liquefaction of C. pyrenoidosa microalga	Acids; Phenols; Esters; Ketones; Aldehydes: C; H; O; N: HHV: H ₂ O: pH:	N/A 80.4; 10.0; 5.6; 4.0 40.5 N/A N/A	T: P: t: Solvents: Feed: Solvent Reactor	400 24 240 Water 3.0g:1.5mL 58mL autoclave	H ₂ : 6MPa Catalysts: Two component catalyst mixtures with Ru as baseline catalyst	Acids; Phenols; Esters; Ketones; Aldehydes: Oil yield: C; H; O; N: HHV: H ₂ O: pH:	N/A 77.2 (Ru/C+Mo ₂ C); ~59 (uncatalyzed) 83.9; 12.9; 0.1; 3.1. (Ru/C:Mo ₂ C (1:1) 79.5; 11.0; 5.4; 4.1 (uncatalyzed) 47.0 (Ru/C:alumina); 41.6 (uncatalyzed) N/A N/A	Xu et al., 2015 [18]

Pre-treated crude algal oil from liquefaction of <i>Chlorella p.</i> (Alga) powder	Acids; Phenols; Esters; Ketones; Aldehydes; C; H; O; N: HHV: H ₂ O: pH:	N/A 79.2; 10.22; 5.04; 4.58 40.49 N/A N/A	T: P: t: Solvents: Feed: Solvent Reactor	400 28 240 Water 3.0g:1.5mL 58mL batch	H ₂ : 6MPa Catalysts: Nine zeolites Including MCM-41(100%Si)	Acids; Phenols; Esters; Ketones; Aldehydes: Oil yield: C; H; O; N: HHV: H ₂ O: pH:	N/A 54.5; 55.6 (uncatalyzed) 83.6; 12.09; 1.73; 1.87 82.4; 10.66; 4.32; 3.45 (uncatalyzed) 45.23; 42.32 (uncatalyzed) N/A N/A	Duan et al., 2015 [52]
Pyrolytic lignin from fast pyrolysis of rice husk	Acids; Phenols; Esters; Ketones; Aldehydes; Alcohols: C; H; O; N: HHV: H ₂ O: pH/TAN:	N/A 60.21; 6.42; 31.3; 2.07 N/A N/A N/A	T: P: t: Solvents: Feed: Solvent Reactor	260 9.5 480 Ethanol 3g:33.3g 150mL autoclave	H ₂ : 2MPa Catalysts: SBA-15; Zr; RuZr; SZr; RuSZr;	Acids; Phenols; Esters; Ketones; Aldehydes; Alcohols: Oil yield: C; H; O; N: HHV: H ₂ O: pH/TAN:	N/A 99.51(RuZr50); 51.28(uncatalyzed) N/A N/A 3.24 (RuZr); 4.74(uncatalyzed) N/A	Yao et al., 2015 [44]
Bio-oil from pyrolysis of pine sawdust	Acids; Phenols; Esters; Ketones; Aldehydes; Alcohols: C; H; O: HHV: H ₂ O: pH:	45.52; 21.35; N/A; 18.22; 1.41; 2.22 53.9; 3.3; 41.3 18.5 39.05 2.45	T: P: t: Solvents: Feed: Solvent Reactor	380 23 N/A Water N/A 12mL micro-bomb reactor	H ₂ : N/A Catalysts: Ni-Co supported on carbon nanofibers	Acids; Phenols; Esters; Ketones; Aldehydes; Alcohols: Oil yield: C; H; O: HHV: H ₂ O: pH:	9.10; 53.88; N/A; 23.98; N/A; 0.18.9; 51.92; N/A; 21.95; N/A; 0 (uncatalyzed) 56.0; 45.1 (no catalyst) 72.1; 7.4; 19.8; 67.4; 7.0; 25.2 (uncatalyzed) 31.9; 29.2(uncatalyzed) N/A N/A	Remon et al., 2016 1 [24]
Bio-oil from pyrolysis of pine sawdust	Acids; Phenols; Esters; Ketones; Aldehydes; Alcohols: C; H; O: HHV: H ₂ O: pH:	45.52; 21.35; N/A; 18.22; 1.41; 2.22 53.91; 3.32; 41.31 18.5 39.05 2.45	T: P: t: Solvents: Water: bio-oil Reactor	310-450 20-26 0-60 Water 6.5 to 12.5 12mL micro-bomb reactor	H ₂ : N/A Catalysts: Ni-Co/Al-Mg	Acids; Phenols; Ketones: Oil yield: C; H; O: HHV: H ₂ O: pH:	1.39; 0; 0. 0; 27.27; 4.28(uncatalyzed) 64.5 (Run No. 25); 54.4 (uncatalyzed) 77.34; 7.82; 12.66 (Run No. 16) 70.31; 7.59; 21.43 (uncatalyzed) 35.01 (Run No. 16); 31.29 (uncatalyzed) N/A N/A	Remon et al., 2016 2 [60]
Bio-oil from fast pyrolysis of empty palm fruit bunch	Acids; Phenols; Esters; Ketones; Aldehydes; Alcohols C; H; O; N: HHV: H ₂ O: TAN:	0.985; 56.455; 0; 9.024; 0.878; 0.520 69.1; 6.1; 26.8; 1.6 24.3 14.0 69.4	T: P: t: Solvents: Feed: Solvent Reactor	300; 350; 400 16.8-41.3 30; 60; 120 Ethanol 2.0g:66.0g 140mL reactor	N ₂ : 1MPa Catalysts: N/A	Acids; Phenols; Esters; Ketones; Aldehydes; Alcohols: Oil yield: C; H; O; N: HHV: H ₂ O: TAN:	0.269; 34.127; 13.866; 1.488; 0.864; 29.724 (Case 3) 83.0 76.9; 7.1; 12.6; 1.4 (Case 3) 34.1 (Case 3) 0.2 (Case 1) 3.6 (Case 2)	Prajitno et al., 2016 [19]

Bio-oil from hydrothermally liquefied dried cornstalk powder	Acids; Phenols; Esters; Ketones; C; H; O; N: HHV: H ₂ O: TAN:	23.8; 18.2; 14.3; 10.4; 72.0; 7.78; 20.2; 0 32.1 25.6 19.7	T: P: t: Solvents: Feed: Solvent Reactor	280; 310; 340; 370 N/A 60 Ethanol 10g:20g 500mL autoclave	H ₂ : 4MPa Catalysts: Bimetallic ammonium nickel molybdate	Acids; Phenols; Esters; Ketones: Oil yield: C; H; O; N: HHV: H ₂ O: TAN:	1.6; 5.9; 12.3; 3.8 (at 370°C) 26.7 82.6; 8.3; 6.0; 2.0 (at 370°C) 38.3 (at 370°C) 1.6 (at 370°C) 1.3 (at 310°C)	Yang et al., 2016 [58]
Pretreated crude duckweed bio-oil	Acids; Phenols; Esters; Ketones; Aldehydes; Alcohols C; H; O; N: HHV: H ₂ O: TAN:	N/A 79.8; 8.9; 3.5; 1.81 39.06 N/A 28.13	T: P: t: Solvents: Feed: Solvent Reactor	400 N/A 60 Water 3.0g: 1.5mL 37mL autoclave	H ₂ : 6MPa Catalysts: Activated Carbon	Acids; Phenols; Esters; Ketones; Aldehydes; Alcohols: Oil yield: C; H; O; N: HHV: H ₂ O: TAN:	N/A 76.3; 74.7(Ru/C) 86.2; 10.7; 1.9; 1.24 85.1; 10.2; 2.2; 1.79 (uncatalyzed) 44.08; 42.94(uncatalyzed) N/A 9.81(Ru/C); 17.84(AC); 26.57(uncat-)	Duan et al., 2016 [45]
Pyrolysis oil from biomass	Acids; Phenols; Esters; Ketones; Aldehydes; Alcohols C; H; O; N: HHV: H ₂ O: pH/ TAN:	N/A 48.4; 7.0; 44.4; 0.2 N/A 34 N/A	T: P: t: Solvents: Feed: Solvent Reactor	410 32 60 Water 1.0:9.3 75mL	N ₂ : 0.2MPa Catalysts: N/A	Acids; Phenols; Esters; Ketones; Aldehydes; Alcohols: Oil yield: C; H; O; N: HHV: H ₂ O: pH/ TAN:	N/A 41.6 77.2; 6.8; 15.6; 0.4 N/A N/A N/A	Isa et al., 2016 [20]
Fast pyrolysis of rice husk	Acids; Phenols; Ketones; Aldehydes; Alcohols C; H; O; N: HHV: H ₂ O: pH:	19.8; 31.46; 10.06; 14.33; 2.88 N/A 13.1 51.4 2.38	T: P: t: Solvents: Feed: Solvent Reactor	280 N/A 300 Ethanol 15g:35g 250mL	H ₂ : 1.5MPa Catalysts: Ni/MgO	Phenols; Esters; Ketones; Alcohols Oil yield: C; H; O; N: HHV: H ₂ O: pH:	50.84; 11.03; 17.8; 6.57 >80 N/A 24.9 14.3 5.01	Zhang et al., 2016 [55]
Hardwood sawdust fast pyrolysis oil	Acids; Phenols; Esters; Ketones; Aldehydes; Alcohols C; H; O: HHV: H ₂ O: pH/TAN:	N/A 56.21; 7.38; 36.40 24.56 20.99 N/A	T: P: t: Solvents: Feed: Solvent Reactor	350 22.5 180 Ethanol 50g:100g 500mL	H ₂ : 5MPa Catalysts: CoMo catalysts supported on various nanostructur ed materials; Ru/C	Acids; Phenols; Esters; Ketones; Aldehydes; Alcohols: Oil yield: C; H; O: HHV: H ₂ O: pH/TAN:	N/A 61.9 (CoMo/MCM-41); 66.6 (Ru/C) 83.00; 7.35; 9.65 (CoMo/MCM-41) 36.86 0.41 N/A	Ahmadi et al., 2016 [25]
Biocrude from HTL of microalgae	Acids; Phenols; Esters;	N/A	T: P:	400 22.5	H ₂ : 4MPa Catalysts:	Acids; Phenols; Esters;	N/A	Barreiro et al., 2016

	Ketones; Aldehydes; Alcohols C; H; O; N: HHV: H ₂ O: pH/TAN:	74.4; 10.1; 10.3; 4.8 37.0 N/A N/A	t: Solvents: Feed: Solvent Reactor	240 Water 1.00g:0.55mL 10mL micro autoclave	Pt/Al ₂ O ₃ ; HZSM-5	Ketones; Aldehydes; Alcohols: Oil yield: C; H; O; N: HHV: H ₂ O: pH/TAN:	49.2 (Pt/Al ₂ O ₃); 49.8 (uncatalyzed) 82.0; 11.2; 4.0; 2.8 (Pt/Al ₂ O ₃) 81.4; 10.9; 5.2; 2.3 (uncatalyzed) 41.5 (Pt/Al ₂ O ₃); 40.9 (uncatalyzed) N/A N/A	[48]
Bio-oil from pyrolysis of pine sawdust	Acids; Phenols; Esters; Ketones; Aldehydes; Alcohols C; H; O; N: HHV: H ₂ O: TAN:	16.54; 13.29; 18.25; 27.99; 5.69; 6.13 N/A 22.38 ^f 14.50 320.03	T: P: t: Solvents: Feed: Solvent Reactor	300 N/A 300 Methanol 50g:50g 500mL autoclave	H ₂ : 3.4MPa Catalysts: Co; Zn; Co- Zn Support: HZSM-5	Acids; Phenols; Esters; Ketones; Aldehydes; Alcohols: Oil yield: C; H; O; N: HHV: H ₂ O: TAN:	2.01; 18.89; 35.71; 11.58; 1.56; 0.92 (5%Co15%Zn/HZSM-5) 22.13 (5%Co15%Zn/HZSM-5) N/A 31.98 ^f (10%Co10%Zn/HZSM-5) 3.61 (20%Co/HZSM-5) 72.45 (20%Zn/HZSM-5)	Cheng et al., 2017 [57]
Low boiling fraction of bio-oil from fast pyrolysis of empty palm fruit bunch	Acids; Phenols; Esters; Ketones; Aldehydes; Alcohols C; H; O HHV: H ₂ O: TAN:	23.28; 16.95; 1.36; 18.53; 5.70; 1.65 42.5; 4.7; 41.7 12.5 23.7 92.2	T: P: t: Solvents: Feed: Solvent Reactor	400 22.5-46.7 30 Methanol; N/A 140mL	N ₂ : 1MPa Catalysts: N/A	Acids; Phenols; Esters; Ketones; Aldehydes; Alcohols: Oil yield: C; H; O: HHV: H ₂ O: TAN:	N/A 78.4 68.2; 7.3; 23.7 29.9 4.4 4.0	Jo et al., 2017 [59]
Pyrolysis oil from hardwood sawdust fast pyrolysis	Acids; Phenols; Esters; Ketones; Aldehydes; Alcohols C; H; O: HHV: H ₂ O: pH/TAN:	N/A 53.11; 6.24; 40.65 21.48 27.92 N/A	T: P: t: Solvents: Feed: Solvent Reactor	300 N/A 180 Ethanol 50g:100g; 100g:50g 500mL autoclave	H ₂ : 10MPa Catalysts: Ru/C	Acids; Phenols; Esters; Ketones; Aldehydes; Alcohols: Oil yield: C; H; O: HHV: H ₂ O: pH/TAN:	N/A ~80 82.85; 8.76; 8.38 ~39 6.40 N/A	Ahmadi et al., 2017 [61]
Bio-oil from pine sawdust pyrolysis	Acids; Phenols; Esters; Ketones; Aldehydes; Alcohols C; H; O; N: HHV: H ₂ O: TAN:	10.38; 21.79; 17.34; 15.64; 14.65; 9.23 45.38; 5.12; 48.78; 0.73 22.38 ^f 14.5 320.03	T: P: t: Solvents: Feed: Solvent Reactor	300 N/A 300 Methanol 50g:50g 500mL	H ₂ : 3.45MPa Catalysts: Fe-Co/SiO ₂ or Co/HZSM-5	Acids; Phenols; Esters; Ketones; Aldehydes; Alcohols: Oil yield: C; H; O; N: HHV: H ₂ O: TAN:	0.69; 8.72; 61.47; 0.88; 2.42; 3.38 (Fe- Co (1)/SiO ₂) 33.91(Fe/SiO ₂) 63.46;6.75; 28.96; 0.83 (Fe-Co (1)/SiO ₂) 30.97 ^f (Fe-Co (1)/SiO ₂) 2.68 (Fe-Co (3)/SiO ₂) 67.75 (Fe/SiO ₂)	Cheng et al., 2017 2 [56]

Bio-oil from pine sawdust pyrolysis	Acids; Phenols; Esters; Ketones; Aldehydes; Alcohols C; H; O; N: HHV: H ₂ O: TAN:	10.38; 21.79; 17.34; 15.64; 14.65; 9.23 45.38; 5.12; 48.78; 0.73 22.38 14.5 320.03	T: P: t: Solvents: Feed: Solvent Reactor	300 N/A 300 Methanol 50g:50g 500mL	H ₂ : 3.4MPa Catalysts: Fe- Ni/HZSM-5	Acids; Phenols; Esters; Ketones; Aldehydes; Alcohols: Oil yield: C; H; O; N: HHV: H ₂ O: TAN:	1.72; 19.3; 47.83; 2.55; 0; 0 28.70 N/A 30.21 6.07 65.60	Cheng et al., 2017 3 [53]
-------------------------------------	--	---	--	---	---	---	---	---------------------------------

In cases with more than one experiment result, maximum conditions are selected and corresponding upgraded oil properties are based on the maximum reaction conditions reported in the literature.

^aHeating value after removing ethanol

^bHeating value after removing solvent and water

^cCalculated by difference

^d 4 ml of bio-oil and LBF were diluted to 50 ml solution with methanol respectively.

^eY_{oil} is defined as the mass of oil after reaction/(the mass of consumed ethanol + the mass of oil before reaction) x 100%

^fHeating value after removing methanol

3.4. Conclusion

The proforma Table 3.1. shows the precious metal catalysts platinum, palladium and ruthenium are the most commonly used in the papers examined in this literature review. Additionally, methanol, ethanol and water are frequently used as solvents for the supercritical fluid upgrading. Majority of the papers highlight the improvement in the properties and characteristics of the bio-oil after upgrading. Moreover, the supercritical solvents are consistently recognised for their active effects on the upgrading process which is more than what is observed in ordinary liquid solvent conditions. The literature review demonstrates that non-precious metal catalysts are a viable and economic alternative to expensive precious metal catalysts for bio-oil upgrading. Particularly when supercritical fluids are used in conjunction which provide some catalyst-like activities.

Table 3.1. shows that the reported crude bio-oil properties are different in the research papers even when the feed is the same, e.g. rice husk. This may be considered advantageous because the diversity in processing makes the biomass and bio-oil processes more flexible and accessible to researchers/industries/individuals with different resource availabilities. On the other hand, this may be disadvantageous because there is no standard bio-oil upgrading process.

The next chapter reports on the experimental work involving bio-oil reactions under supercritical alcohol conditions. The literature review demonstrates the ability of supercritical alcohols to participate in esterification reactions. Therefore, it was expected that the level of acid in the product bio-oil from the experiments will be reduced, hence improving the chemical stability of the bio-oil.

4. Production of Renewable Fuels by Blending Bio-oil with Alcohols and Upgrading under Supercritical Conditions

4.1. Introduction

Bio-oil upgrading by hydrotreatment has been widely researched and proven to effectively remove or reduce the oxygen content in the bio-oil to improve its quality and stability [37]. However, the severe process conditions (350-450 °C, 5-15 MPa) leads to the formation of excessive amounts of gases and char as by-products [62]. Moreover, due to the high oxygen content (30-55 wt.%) of bio-oil, a substantial amount of hydrogen is necessary for complete hydrogenation [63]. For example, under hydrodeoxygenation (HDO) conditions of 523 K and 10 MPa, two liquid phases (water and oil) and char were produced with mass balance between 77-96 wt % and with oil oxygen content of 18-27 wt% [64]. Thus, the direct hydrodeoxygenation of bio-oil is a high cost and low hydrogen efficiency process. This has motivated research into developing the hydrotreatment process to operate at lower temperature and without excessive supply of hydrogen.

In conventional liquid-phase catalytic hydrogenation reactions, hydrogen is mixed with a liquid substrate and a solid catalyst. Thus, gas-liquid transfer resistances and external fluid film diffusion resistances take place [7]. These mass transfer resistances can be removed by operating in supercritical conditions [13]. Hydrogen is insoluble in most organic solvents, but it is soluble in supercritical fluids. Thus, hydrogen concentration at the catalyst surface is increased under supercritical conditions resulting in higher reaction rates than in liquid phase reactions [7]. Bio-oil upgrading in supercritical fluids has been researched as an alternative to promote the bio-oil upgrading processes, since the challenges associated with catalytic bio-oil upgrading processes (i.e. expensive precious metal catalyst and external H₂ addition, possibility of catalyst deactivation due to contaminants in crude bio-oil and coking on active sites) are not encountered with supercritical fluid upgrading [8,19,25].

Alcohols, such as methanol, ethanol, and isopropanol have been used to blend with bio-oil to increase its homogeneity and reduce its viscosity and the rate of ageing [65,66,75,67–74]. Diebold and Czernik found additives such as methanol and ethanol can drastically reduce the ageing rate of pyrolysis oil [75]. Methanol participated in molecular dilution to slow the chemical reactions and formation of intermediate products during storage. Boucher et al. also demonstrated the effective role of methanol solvent in reducing ageing and improving stability of bio-oil [65]. The addition of methanol to bio-oil hindered phase separation, lowered ageing rate and restricted polymerisation of the bio-oil components. Moreover, the viscosity of the methanol/oil blend was significantly lower than the untreated bio-oil. Likewise, Pidtasang et al.

found the addition of methanol or ethanol significantly reduced the bio-oil viscosity (initial bio-oil viscosity 21 cSt to 7 cSt bio-oil/alcohol blend) [68]. Yu et al. found blending methanol or ethanol with bio-oil proved to be a simple and cost-effective method for reducing the viscosity and improving homogeneity and stability of the bio-oil [72].

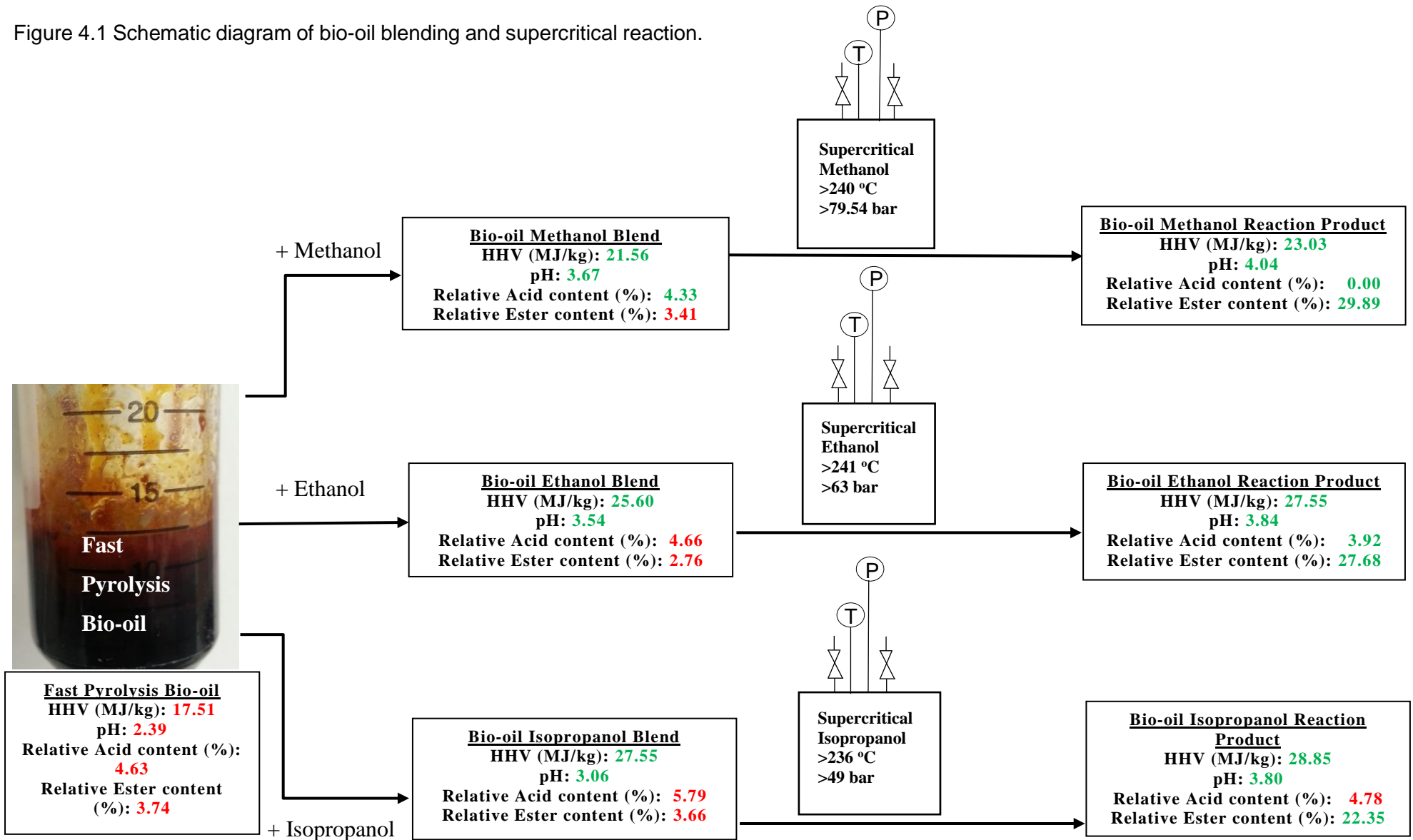
Udomsap et al. prepared various bio-oil-solvent samples including two samples of 10 wt.% methanol, or ethanol in pure bio-oil [74]. The authors reported that the solvents could terminate the chain of oligomers, and break polymer chains to lower molecular weight compounds. For example, oligomeric esters in the bio-oil may undergo transesterification with methanol or ethanol to form lower molecular weight methyl or ethyl esters, respectively [74,75].

Oasmaa et al. tested the effects of adding up to 10 wt.% methanol, ethanol and isopropanol on the quality of liquids from fast pyrolysis forestry residue and pine [67]. The authors reported that the addition of alcohols improved the homogeneity and heating value and reduced the viscosity of pyrolysis liquids. After the addition of alcohol, the solubility of poorly water-soluble compounds (e.g. lignin dimers) in the pyrolysis liquids was improved. The decrease in viscosity was reportedly due to the stabilising effect of the alcohols on the water-insoluble fraction.

Weerachanchai et al. experimented with two alcohols (ethanol and n-butanol) as co-solvent to improve miscibility of bio-oil in diesel and produce a stable homogenous phase fuel [71]. A miscible bio-oil-diesel-alcohol fuel blend was obtained with 40 vol% bio-oil, 10 vol% diesel and 50 vol% ethanol or butanol. The product fuel properties were improved (i.e. reduced viscosity, acidity, and carbon residue) relative to the bio-oil. Similarly, Nguyen and Honnery investigated combustion capabilities of 10% 20% and 40% bio-oil in ethanol blends [66]. The burning rates for the product fuel blends were comparable to diesel fuel.

Many researchers have reported on bio-oil blending with alcohols, and bio-oil upgrading using supercritical fluids, respectively. However, to the best of the authors' knowledge, a detailed study of blending bio-oil with alcohols followed by treatment with supercritical alcohols has not been conducted. Figure 4.1 illustrates the bio-oil blending and supercritical alcohol reactions carried out. This chapter further outlines the effects of bio-oil blending with alcohols (methanol, ethanol and isopropanol) followed by the effects of non-catalytic supercritical alcohol treatment of crude bio-oil.

Figure 4.1 Schematic diagram of bio-oil blending and supercritical reaction.



4.2. Materials and Methods

4.2.1. Materials

The bio-oil used for this research was derived from softwood and obtained from Biomass Technology Group (BTG) in the Netherlands. Chemically pure grade methanol, ethanol and isopropanol were obtained from the company VWR chemicals. The samples were labelled BM1 (bio-oil methanol blend), BE1 (bio-oil ethanol blend), BI1 (bio-oil isopropanol blend), BM2 (bio-oil methanol reaction products), BE2 (bio-oil ethanol reaction products), and BI2 (bio-oil isopropanol reaction products).

4.2.2. Bio-oil blending and upgrading reactions

The bio-oil-alcohol blends were each prepared by weighing a 50 wt.% sample of bio-oil in a glass container, then adding 50 wt.% alcohol solvent. Figure 4.2 illustrates the 50 mL stainless steel autoclave with a maximum operating pressure of 210 bar which was used for the bio-oil-alcohol reactions. In a typical run, a magnetic stirrer, bio-oil and alcohol (1:1 mass ratio) was transferred into the autoclave. Then the autoclave was sealed and placed on an Asynt ADS-HP-NT magnetic hotplate stirrer and an Asynt ADS-TC-NT temperature sensor with controller was inserted. The autoclave was purged with N₂ to remove dissolved oxygen in the liquid and the oxygen in the reactor. A 2-way ball valve on the autoclave was connected to the N₂ line in the fume cupboard with a rubber tube. The hotplate and the temperature controllers were set to the maximum temperatures of 310 °C and 450 °C, respectively. The bio-oil methanol reaction gradually increased in temperature and after 40 minutes of continuous heating the autoclave contents exceeded methanol's critical point (240 °C and 79.54 bar). Likewise, the bio-oil ethanol and bio-oil isopropanol reactions gradually increased in temperature and after 30 minutes of continuous heating surpassed the ethanol (241 °C and 63 bar) and isopropanol (236 °C and 49 bar) critical points, respectively. Each reaction lasted 2 h and the stirring rate was set to 1500 rpm. At the end of the reaction, the hot plate was switched off and the reactor was placed in a water bath to cool.

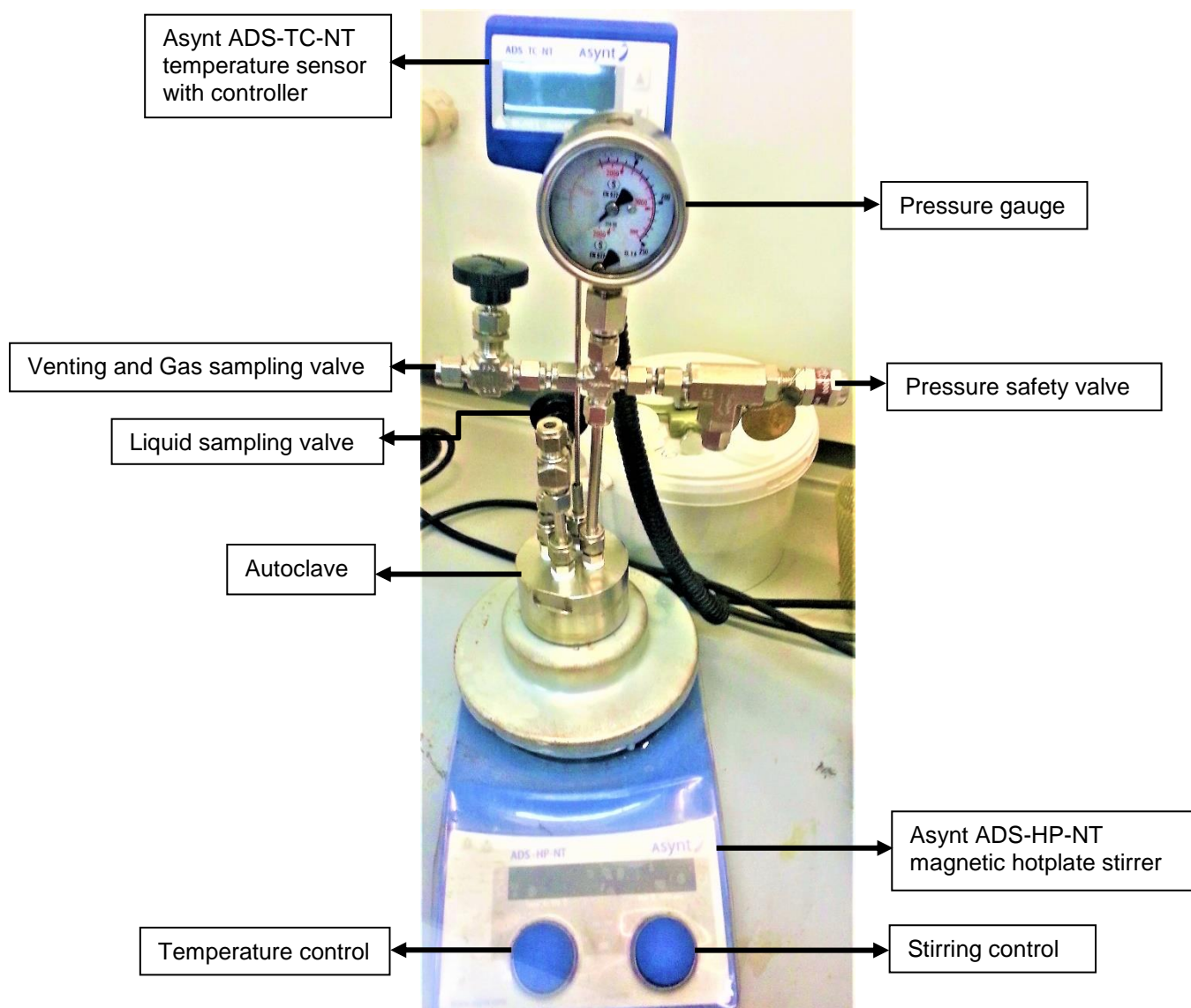


Figure 4.2 The 50 mL stainless steel autoclave used for the bio-oil-alcohol reactions.

4.2.3. Product analysis and characterisation

The mass balance was calculated by the difference in the weight of the autoclave body before and after the reaction. The solid products readily settled at the bottom of the autoclave. The liquid product was collected with a pipette and transferred into a glass sample vial. The solid product in the autoclave with the magnetic stirrer was weighed and the total solid product was calculated by subtracting the weight of the autoclave and the magnetic stirrer. The liquid product was determined by the difference between the total product (liquid + solid) and the solid product. The yields of the liquid product, solid residue, and gaseous products were calculated using Equation 4.1 Equation 4.2 and Equation 4.3 [76].

The product yields were calculated using the following equations.

Equation 4.1 Liquid yield

$$\text{Liquid yield (wt.\%)} = \frac{\text{Liquid product (g)}}{\text{Bio-oil (g) + Solvent (g)}} \times 100 \%$$

Equation 4.2 Solid yield

$$\text{Solid yield (wt.\%)} = \frac{\text{Solid product (g)}}{\text{Bio-oil (g) + Solvent (g)}} \times 100 \%$$

Equation 4.3 Gas yield

$$\text{Gas yield (wt.\%)} = 100 \% - [(\text{Liquid yield (wt.\%)} + \text{Solid yield (wt.\%)})]$$

By measuring the water content, pH and heating value of the original bio-oil, the bio-oil blends and the liquid reaction products a comparison can be made to discuss the effects of blending and supercritical alcohol reactions on bio-oil. Additionally, characterisation techniques such as GCMS, ¹³C NMR and FTIR provide insight into the changes in chemical compounds in the bio-oil samples.

The moisture content of the pyrolysis oil and the distillate products was determined using Karl Fischer titration. The titration was performed using a Mettler Toledo V20 Volumetric Karl Fischer Titrator Solvent: 34817 Fluka Hydranal™ and Working Medium K Reagent: 34816 Fluka Hydranal™ - Composite 5 K. The acidity of the samples was measured using a Hanna instruments pH tester. The higher heating value (HHV) was measured using an IKA C 1 static jacket oxygen bomb calorimeter.

The composition of the bio-oil and treated bio-oils was analysed using a Varian 450 gas chromatograph, and a Varian 220 mass spectrometer. A Column Elite-1701 was used to separate the components (30 m, 0.25 mm internal diameter, 0.25 μm film thickness, 14% cyanopropylphenyl/86% dimethyl polysiloxane stationary phase). Before GCMS analysis, each sample was first mixed with high performance liquid chromatography (HPLC) grade acetone at a sample: acetone ratio 1:3. Then, this sample/acetone was filtered with a 0.2 μm polytetrafluoroethylene (PTFE) filter using a syringe. For each analysis, 0.5 μL of sample was injected into the GC column, and the injection port was 250 °C. Helium was used as the carrier gas, with a 1:20 split ratio (sample to helium). The GC oven was held at 45 °C for 2.5 min, then heated at 5 °C min⁻¹ to 260 °C, and held at this temperature for 7.5 min. The flame ionisation detector (FID) was kept at a temperature of 50 °C. The mass spectra were obtained for a range of 45–300 (m/z). Peak assignments were performed on the mass spectra using the NIST05 MS library and from assignments found in the literature.

¹³C NMR characterization of bio-oil was recorded in dimethyl sulfoxide DMSO-d₆ (Cambridge Isotope Laboratories, DLM-10TB) solution (25% wt/wt) in a 5 mm NMR tube (Wilmad, 528 PP-

7) using a Bruker Advance 300 MHz NMR spectrometer. The ^{13}C NMR spectrum was obtained by powergated decoupling pulse sequence (zgpg), 90° pulse angle, 3 s pulse delay time, and a total of 12288 scans at 25°C . The spectra phase, baseline correction, and integration were conducted with Topspin software 3.5.

A Perkin Elmer Pyris 1 thermogravimetric analyser was used to carry out thermogravimetric analysis (TGA) of the crude and treated bio-oils. TGA was carried out over the range $25\text{-}750^\circ\text{C}$ at a heating rate of $10^\circ\text{C min}^{-1}$ under a nitrogen flow rate of 2 mL min^{-1} .

Elemental analysis to determine the carbon, hydrogen, nitrogen, sulphur, oxygen (CHNSO) contents of the bio-oil and treated bio-oils was conducted using a Thermo Fisher Scientific Flash 2000 CHNS-O Organic Elemental Analyzer, where the oxygen content was calculated by difference. The H_2O content from the Karl Fisher moisture content analysis was used to present the C H N S of the treated samples on a dry basis i.e. water-free basis.

The functional groups of the bio-oil and the treated bio-oils were characterised using a Perkin Elmer Frontier FTIR spectrometer. A spectral range of $400\text{ to }4000\text{ cm}^{-1}$ was used and 16 scans were applied to each sample. Prior to all analysis, a background scan was carried out under ambient atmosphere.

4.3. Results and Discussions

4.3.1. Reproducibility

To determine the reproducibility of the mass balance and product yields, the bio-oil reactions with methanol, ethanol and isopropanol was repeated. The same experimental procedure was followed as described in the Materials and Method section 4.2.2. The comparable liquid yield and total solid and gas yield is displayed in Table 4.1. The liquid product yield was calculated using Equation 4.1 described in section 4.2.3. The total solid and gas yield was calculated as follows:

$$\text{Total Solid and Gas yield (wt.\%)} = (\text{Feed (g)} - \text{Liquid Product (g)}) / \text{Feed (g)} \times 100 \%$$

Table 4.1 Analysis of mass balance reproducibility

Solvent	Liquid yield wt.%		^a Total Solid and Gas yield wt.%		Mean \pm standard deviation
	Run 1	Run 2	Run 1	Run 2	
Methanol	59.68	68.53	40.32	31.47	6.26
Ethanol	82.84	81.15	17.16	18.85	1.20
Isopropanol	86.23	88.79	13.77	11.21	1.81

^aTotal solid and gas yield was calculated by difference assuming no losses.

Table 4.1. illustrates that both experimental runs achieved very similar liquid, gas and solid yields. The methanol reaction repeatedly produced the lowest liquid yield and highest solid

and gas yield. The ethanol reactions generated highly comparable yields and the mean standard deviation was only ± 1.20 . In both runs, the isopropanol reaction produced the highest liquid yield and lowest solid and gas yield.

4.3.2. Product yields

The total liquid and solid obtained was 80.90 %, 90.75 %, and 91.37 % after bio-oil methanol, ethanol and isopropanol reactions, respectively (Table 4.2). All the liquid products were visibly less viscous than the crude bio-oil, and no significant change in colour was observed after reacting the bio-oil with the alcohols. Apart from the water contained in the crude bio-oil, water can also originate from esterification reactions, re-polymerization of oligomers, hydrodeoxygenation, and hydrocracking of the solvents during the upgrading process [76].

Table 4.2 Mass balance of bio-oil reactions

Mass balance (% mass fraction with respect to the original feed amount) of the products of bio-oil reactions with methanol, ethanol and isopropanol, respectively. (270 °C, 100 bar, 2 h).

Solvent	Liquid yield wt. %			Total Solid yield wt. %	Total Gas yield ^(a) wt. %
	Total Liquid Yield	Water-free Liquid yield	Water yield ^b		
Methanol	59.68	41.91	17.77	21.22	19.10
Ethanol	82.84	63.48	19.36	7.91	9.25
Isopropanol	86.23	69.96	16.27	5.14	8.63

^a Gas yield was calculated by difference assuming no losses. ^b Water yield was calculated using the water content measured in Table 4.3

Compared to ethanol (C₂H₅OH) and isopropanol (C₃H₈O), the hydroxyl concentration is the highest with methanol (CH₃OH) and its molecular structure enables higher activity [23]. The hydrocarbon contribution is the highest with isopropanol and the longer alkyl chain could dissolve higher molecular weight products, which leads to relatively lower solid products [23]. This functional group contribution change affects the reactivity of the solvents and leads to differences in the mass balance of each reaction. These findings also correspond with the CHNS results (Table 4.3) which showed methanol treated bio-oil had the highest oxygen content, lowest carbon and hydrogen content while isopropanol treated bio-oil had the lowest oxygen content, highest carbon and hydrogen content. Prajitno et al. also reported higher oil and lower coke yield after supercritical ethanol reaction compared to supercritical methanol [19].

Coke, commonly reported as an undesired by-product in bio-oil hydrocracking and hydrotreatment processes, is generally derived from the re-polymerization and over-dehydration of oligomers [76]. Table 4.2 shows methanol reacted bio-oil (BM2) generated the highest solid yield, this is reflected in the CHNS and TGA results and is further discussed in section 4.3.3 Physicochemical properties of bio-oil and treated bio-oils. Shafaghat et al. also

found relatively higher char/coke yield after reacting bio-oil with supercritical methanol compared to supercritical ethanol [77].

Gaseous products can be formed from various reactions during the bio-oil upgrading process namely; cracking, decarboxylation, decarbonylation, methanation, and hydrodenitrogenation [78]. Table 4.2 indicates the bio-oil methanol reaction generated lower total liquid and solid product yield compared to the ethanol and isopropanol. This indicates higher gas yield was obtained after the methanol reaction and more of the bio-oil-methanol was decomposed into gas products than bio-oil-ethanol or bio-oil-isopropanol. This suggests methanol had a higher tendency, than ethanol or isopropanol, to promote cracking of the higher-molecular-weight bio-oil fractions and gas formation reactions during the upgrading process. The increase in methanol activity may have led to higher mass losses due to the increased volatility of the product. In addition, self-decomposition of the alcohols in their supercritical state may contribute to some fractions of the gas products [59].

4.3.3. Physicochemical properties of bio-oil and treated bio-oils

Table 4.3 summarises the results from the water content, heating value, pH and CHNS analysis. The water content was reduced after blending the bio-oil with methanol, ethanol, and isopropanol. This decrease in the water content of bio-oil after blending with an alcohol solvent was previously observed by Yu et al. [72] Pidtasang et al. reported that the water reduction is due to the dilution effect of the anhydrous alcohols [68]. After the supercritical alcohol reactions, BM2 exhibited the highest water content. This is due to esterification reactions of methanol and acids in the bio-oil occurred and generated water as a product [21,68,79]. Another reason for the increased water content after the supercritical methanol reaction compared to the methanol blend may be linked to the high gas yield after the methanol reaction (Table 4.2). As methanol and volatile products are decomposed to gas, the resulting liquid product obtains an increased concentration of water. On the other hand, lower gas yield (compared to methanol) after the bio-oil-isopropanol reactions indicates isopropanol did not decompose to gas and the water content does not significantly increase. Reducing the moisture in the bio-oil is crucial as it can lead to increased ignition delay and decreased combustion rate in an engine [56]. On the other hand, water in bio-oil is beneficial as it reduces the viscosity [72].

Table 4.3 Physicochemical properties of liquid products of bio-oil reactions with methanol, ethanol and isopropanol.

Properties	Bio-oil alcohol blends ^a			Bio-oil alcohol reaction liquid products ^a			Bio-oil
	BM1	BE1	BI1	BM2	BE2	BI2	
H ₂ O wt.%	13.42 (0.9) ^b	12.27 (0.3)	11.90 (0.7)	29.78 (0.3)	23.37 (0.2)	18.87 (0.4)	31.69 (0.3)
pH	3.67	3.54	3.06	4.04	3.84	3.80	2.39
C wt.% ^c	48.13 (0.5)	55.16 (0.0)	58.28 (0.0)	46.05 (1.3)	58.76 (0.3)	61.91 (0.3)	49.26 (0.4)
H wt.% ^c	9.52 (0.1)	10.06 (0.1)	10.35 (0.1)	9.60 (0.4)	10.52 (0.1)	10.36 (0.1)	7.91 (0.0)
N wt.% ^c	0.20 (0.0)	0.18 (0.0)	0.17 (0.0)	0.71 (0.0)	0.18 (0.0)	0.19 (0.0)	0.20 (0.0)
O wt.% ^{c, d}	42.16 (0.6)	34.60 (0.1)	31.20 (0.0)	43.63 (1.7)	30.53 (0.4)	27.54 (0.2)	42.63 (0.4)
HHV MJ/kg ^e	21.56 (0.9)	25.60 (0.2)	27.55 (0.0)	23.03 (1.1)	27.55 (0.2)	28.85 (0.1)	17.51 (0.1)

^a BM1, BE1, BI1 refers to bio-oil- methanol, bio-oil-ethanol and bio-oil-isopropanol blends; BM2, BE2, BI2 refers to bio-oil- methanol, bio-oil-ethanol and bio-oil-isopropanol reaction products; ^b Mean \pm standard deviation; ^c CHNO water-free basis for the blends and reaction products; ^d Oxygen content calculated by difference; ^e HHV dry basis for the blends and reaction products HHV dry basis = HHV_{wet} / (1-H₂O/100). ^f S contents are zero in all samples.

After the methanol, ethanol and isopropanol reactions a modest increase in pH was observed (Table 4.3). This correlates with the GCMS results (Table 4.4) which showed a decrease in acidic compounds in the bio-oil after the reactions compared to the blends and the untreated bio-oil. The elemental analysis gives the weight per cent of C, H, N, and S in the sample. The oxygen content was calculated by difference. The CHNS results in Table 4.3 show the C content slightly decreased while the O content increased after the methanol reaction compared to the bio-oil methanol blend. This may be linked to the high solid and gas yield after the supercritical methanol reaction which led to C and H loss and subsequent increased proportion of O. Carbon may be lost as solid and gas due to polymerisation reactions and decarboxylation, decarbonylation, methanation reactions, respectively [78]. This indicates the supercritical reaction is more reactive with methanol solvent than ethanol or isopropanol. Similarly, the mass balance results (Table 4.2) showed the highest solid yield was obtained after bio-oil-methanol reactions, hence heavy components from polymerisation reactions were collected as solid residue leaving a liquid product with lighter volatile compounds [19].

The heating value of the crude bio-oil was 17.51 MJ kg⁻¹. Increasing the heating value of the crude bio-oil is essential for improving its combustion efficiency in engines [56]. Table 4.3 shows minimal changes in the heating value after the reactions compared to the respective blends. Hence, in this work the reaction provides insufficient improvements for the heating

value compared to blending. The heating values of the blends and the reaction products increased according to the heating value of the added solvent, i.e. methanol<ethanol<isopropanol. Isopropanol treated bio-oil had the highest heating value because isopropanol has higher heating value than methanol and ethanol. An increase in C and H and reduction in O leads to higher energy density [26]. This is confirmed in this study where isopropanol treated bio-oil exhibited the highest C and H and lowest O content as well as the highest heating value (28.85 MJ kg⁻¹). The heating values after the reactions (23.03 MJ kg⁻¹ BM2; 27.55 MJ kg⁻¹ BE2; 28.85 MJ kg⁻¹ BI2) are comparably low compared to crude oil (45.54 MJ kg⁻¹) or conventional gasoline (46.54 MJ kg⁻¹) [80]. Nevertheless, the improvements in the heating value compared to the crude bio-oil indicates solvents addition is a simple and effective means for improving bio-oil properties.

4.3.4. Characterisation of bio-oil and treated bio-oils

4.3.4.1. GC-MS analysis

Gas chromatography mass spectrometry (GC-MS) was used to identify and quantify many of the molecular compounds present in the crude bio-oil, and the treated bio-oils. In order to examine the product distribution in the different samples, the chemicals identified in the GCMS were classified into eight groups (acids, phenols, esters, ketones, alcohols/ethers, aldehydes, sugar derivatives, and hydrocarbons) based on their functional groups. Table 4.4 provides a summary of the relative amounts of compound classes in the crude bio-oil and the treated bio-oils. Detailed composition including the compounds in each group is included as a supplementary material in Appendix 1. GCMS results of bio-oil blending and reactions. The total relative area % of each group was obtained by adding the area % of each compound in each category. The chromatographic peak area % of a compound is considered linear with its concentration. Therefore, the corresponding chromatographic peak area % of the compounds can be compared. For example, the peak area % of acetic acid after each reaction can be compared to examine the effects of the supercritical alcohols. Additionally, the peak area % can be used to compare the change of the relative content of the compound among the detected compounds [43,56].

Phenolic compounds, which can be produced from the degradation of lignin [59], exhibited the highest total area % (37.0 %) in the raw bio-oil with compounds such as 2-methoxy-4-methylphenol and 2-methoxy-4-(1-propenyl)-phenol, contributing to the high area %. Although the percentage of peak area does not represent the actual content of the compound, it is a strong indication that the crude bio-oil contains a large amount of phenolic compounds. The presence of the phenolic compounds in the crude bio-oil and after the reactions is consistent with the results reported by other researchers [19,22,51,59].

Table 4.4. Distribution of chemical composition in bio-oil samples.

Detailed composition including the compounds in each group is included as a supplementary material in Appendix 1. GCMS results of bio-oil blending and reactions.

Compound	Total relative content area %						
	Bio-oil	BM1	BM2	BE1	BE2	BI1	BI2
Acids	4.63	4.33	0.00	4.66	3.92	5.79	4.78
Phenols	37.03	27.85	32.73	28.49	28.76	31.12	38.04
Esters	3.74	3.41	29.89	2.76	27.68	3.66	22.35
Ketones	17.40	12.99	13.12	13.22	11.42	13.64	15.33
Alcohols/Ethers	9.62	23.60	10.75	22.54	14.31	13.57	4.75
Aldehydes	8.57	6.01	0.00	7.23	0.00	7.12	0.00
Sugar Derivatives	6.83	7.19	0.00	7.94	0.00	9.01	0.00
Hydrocarbons	0.00	0.00	0.30	0.00	0.00	0.00	0.00
Others	12.22	14.61	13.24	13.19	13.89	16.10	14.73

After reacting the bio-oil with the various solvents, the number of identified esters and the relative area % of esters significantly increased relative to the crude bio-oil and the blends. Compared to acids, esters are more favoured in the fuel composition due to their reduced corrosive effect on the engine surface [77]. Esters could be produced from the esterification reaction between acids in the bio-oil and the corresponding alcohols (methyl/ethyl/isopropyl esters after bio-oil methanol/ethanol/isopropanol reactions, respectively). Further esters can form during reactions between the alcohol solvents and acids derived from the intermediate products from the conversion of oxygenated compounds during the process [22,23]. Udomsap et al. reported that solvents such as methanol and ethanol could terminate the chain of oligomers when added to crude bio-oil and break polymer chains to lower molecular weight compounds [74]. For example, the transesterification of polymeric esters with alcohol to form lower molecular weight methyl or ethyl esters. The GCMS results in this report confirms this phenomenon. The product distribution of esters changed after reacting the bio-oil with each alcohol solvent. For example, Propanoic acid methyl ester, Propanoic acid ethyl ester, and Propanoic acid 1-methylethyl ester was detected after reacting the bio-oil with methanol, ethanol and isopropanol, respectively. These findings indicate supercritical methanol, ethanol and isopropanol can promote ester formation during bio-oil reactions without catalyst addition.

A corresponding decrease in acids was observed after the reactions which resulted in higher pH compared to the bio-oil-alcohol blends (Table 4.3). Ester formation could be the major deacidification mechanism for reducing the acidity of the bio-oil and improving its pH value. The bio-oil-methanol reaction generated the lowest acid content, this agrees with the pH

results which showed methanol treated bio-oil exhibited the highest pH (4.04) compared to ethanol (3.84) or isopropanol (3.80). One reason for the lower pH in BI2 may be the higher presence of acids in BI2 compared to BM2 and BE2. The acids in the bio-oil were eliminated after reacting with methanol and decreased by 15.88% and 17.44% with after ethanol and isopropanol reaction compared to their respective blends

Esterification reactions produce water as a by-product, one of the reasons for the increased water content after reacting the bio-oil with methanol may be the higher esterification activity when reacting the bio-oil with methanol [21,23,68,79]. Methanol treated bio-oil exhibited the highest water and ester content (29.78 wt.%; 29.89 area%, respectively), followed by ethanol (23.37 wt.%; 27.68 area% respectively) and isopropanol (18.87 wt.%; 22.35 area% respectively). These findings indicate that the non-catalytic and non-external hydrogen supercritical alcohol process can stabilize the bio-oil by reducing the corrosive acidic components and increasing the desirable compounds such as esters [19,59].

The relative area count of phenolic compounds slightly increased after the reactions compared to the respective blends. Li et al. also found the phenols were difficult to reduce without co-feeding the upgrading reactions with Pt/C and hydrogen [28]. The ^{13}C NMR results (Figure 4.6) also show increased content of aromatic carbons after the bio-oil methanol, bio-oil-isopropanol reactions and most of the aromatics are phenol derivatives [42]. Aromatics and cyclic compounds are less likely to transform compared to light oxygenated compounds due to the stronger C-C bonds involved [24]. Additionally, the increase in methoxy-phenolic compounds after the reactions compared to the blends may be due to the depolymerisation of the lignin fraction in the bio-oil [24,55].

The unsaturated double bonds at the substituted groups of phenols such as 2-methoxy-4-(1-propenyl)-phenol in the crude bio-oil and blends, significantly decreased after the reactions and the phenols with saturated substituted groups such as, 2-methoxy-4-propyl-phenol increased. Similar findings were also reported by Tang et al. who explained the double bonds were reduced by hydrotreating the bio-oil [39]. Moreover, the ^{13}C NMR findings (Figure 4.6) also indicate supercritical alcohol treatment facilitate in the saturation of C=O bonds. A decrease in carbonyl carbon content was observed after the supercritical alcohol reaction compared to the bio-oil-alcohol blends. This suggests the alcohols functioned as hydrogen donors and facilitated in situ hydrogenation of the unsaturated bonds. Another reason for the increase in the proportion of 2-methoxy-4-propyl-phenol after the reactions could be due to conversion of 4-Hydroxy-2-methoxycinnamaldehyde, which was not detected after the reactions [55].

Phenols and aldehydes in bio-oil can lead to thermal instability and can form carbonaceous deposits hence their removal or conversion into more stable compounds is favourable [28,50]. Aldehydes such as 5-hydroxymethyl-2-furancarboxaldehyde (HMF) which are prevalent in the

crude bio-oil and the blends are not detected after the reactions. 2,5-dimethylfuran (DMF) was detected in BM2, BE2, and BI2 although it was not present in the crude bio-oil and blends. Several researchers have examined the production of DMF by hydrogenolysis of biomass derived hydroxymethylfurfural [81–83]. DMF has received significant attention as a potential renewable liquid transportation fuel due to its favourable physical properties including high energy density (30 MJ L^{-1}), high research octane number (RON = 119), and low volatility (boiling point range $92\text{--}94 \text{ }^\circ\text{C}$) [82]. These values correspond to that of gasoline (34 MJ L^{-1} , RON = 89–96 and $96.3 \text{ }^\circ\text{C}$ boiling point) [82]. Additionally, unlike ethanol, the low solubility of DMF in water (2.3 g L^{-1}) enables its use as a fuel blend [82]. Interestingly, after bio-oil-ethanol reactions, 2-ethyl-5-methyl-furan is detected and after bio-oil-isopropanol reactions, 2-methyl-furan is detected. Supercritical methanol may also transform furfural to 1,2-butanediol by hydrogenation and hydrolysis. This indicates the different effects of the solvents on the bio-oil.

The ketones were relatively unchanged by the varying alcohols in the blends and the reaction products and remained between 11–13 area % except after the isopropanol reaction. A slightly higher total relative area count of ketones was observed after the bio-oil-isopropanol reaction (15.33 area %). The increase in ketones could be due to cracking and transformations from carbohydrates in the bio-oil [21]. This indicates compared to aldehydes, reducing or converting ketones was more difficult.

4.3.4.2. FT-IR analysis

Fourier-transform infrared spectroscopy (FTIR) enables identification of the molecules present in a sample and was used to gain insight into the class of compounds present in the crude bio-oil and the treated bio-oils. Table 4.5 shows the chemical compounds that can be found in the crude bio-oil, blends, and treated bio-oil at various frequency ranges. Figure 4.3, Figure 4.4, Figure 4.5 show the FTIR spectra of the crude bio-oil, and the alcohol treated bio-oils. The IR absorption bands were assigned based on literature [36]. The relative differences between the band heights correlate with the relative differences in the concentrations of the corresponding functional groups between the samples [45].

Table 4.5 Classes of compounds identified in the bio-oil and treated bio-oils using FTIR analysis.

Frequency range 1/cm	Frequency range 1/cm							Group	Class of Compound
	Bio-oil	BM1	BM2	BE1	BE2	BI1	BI2		
3500-3200	3367	3357	3346	3359	3360	3359	3360	O-H stretching	Phenols, polymeric O-H, water impurities
3200-2800	2927, 2853	2929, 2840	2946, 2837	2974, 2929	2975, 2930	2971, 2932	2972, 2934	C-H stretching	Alkanes – methyl group
1750-1650	1709,	1710	1703	1710	1703	1711	1707, 1651	C=O stretching	Ketones, aldehydes,
1650-1590	1648	1603	1610	1603	1603	1605		C=C stretching alkene	C-C multiple bond stretching
~1600-1450	1515	1515	1515	1515	1515	1515	1515	C=C stretching aromatic	
1470-1350	1450, 1363	1449, 1361	1449, 1377	1448, 1378	1452, 1378,	1465, 1380,	1466, 1380,	C-H deformation	Alkanes – methylene group
1300-950	1268, 1033	1268, 1193, 1031,	1268, 1219, 1114, 1018	1270, 1043	1271, 1086, 1044,	1276, 1160, 1126, 1100, 1051,	1288, 1161, 1127, 1106, 1034	C-O stretching O-H bending	Primary, secondary, tertiary alcohols, phenols
975-525	861, 811,	889, 812,		878, 811,	878,	949, 815,	949, 816,	C-H bending	Mono-, polycyclic, substituted aromatic rings

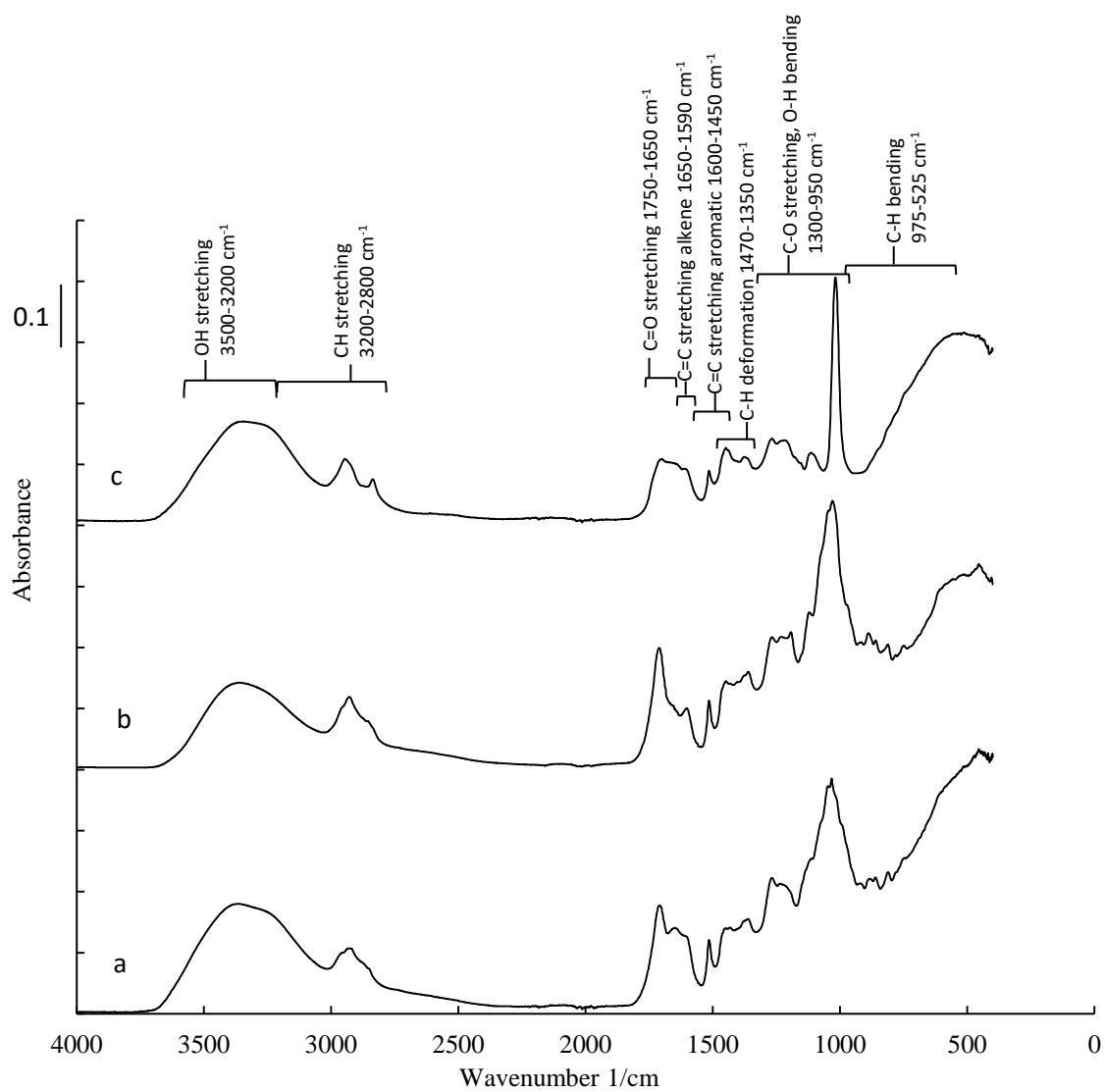


Figure 4.3 FTIR spectra of (a) bio-oil, (b) bio-oil-methanol blend, and (c) bio-oil-methanol reaction products.

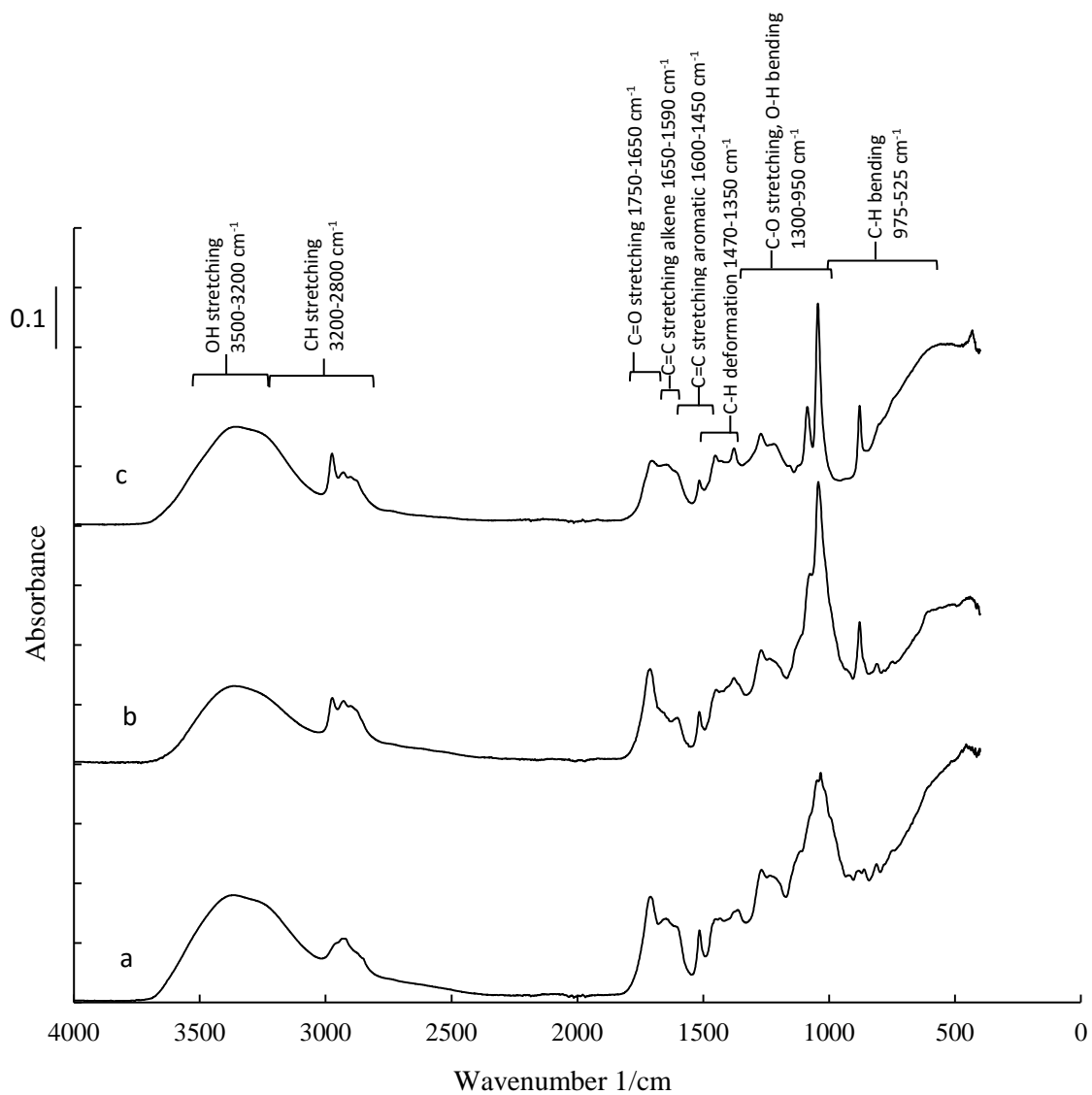


Figure 4.4 FTIR spectra of (a) bio-oil, (b) bio-oil-ethanol blend, and (c) bio-oil-ethanol reaction products.

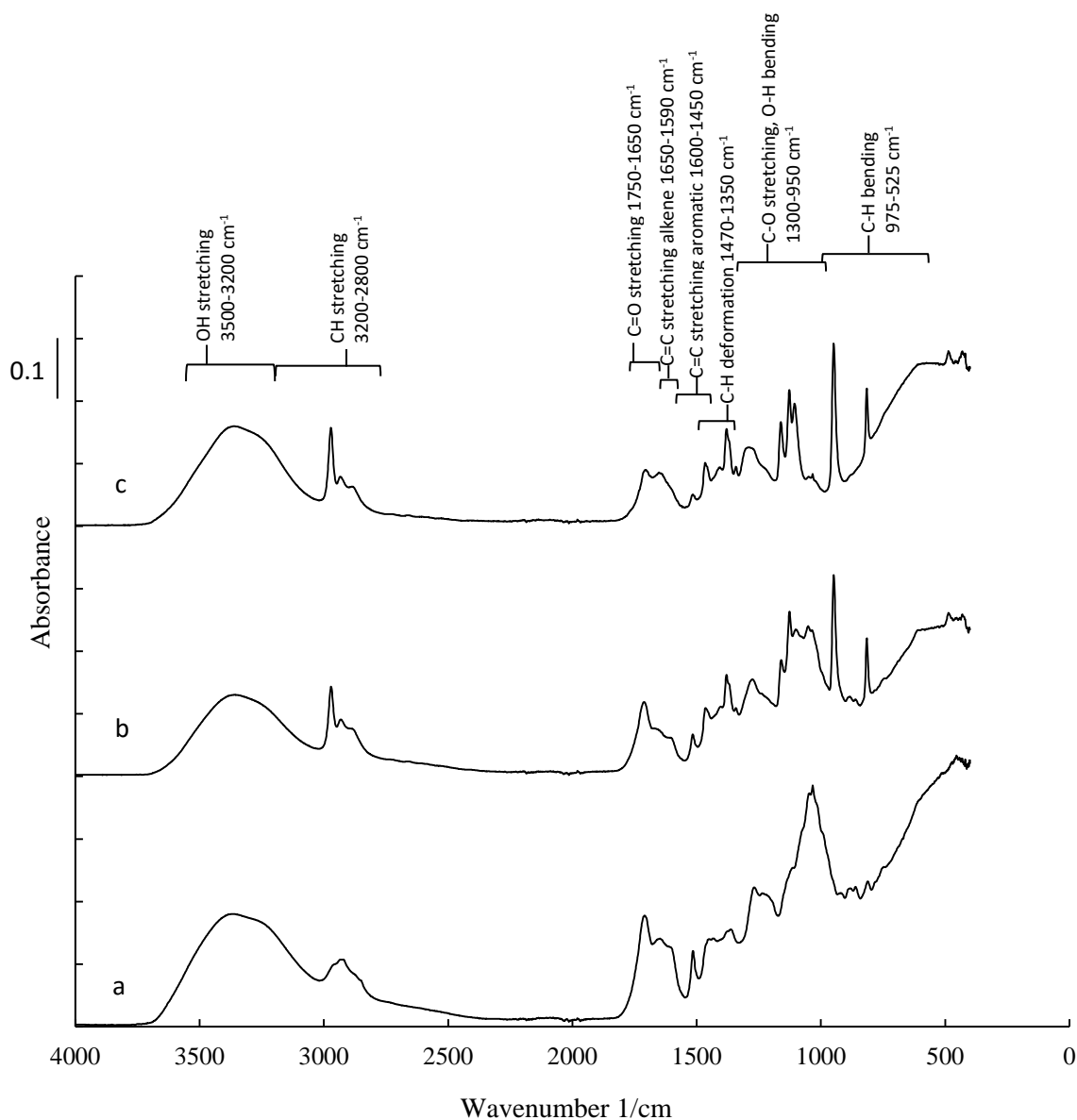


Figure 4.5 FTIR spectra of (a) bio-oil, (b) bio-oil-isopropanol blend, and (c) bio-oil-isopropanol reaction products.

The peaks between $3500\text{-}3200\text{ cm}^{-1}$ were ascribed to O-H stretching vibrations of phenols, polymeric O-H and water impurities. The O-H stretching intensity was increased in BM2, BE2, and BI2, respectively compared to their corresponding blends (i.e. BM1, BE1, BI1). This correlates with the results from the water content analysis which showed an increase in water content after the reactions compared to the blends. Likewise, the GCMS results showed the ester content significantly increased after the reactions indicating esterification reactions occurred which evolves water as a by-product. Additionally, the total relative area % of phenol compounds increased after the reactions compared to the blends, thus, further contributing to the increased intensity in the peaks between $3500\text{-}3200\text{ cm}^{-1}$.

The peaks between 3200-2800 cm^{-1} and 1470-1350 cm^{-1} were caused by C–H stretching in methyl groups and deformation in methylene groups, respectively. These absorption bands increased in intensity from BM2, BE2 to BI2, where the strongest absorbance in these ranges was observed after the bio-oil-isopropanol reactions. This is because isopropanol has two methyl groups, ethanol has a methyl and methylene group, and methanol has a methyl group. This aligns with the GCMS results which showed longer chain esters formed in BI2 such as acetic acid, (1-methylethoxy)-, 1-methylethyl ester, compared to BE2 (acetic acid, ethoxy-, ethyl ester) and BM2 (acetic acid, methoxy-, methyl ester).

The carbonyl stretch C=O appears as an intense band from 1750-1650 cm^{-1} . The supercritical methanol, ethanol, and isopropanol treated bio-oils show a notably decreased absorbance in this wavenumber range compared to the corresponding blends and the original bio-oil. This indicates the supercritical alcohol conditions was effective in transforming carbonyl containing compounds such as carboxylic acids and aldehydes. This confirms the GCMS results which showed a complete removal of aldehydes after the reactions, as well as, elimination of carboxylic acids with methanol treatment and decrease of acids after ethanol and isopropanol treatments. Additionally, the ^{13}C NMR results (Figure 4.6) showed after the supercritical treatment the carbonyl carbons were reduced.

The peak at 1515 cm^{-1} is attributed to C=C aromatic stretching. This peak is prominent in the bio-oil and the blends and decreases after the reactions in BM2, BE2, and BI2. This agrees with the GCMS results which indicated to the decrease in unsaturated double bonds at the substituted groups of phenols such as 2-methoxy-4-(1-propenyl)- phenol and increase in phenols with saturated substituted groups such as, 2-methoxy-4-propyl-phenol.

The frequency range 1300-950 cm^{-1} corresponds to O-H bending and C-O stretching of primary, secondary, tertiary alcohols, and phenols, as well as C-O stretching of ethers. Isopropanol treated bio-oil exhibits a cluster of sharp peaks in this region which is ascribed to the long ester chains and propylated compounds formed after the reaction.

The 975-525 cm^{-1} wavenumber range corresponds to C-H bending from aromatic rings. The spectrums of the bio-oil ethanol blend, and the supercritical ethanol treated bio-oil exhibit a sharp peak at 878 cm^{-1} which comes from the ethanol in the sample. The spectrums of the isopropanol blended, and supercritical isopropanol treated bio-oil shows a sharp peak at 950 cm^{-1} and 815-817 cm^{-1} , which originates from the isopropanol in the sample.

4.3.4.3. ^{13}C NMR analysis

Carbon-13 nuclear magnetic resonance (^{13}C NMR) identifies the specific carbon atoms in a molecule and enables analysis of the carbon distribution in the bio-oil and the bio-oil treated samples. To obtain a complete characterization of the bio-oil and the treated bio-oils, ^{13}C NMR analysis was carried out and summarised in Figure 4.6. The integrated ^{13}C NMR spectra were

separated into five chemical shift ranges and the regions were assigned according to literature [84]: 215–163 ppm (carbonyl carbons), 163–110 ppm (aromatic and C=C carbons), 110–84 ppm (carbohydrate-type carbons), 84–54 ppm (methoxy- or hydroxy-bound carbons), 54–1 ppm (primary, secondary, tertiary, and most quaternary alkyl carbons).

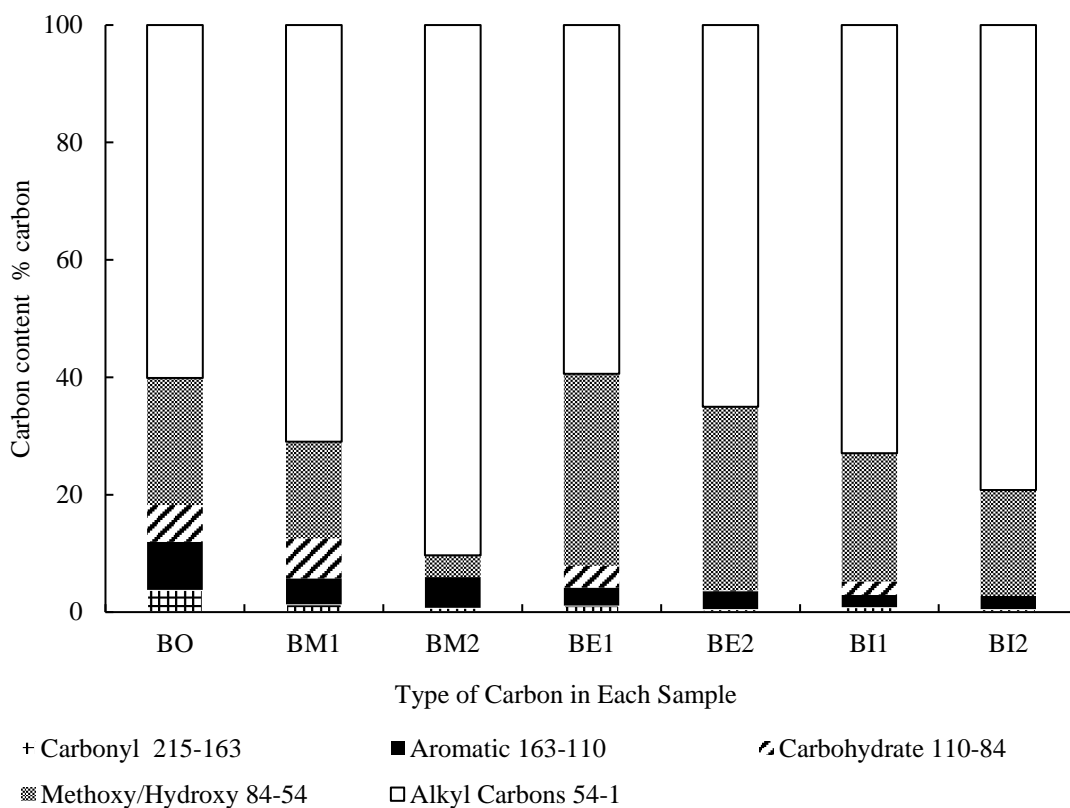


Figure 4.6 Quantitative ^{13}C NMR characterisation of bio-oil and treated bio-oils.

The integration range was selected based on ^{13}C NMR bio-oil characterisation by Meng et al. [84].

The alkyl carbons increased after the reactions relative to the crude bio-oil and the respective blends. This may be due to the dissociation of methyl, ethyl or isopropyl from methanol, ethanol and isopropanol, respectively as a result of the high temperature supercritical conditions.

After the bio-oil methanol reaction, the methoxy/hydroxy carbons decreased, this is in line with the GCMS results where the alcohol and ether contents decreased in BM2 compared to BM1. According to ^{13}C NMR results the methoxy/hydroxy carbons did not significantly change after the bio-oil ethanol reaction, however, the GCMS results show alcohol and ether contents decreased in BE2. The latter is in line with the FTIR findings which showed after the bio-oil-ethanol reaction, the intensity of the peaks in $1300\text{-}950\text{cm}^{-1}$ frequency range (which corresponds to O-H bending and C-O stretching of primary, secondary, tertiary alcohols, as well as C-O stretching of ethers) decreases compared to the bio-oil-ethanol blend and the crude bio-oil. The isopropanol treated bio-oil also demonstrated a decrease in

methoxy/hydroxy carbons as well as alcohol and ether content in the ^{13}C NMR and GCMS results, respectively.

After the reactions, no resonances occurred in the carbohydrate carbon chemical shift ranges 110 to 84 ppm. Likewise, in the GCMS analysis, the sugar derivatives which were present in the crude bio-oil and blends were not detected after the reactions. This may be due to the depolymerisation of these compounds due to the supercritical conditions. Meng et al. reported that under high temperature conditions, the carbohydrates in bio-oil could decompose into various light-oxygenates [84]. Additionally, Li et al. indicated large amount of water from processed high boiling fraction of bio-oil may be linked to the dehydration of sugars [21].

The aromatic carbons in the bio-oils include carbons in phenolic compounds. The GCMS analysis demonstrated that phenolic compounds were less likely to transform during upgrading reactions compared to light oxygenated compounds due to the stronger C-C bonds involved [24]. Likewise, the ^{13}C NMR findings show minimal changes occurred to the aromatic carbon content after the reactions.

After the supercritical treatment the carbonyl carbons were reduced. This is consistent with the GCMS results of BM2, BE2, and BI2 which demonstrated transformations of acids and aldehydes. These findings also correspond to the FTIR results which showed supercritical alcohol treated bio-oil exhibited a decrease in carbonyl stretching compared to the crude bio-oil or bio-oil-alcohol blends.

4.3.4.4. TGA analysis

Thermogravimetric analysis (TGA) provides insight into the changes in the physical and chemical properties of a material as a function of increasing temperatures. The analysis results outlined the relative proportions of light and heavy fractions in bio-oil. Figure 4.7, Figure 4.8, Figure 4.9, compile the thermographic (TG) curves of the crude bio-oil and the methanol, ethanol and isopropanol treated bio-oils. The TG curve of the crude bio-oil shows the evaporation of moisture and highly volatile compounds in the bio-oil occurred between 27.69-337.36 °C which resulted in 69.66 % weight loss. The first decomposition of less volatile compounds in the bio-oil was observed between 384.01-472.85 °C and 5.63% of these compounds were removed. The final bio-oil decomposition region was between 521.98-696.60 °C and 17.83 % of heavy compounds were decomposed.

Figure 4.7 demonstrates the presence of the lighter methylated and methoxylated compounds in supercritical methanol treated bio-oil leads to the formation of a TG curve with faster weight loss rate than crude bio-oil and methanol blended bio-oil which contain relatively heavier compounds. In all three cases (methanol, ethanol and isopropanol) the weight loss rate of the supercritical alcohol treated bio-oils are all faster than that of the original bio-oil. This is due to the volatilization of alcohol, water and other light components [39]. In supercritical methanol

treated bio-oil a second peak can be observed at ~100°C which is not apparent in the bio-oil-methanol blend. This may indicate to the formation of more water after the reaction which corresponds to the FTIR results which showed a higher absorbance in the O-H wavenumber range after supercritical methanol treatment relative to the bio-oil-methanol blend.

The boiling point distribution of the bio-oil and treated bio-oils is illustrated in Table 4.6 and the distillation range was selected based on the reference [85]. Bio-oil treatment with supercritical methanol produced a liquid product with 62.79 % of the material boiling between 35-150 °C, compared to 54.62 % and 50.46 % with supercritical ethanol and isopropanol, respectively. This agrees with the GCMS results which showed the greatest ester content after the bio-oil-methanol reactions. The methylated or methoxylated compounds present in the bio-oil-methanol liquid products are more volatile than the ethanol and isopropanol counterparts. Additionally, the highest water content was observed after the bio-oil-methanol reactions; primarily due to water formed as a by-product of esterification reactions. These factors contribute to the increased volatile light compounds present after the supercritical methanol treatment. The material boiling between 35-150 °C increased in BM2 and BE2 compared to their respective blends (i.e. BM1 and BE1) but decreased after supercritical isopropanol reaction compared to the isopropanol blend. This may be due to the formation of higher boiling longer chain compounds after the isopropanol reaction.

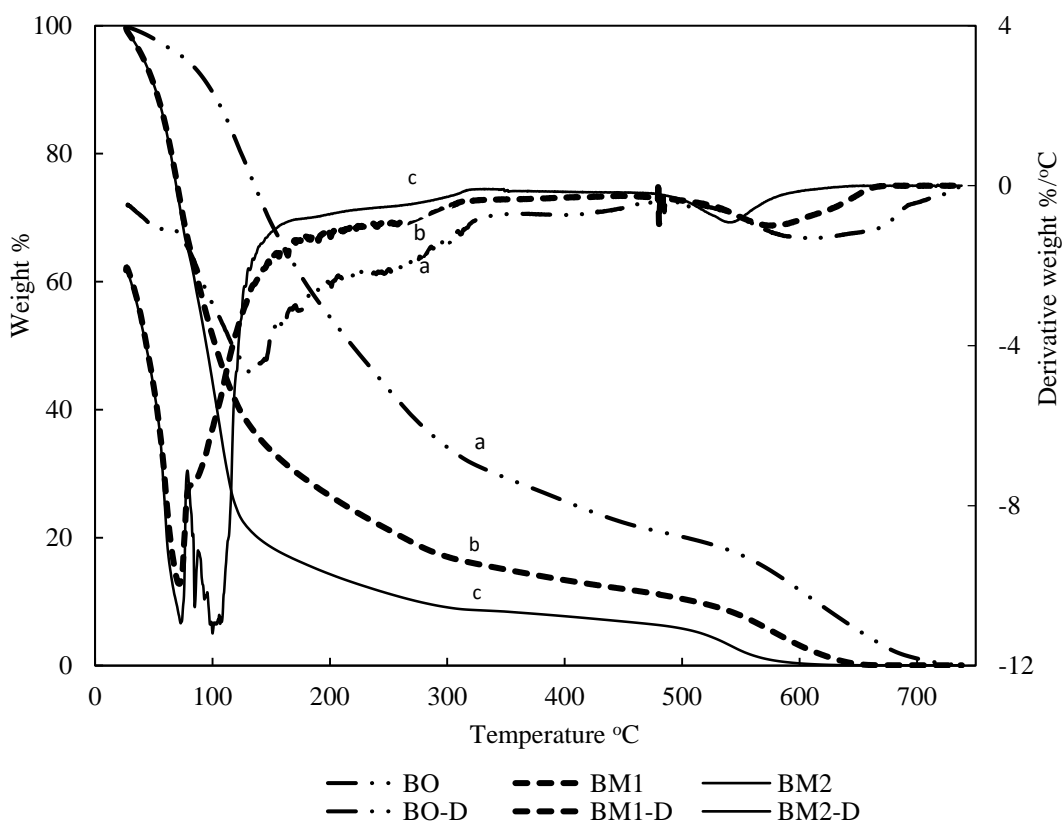


Figure 4.7 TGA and DTG profiles of (a) bio-oil, (b) bio-oil-methanol blend, and (c) bio-oil-methanol reaction products.

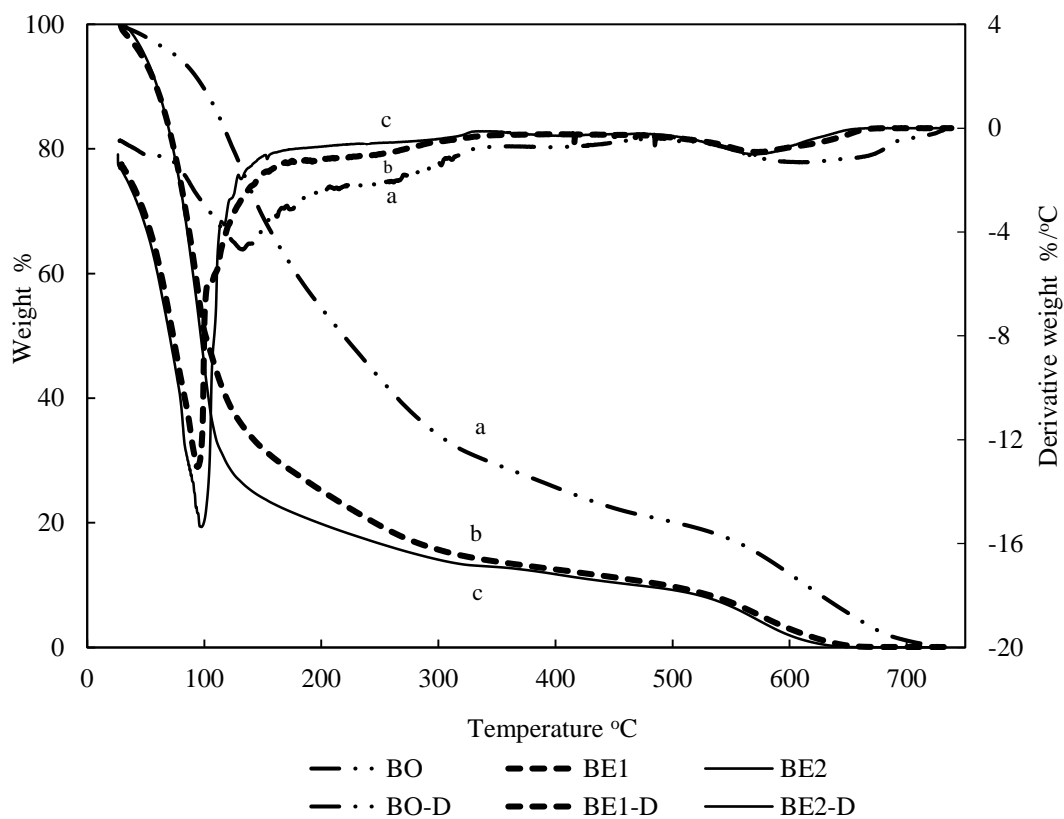


Figure 4.8 TGA and DTG profiles of (a) bio-oil, (b) bio-oil-ethanol blend, and (c) bio-oil-ethanol reaction products.

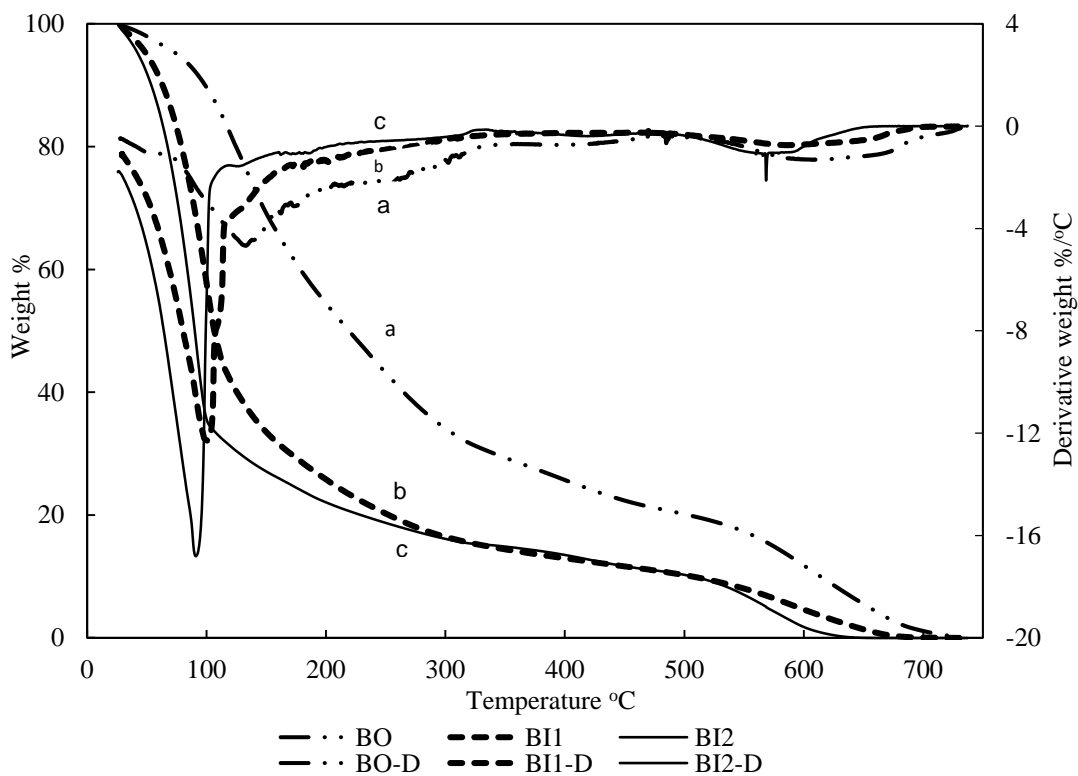


Figure 4.9 TGA and DTG profiles of (a) bio-oil, (b) bio-oil-isopropanol blend, and (c) bio-oil-isopropanol reaction products.

Table 4.6 Boiling point distribution of bio-oil and treated bio-oils.

The distillation range was selected based on [85].

Distillation range °C	Weight %						
	BO	BM1	BM2	BE1	BE2	BI1	BI2
35-150	41.31 (0.5) ^a	50.17 (0.0)	62.79 (0.4)	52.80 (0.1)	54.62 (0.7)	52.50 (0.2)	50.46 (0.2)
150-200	11.79 (0.1)	10.17 (0.0)	7.83 (0.0)	9.77 (0.0)	8.38 (0.2)	9.62 (0.2)	9.14 (0.1)
200-250	9.66 (0.1)	8.33 (0.0)	6.32 (0.0)	7.91 (0.0)	7.22 (0.2)	7.73 (0.2)	7.86 (0.1)
250-300	7.64 (0.1)	6.66 (0.0)	5.03 (0.0)	6.20 (0.1)	6.09 (0.2)	6.14 (0.1)	6.72 (0.1)
300-350	6.29 (0.1)	5.66 (0.0)	4.38 (0.0)	5.28 (0.0)	5.35 (0.1)	5.24 (0.1)	5.99 (0.1)
<350	76.70 (0.9)	80.99 (0.0)	86.36 (0.4)	81.97 (0.0)	81.66 (0.0)	81.24 (0.3)	80.18 (0.2)
350-400	5.50 (0.0)	5.00 (0.0)	4.07 (0.0)	4.70 (0.0)	4.94 (0.2)	4.64 (0.1)	5.53 (0.1)
400-450	4.72 (0.1)	4.42 (0.1)	3.63 (0.0)	4.20 (0.0)	4.38 (0.1)	4.13 (0.1)	4.83 (0.0)
450-500	4.20 (0.1)	3.93 (0.1)	3.17 (0.0)	3.74 (0.0)	3.90 (0.0)	3.67 (0.1)	4.20 (0.0)
>500	8.88 (1.1)	5.66 (0.2)	2.77 (0.4)	5.39 (0.0)	5.13 (0.3)	6.32 (0.6)	5.25 (0.3)

^a Mean ± standard deviation.

4.4. Conclusion

The physical and chemical characteristics and the effects of blending crude bio-oil with methanol, ethanol, and isopropanol were investigated and compared to those of bio-oil treated with supercritical methanol, ethanol, and isopropanol. Additionally, the in situ hydrogenation method was examined for treating the crude bio-oil, rather than using external hydrogen addition.

Bio-oil-supercritical methanol treatment tended towards high solid and gas yields which may be due to its higher reactivity compared to ethanol or isopropanol as indicated by the GCMS findings. GCMS analysis demonstrated that only supercritical methanol treatment eliminated the acids in the bio-oil, consequently, the pH increased from 2.39 in the crude bio-oil to 4.04 after the methanol reaction. This was attributed to the high esterification ability of supercritical methanol based on the significant amount of newly formed esters and the high water by-products from esterification reactions. Due to the high hydrocarbon contribution of isopropanol, after blending, the C and H content increased, and the O content was reduced compared to the crude bio-oil. As a result, the heating value improved from 17.51 MJ kg⁻¹ in the crude bio-oil to 27.55 MJ kg⁻¹ in the bio-oil-isopropanol blend. After the supercritical isopropanol reaction, the heating value of the liquid product further increased to 28.85 MJ kg⁻¹.

The improvements in the heating value compared to the crude bio-oil indicates solvents addition is a simple and effective method for improving bio-oil properties.

In situ hydrogenation proceeded in all the reactions which was confirmed by the GCMS results which showed the transformation of aldehydes such as hydroxymethylfurfural to 2,5-dimethylfuran. ^{13}C NMR and FTIR results also indicated that in situ hydrogenation occurred due to the reduction in carbonyl compounds after the supercritical reactions and an increase in alkyl carbons in the ^{13}C NMR results. Although the bio-oil-alcohol blends improved certain bio-oil properties, (e.g. heating value and pH), the supercritical reactions further enhanced the bio-oil properties by promoting reactions such as esterification and hydrogenation thus further improving the physicochemical properties of the bio-oil. For future work, efficient solvent recovery and reuse is necessary to optimise the process.

5. In situ Catalytic Hydrogenation of Phenol using Raney-Ni Catalyst and Near-Critical Water-Methanol Mixtures

5.1. Introduction

Lignin is an abundant aromatic biopolymer and a vital structural material in plants [86,87]. It contains substituted C₆ phenol and C₉ propyl-phenol units [86]. Pyrolysis of lignocellulosic biomass (e.g. woods, grass, agricultural waste) leads to the production of a bio-oil with a high proportion of phenolic compounds due to the decomposition of lignin in the lignocellulosic biomass [64]. The analysis of a sample of raw bio-oil from a softwood feedstock in chapter 4 section 4.3.4.1 GC-MS analysis, showed that it contained 37.03 % of phenols. Minimal changes to the bio-oil phenol content was found after blending and supercritical reactions. Moreover, it was found that the phenols were less likely to transform compared to light oxygenated compounds due to the stronger C-C bonds involved [24].

The hydroxyl group in phenol is very acidic. Therefore, the hydrogen is detachable and as a result phenol can behave like an acid. The presence of an aromatic acid, such as phenol, in bio-oil is less desirable than a conventional alcohol. Weak alcohols are undissociated, e.g. hexanol whereas strong alcohols e.g. phenol are more dissociated. The dissociation of phenol increases the concentration of hydrogen ions and makes the bio-oil more acidic. As a result, phenol can be highly reactive in bio-oil [64].

In practical terms, phenols are undesirable in bio-oil because the high oxygen content causes unfavourable properties such as low energy density, instability, high viscosity, corrosion, and tendency to polymerize [5]. Moreover, the presence of phenolic compounds is reported as the main cause for coke formation and catalyst deactivation [5]. However, the deoxygenation of phenol by cleavage of its C-O bond is difficult and is typically performed after hydrogenation of phenol. This is because the bond energy of the OH group attached to the aromatic carbon on phenol (Ar-OH) is very high. As shown in Table 5.1, Ar-OH has the highest bond energy compared to R-OR (aliphatic ether), R-OH (alcohols) and Ar-OR (aryl ethers) [64]. Therefore, firstly hydrogenating phenol to cyclohexanol thereby converting the Ar-OH bond to an R-OH bond enables enhanced deoxygenation. Because less energy is required to cleave the R-O bond than the Ar-O bond.

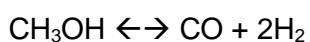
Table 5.1 Bond Dissociation Energies [64]

Bond	Dissociation energy (kJ/mol)
R-OR	339
R-OH	385
Ar-OR	422
Ar-OH	468

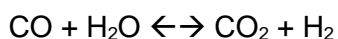
Conventional liquid-phase catalytic hydrogenation involves using hydrogen-transfer or hydrogen gas to achieve hydrogenation [88]. The costly hydrogen requirements of the conventional hydrogenation processes can be avoided by using an in-situ catalytic hydrogenation technique. This system involves aqueous phase reforming of oxygenated hydrocarbons (e.g. methanol) to generate hydrogen molecules which are in situ used for hydrogenation of an organic compound. This process has several advantages including the increased selectivity to the desired product during hydrogenation of the organic compound [88].

The reforming of methanol (Equation 5.1) produces CO as an intermediate product which is converted to CO₂ by a water-gas-shift reaction (Equation 5.2). The overall reaction (Equation 5.3) is referred to as aqueous phase reforming (APR) [62].

Equation 5.1 Methanol reforming



Equation 5.2 Water-gas shift reaction

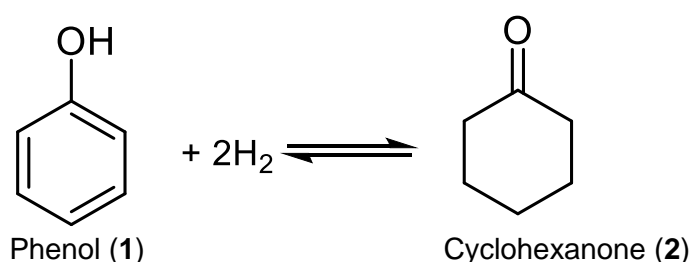


Equation 5.3 Aqueous phase reforming

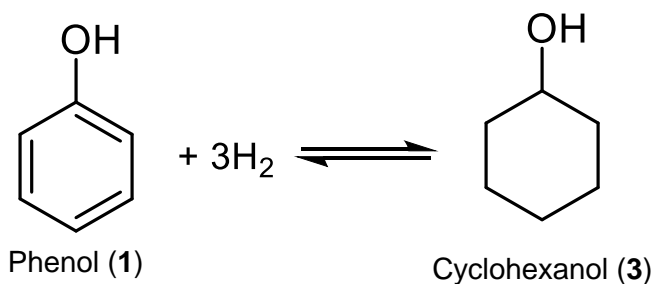


The hydrogenation of phenol (1) to cyclohexanone (2) and cyclohexanol (3) takes place according to the following reactions [88]:

Equation 5.4 The hydrogenation of phenol (1) to cyclohexanone (2)

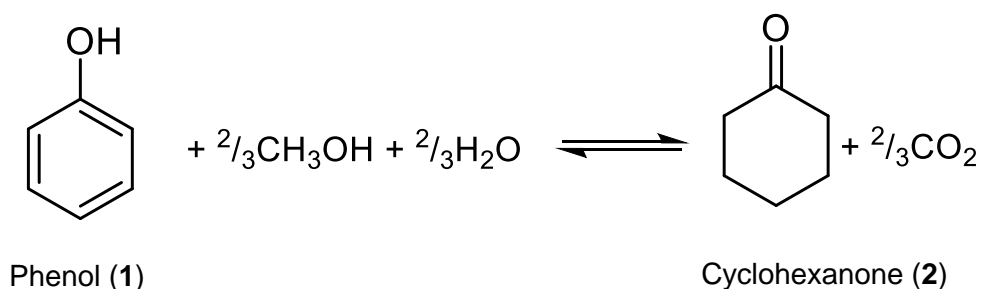


Equation 5.5 The hydrogenation of phenol (1) to cyclohexanol (3)

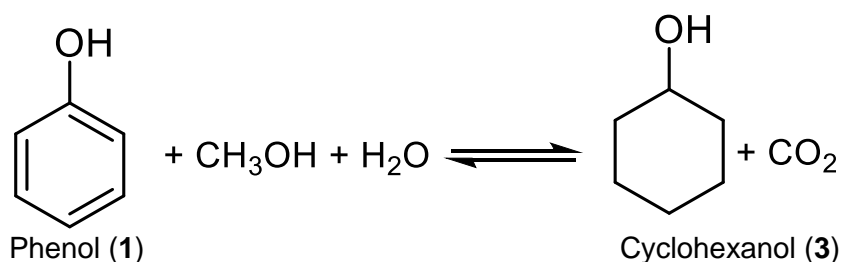


Hence, the combination of the aqueous phase reforming of methanol for hydrogen production and in-situ hydrogenation of phenol to cyclohexanone and cyclohexanol can be demonstrated by the following reactions [88]:

Equation 5.6 Aqueous phase reforming of methanol and hydrogenation of phenol to cyclohexanone



Equation 5.7 Aqueous phase reforming of methanol and hydrogenation of phenol to cyclohexanol



In Chapter 4, methanol proved to be the best solvent for generating a bio-oil with improved properties. Additionally, studies have shown methanol as a good hydrogen donor for in situ hydrogenation of phenol [89]. Catalysts with good hydrogenation activity are ideal for the hydrogenation of phenol and noble metal catalysts such as Pd and Pt have been researched [64]. However, one study found a higher catalytic performance of Raney Ni on aqueous phase reforming of methanol and hydrogenation of phenols compared to noble metal catalysts such as Pt/Al₂O₃, Pd/Al₂O₃ and Pd/C [90]. Raney Ni has been recognised as effective for both aqueous phase reforming of methanol and hydrogenation of phenol [90]. Moreover, Raney Ni

is a highly active metal catalyst industrially used for hydrodeoxygenation of bio-derived phenols [15,41,91]. Therefore, methanol and Raney-Ni were used as solvent and catalyst in this work, respectively.

This chapter continues on the work of Chapter 4 which showed phenols did not transform after blending with alcohols or after non-catalytic supercritical upgrading. This work aims to convert and study phenol alone; in order to clearly follow its reaction pathway without the presence of the complex mixture in crude bio-oil. Secondly, the work aims to utilise Raney-Ni to catalyse the aqueous phase reforming of methanol and in situ hydrogenation of phenol. The effects of varying reaction temperature, time, catalyst loading and starting material ratio on the conversion of phenol will also be investigated.

5.2. Materials and Method

5.2.1. Materials

Phenol (white solid crystals at room temperature) was obtained from Sigma-Aldrich. Cyclohexanol and Cyclohexanone were purchased from Fisher Scientific. Raney 2800 Nickel active catalyst (slurry at room temperature) was also obtained from Sigma-Aldrich. Methanol from VWR Chemicals was used as a co-solvent with deionised water. All the chemicals in the study are commercially available and used without purification.

5.2.2. Experimental procedure

In a typical experiment, phenol, deionised water, methanol and Raney-Ni catalyst were transferred to a 70 mL high-pressure stainless steel autoclave along with a magnetic stirrer which was set to rotate at 1500 rpm. Then the autoclave was sealed and placed on a magnetic stirring heating mantle and a temperature sensor was inserted. The starting material amounts and reaction operating parameters were varied to investigate their effects on the conversion, selectivity and yield of the reaction. The following experiments were performed:

1. Varying catalyst loading (0.2 g, 0.4 g, 0.6 g, 0.8 g and 1.0 g) at constant deionised water, methanol and phenol molar ratio of 40:20:1, heating setting temperature of 300 °C, reaction time of 2 h.
2. Varying reaction time (1 h , 2 h, 3 h, 4 h, and 5 h) at constant deionised water, methanol and phenol molar ratio of 40:20:1, heating setting temperature of 300 °C and catalyst loading of 1 g.
3. Varying reaction heating setting temperature (100 °C , 200 °C and 300 °C) at constant deionised water, methanol and phenol molar ratio of 40:20:1, reaction time of 2 h and catalyst loading of 1 g.
4. Varying deionised water, methanol and phenol molar ratio (0:100:1, 80:10:1, 40:5:2, 40:10:0.5, 20:20:0.5, and 40:20:1) at constant heating setting temperature of 300 °C, reaction time of 2 h and catalyst loading of 1 g.

At the end of the reaction, the temperature and stirring was turned off and the autoclave was placed in a water bath to cool to room temperature. Once cooled, 2mL samples of the product were collected into Thermo Scientific autosampler vials for gas chromatography mass spectrometry analysis.

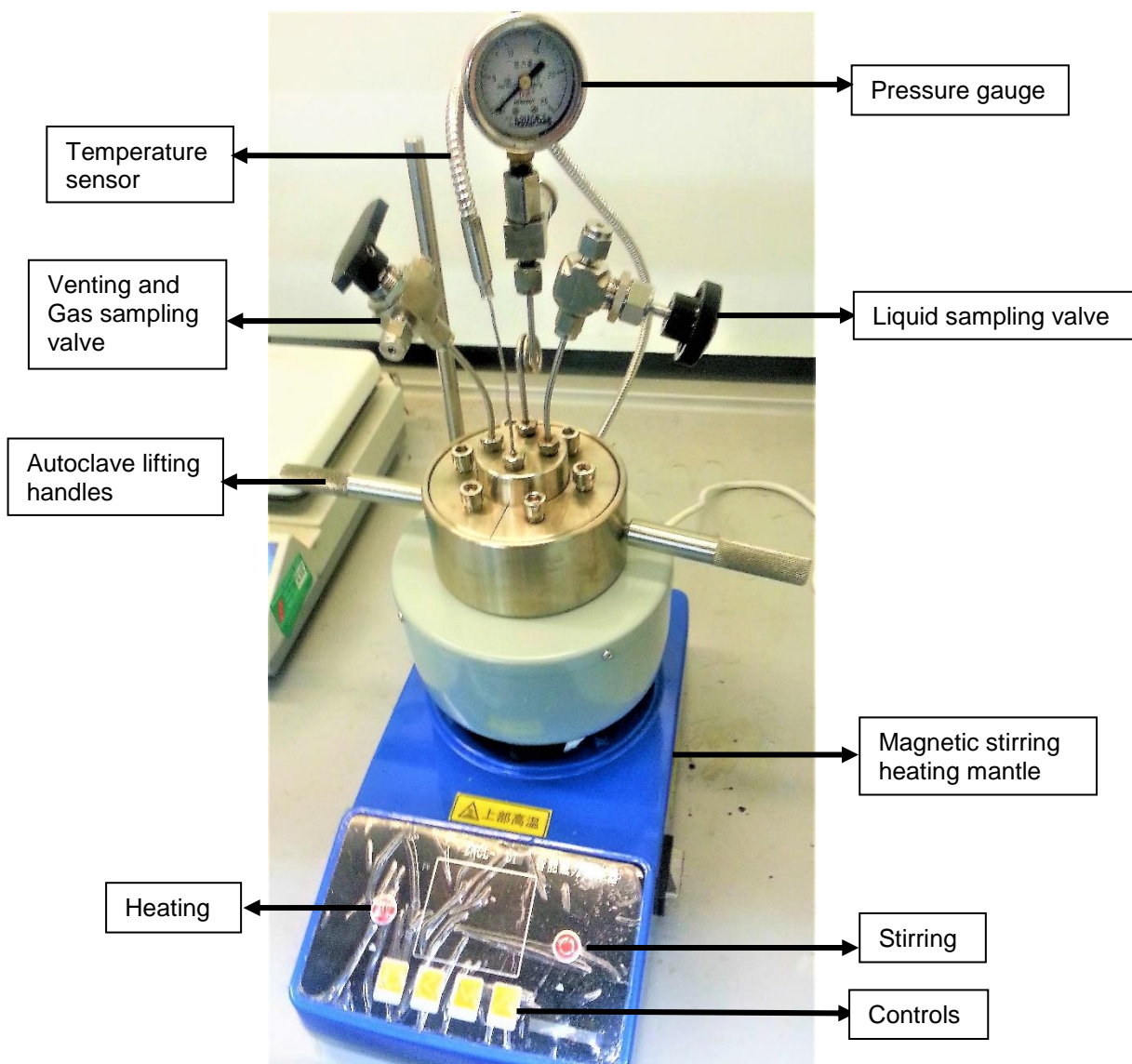


Figure 5.1 The 70 mL stainless steel autoclave used for the experiments.

5.2.3. Analytical methods

The liquid samples were analysed using gas chromatography mass spectrometry (GCMS). The aim of using GCMS analysis was to identify the components and their relative percentages in the samples. A Thermo scientific TRACE 1300 Gas Chromatograph and ISQ LT Single Quadrupole Mass Spectrometer was used. The GC column used for separation was Agilent J&W DB-1701 polysiloxane column, i.d. 0.25mm, 15m length, 0.25 μ m film thickness. The column oven temperature program was as follows: the GC oven temperature was initially held

at 45 °C for 2.5 min, then ramped up at 10 °C/min to 280 °C, and held at 280 °C for 7.5 min. Helium was used as the GC carrier gas at a flow rate of 1.25mL/min. The total time for each injection run was 33.5 min and the injection temperature was 280 °C. Split injection mode was used at split ratio of 20 with 25 ml/min split flow and 5 ml/min purge flow. The mass spectrometer was configured for electron impact ionization at 70 eV, with an interface temperature of 250 °C and an ion source temperature of 200 °C. Full scan data were acquired and processed using Chromeleon™ 7.2 Chromatography Data System (CDS) software.

External standard quantitation was carried out to determine the concentrations of phenol, cyclohexanol and cyclohexanone in the products. The calibration curves are presented in Appendix 2. For the phenol and the cyclohexanone calibration curves the concentrations of the calibration standards were 0.2 mg/mL, 0.4 mg/mL, 0.6 mg/mL, 0.8 mg/mL and 1 mg/mL. For the cyclohexanol calibration curve the concentrations of the calibration standards were 0.6 mg/mL, 0.8 mg/mL, 1.0 mg/mL, 1.2 mg/mL, 1.6 mg/mL, and 2.0 mg/mL. Methanol was the solvent used to prepare the standard solutions. A blank sample (methanol only) was prepared and processed in the same manner as the standards. GCMS analysis of the calibration standards provided their corresponding peak area count and the calibration curve was prepared using Microsoft excel. Each standard was analysed twice and an average of the peak area counts was used for the calibration curve. The calibration curves include the standard deviations of the peak area counts. The blank sample was analysed at the beginning of the series of analyses and after the highest concentration calibration standard to confirm there was no contamination and no analyte was carried over.

The conversion of phenol and the yield and selectivity of cyclohexanol and cyclohexanone were calculated based on the following equations:

Equation 5.8 Conversion

$$\text{Conversion (\%)} = (\text{moles}_{\text{phenol,in}} - \text{moles}_{\text{phenol,out}}) / \text{moles}_{\text{phenol,in}} \times 100\%$$

Equation 5.9 Selectivity

$$\text{Selectivity}_i (\%) = \text{moles}(\text{product})_i / \sum \text{moles}(\text{product}) \times 100\%$$

Equation 5.10 Yield_i

$$\text{Yield}_i (\%) = \text{Selectivity}_i \times \text{Conversion (\%)}$$

5.3. Results and Discussions

5.3.1. Reproducibility

To determine the reproducibility of the experimental procedure and set up, the phenol conversion experiment was repeated. For both experiments, 1.0 g of catalyst was used, at

deionised water, methanol and phenol molar ratio of 40:20:1, heating setting temperature of 300 °C and reaction time of 2 h. Each product sample was analysed by GCMS twice and an average of the relative area % of the two runs was taken. The resulting phenol conversion, cyclohexanone and cyclohexanol yield and selectivity is displayed in Table 5.2. The full GCMS analysis results including the standard deviations is provided in Appendix 2. Tables 1, 2 and 3.

Table 5.2 Reproducibility analysis of phenol conversion experiments

	Experiment 1	Experiment 2	Mean \pm standard deviation
Phenol Conversion (%)	99.07	97.13	1.37
Cyclohexanone Selectivity (%)	5.77	7.52	1.24
Cyclohexanol Selectivity (%)	94.23	92.48	1.24
Cyclohexanone Yield (%)	5.72	7.31	1.12
Cyclohexanol Yield (%)	93.35	89.82	2.50

Table 5.2 illustrates that both experimental runs achieved very high conversions of phenol with a mean standard deviation of ± 1.37 . The same products are formed after both experiments; cyclohexanol and cyclohexanone. The selectivity of the products is also very similar with a small mean standard deviation of ± 1.24 . Likewise, the cyclohexanone yield is highly comparable after both experimental runs with a mean standard deviation of ± 1.12 . The cyclohexanol yield after the two experimental runs has a slightly higher mean standard deviation but is still lower than ± 3 .

As both experiments achieved over 90 % conversion of phenol and the conversion, yield and selectivity results are in < 5 % range, it can be expected that further experiments will generate reproducible results. Therefore, each phenol conversion experiment was performed once and analysed by GCMS twice.

5.3.2. Effect of varying Raney-Ni catalyst loading

The experimental results of hydrogenation of phenol to cyclohexanone and cyclohexanol using in situ generated hydrogen from methanol reforming at various catalyst amounts is presented in Figure 5.2 and Figure 5.3. The full GCMS analysis results including the standard deviations is provided in Appendix 2. Tables 1, 2 and 3. The experiments were carried out at various catalyst loadings, heating setting temperature of 300 °C, reaction time of 2 h and deionised water, methanol and phenol molar ratio of 40:20:1.

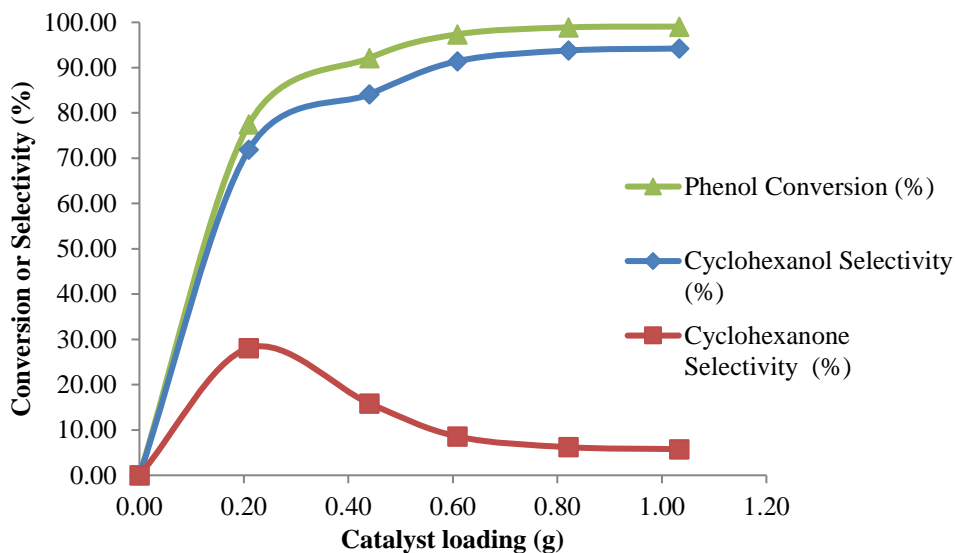


Figure 5.2 Phenol conversion and product selectivity at various catalyst loading.

Heating setting temperature of 300 °C, reaction time of 2 h and deionised water, methanol and phenol molar ratio of 40:20:1

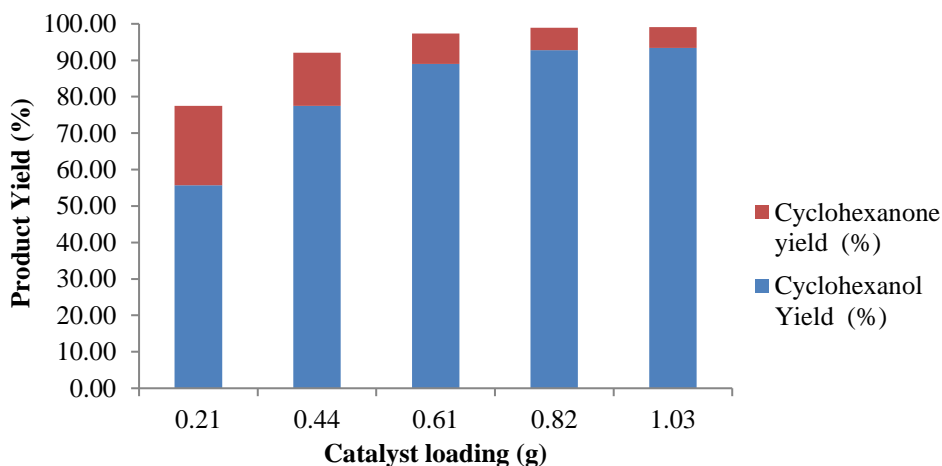


Figure 5.3 Product yield at various catalyst loading.

Heating setting temperature of 300 °C, reaction time of 2 h and deionised water, methanol and phenol molar ratio of 40:20:1.

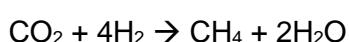
As shown in Equation 5.6 and Equation 5.7, the reforming of methanol for hydrogen production and in situ hydrogenation of phenol (1) simultaneously occur, therefore an external hydrogen source is unnecessary. Raney Ni effectively catalyses both the methanol reforming to produce hydrogen and the hydrogenation of phenol (1) to cyclohexanone (2) to cyclohexanol (3). As shown in Figure 5.2, at 0g catalyst the reaction was unsuccessful, and no products were

formed. This suggests Raney Ni functioned as an essential catalyst for both aqueous phase reforming of methanol and hydrogenation of phenol.

The total selectivity to cyclohexanone (**2**) and cyclohexanol (**3**) is consistently 100 % under all the catalyst loading amounts. However, the catalyst loading amount influenced the ratio of cyclohexanone (**2**) to cyclohexanol (**3**). The selectivity to cyclohexanol (**3**) rapidly increased with increasing catalyst addition from 0 g to 0.61 g. Then its selectivity appears to plateau with increased catalyst addition up to 1.03 g. A similar trend is observable with phenol (**1**) conversion. On the other hand, cyclohexanone (**2**) selectivity rapidly decreased with increased catalyst loading, but gradually decreased after 0.61 g of catalyst loading. Therefore, very high phenol conversion (up to 99 %) and cyclohexanol selectivity (>90 %) can be achieved at catalyst loading around the range of 0.6 g – 1 g. Moreover, these findings indicate to the improved hydrogenation activity with increased presence of Raney Ni catalyst in the system. The large catalytic surface area of Raney Ni potentially increases the reaction surface and improves reactivity [90]. Similarly, Xu et al. reported the high performance of Raney Ni catalyst in both APR of methanol for hydrogen production and in situ hydrogenation of the bio-oil [62].

Figure 5.3 demonstrates consistently high product yields which increased with catalyst loadings. At 0.21 g of catalyst the highest cyclohexanone (**2**) yield was obtained. This indicates that less hydrogen was available therefore the reaction generated more cyclohexanone (**2**) compared to a higher catalyst loading. Additionally, the lowest overall product yield was obtained at 0.21 g of catalyst which may indicate to more gas formation due to side reactions, e.g. methanation (Equation 5.11). The product yields were significantly improved with catalyst loading 0.61 g – 1.03 g.

Equation 5.11 Methanation



The use of hydrogen generated from methanol reforming for in situ hydrogenation of phenol has several advantages. It allows prompt transfer of adsorbed active hydrogen from the catalyst surface into phenol [88]. Also, the alkylation of CO and or CO₂ with H₂ by methanation and Fischer-Tropsch reactions is repressed [88]. Additionally, the selectivity to H₂ during methanol reforming is increased and the selectivity to desired products of phenol hydrogenation is improved because the in situ generated hydrogen is different from externally adsorbed hydrogen gas [88,90]. Therefore, the process is simpler and more resource-efficient than traditional liquid phase hydrogenation processes.

5.3.3. Effect of varying reaction time

The experimental results of hydrogenation of phenol (**1**) to cyclohexanone (**2**) and cyclohexanol (**3**) using in situ generated hydrogen from methanol reforming at various reaction times is presented in Figures 5.4 and 5.5. The full GCMS analysis results including the

standard deviations is provided in Appendix 2. Tables 4, 5 and 6. The experiments were carried out at various reaction time (1 h, 2 h, 3 h, 4 h, and 5 h) at constant deionised water, methanol and phenol molar ratio of 40:20:1, heating setting temperature of 300 °C and catalyst loading of 1 g.

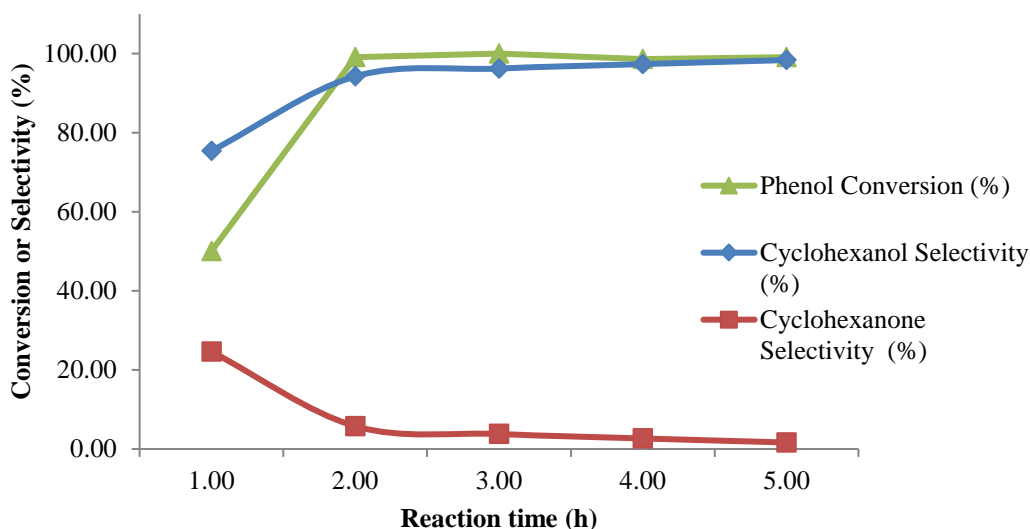


Figure 5.4 Conversion and selectivity at various reaction times.

1 g catalyst loading, heating setting temperature of 300 °C, and deionised water, methanol and phenol molar ratio of 40:20:1

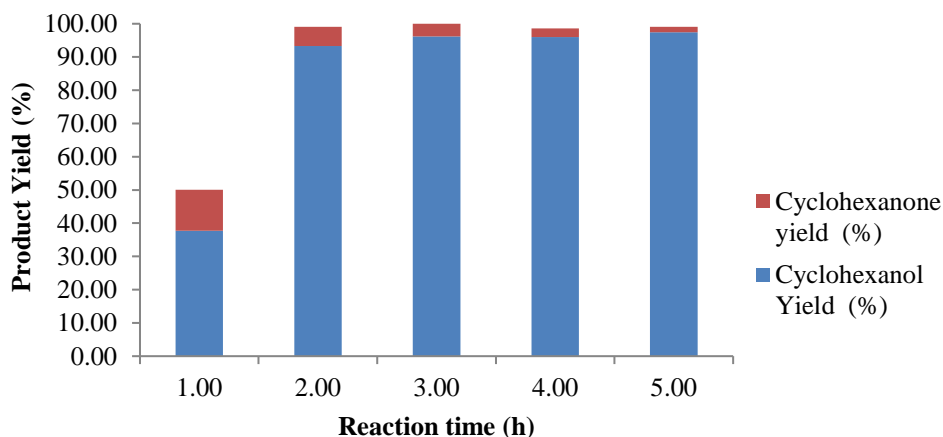


Figure 5.5 Product yield at various at various reaction times.

1 g catalyst loading, heating setting temperature of 300 °C, and deionised water, methanol and phenol molar ratio of 40:20:1

All the reaction times generated a product with 100 % total selectivity to cyclohexanone (2) and cyclohexanol (3). Phenol (1) conversion was lowest after the 1 h reaction (50.05 %) and as a result, the lowest product yield was also obtained. This suggests 1 h reaction time is insufficient for high phenol (1) conversion to cyclohexanone (2) and cyclohexanol (3).

Phenol (1) conversion to cyclohexanone (2) is faster than cyclohexanol (3) because cyclohexanone (2) formation requires less hydrogen atoms. However, all the reaction times generated a product with a significantly higher selectivity to cyclohexanol (3) than cyclohexanone (2). The lowest cyclohexanol (3) selectivity and yield was observed after the 1 h reaction time but rapidly increases to over 90 % after the 2 h reaction and then the selectivity minimally increases with increasing reaction times. This indicates that these methanol reforming and in situ hydrogenation reactions are thermodynamically operative. In thermodynamically controlled chemical reactions, longer reaction times and the formation of a more stable product is favoured; in this case cyclohexanol (3).

The reaction shows some tendency towards kinetic control in the shorter 1 h reaction time compared to the longer reaction times. In kinetically controlled chemical reactions, the molecules of the starting material follow the route of the lower energy transition state to form the kinetic product. These reactions involve short reaction times and or low temperature. The short reaction time prevents the products further converting to more thermodynamically stable products. Because phenol (1) conversion to cyclohexanone (2) requires less hydrogen atoms than cyclohexanol (3), cyclohexanone (2) is more easily formed and therefore it is the kinetic product. The cyclohexanone selectivity and yield was the highest after the 1 h reaction at 24.61 % and 12.32 %, respectively. This suggests that less hydrogen was available for in situ hydrogenation at the 1 h reaction time, therefore a higher tendency to cyclohexanone formation was found compared to the longer reaction times.

5.3.4. Effect of varying reaction temperature

The experimental results of hydrogenation of phenol to cyclohexanone and cyclohexanol using in situ generated hydrogen from methanol reforming at various reaction temperatures is presented in Figures 5.6 and 5.7. The full GCMS analysis results including the standard deviations is provided in Appendix 2. Tables 7, 8 and 9. The experiments were carried out at various reaction temperatures at constant deionised water, methanol and phenol molar ratio of 40:20:1, reaction time of 2 h, and catalyst loading of 1 g.

Once again, the products formed at the different reaction temperatures showed 100 % total selectivity to cyclohexanone (2) and cyclohexanol (3). The temperature setting greatly influenced the conversion, selectivity and yield of the reaction. Phenol (1) conversion was lowest after the 100 °C reaction (9.89 %) and as a result, the lowest product yield was also obtained. The conversion remained at a low 13.61 % at 200 °C reaction temperature setting, consequently, the product yield was also quite low. With increased temperature phenol conversion and cyclohexanol yield rapidly escalated and at the 300 °C reaction temperature setting, phenol conversion peaked to 99.07 %.

At 100 °C and 200 °C although the overall product yield is low, cyclohexanone (2) forms majority of the product and its selectivity is 95.64 % and 82.13 %, respectively. This indicates

cyclohexanone (**2**) is a kinetic product that preferentially forms at lower reaction temperatures. On the other hand, cyclohexanol (**3**) is the more thermodynamically stable compound and readily forms at higher reaction temperatures. At 300 °C heating setting temperature, cyclohexanol selectivity and yield reached 94.23 % and 93.35 %, respectively. Therefore, the reforming of methanol for hydrogen production and in-situ hydrogenation of phenol to predominantly form cyclohexanol is most successful at temperatures above 200 °C.

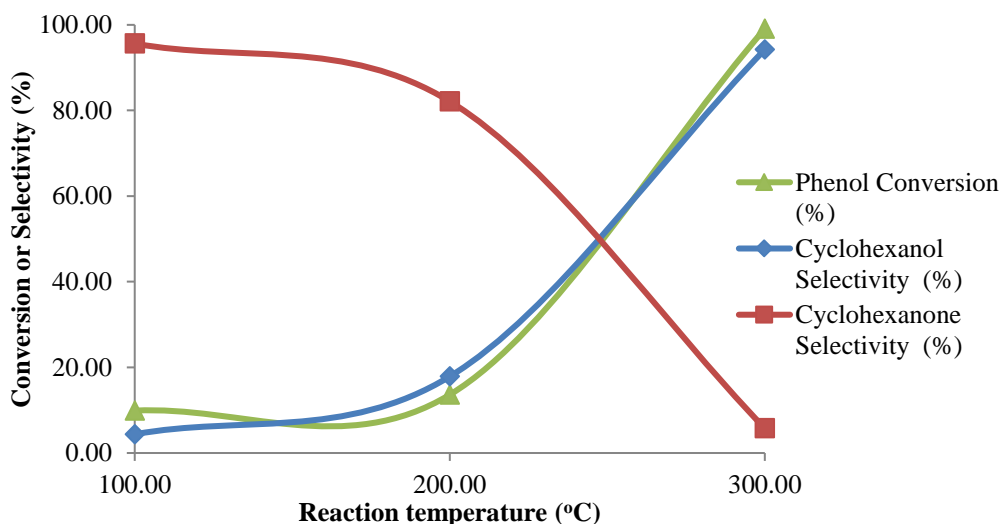


Figure 5.6 Conversion and selectivity at various reaction temperatures.

1 g catalyst loading, reaction time 2 h, and deionised water, methanol and phenol molar ratio of 40:20:1

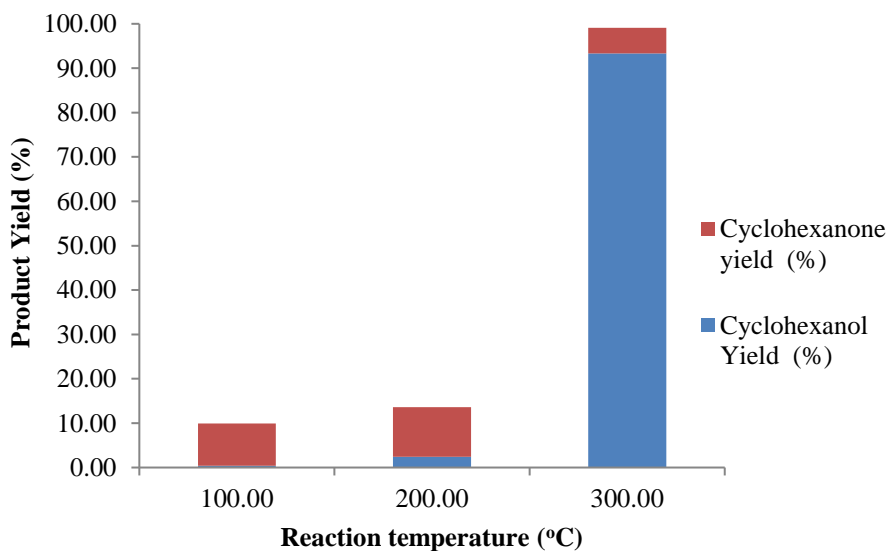


Figure 5.7 Product yield at various reaction temperatures.

1 g catalyst loading, reaction time 2 h, and deionised water, methanol and phenol molar ratio of 40:20:1

5.3.5. Effect of varying reaction starting material ratios

Because 1 g catalyst loading, 2 h reaction time and maximum reaction setting temperature proved ideal for high phenol conversion and cyclohexanol yield these parameters were kept constant and the effect of varying reaction starting material was investigated. The experimental results of hydrogenation of phenol to cyclohexanone and cyclohexanol using in situ generated hydrogen from methanol reforming at various starting material ratios is presented in Figures 5.8 and 5.9. The full GCMS analysis results including the standard deviations is provided in Appendix 2. Tables 10, 11 and 12. The experiments were carried out at various deionised water, methanol and phenol molar ratio (0:100:1, 80:10:1, 40:5:2, 40:10:0.5, 20:20:0.5, and 40:20:1) at constant heating setting temperature of 300 °C, reaction time of 2 h and catalyst loading of 1 g. Except at the H₂O:methanol:phenol molar ratio 0:100:1 and 20:20:0.5, all the reaction ratios generated a product with 100 % total selectivity to cyclohexanone (**2**) and cyclohexanol (**3**).

At the H₂O:methanol:phenol molar ratio 0:100:1 the reaction was unsuccessful as 0 % phenol converted and no products were detected. This highlights the important role of water in this aqueous-alcohol-solvent reaction system. Water is necessary for the reforming of methanol to proceed (Equation 5.3) and without it, no hydrogen can be produced. Due to the absence of water and the resulting lack of hydrogen, the in situ hydrogenation of phenol (**1**) cannot take place and therefore cyclohexanone (**2**) and cyclohexanol (**3**) were not formed. By comparing this experiment run to the other ratios, it confirms that the aqueous methanol reforming and in situ hydrogenation method is an effective alternative to external hydrogen application. Additionally, the method improves the selectivity to desired products of phenol hydrogenation. Researchers have noted that this is because the in situ generated hydrogen is different from externally adsorbed hydrogen gas [88,90].



Equation 5.3

Supercritical solvents such as methanol are recognised as good mediums for chemical reactions, enabling increased reaction rate and controllable selectivity [92]. This is because the properties of supercritical fluid solvents such as heat capacity, heat conductivity and diffusivity change under small temperature and pressure variations [93]. Lower alcohols such as methanol possess high solvating power, relatively low critical parameters, and are thermally stable as they do not decompose in supercritical reactions [94]. Therefore, they are frequently used as supercritical solvents for chemical reactions. In this aqueous methanol reforming and in situ hydrogenation method, methanol has a dual function as a solvent and starting material in the reforming reaction. Therefore, the process is simpler and more resource-efficient than traditional liquid phase hydrogenation processes. At the H₂O:methanol:phenol molar ratio 0:100:1, although temperatures and pressures above the critical point of methanol (240 °C and 74 bar) was achieved, supercritical methanol alone was unable to promote product formation.

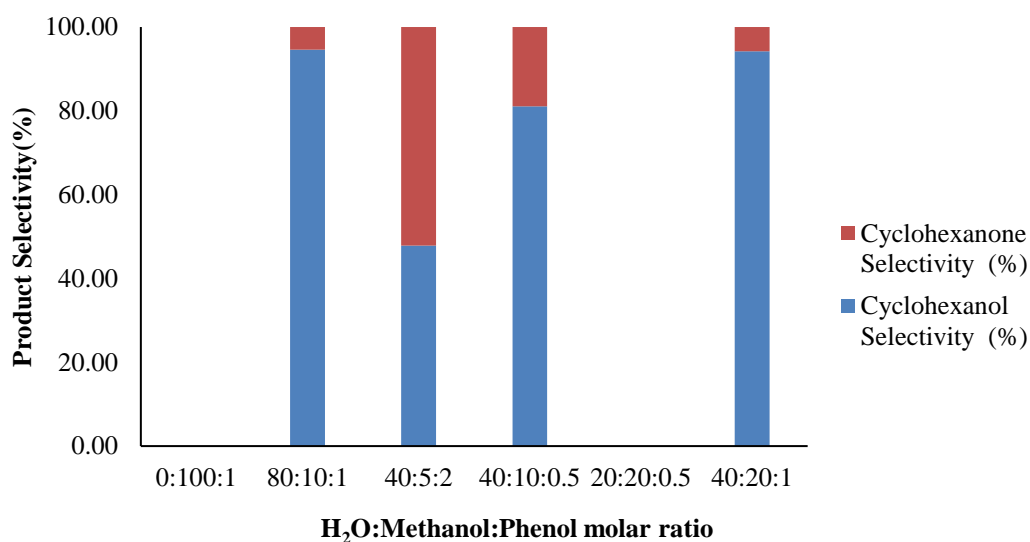


Figure 5.8 Product selectivity at various starting material ratios.

1 g catalyst loading, reaction time 2 h, and heating setting temperature of 300 °C.

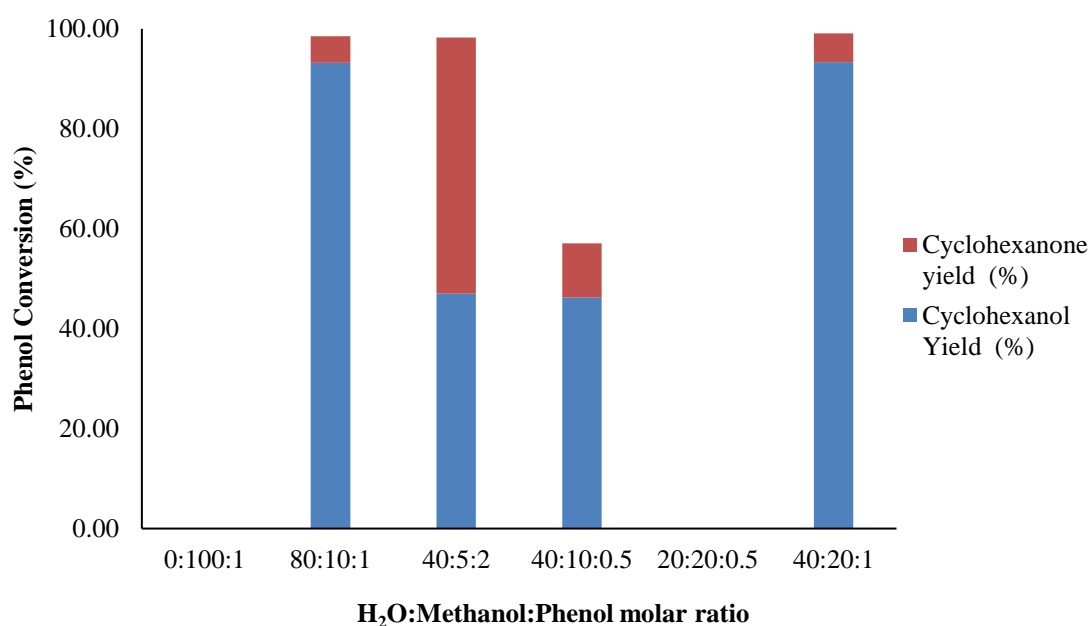


Figure 5.9 Product yield at various at various starting material ratios.

1 g catalyst loading, reaction time 2 h, and heating setting temperature of 300 °C.

At the H₂O:methanol:phenol molar ratio 20:20:0.5 the reaction was also unsuccessful because 0 % phenol converted, and no products were detected. This may be due to conflicting effects of the methanol and water on the reaction when equimolar amounts are used which hinders the product formation. Similar findings were also observed by researchers who used equimolar water-methanol ratio under supercritical conditions for chemical reactions [95].

At the various starting material ratios, the concentration of phenol was consistently kept low relative to the solvents because phenols are one of several other compounds present in the

bio-oil. Therefore, the objective was to keep the reactions of phenol similar to what would happen to it in a sample of bio-oil. At the H₂O:methanol:phenol molar ratio 80:10:1 and 40:20:1, similar phenol conversion, cyclohexanone (**2**) and cyclohexanol (**3**) yield and selectivity was observed. At 40:10:0.5, phenol conversion was relatively low at 57.07 %, and this was reflected in the product yield. However, a higher cyclohexanone (**2**) selectivity (18.92 %) was found compared to 80:10:1 and 40:20:1. The selectivity and yield at 40:5:2 is interesting due to the high phenol conversion of 98.29 % and almost 1:1 ratio of cyclohexanone (**2**) and cyclohexanol (**3**) was formed. This may be due to the higher concentration of phenol in the starting material compared to the other ratios.

Overall, by varying the reaction parameters the selectivity to cyclohexanone (**2**) and cyclohexanol (**3**) can be controlled. If a reaction with a high phenol conversion but with similar amounts of cyclohexanone (**2**) and cyclohexanol (**3**) is desired, a H₂O:methanol:phenol molar ratio of 40:5:2 is suitable. Generally, for the reaction to proceed water must be present, and a higher ratio of water to methanol is preferred over an equimolar ratio.

5.3.6. Comparing the experimental reaction temperatures and pressures and the critical properties calculated by ASPEN HYSYS simulator

ASPEN HYSYS simulation was utilised to examine if the experimental conditions achieved the critical point of the water-methanol-phenol reaction mixture. A fluid package using the Peng Robinson property method was applied to use the Critical Properties Analysis tool on ASPEN HYSYS. The critical properties were calculated by ASPEN HYSYS using the mixing rules associated with the Peng Robinson property package.

Table 5.3 includes the results of the ASPEN HYSYS calculated critical properties of various water-methanol-phenol ratios. Figure 5.10 shows the relationship between increasing concentration of water and the critical properties of the reaction mixture, from the critical data calculated using ASPEN HYSYS. Expectedly, with higher water concentration, the critical point of the reaction mixture increases because the critical point of water (374 °C, 221 bar) has a greater influence.

At the H₂O:Methanol:phenol molar ratios 80:10:1, 40:10:0.5, and 40:20:1 the temperature and pressures reached the same values of around 285 °C and 110 bar. Interestingly, at the lower concentrations of water of 0 % and 34.3 %, the reaction temperatures peaked at 268 °C, however the pressures did reach 100 bar. At starting material ratio 40:5:2, the highest temperature of 290 °C was achieved- although only around 5 °C higher than at the other ratios on average. Generally, all the reaction conditions were quite close to reaching the temperature setting of 300 °C.

Table 5.3 indicates that none of the experiments achieved the ASPEN HYSYS calculated critical properties except at 0:100:1. At 0 % water, the critical properties at this ratio mainly accounts for that of methanol (240 °C and 74 bar), therefore the ASPEN HYSYS calculated critical conditions are 242.6 °C and 75.09 bar. With temperature setting of 300 °C, the reaction managed to surpass the critical point of methanol and reach 268 °C and 115 bar. Therefore, the reactions at the other ratios may have been limited by the operating capacity of the autoclave. However, as mentioned, the results in section 5.3 demonstrated that 300 °C was sufficient temperature setting to achieve very high phenol (**1**) conversion (>90 %), and high cyclohexanol selectivity (**3**) and yield (>90 %). This highlights that subcritical conditions can be considered a favourable alternative to energy-intensive and resource-demanding supercritical conditions.

Table 5.3 Comparing the critical properties of phenol experiments and ASPEN HYSYS.

Experiment conditions are 300 °C heating temperature setting, 2 h reaction time, 1 g Raney Ni catalyst and various H₂O:Methanol:phenol molar ratio.

H ₂ O:Methanol:Phenol	Equivalent H ₂ O concentration (%)	ASPEN HYSYS Critical Properties		Experiment properties	
Molar ratio	(%)	Tc (°C)	Pc (bar)	T max (°C)	P max (bar)
80:10:1	77.6	353.8	183.6	286	105
40:10:0.5	66.2	339.8	163.4	285	112
40:20:1	49.5	322.1	139.8	285	110
20:20:0.5	34.3	300.7	117.9	268	100
0:100:1	0	242.6	75.09	268	115
40:5:2	67.3	353.5	173.0	290	110

Tc, Pc, T max and P max refers to critical temperature, critical pressure, maximum reactor content temperature and maximum reactor content pressure, respectively.

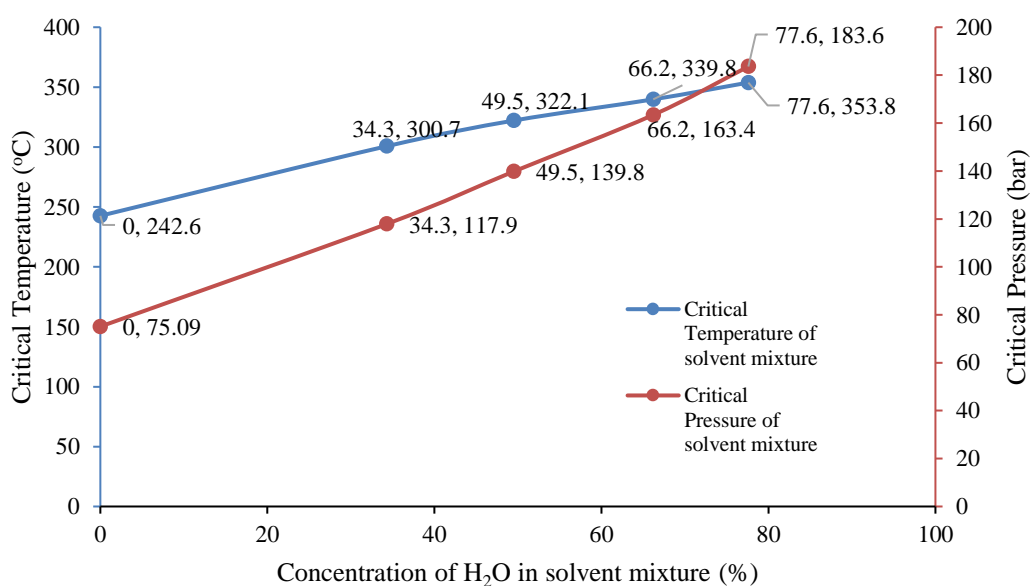


Figure 5.10 Changes in the critical properties of the reaction mixture at different concentration of H₂O.

5.4. Conclusion

This chapter developed on the work of Chapter 4 which showed phenols remained relatively unchanged after blending and supercritical alcohol treatment. The analysis of a sample of raw bio-oil from a softwood feedstock in Chapter 4, showed that it contained 37.03 % of phenols. The high phenol content in raw bio-oil is undesirable because phenol can behave like an acid thus it can be highly reactive in bio-oil [64]. Moreover, the presence of phenolic compounds is reported as the main cause for coke formation and catalyst deactivation during bio-oil processes [5]. Additionally, phenols are undesirable in bio-oil because the high oxygen content causes unfavourable properties such as low energy density, instability, high viscosity, corrosion, and tendency to polymerize [5]. Therefore, the conversion of phenols in bio-oil to less reactive compounds such as cyclohexanol is highly desired to improve the bio-oil properties.

This work aimed to study phenol alone; in order to clearly follow its reaction pathway without the presence of the complex mixture in crude bio-oil. The objective was to utilise Raney-Ni to catalyse the aqueous phase reforming of methanol and in situ hydrogenation of phenol. The effects of varying reaction temperature, time, catalyst loading and starting material ratio on the conversion of phenol was also investigated.

The reaction parameters greatly influenced phenol conversion, product selectivity and yield. Phenol conversion increased with catalyst loading amount and up to 1 g of catalyst proved sufficient to generate high cyclohexanol yield (93.35 %) and selectivity (94.23 %). Varying the reaction time and temperature indicated that the hydrogenation of phenol is a kinetics versus thermodynamics situation because two products are formed at different distribution depending on the variation in the reaction temperature and time. Cyclohexanone (**2**) was the kinetically favoured product in the reaction because its highest selectivity and yield was observed at the shortest reaction time and lowest reaction temperatures. On the other hand, cyclohexanol (**3**) was the thermodynamically favoured product in the reaction because its selectivity and yield increased with reaction time and it formed a high proportion at the maximum reaction temperature. Varying the ratio of deionised water, methanol and phenol at the start of the reaction showed some interesting findings. If a reaction with a high phenol conversion but with similar product amounts of cyclohexanone (**2**) and cyclohexanol (**3**) is desired, a H₂O:methanol:phenol molar ratio of 40:5:2 is suitable. Generally, for the reaction to proceed water must be present, and a higher ratio of water to methanol is preferred over an equimolar ratio.

Chapter 4 showed a non-catalytic supercritical methanol process was advantageous for generating a product bio-oil with a high proportion of esters and reduced acidity. In order to further enhance the properties of bio-oil, the aqueous phase reforming of methanol and in situ hydrogenation process can be applied to transform the phenols in bio-oil and generate a bio-

oil with further enhanced properties. Raney-Ni proved to be an excellent catalyst for both methanol reforming and phenol hydrogenation. Therefore, this process is an economic alternative to conventional catalytic hydrogenation processes which involve precious metal supported catalysts and external molecular hydrogen.

6. A One-pot Synthesis of Monoterpenes by Transforming a Bio-oil Compound using Near-Critical Water-Methanol Mixtures as Solvent and Catalyst

6.1. Introduction

Most key molecules in the chemical industry are produced by fossil-fuel based processes. This is largely due to the historically challenging task of maintaining a continuous and steady year-round supply of raw materials and increasing production costs [96]. This resulted in many industries replacing natural products/intermediates with petrochemicals. For example, citral is a terpene naturally derivable from lemongrass and commonly used in the flavours and fragrances industry for the synthesis of ionones [96]. However, it has been mostly replaced by its synthetic counterpart which is produced from isobutene [96]. Recently, plant-based chemicals are increasingly being considered for application as chemical building blocks in order to decrease reliance on fossil feedstocks, reduce the impact of chemical processing on the environment, and decrease greenhouse gas emissions along the production chain [96,97].

Terpenes are a class of organic compounds produced by a variety of plants and certain insects. These valuable compounds are used to produce fine and bulk chemicals such as flavours, fragrances, solvents, and pharmaceuticals [96,98]. Terpenes are frequently used in the fragrance and perfume industry due to their distinct scent. For instance, hydroformulation of the monoterpene limonene (an industrial process developed by Celanese) results in limonenal, a citrus fruit scented compound found in soaps and lotions [97]. Monoterpenes are also of practical value for the production of alkyl-substituted aromatic C₇-C₁₀ hydrocarbons and mono/poly-oxygenated compounds for the medical industry [92]. Monoterpenes are also important for producing unsaturated diene and triene compounds and monomers for the synthesis of polymers [92]. Monoterpenes are available from natural sources by distillation and extraction and they are the main components of essential oils obtained from plants [99]. For example, limonene is found in the foliage, fruit and peels of orange trees. Terpenes are also industrially synthesised via chemical synthesis, microbial fermentation and plant cell culture.

However, rather than ad hoc synthesis or growing crops specifically for chemicals production, agricultural wastes and residues have been identified as good sources of terpenes [97]. For example, the terpenes alpha- and beta-pinene can be obtained by fractional distillation of turpentine oil which is a waste product in paper pulp production [97]. Furthermore, approximately 30,000 ton per year of limonene is produced [98]. Conveniently, there is a global c.7 million tons of peel waste from orange juice production [97]. This waste is a viable source

of limonene which can be recycled and transformed to chemicals for flavours, fragrances, pharmaceuticals and other industries. This is an economic and environmentally effective alternative to ad hoc synthesis or growing of biomass for plant-based chemicals which is not entirely carbon neutral and may have a greater CO₂ emissions than fossil-based routes. Additionally, although waste with high concentration of organic compounds is biodegradable and can be safely disposed, large amounts of waste can be difficult to dispose of. Terpene production from waste offers an alternative application of organic wastes alongside common uses such as composting, as a source of heat, to generate electricity or for fuel.

Several researchers have discussed the production of fine chemicals from renewable resources such as biomass. Gallezot discussed three methods of converting biomass into chemical products [100]. One method involves firstly converting biomass to bio-oil via pyrolysis, followed by separation of the molecules in the bio-oil and transformation to chemicals by existing chemicals synthesis methods. However, as mentioned by the author, this is an energy-intensive and environmentally unsustainable method due to the degradation of the functionalised molecules in the biomass during pyrolysis only to re-functionalise during chemical synthesis.

Another method for converting biomass into chemical products involves using biorefineries. Biorefineries are production facilities that combine various biomass conversion processes to produce fuels and chemicals. A fraction of the biomass is converted to fuels by processes such as pyrolysis and gasification. Another fraction of the biomass is converted by fermentation or chemo-catalytic routes to platform molecules which can be used as building blocks in chemical synthesis.

A final method proposed by Gallezot involves one-pot reactions where enzymatic and chemical steps are conducted in series to transform biomass into chemicals [100]. For example, some production processes (e.g. cosmetics, paints) use a mixture of molecules with the same functionalities such as a mixture of diols or polyols. This mixture can be acquired from biomass by one-pot processes with catalytic steps completed in series. This method reduces processing cost because it prevents product isolation, does not require intermediate product recovery, reduces operating time and potentially reduces the quantity of waste produced.

6.1.1. Catalytic production of terpenes

Catalytic conversion of monoterpenes has received increasing attention by academia and industry to overcome issues including waste reduction, managing production cost, and selectivity challenges in catalytic processes [97].

Costa et al. examined the effect of various catalysts including alumina catalyst, and different zirconium catalysts on the dehydration of the monoterpenoid alcohols nerol (**4**) and geraniol (**3**) [101]. The gas-phase reactions were conducted in a glass reactor tube held at either 150

or 250 °C with 0.1 g catalyst, 0.5 g substrate, and 0.5 L/min nitrogen gas. The product compositions of geraniol (**3**) and nerol (**4**) dehydration over alumina catalyst were reportedly very similar due to the lack of steric differentiation between the two alcohols. Generally, the acid-catalysed dehydration of nerol (**4**) and geraniol (**3**) leads to cyclisation to monoterpenes [101]. The ratio of acyclic to cyclic products after reacting with alumina catalyst was 90:10 for geraniol (**3**) and similarly for nerol (**4**) it was 86:13. In fact, the ratio of acyclic to cyclic products was repeatedly around 90:10 after the four geraniol (**3**) dehydration reactions with the different zirconium phosphate catalysts.

The authors reported average ratio of 50:50 acyclic to cyclic after the nerol (**4**) dehydration reactions with the various zirconium phosphate catalysts. This suggests under these catalytic conditions, the dehydration of nerol (**4**) favours cyclic product formation compared to geraniol (**3**) dehydration. This may be because, geraniol (**3**) and nerol (**4**) are E and Z isomers about the allylic double bond, respectively. Therefore, reactions of geraniol (**3**) derivatives prefer forming acyclic products and nerol (**4**) derivatives favour monocyclic products [101].

Costa et al. reported minimal difference in the product composition/distribution after geraniol (**3**) dehydration with zirconium or alumina catalyst. On the other hand, the nerol (**4**) dehydration product distribution varied depending on the catalyst used for the reaction.

In another study on catalytic processes to produce terpenes, Eisenacher et al. obtained 99% total product selectivity of the monoterpene's linalool, myrcene, phellandrene and ocimene by dehydrating geraniol (**3**) using gas-phase reactions over a weak acidic boron pentasil zeolite catalyst [99]. The geraniol (**3**) dehydration was conducted in a plug flow fixed bed reactor which was filled with the solid catalyst and placed in a temperature-controlled oven. Subsequently, geraniol (**3**) was pumped into the reactor. The authors investigated the effect of nitrogen flow, geraniol (**3**) feed, temperature, pressure and catalyst loading on the reaction. The study showed that the selectivity to the monoterpenes (linalool, myrcene, phellandrene and ocimene) could be controlled by varying the reaction parameters.

Furthermore, unlike Costa et al. who reported an acyclic to monocyclic ratio of 9:1 after acidic gas phase treatment of geraniol (**3**), Eisenacher et al. reported a product mix with a lower acyclic to monocyclic ratio of 4:1 [99,101]. Additionally, Eisenacher et al. reported increasing the reaction temperature up to 250 °C or higher leads to over 50 % geraniol (**3**) conversion. However, the authors observed CO, CO₂ and H₂O were the main products at those conditions.

6.1.2. Non-catalytic terpene production using supercritical alcohol solvents and supercritical water as acid catalyst

To obtain high conversion (90-95%) of monoterpenes in gas or liquid phase processes, the reaction mixture requires long contact times; hence the reaction can take up to tens of hours [92]. Fortunately, the reaction can be accelerated with a catalyst or supercritical solvents which

are considered an attractive medium for chemical reactions, offering increased reaction rate and controllable selectivity [92]. This is because the properties of supercritical fluid solvents such as heat capacity, heat conductivity and diffusivity change under small temperature and pressure variations [93]. Lower alcohols such as methanol possess high solvating power, relatively low critical parameters, and are thermally stable as they do not decompose in supercritical reactions [94]. Therefore, they are frequently used as supercritical solvents for chemical reactions.

Anikeev used supercritical alcohols for thermal transformations of a selection of terpenes (alpha-pinene, beta-pinene, turpentine, and cis-verbenol) [92]. The results demonstrated increased thermal isomerization of the monoterpenes and same selectivity towards desired reaction products in supercritical conditions compared to reactions in gas or liquid phase. Moreover, the author found supercritical solvents significantly increased the isomerization reaction rate compared to gas or liquid phase. Anikeev reported that the pressure of the supercritical solvent effectively enabled accelerated reactions.

More recent research has also proven the effectiveness of supercritical fluid technology for chemical transformation of essential oil compounds [102]. Yilmazoglu and Akgun used supercritical ethanol and 2-propanol for catalytic reactions of orange peel oil containing 96.56% d-limonene (**8**) [102]. The supercritical phase enhanced the selectivity of the main product (p-cymene) and enabled high conversion in short reaction time.

Ermakova et al. studied the influence of water on the transformation of alpha-pinene in a supercritical aqueous-alcohol solvent [103]. Generally, the transformation of alpha-pinene occurs under acid catalysis. Water can be used as an acid catalyst because it is strongly dissociated and produces ions at its critical region [92]. Additionally, it is well recognised that the ionic product of water increases in supercritical conditions [102]. Therefore, in the work of Ermakova et al. supercritical water was described as a cosolvent and catalyst in the reaction [103]. In another paper, the authors found raising the pressure of a mixture of supercritical ethanol-water- alpha-pinene results in an increase in the density of the supercritical medium in the critical region [94]. This consequently leads to an increase in the H⁺ ion concentration due to the increasing degree of ionisation of water. Therefore, water functioned as an acid catalyst and accelerated the reaction rate. Moreover, the study by Ermakova et al. showed an increased concentration of water in the supercritical solvent led to an increase in the yield of the target product (limonene) in reaction products [103].

Similarly, Ikushima and Sato reported on using supercritical water (SCW) as an acid catalyst and solvent for the successful synthesis of lavandulol (a monoterpene alcohol) from hemiterpene alcohols [95]. The authors reported higher yield in the non-catalytic SCW system compared to a conventional method using organometallic catalysts. Additionally, low yield was observed when the reaction was conducted in hot water, even with extended reaction time.

Ikushima and Sato discussed the reduced strength of the hydrogen bonding in H₂O near the critical point which leads to the activation of protons or H₃O⁺ ions. This causes the acid or base-catalysed reactions under a SCW solvent. The authors concluded, the acidic ability of SCW promotes high selectivity.

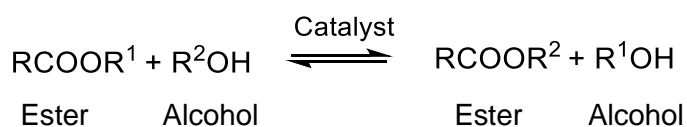
Acidic media are recognised for facilitating a variety of transformations of acyclic monoterpene alcohols such as geraniol (**3**) and nerol (**4**) and their esters [104]. Supercritical water provides the functions of an acidic catalyst and it is a favourable solvent because it is environmentally safe, relatively inexpensive compared to organic solvents, and possesses physicochemical properties that can be manipulated with pressure and temperature [95]. The work by Ermakova et al., Anikeev, Ikushima and Sato, and Yilmazoglu and Akgun show non-catalytic reactions to produce terpenes can be successfully achieved with supercritical alcohol-water solvents.

6.1.3. Transesterification

The starting material for the monoterpene production for this work is geranyl isovalerate (**1**) a compound detected in a sample of bio-oil analysed in chapter 4. The transesterification of geranyl isovalerate (**1**) and the dehydration of its intermediates leads to the formation of methyl isovalerate (**2**) and a mixture of monoterpenes, respectively.

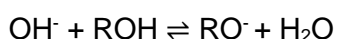
Transesterification involves the conversion of an ester into a different ester through interchange of the alkoxy group (Equation 6.1) [105].

Equation 6.1 General equation for transesterification [106]



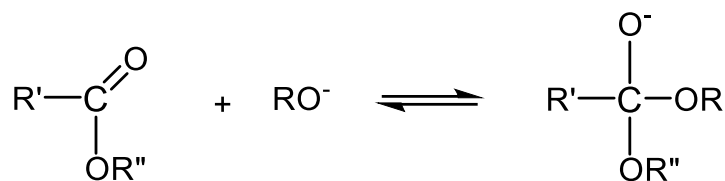
The equilibrium reaction can proceed by simply mixing the ester and alcohol. However, without a catalyst the reaction progresses at a slow rate and an acid (e.g. sulfuric acid and hydrochloric acid) or base (e.g. sodium hydroxide and potassium hydroxide) catalyst is typically used [105]. The reaction is reversible and molar excess of alcohol is used to shift the equilibrium towards the forward reaction [106]. Alternatively, following Le Chatelier's principle, continuous removal of the alcohol produced is essential for good yield of the desired esters [105].

Base catalysed transesterification begins with a pre-step involving an acid-base equilibrium where an alkoxide ion is produced for the main transesterification reaction: [107]



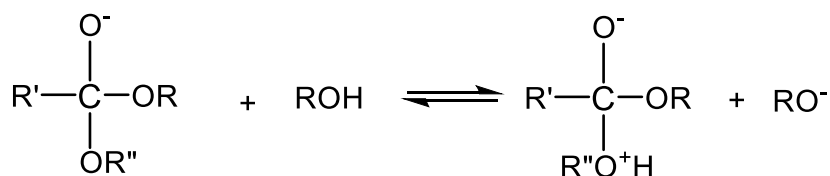
In step one, the alkoxide ion nucleophilic attacks the carbonyl carbon of the ester molecule to form a tetrahedral intermediate [106].

Step 1.



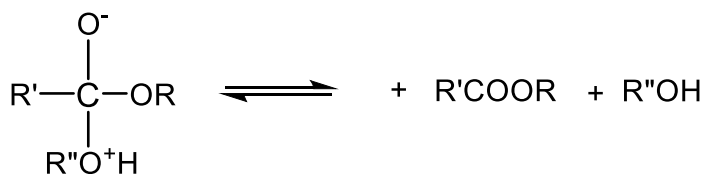
The intermediate subsequently reacts with an alcohol and forms an alkoxide ion in the second step [106].

Step 2.



In the final step, the tetrahedral intermediate rearranges and an ester and alcohol is produced [106].

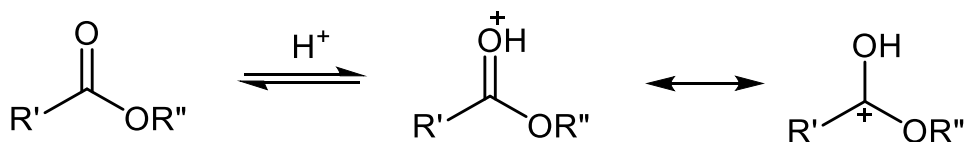
Step 3.



Where, R, R' and R'' indicate any alkyl or aryl group.

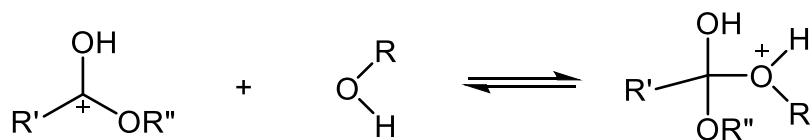
Acid catalysed transesterification begins with the protonation of the carbonyl group of the ester by the Bronsted acid which leads to the formation of a carbocation [107].

Step 1.



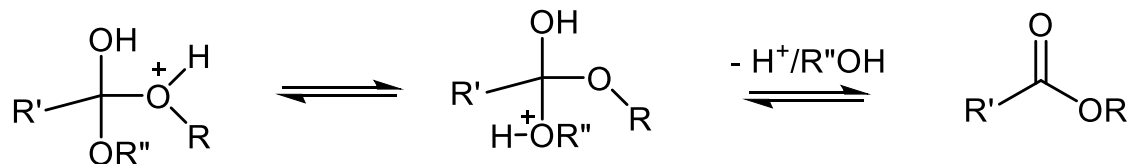
The second step is nucleophilic attack on the carbocation by the alcohol group which leads to the formation of a tetrahedral intermediate [107].

Step 2.



The final steps are proton transfer, removal of the leaving alcohol group, and deprotonation subsequently formation of a new ester.

Step 3.



Where, R, R' and R'' indicate any alkyl or aryl group.

Transesterification reactions are essential in biodiesel production and homogenous base catalyst are frequently used in commercial biodiesel plants [8]. However, base catalysts are not ideal if the vegetable oil contains a high content of free fatty acids (FFA) or water as side reactions producing soap can occur which affect the biodiesel yield. Alternatively, with homogenous acid catalysts, no side formations of soap occur when the oil contains high FFA or water content. However, transesterification reactions using homogenous acid and alkaline catalysts can present several shortcomings including [107]:

1. Complex and energy-intensive post-reaction treatment to separate the catalyst from the biodiesel due to the homogenous phase of the catalyst and product.
2. Additional costs for the treatment and disposal of the alkaline and acidic wastewater from the process.
3. Challenge of glycerol recovery due to the solubility of excess methanol and catalyst.
4. If the vegetable oil contains a high content of FFA or water the biodiesel production process would be limited to using acid catalysts due to saponification if base catalyst is used.

Heterogenous catalytic transesterification reactions do not present these weaknesses, and are considered alternatives to homogenous reactions. Heterogenous reactions do not require catalyst and product separation and purification of biodiesel. Moreover, the cost of catalyst can be reduced due to simpler recovery and reuse processes. Also, unlike homogenous base catalysts, heterogenous catalysts are unaffected by oils with high content of FFA. However, the reaction rate is slower with heterogenous catalysts due to the three-phase mixture of oil, alcohol and solid catalyst. Furthermore, water in the reaction mixture can result in leaching of active compounds in the solid catalyst, reducing catalyst efficiency and ultimately lowering biodiesel yield.

Non-catalytic supercritical fluid techniques have been investigated to circumvent the challenges in catalytic transesterification reactions, particularly for biodiesel production [8,9,108]. In supercritical alcohol transesterification, the triglycerides and alcohol are heated to the critical temperature and pressure of the alcohol [8]. Due to these conditions, the solubility of the alcohol is decreased to a level that corresponds to the solubility of the triglycerides [8]. Consequently, the contact area between the two reactants is improved and the usually immiscible oil and alcohol forms a single homogenous phase [8]. This means, for a given triglyceride alcohol mixture, below the critical temperature the mixture is in a heterogenous

phase and above the critical temperature the mixture is in a homogenous supercritical phase [9]. This enables the transesterification reaction to proceed at an enhanced rate without a catalyst. A key concern with conventional transesterification reactions is the requirement of excess alcohol to shift the equilibrium reaction forward. However, a review by Anitescu and Bruno showed at higher temperature supercritical conditions the reverse reaction is reduced and less alcohol is necessary to favour the desired forward reaction [9]. For instance, at 350 °C a supercritical phase can be achieved at methanol: triglyceride molar ratios of 15. At 400 °C the molar ratio can be reduced to 8 [9]. Therefore, solvent costs can be reduced with high-temperature supercritical transesterification processes.

Some notable advantages of supercritical alcohol transesterification reactions include [8]:

1. Reduced production costs due to the elimination of catalyst from the process.
2. Simpler separation of glycerol and biodiesel due to the absence of catalyst.
3. High tolerance to feedstocks with high concentration of FFA and water [8,9].
4. Promotes the use of inexpensive feedstocks such as waste oils or fats which typically contain significant amounts of FFA and water.
5. Higher biodiesel yield as esterification of FFA and transesterification of triglycerides simultaneously occur.
6. High conversion at reduced reaction time with supercritical transesterification (5-9 min) compared to base/acid catalysed transesterification (1-6 h) [9].
7. Lower manufacturing cost of biodiesel fuel using supercritical transesterification compared to base/acid catalysed transesterification [9].

Generally, ethanol is considered more favourable for transesterification processes compared to methanol. This is because bioethanol can be produced from agricultural products, which is renewable and environmentally benign [108]. However, methanol is commonly used due to its low cost, physical and chemical advantages such as polarity and it possesses the shortest chain alcohol [108].

6.1.4. Summary

In chapter 4, GCMS analysis of a sample of bio-oil showed the presence of geranyl isovalerate (**1**). A potentially useful compound for chemicals production. This compound and its derivatives (geraniol (**3**) and nerol (**4**)) can be obtained from renewable/sustainable sources, e.g. from agricultural residue, specifically plant /food waste.

In this work, a one-pot synthesis of valuable compounds including methyl isovalerate (**2**) and a mixture of monoterpenes was completed by transesterification of geranyl isovalerate (**1**) and dehydration of the intermediates (geraniol (**3**) and nerol (**4**)) of the transesterification reaction. A sub/supercritical water-methanol mixture was utilised as solvent and catalyst to transform the reagents. This work explored the transformation of the bio-oil based compound to valuable compounds which are highly desirable in the chemicals industry as intermediates for bulk/fine

chemicals production. In this report, the effect of various reaction parameters on the conversion of geraniol (**3**) and nerol (**4**) to monoterpenes was also investigated. Additionally, a tentative explanation of the mechanism towards the formation of the monoterpenes was proposed. To the best of our knowledge, formation of monoterpenes via a one-pot, cascade transesterification dehydration of geranyl isovalerate (**1**) and its intermediate products geraniol (**3**) and nerol (**4**) in a non-catalytic sub/supercritical water-methanol process has not been previously reported.

6.2. Materials and Method

6.2.1. Materials

Natural, food grade geranyl isovalerate was obtained from Sigma-Aldrich. Geraniol and nerol were obtained from Alfa Aesar and Fisher Scientific, respectively. Methanol from VWR Chemicals and deionised water were used as a co-solvents and catalysts. All the chemicals in the study are commercially available and used without purification.

6.2.2. Experimental procedure

For the geranyl isovalerate (**1**) experiments, deionised water, methanol and geranyl isovalerate (**1**) at molar ratios of 40:20:1 was used for the reaction. The materials were transferred to a 70 mL high-pressure stainless steel autoclave along with a magnetic stirrer. Then the autoclave was sealed and placed on a magnetic hotplate and a temperature sensor was inserted. The hotplate was set to the maximum temperature of 400 °C and 1500 rotation per minute (rpm) was used. After a 2 h reaction time, the temperature and stirring was turned off and the autoclave was placed in a water bath to cool to room temperature. Once cooled, 2mL samples of the product were collected into Thermo Scientific autosampler vials for gas chromatography mass spectrometry analysis. The geranyl isovalerate (**1**) experiment was repeated for reproducibility analysis.

The same procedure was used for the geraniol (**3**) and nerol (**4**) experiments except for the following changes. The effect of various molar ratios of deionised water, methanol and geraniol (**3**) or nerol (**4**) were examined. The ratios examined were 40:20:1, 80:10:1, 40:5:2, 40:10:0.5, 20:20:0.5, 0:100:1, respectively at a constant temperature setting 400 °C, 1500 rpm, and reaction time of 2 h. For the geraniol (**3**) experiments a ratio of 100:0:1 was also examined. The influence of various reaction times of 1 h, 2 h, 3 h, 4 h, and 5 h was also examined at constant reaction ratios of 40:20:1 and reaction temperature of 400 °C. Finally, the effect of various reaction temperature setting of 400 °C, 200 °C, 150 °C and 100 °C at constant reaction ratios of 40:20:1 and reaction time of 2 h was investigated.

6.2.3. Analytical methods

The liquid samples were analysed using gas chromatography mass spectrometry (GCMS). The aim of using GCMS analysis was to identify the components and their relative percentages in the samples. A Thermo scientific TRACE 1300 Gas Chromatograph and ISQ LT Single Quadrupole Mass Spectrometer was used. The GC column used for separation was Agilent J&W DB-1701 polysiloxane column, i.d. 0.25mm, 15m length, 0.25 μ m film thickness. The column oven temperature program was as follows: the GC oven temperature was initially held at 45 °C for 2.5 min, then ramped up at 10 °C/min to 280 °C, and held at 280 °C for 7.5 min. Helium was used as the GC carrier gas at a flow rate of 1.25mL/min. The total time for each injection run was 33.5 min and the injection temperature was 280 °C. Split injection mode was used at split ratio of 20 with 25 ml/min split flow and 5 ml/min purge flow. The mass spectrometer was configured for electron impact ionization at 70 eV, with an interface temperature of 250 °C and an ion source temperature of 200 °C. Full scan data were acquired and processed using Chromeleon™ 7.2 Chromatography Data System (CDS) software.

6.3. Results and Discussions

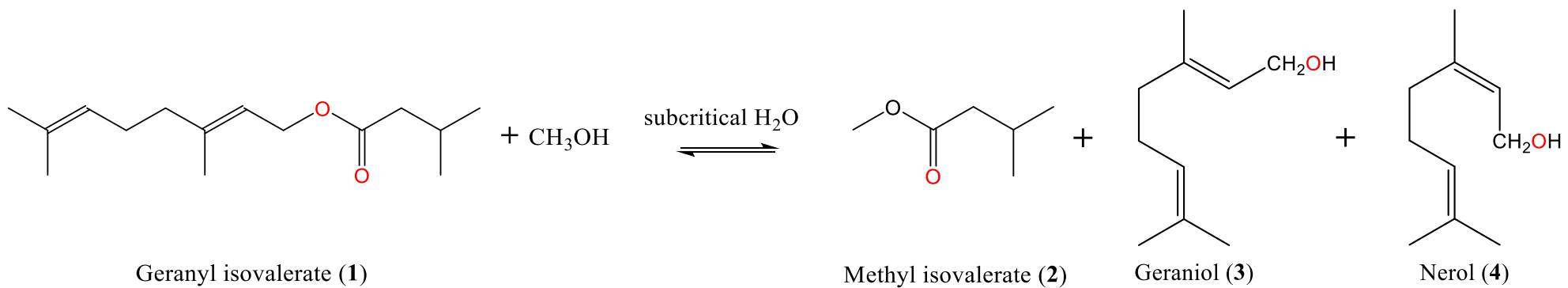
6.3.1. Transformation of the bio-oil compound geranyl isovalerate to methyl isovalerate and a mixture of monoterpenes

In chapter 4, the compound geranyl isovalerate (**1**) was identified by GCMS in the sample of crude bio-oil. In this chapter, the ester was transformed in a one-pot process without any catalysts and with a sub/supercritical water-methanol mixture which performed the role of co-solvents. Additionally, the subcritical water behaved like a catalyst. The transformation included a cascade reaction of transesterification and dehydration as illustrated in Schemes 6.1 and 6.2. Firstly, the transesterification of geranyl isovalerate (**1**) produced methyl isovalerate (**2**) and the intermediates geraniol (**3**) and nerol (**4**). Subsequently, geraniol (**3**) /nerol (**4**) underwent a dehydration reaction which produced a mixture of monoterpenes.

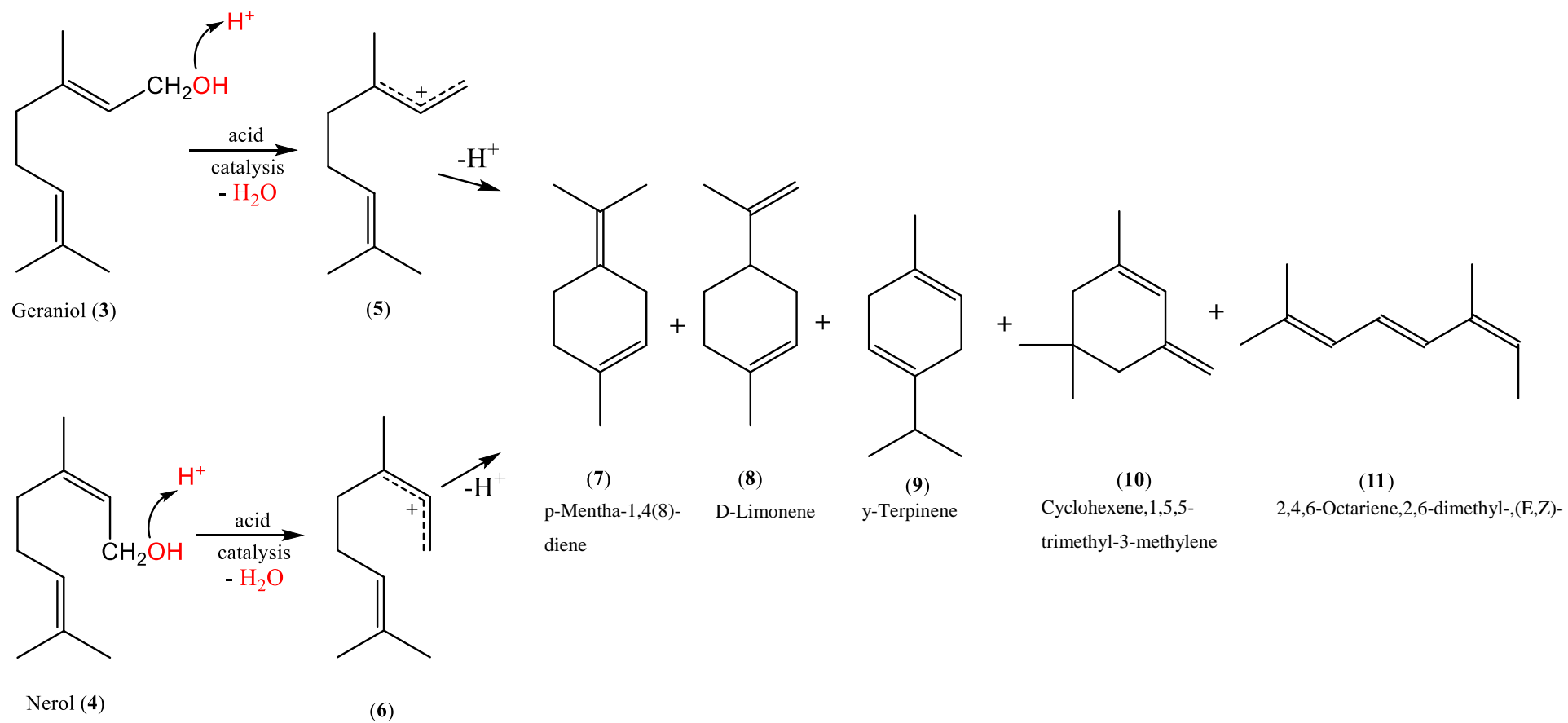
With Schemes 6.1 and 6.2, a tentative mechanistic explanation of monoterpene formation from geranyl isovalerate (**1**) is described as follows. Acid catalysed transesterification of geranyl isovalerate (**1**) (using subcritical water as the acid catalyst and sub/supercritical water-methanol mixture as solvent), forms methyl isovalerate (**2**), geraniol (**3**) and nerol (**4**). This follows the general steps of acid catalysed transesterification described in section 6.1.3 Transesterification. The alcohols geraniol (**3**) and nerol (**4**) form as side products of the transesterification reaction and function as intermediates to monoterpene formation.

The next steps are similar to literature reports by Costa et al. and Eisenacher et al. [99,101]. The oxygen atom of the hydroxyl group in geraniol (**3**) or nerol (**4**) uses a pair of electrons to bond with a hydrogen ion available in the acidic solution. The formed H₂O molecule leaves i.e. dehydration of geraniol (**3**) and nerol (**4**). An allylic carbocation is formed (**5**) (**6**) at the terminal

trisubstituted bond. Dehydrogenation of **(5)** and **(6)** leads to the formation of monoterpenes including : p-Mentha-1,4(8)-diene **(7)**, D-Limonene **(8)**, γ -Terpinene **(9)**, Cyclohexene,1,5,5-trimethyl-3-methylene **(10)**, 2,4,6-Octariene,2,6-dimethyl-,(E,Z)- **(11)**.



Scheme 6.1 Transesterification of geranyl isovalerate.



Scheme 6.2 Dehydration and cyclisation of geraniol and nerol

Table 6.1 Summary of the GCMS analysis results of the geranyl isovalerate reaction products.

Full GCMS data is available in Appendix 3.- Table 1 and 2

Compound	Formula	Average Relative Area% TIC Experiment 1	Average Relative Area% TIC Experiment 2	Mean ± standard deviation
Methyl isovalerate	C ₆ H ₁₂ O ₂	28.77	27.28	1.05
Isovaleric acid	C ₅ H ₁₀ O ₂	0.47	0.82	0.25
1,3-Cyclohexadiene,1,3,5,5-tetramethyl- y-Terpinene	C ₁₀ H ₁₆	1.05	1.04	0.01
Cyclohexene,1,5,5-trimethyl-3-methylene	C ₁₀ H ₁₆	10.92	11.75	0.59
1,3-Cyclopentadiene,5,5-dimethyl-1-propyl	C ₁₀ H ₁₆	6.84	6.81	0.02
p-Mentha-2,8-diene,(1R,4R)-(+)- D-Limonene	C ₁₀ H ₁₆	0.15	0.21	0.04
p-Mentha-1,4(8)-diene	C ₁₀ H ₁₆	0.70	1.00	0.21
3-Carene	C ₁₀ H ₁₆	7.65	3.96	2.61
Cyclohexene, 5-methyl-3-(1-methylethenyl)- ,trans(-)	C ₁₀ H ₁₆	33.89	37.27	2.39
2,4,6-Octariene,2,6-dimethyl-,(E,Z)-	C ₁₀ H ₁₆	2.62	1.62	0.71
2,6-Octadiene,1-(1-ethoxyethoxy)-3,7-dimethyl	C ₁₄ H ₂₆ O ₂	0.47	1.31	0.59
Geranyl Isovalerate	C ₁₅ H ₂₆ O ₂	4.00	5.22	0.86
Total		0.35	0.14	0.15
		2.13	1.57	0.40
		100.01	100.00	

Table 6.1 displays the GCMS analysis results of the geranyl isovalerate (**1**) reaction products. The chromatographic peak area % of a compound is considered linear with its concentration. Therefore, the corresponding chromatographic peak area % of the compounds can be compared. 10 out of 13 product compounds detected by the GCMS after the reaction were monoterpenes and approximately 69.24 % of the total relative area count was identified as monoterpene compounds. Methyl isovalerate (**2**) was identified as the newly formed ester from the transesterification reaction and constituted roughly 28 % of the total product. The reaction was repeated to confirm the findings and both experiments achieved 99 % conversion of the reactant geranyl isovalerate (**1**). The compound p-Mentha-1,4(8)-diene (**7**) dominated the monoterpene products, accounting for over 50 % of the monoterpene products. γ -Terpinene (**9**) also formed a notable proportion of the monoterpene products at 17 %. This was closely followed by D-Limonene (**8**) and Cyclohexene,1,5,5-trimethyl-3-methylene (**10**) accounting for 9 % and 10 % of the total monoterpene products, respectively. Interestingly, the compound 2,4,6-Octariene, 2,6-dimethyl-, (E,Z)- (**11**) was the only acyclic monoterpene detected. This indicates the reaction favours the formation of cyclic monoterpenes, specifically with six-membered carbon rings.

In order to gain further insight into the formation of the monoterpenes, experiments were carried out using the geranyl isovalerate (**1**) transesterification reaction intermediates; geraniol (**3**) and nerol (**4**). The reaction intermediates, which are not detected in the GCMS results of the geranyl isovalerate (**1**) reaction products (Table 6.1), are speculated to appear based on the tentative mechanism discussed in Schemes 6.1 and 6.2. Various operating conditions were applied, and their influence was discussed. A selection of different molar ratios of the reactant (geraniol (**3**) or nerol (**4**)), methanol and water was utilised to examine the effects of varying ratios of starting materials can have on the product distribution, reactant conversion and product selectivity. Additionally, the effects of temperature and time on the reaction and its products was also investigated.

6.3.2. Reproducibility

To determine the reproducibility of the experimental procedure and set up, two monoterpene production experiments were performed using geranyl isovalerate (**1**) as the feedstock. The same molar ratio (40:20:1) of deionised water, methanol and geranyl isovalerate (**1**) was used. Also, the same temperature setting of 400 °C, reaction time of 2 h, and 1500 rpm was used. This was done to ensure the results could be accurately compared. Each product sample was analysed by GCMS twice and an average of the relative area % of the two runs was taken. A summary of the GCMS analysis results is provided in Table 6.1 and the full GCMS analysis results including the standard deviations is provided in Appendix 3 Table 1 and 2.

For the geraniol (**3**) and nerol (**4**) experiments, each product was analysed by GCMS three times to calculate the mean standard deviation and to indicate the experimental error range.

The GCMS analysis results provided in the main text are summaries and include averages of the relative area % of the three runs taken. The full GCMS analysis results including the standard deviations is provided in Appendix 3.

Table 6.1 shows that both experiments achieved very high conversion of geranyl isovalerate (1) as only 2.13 % and 1.57 % of it was detected in both products and the mean standard deviation is only ± 0.40 . The product distribution is very similar and both products contained 14 different compounds. As both experiments achieved over 90 % conversion and the relative area % of the components in each product are in < 5 % range, it can be expected that further experiments will produce reproducible results. Therefore, each geraniol (3) and nerol (4) experiment was performed once and analysed by GCMS three times.

6.3.3. Various molar ratio of water, methanol, and geraniol

Different molar ratios of water, methanol and geraniol (3) were examined to study the effect of varying conditions on the product. Table 6.2 provides a summary of GCMS analysis results of the geraniol (3) reaction products at various starting material ratios, constant heating temperature (400 °C) and time (2 h). As the chromatographic peak area % of a compound is considered linear with its concentration, the corresponding chromatographic peak area % of the compounds can be compared. For example, the peak area % of p-Mentha-1,4(8)-diene (7) after each reaction can be compared to examine the effects of the varying reaction parameters on the products. Additionally, the peak area % can be used to compare the change of the relative content of the compound among the detected compounds [43,56].

All the reactions with varying ratios proceeded and generated products except 0:100:1 (H₂O:methanol:geraniol) molar ratio. Comparably, with no methanol addition (100:0:1) the reaction comfortably progresses forming 90.91 % cyclic products. This highlights the distinct roles of methanol and water in this aqueous-alcohol-solvent reaction system. Water is strongly dissociated at its critical point and can display the properties of an acid catalyst [92]. As reported by several researchers, water in the critical region can be used to catalyse terpene transformation reactions [92,95,103]. Water interacts with the reagent by donating hydrogen ions which initiates the reaction. Therefore, water can function as a solvent and catalyst in non-catalytic reactions to produce terpenes. Supercritical methanol can offer advantages due to its high pressure which influences the rate of the chemical reaction due to: a specific interaction of methanol with the molecules of the dissolved substance, the unique properties of the supercritical methanol, and the interaction of the clusters of dissolved substances with the solvent [92].

Table 6.2 Summary of GCMS analysis results of the geraniol reaction products at various starting material ratios.

Constant heating setting temperature (400 °C) and time (2 h). Full GCMS data is available in Appendix 3.- Table 3 to 8.

Compound	Relative Area% at various molar ratios of H ₂ O:Methanol:Geraniol						
	40:20:1	80:10:1	40:5:2	40:10:0.5	20:20:0.5	100:0:1	0:100:1
D-Limonene	17.71	20.60	8.48	15.24	11.87	27.35	
p-Mentha-1,4(8)-diene	42.05	32.16	38.73	41.93	12.64	17.80	
γ-Terpinene	11.43	5.45	10.01	7.67	0.81	8.47	
Beta-Pinene	3.71	2.54	0.50	1.91	0.21	3.39	
Alpha-Terpineol	0.15	3.84	2.49	2.94	17.63	2.02	
1,3-Cyclohexadiene,1,3,5,5-tetramethyl	3.39	5.62	6.64	6.68	6.10	6.44	
1,2,4,4-Tetramethylcyclopentene	0.16	0.19	0.54	0.20	0.12		
1,3-Cyclopentadiene,5,5-dimethyl-1-propyl	0.27		0.38				
o-Cymene	0.89	1.16	7.22	2.72	2.73	17.58	
p-Mentha-3,8-diene	0.10		0.75		1.71	0.87	
1,3-Cyclopentadiene,5,5-dimethyl-2-propyl	0.45	0.60	1.44	1.37	1.39		
2H-Pyran,2-ethenyltetrahydro-2,6,6-trimethyl						0.64	
5-Caranol,(1S,3R,5S,6R)-(-)-			0.10		0.41		
Terpinen-4-ol		0.12	0.10		0.27		
Cyclopentane,2-methyl-1-methylene-3-(1-methylethenyl)-		0.54			1.43		
4-Caranone,cis		0.16	0.30	0.63	0.07	0.13	
2-Norbornanone,1,3,3-trimethyl			0.24		0.30		

Compound	Relative Area% at various molar ratios of H ₂ O:Methanol:Geraniol						
	40:20:1	80:10:1	40:5:2	40:10:0.5	20:20:0.5	100:0:1	0:100:1
p-Menth-2-ene			0.10				
2-tert-Butyltoluene			0.41		0.85		
Cyclopentanol,3-isopropenyl-1,2-dimethyl-,(1R,2S,3S)-(-)-					1.87		
p-Menth-3-ene,(R)-(+)-					0.30		
2-Bornene						1.24	
p-Mentha-2,8-diene,(1R,4R)-(+)-						3.48	
p-Cymene						0.32	
p-Menth-3-ene						1.03	
p-Mentha-1,3,8-triene						0.15	
Total Cyclic Compounds	80.31	72.98	78.44	81.29	60.70	90.91	0.00
Beta-Ocimene	7.49	7.21	5.06	5.34	1.89		
2,4,6-Octariene,2,6-dimethyl-,(E,Z)-	4.39	5.60	0.90	0.53			
(2E)-1-Methoxy-3,7-dimethylocta-2,6,diene	4.32	2.21	2.98	1.79	29.30	0.81	
Nerol, methyl ether	1.11				0.15		
Geraniol		9.24	5.89	6.70	5.18	4.09	100.00
Beta-Linalool	0.41	2.65	4.21	2.26	0.99	3.73	
Linalool, methyl ether	1.96		2.53	2.11	1.41	0.13	
Linalyl 3-methylbutanoate						0.12	
2,6-Dimethyl-2-trans-6-octadiene		0.13			0.38		

Compound	Relative Area% at various molar ratios of H ₂ O:Methanol:Geraniol						
	40:20:1	80:10:1	40:5:2	40:10:0.5	20:20:0.5	100:0:1	0:100:1
2,6-Octadiene,1-(1-ethoxyethoxy)-3,7-dimethyl						0.22	
Total Acyclic Compounds	19.67	27.03	21.57	18.71	39.30	9.09	100.00
Total Compounds	99.99	100.01	100.01	100.00	100.00	100.00	100.00

Although a high proportion of cyclic products are formed at the H₂O:methanol:geraniol molar ratio of 100:0:1, this reaction has one of the highest number of different product compounds, therefore the product selectivity is low. This may be because although a heating setting temperature of 400 °C was applied, this reaction peaked at 369 °C and 92 bar. This is below the critical point of water (374 °C and 221 bar) so it can only be considered a subcritical water reaction. Therefore, this reaction does not have the advantage of high selectivity that come with operating in the supercritical phase [92,102].

The results show supercritical methanol has a positive effect on the product selectivity. The H₂O:methanol:geraniol molar ratios 40:10:0.5, 40:20:1 and 80:10:1 there are a total of 15, 17, and 17 different product compounds, respectively. It seems the product selectivity is improved with more methanol present in the feed because with feed ratios with less methanol such as 40:5:2 and 100:0:1 the number of different compounds is 22 and 20, respectively. At the equimolar water and methanol condition (H₂O:methanol:geraniol molar ratios 20:20:0.5), the lowest product selectivity is observed as 24 different compounds are present in the product. This may be due to the conflicting effects of the methanol and water on the reaction when equimolar amounts are used which hinders the product selectivity. Ikushima and Sato reported similar findings when they used an equimolar solution of water and methanol to form monoterpene alcohols under supercritical conditions [95]. At 1:1 water-methanol ratio, no monoterpene alcohols were formed. The authors mentioned that methanol in the high-temperature water medium suppresses the acidic ability of supercritical H₂O. This interfered with the protonation of the intermediate and ultimately prevented product formation.

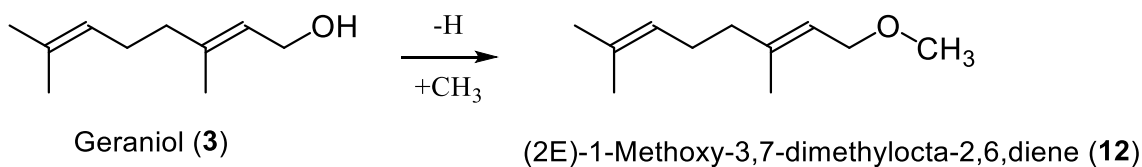
Comparing the products of the different molar ratio reactions, there is a consistently higher proportion of cyclic compounds than acyclic compounds in the products; regardless of the varying molar ratio. Therefore, this non-catalytic sub/supercritical aqueous-alcohol solvent condition tends more towards the conversion of geraniol (**3**) to cyclic compounds than acyclic. In comparison, the research by Costa et al. and Eisenacher et al. showed acidic catalyst gas phase treatment of geraniol (**3**) to form monoterpenes generally led to more acyclic than cyclic compounds [99,101]. Costa et al. reported cyclic to acyclic ratio of 1:9 and Eisenacher et al. reported a ratio of 1:4, respectively. For this work, the target compounds are cyclic monoterpenes, therefore this non-catalytic sub/supercritical aqueous-alcohol solvent condition is ideal and preferred to the acidic catalyst gas phase treatment method reported in literature.

Except for the equimolar solvent (20:20:0.5) and the non-methanol (100:0:1) reaction conditions, the total cyclic compounds produced at the various ratios is generally in the range of 70-80%. The lowest proportion of cyclic compounds is at H₂O:methanol:geraniol molar ratios 20:20:0.5. At the H₂O:methanol:geraniol molar ratios 100:0:1, 90.91 % of the products formed are cyclic compounds. However, as mentioned this ratio does not present the highest product selectivity.

The total acyclic compounds at the H₂O:methanol:geraniol molar ratios 80:10:1 was a noticeably high 27.03 %, relative to the other ratios. Geraniol (**3**) and the acyclic monoterpenes beta-ocimene and 2,4,6-Octatriene,2,6-dimethyl-,(E,Z)- (**11**) accounted for majority of the acyclic product at 9.24 %, 7.21 %, and 5.60 % respectively. The relatively larger content of total acyclic compounds, particularly the amounts of geraniol (**3**) in the product indicates that this reactant ratio was comparably less effective in converting geraniol (**3**) to the desired products. With respect to the other reactant ratios, at 80:10:1 one of the lowest total cyclic compounds (72.98 %) was generated. p-Mentha-1,4(8)-diene (**7**) and D-Limonene (**8**) formed most of the product at 32.16 % and 20.60 %, respectively. Comparing the product distribution of the various ratios, this is the second highest amount of D-Limonene (**8**) in a product only preceded by the reactant ratio 100:0:1 which generated more D-Limonene (27.35 %) than p-Mentha-1,4(8)-diene (**7**) (17.80 %). This may indicate that at the other ratios (40:10:0.5, 40:20:1 and 40:5:2) the dehydration of geraniol (**3**) followed by cyclisation to monoterpenes favoured the formation of p-Mentha-1,4(8)-diene (**7**), however at the ratios 80:10:1 and 100:0:1 this route was challenged by D-Limonene (**8**) formation. The increased tendency to D-Limonene (**8**) formation may also be due to the comparably higher concentration of water at the ratios 80:10:1 and 100:0:1. As Anikeev also found raising the concentration of water in a reaction mixture with supercritical alcohol-water to convert α -pinene led to an increase in the yield of limonene from 57 % to 69 % [92]. This effect is reportedly due to the supercritical conditions imparting acidic catalyst properties to water which affects the reaction mechanism, selectivity and the rate of the overall reaction [92].

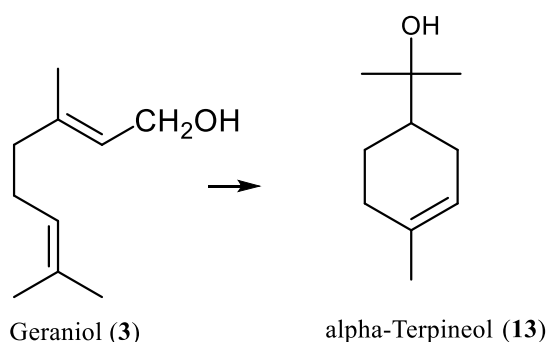
At 40:10:0.5, the monoterpenes, p-Mentha-1,4(8)-diene (**7**) and D-Limonene (**8**) accounted for the highest percentage of the product with 41.93 % and 15.24 %, respectively. As a result, the total cyclic compounds in the product was 81.29 % which is the second highest amount relative to the other various ratios. The high content of p-Mentha-1,4(8)-diene (**7**) demonstrates that this reactant ratio offers good conditions for the dehydration of geraniol (**3**) to selectively produce cyclic monoterpenes. The total acyclic compounds at this reactant ratio was 18.71 %, and geraniol (**3**) accounted for majority of the acyclic products at 6.70 %. This reactant ratio produced one of the lowest amounts of total acyclic compounds in comparison to the products of the other reactant ratios.

At the H₂O:methanol:geraniol molar ratios 20:20:0.5, the lowest proportion of cyclic compounds (60.70 %) and consequently the highest acyclic compounds (39.30 %) was formed. The compound (2E)-1-Methoxy-3,7-dimethylocta-2,6,diene (**12**) constitutes 29.30 % of the product and is a derivative of geraniol. Scheme 6.3 shows the hydrogen on the hydroxyl group of geraniol (**3**) is substituted by a methyl group to produce (2E)-1-Methoxy-3,7-dimethylocta-2,6,diene (**12**).



Scheme 6.3. Geraniol conversion to (2E)-1-Methoxy-3,7-dimethylocta-2,6,diene (**12**)

As described in the tentative mechanistic explanation in section 6.3.1. and Scheme 6.2. the typical steps for the formation of a cyclic monoterpene includes geraniol (**3**) dehydration and cyclisation catalysed by subcritical water as the acid catalyst. However, at H₂O:methanol:geraniol molar ratios 20:20:0.5 it appears the catalytic ability of subcritical water was suppressed because less cyclic monoterpenes were produced and (2E)-1-Methoxy-3,7-dimethylocta-2,6,diene (**12**) dominated the reaction product. This may be due to the incompatible effects of supercritical methanol and subcritical water when equimolar methanol and water is used for the reaction. This interesting solvent effect was also observed by Ikushima and Sato who failed to produce monoterpene alcohols at reaction conditions of 1:1 water-methanol ratio [95]. The authors explained that the presence of methanol in the high-temperature water medium restricts the acidic ability of supercritical H₂O. As a result, this interfered with the protonation of the intermediate and ultimately prevented product formation [95]. This solvent effect may also be associated with the relatively lower product selectivity at this reactant ratio as it also produced the highest number of different compounds. Interestingly, at this reactant ratio, alpha-Terpineol (**13**) accounted for the biggest proportion of the cyclic compounds at 17.63 %. Figure 6.1 highlights the relatively larger alpha-Terpineol (**13**) in this product (20:20:0.5) compared to the other ratios. This is the largest amount of alpha-Terpineol (**13**) present in any of the geraniol (**3**) reaction products. Additionally, gamma-Terpinene (**9**), which forms around 5-11 % of the product in the other reaction ratios, only forms 0.81 % at this ratio (20:20:0.5). The dominant formation of alpha-Terpineol (C₁₀H₁₈O) rather than p-Mentha-1,4(8)-diene (**7**) (C₁₀H₁₆) and D-Limonene (**8**) (C₁₀H₁₆) further indicates the repressed acidic ability of subcritical water to promote dehydration reactions at this reaction condition. Although geraniol (**3**) formed a small 5.18 % of the reaction product, the conversion to the desired cyclic monoterpene compounds was low.



Scheme 6.4 Geraniol conversion to alpha-Terpineol (**13**).

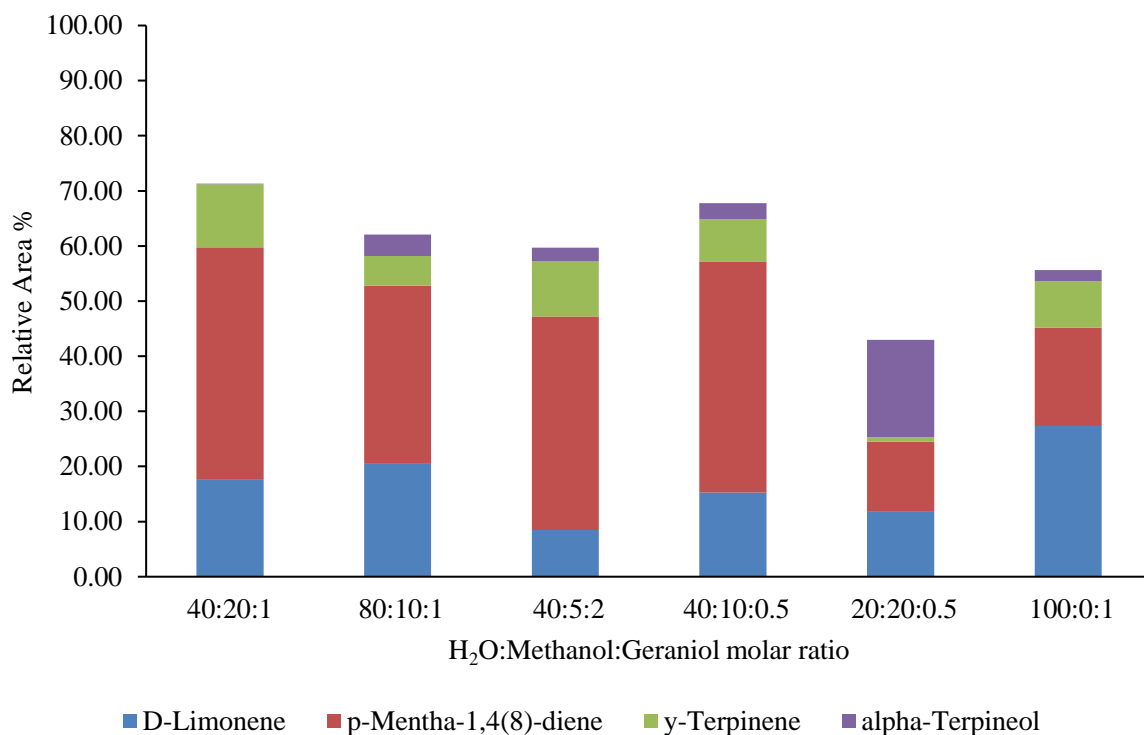
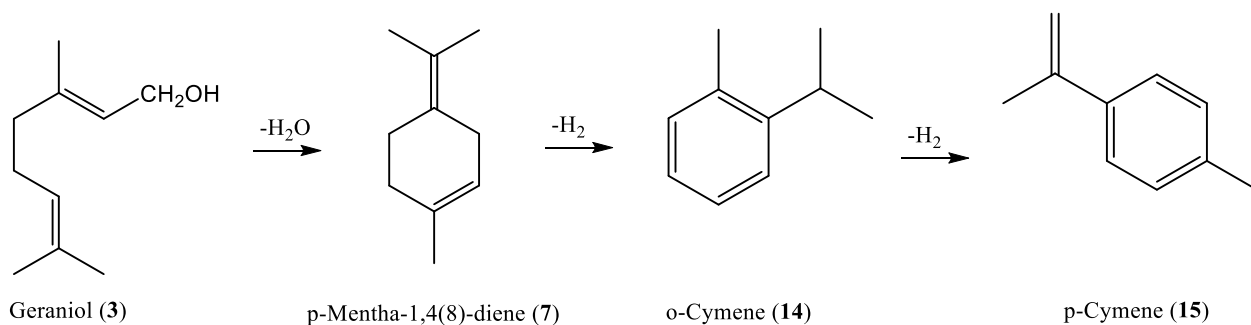


Figure 6.1 Major compounds in the geraniol reaction products at various starting material ratios.

Constant heating temperature (400 °C) and time (2 h)

The product distribution of the H₂O:methanol:geraniol molar ratio 100:0:1 is particularly interesting because of the relatively large amount of o-Cymene (**14**) formed.



Scheme 6.5 Geraniol conversion to o-Cymene (**14**) and p-Cymene (**15**)

o-Cymene (**14**) is an isomer of the favourable and high price monoterpene p-cymene (**15**) [102]. The proportion of o-cymene (**14**) to p-cymene (**15**) in the product is 17.58 % to 0.32 %, hence the reaction tended towards the formation of the less popular cymene isomer (o-cymene (**14**)). The distinctively high amount of cyclic compounds (90.91 %) at 100:0:1 molar ratio is primarily due to the high o-cymene (**14**) content in the product which does not occur at the other reactant ratios. While the o-cymene (**14**) content is high, the amount of p-Mentha-1,4(8)-diene (**7**) is significantly lower than that of all the other ratios, except 20:20:0.5. This may

suggest an enhanced acidic ability of water at the absence of supercritical methanol to catalyse the dehydrogenation of p-Mentha-1,4(8)-diene (**7**) to o-cymene (**14**). As Ikushima and Sato noted, methanol in a high-temperature water medium suppresses the acidic ability of supercritical H₂O [95]. Another unique facet of the product distribution at 100:0:1 molar ratio, is that D-Limonene (**8**) is the major compound accounting for 27.35 % of the total product. This is the highest amount of D-Limonene (**8**) present in a reaction product out of all the various ratios. γ -Terpinene (**9**) and 1,3-Cyclohexadiene,1,3,5,5-tetramethyl account for a modest 8.47 % and 6.44 % of the product, respectively which is a typical amount in all the different ratios. Only 9.09 % of the total product are acyclic compounds, therefore this reactant ratio produced the lowest amount of acyclic compounds. This is ideal because the target compounds are cyclic monoterpenes. However, geraniol (**3**) forms most of the acyclic compounds hence the conversion was not completed at the given time and temperatures at this feed ratio.

The lowest amount of D-Limonene (**8**) (8.48 %) (compared to the other ratios) was produced at the H₂O:methanol:geraniol molar ratio 40:5:2. Even though the ratio of water to methanol at 40:5:2 is the same as the reaction ratio 80:10:1 -which generated a product with one of the highest d-limonene (**8**) contents. The excess geraniol (**3**) at 40:5:2 may have pushed the reaction towards the formation of p-Mentha-1,4(8)-diene (**7**) which was the major reaction product (38.73 %) at this ratio. However, as mentioned earlier, despite the high content of p-Mentha-1,4(8)-diene (**7**), the product selectivity is low as there are 22 different compounds in the product. Moreover, the reaction ratio 40:5:2 produced one of the highest γ -Terpinene (**9**) contents with respect to the various ratios, albeit only 10.01 % of the total product. Furthermore, a higher than average amount of o-Cymene (**14**) compared to the other ratios is observed at 40:5:2. This may be linked to the improved acidic ability of water at lower concentration of supercritical methanol to catalyse the dehydrogenation of p-Mentha-1,4(8)-diene (C₁₀H₁₆) (**7**) to o-cymene (C₁₀H₁₄) (**14**) as shown in Scheme 6.5. The total acyclic compounds at 40:5:2 molar ratio was 21.57 %. Geraniol (**3**) and the acyclic monoterpene beta-ocimene accounted for a similar amount of the total acyclic product at 5.89 % and 5.06 %, respectively.

The selectivity is very high at the H₂O:methanol:geraniol molar ratios 40:20:1. p-Mentha-1,4(8)-diene (**7**), D-Limonene (**8**), and γ -Terpinene (**9**) collectively accounted for 71.19 % of the total product and 88.64 % of the total cyclic compounds. The high content of these monoterpenes demonstrates that this reactant ratio offers excellent conditions for dehydration of geraniol (**3**) to selectively produce cyclic monoterpenes. Moreover, complete conversion of geraniol (**3**) was only observed at this reactant ratio. This indicates excess molar ratio of water is not necessarily ideal for complete conversion of geraniol (**3**) despite its advantages of enhanced acidic ability. The acyclic monoterpenes beta-ocimene and 2,4,6-Octariene,2,6-dimethyl-,(E,Z)- (**11**) formed 7.49 % and 4.39 % and beta-ocimene accounted for the largest percentage

of the total acyclic compounds. The compound (2E)-1-Methoxy-3,7-dimethylocta-2,6,diene (**12**) also formed 4.32 % of the total product. This indicates although complete conversion of geraniol (**3**) was observed, side products such as (2E)-1-Methoxy-3,7-dimethylocta-2,6,diene (**12**) were also prevalent alongside the cyclic monoterpenes.

6.3.4. Various molar ratio of water, methanol, and nerol

Nerol (**4**) is isomeric with geraniol (**3**) and can also form during the transesterification of geranyl isovalerate (**1**). Various molar ratios of water, methanol and nerol (**4**) were examined to study the effect of varying reactant conditions on the product yield and distribution. Table 6.3 shows the GCMS analysis results of the nerol (**4**) reaction products at various starting material ratios constant heating temperature (400 °C) and time (2 h).

Like the geraniol (**3**) results, all the reactions with varying ratios proceeded and generated products except 0:100:1 (H₂O:methanol:nerol) molar ratio. This is a confirmation of the importance of an acid catalyst or sub/supercritical water appropriating the properties of an acid catalyst to initiate the reaction and facilitate product formation. Moreover, even though the reaction at 0:100:1 molar ratio was operated under supercritical methanol conditions which has been shown to promote reactions without catalyst addition, and methanol can offer its own acidic ability [95] the reaction failed to generate product. Therefore, water forms an integral part of this one-pot monoterpene synthesis as a solvent and catalyst.

In terms of selectivity, at the H₂O:methanol:nerol ratio 40:5:2, a total of 18 different compounds were identified and 12 were cyclic which is comparably less than when geraniol (**3**) was used as the reagent (22 compounds identified, 17 of them cyclic). Therefore, the selectivity is higher with nerol (**4**) at this ratio compared to geraniol. The opposite effect is observed at the ratio 40:10:0.5. With nerol (**4**) a total of 24 different compounds were identified and 17 were cyclic. Whereas with geraniol (**3**) a total of 15 different compounds were identified and 10 were cyclic. Therefore, the selectivity is lower with nerol (**4**) at H₂O:methanol:nerol ratio of 40:10:0.5 compared to geraniol at this ratio. Nerol (**4**) showed similarly poor selectivity as geraniol (**3**) at the ratio 20:20:0.5. Both reagents generated products with 24 different compounds. This confirms the solvent effect observed at the equimolar water methanol water ratio 20:20:0.5. The conflicting effects of the methanol and water on the reaction when equimolar amounts are used reduces the product selectivity. As reported by researchers, at a 1:1 ratio, methanol in the high-temperature water medium suppresses the acidic ability of supercritical H₂O consequently limits the formation of the target product [95]. Once again, the highest product selectivity is observed at the ratios 40:20:1 and 80:10:1 with nerol (**4**) as it was with geraniol (**3**) as the reagent.

Table 6.3 Summary of GCMS analysis results of the nerol reaction products at various starting material ratios.

Constant heating setting temperature (400 °C) and time (2 h). Full GCMS data is available in Appendix 3.- Table 9 to 13.

Compound	Relative Area% at various ratios of H ₂ O:Methanol:Nerol					
	40:20:1	80:10:1	40:5:2	40:10:0.5	20:20:0.5	0:100:1
D-Limonene	22.55	5.18	10.46	10.26	18.03	
p-Mentha-1,4(8)-diene	47.05	57.37	47.51	42.84	22.87	
γ-Terpinene	12.88	15.99	10.99	11.06	2.18	
Beta-Pinene	2.26	1.18	0.19	0.62	0.83	
Alpha-Terpineol	0.10	6.04	6.91	7.91	21.94	
1,3-Cyclohexadiene,1,3,5,5-tetramethyl	1.03	1.58	2.72	2.15	2.38	
1,2,4,4-Tetramethylcyclopentene	0.07	0.09	0.18	0.13	0.05	
1,3-Cyclopentadiene,5,5-dimethyl-1-propyl	0.11					
o-Cymene	1.03	1.31	8.65	6.08	2.06	
p-Mentha-3,8-diene	0.13	1.39	0.59	0.75	1.34	
1,3-Cyclopentadiene,5,5-dimethyl-2-propyl	0.24	0.60	0.57	0.51	0.39	
p-Menth-8-en-1-ol				0.08	0.08	

Compound	Relative Area% at various ratios of H ₂ O:Methanol:Nerol					
	40:20:1	80:10:1	40:5:2	40:10:0.5	20:20:0.5	0:100:1
5-Caranol,(1S,3R,5S,6R)-(-)-				0.07	0.22	
Terpinen-4-ol		0.25	0.17	0.16	0.78	
4-Caranone,cis		0.26	0.16	0.65	0.19	
2-Norbornanone,1,3,3-trimethyl					0.15	
2-tert-Butyltoluene				0.39	0.67	
Cyclopentanol,3-isopropenyl-1,2-dimethyl-,(1R,2S,3S)-(-)-					0.75	
2-Cyclohexen-1-one, 4-ethyl-3,4-dimethyl-				0.56		
Carvacrol				0.11		
Total Cyclic Compounds	87.45	91.24	89.09	84.35	74.91	0.00
Beta-Ocimene	3.62	0.85	1.57	2.78	2.16	
2,4,6-Octatriene,2,6-dimethyl-,(E,Z)-	1.64		0.09	0.10		
(2E)-1-Methoxy-3,7-dimethylocta-2,6,diene	3.33	0.13	0.22	1.35	8.02	
Nerol, methyl ether	2.29				0.11	
Geraniol				0.45	0.95	
Beta-Linalool	0.15	0.91	2.51	2.49	1.94	
Linalool, methyl ether	1.45	1.73	1.73	3.84	2.90	

Compound	Relative Area% at various ratios of H ₂ O:Methanol:Nerol					
	40:20:1	80:10:1	40:5:2	40:10:0.5	20:20:0.5	0:100:1
2,6-Octadiene,1-(1-ethoxyethoxy)- 3,7-dimethyl		0.86	0.89	2.72	6.90	
Nerol	0.06	4.28	3.89	1.92	2.12	100.00
Total Acyclic Compounds	12.54	8.76	10.90	15.65	25.09	100.00
Total Compounds	100.00	100.00	99.99	100.00	100.00	100.00

The products of the nerol (**4**) reaction at various molar ratios all show higher proportion of cyclic compounds than acyclic compounds and the total cyclic compounds ranged from 74.91-91.24%. This is comparably higher than with geraniol (**3**) which produced total cyclic compounds ranging from 60.70-81.29% at the corresponding molar ratio conditions. Similarly, Costa et al. found the dehydration of nerol (**4**) more readily formed cyclic products than geraniol (**3**) dehydration [101]. As shown in Scheme 6.2, this may be because geraniol (**3**) and nerol (**4**) are E and Z isomers about the allylic double bond, respectively. Therefore, reactions of nerol derivatives (**6**) can more easily form cyclic products than geraniol derivatives (**5**). The structure of nerol (**4**) enables its dehydrated intermediate (**6**) to have an allylic cation which interacts with the other terminal trisubstituted bond. This interaction less readily happens with geraniol dehydrated intermediate (**5**) because the allylic cation is positioned away from the other terminal trisubstituted bond.

Like the geraniol (**3**) result at various molar ratios, the lowest proportion of cyclic compounds is at H₂O:methanol:nerol molar ratio 20:20:0.5. This may be associated with the relatively lower selectivity at this ratio which could be due to the incompatible methanol-water effects at this ratio. Additionally, like the geraniol (**3**) results at this reaction ratio, the compound (2E)-1-Methoxy-3,7-dimethylocta-2,6,diene (**12**) formed the largest fraction of the total acyclic compounds. Alongside the compound 2,6-Octadiene,1-(1-ethoxyethoxy)-3,7-dimethyl, these two acyclic non-monoterpene compounds accounted for over half of the total acyclic compounds. Hence, although the nerol (**4**) content in the final product was only 2.12 %, its conversion to the target compounds was low. As previously mentioned, this could be a result of the reduced catalytic ability of subcritical water because of the solvent effects at the 1:1 water-methanol ratio. Similar to the geraniol (**3**) results at 20:20:0.5 molar ratio, alpha-Terpineol (**13**) (C₁₀H₁₈O) accounted for a significant proportion of the cyclic compounds at 21.94 %. Figure 6.2 highlights the relatively larger alpha-Terpineol (**13**) in 20:20:0.5 compared to the other ratios. In the other reaction ratios, alpha-Terpineol (**13**) only forms between 0.10-7.91 % of the total product. p-Mentha-1,4(8)-diene (**7**) (C₁₀H₁₆) which typically forms around 42.84-57.37% of the total products at the other reaction ratios only formed 22.87 % at this reaction ratio. Additionally, γ-Terpinene (**9**), which forms 10.99-15.99 % of the product in the other reaction ratios, only forms 2.18 % at this ratio. The removal of a H₂O molecule from alpha-Terpineol (**13**) (C₁₀H₁₈O) would result in a monoterpene in the class C₁₀H₁₆. Therefore, the large content of alpha-Terpineol (**13**) at 20:20:0.5 indicates to a suppressed acidic ability of subcritical water to promote dehydration reactions at this reaction condition.

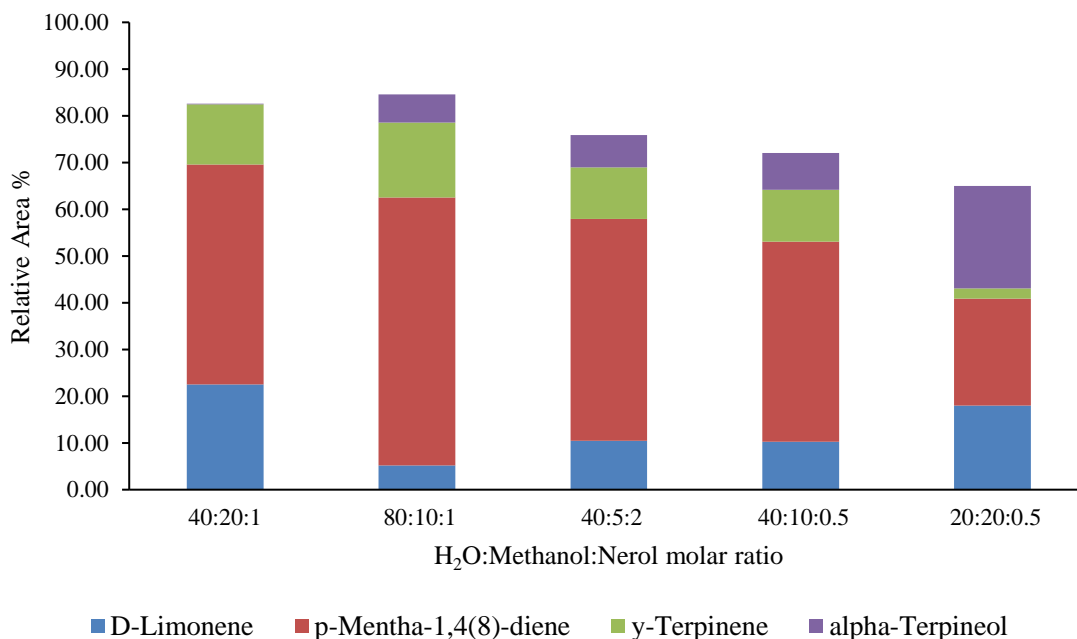


Figure 6.2 Major compounds in the nerol (**4**) reaction products at various starting material ratios.

Constant heating temperature (400 °C) and time (2 h)

At the H₂O:methanol:nerol molar ratio 40:10:0.5, p-Mentha-1,4(8)-diene (**7**), y-Terpinene (**9**) and D-Limonene (**8**) constituted major fractions of the products at 42.84 %, 11.06 % and 10.26 %, respectively. When geraniol (**3**) is used as the reagent, more D-Limonene (**8**) is usually formed than y-Terpinene (**9**) at the various reaction ratios. However, when nerol (**4**) is used as the reagent, similar amounts of y-Terpinene (**9**) and D-Limonene (**8**) are formed (at ratios 40:10:0.5 and 40:5:2) and in some cases (80:10:1) there is more y-Terpinene (**9**) than D-Limonene (**8**). Therefore, geraniol (**3**) as the reactant enables a push towards more D-Limonene formation than y-Terpinene (**9**) regardless of the reactant ratio. On the other hand, with nerol (**4**) the selectivity to D-Limonene (**8**) can be modified as necessary by varying the reactant ratios. For example, H₂O:methanol:nerol molar ratio 40:20:1 generates a product with D-Limonene (**8**) content almost double that of y-Terpinene (**9**) and 80:10:1 produces significantly lower D-Limonene (**8**) than y-Terpinene (**9**). At the ratio 40:10:0.5, alpha-Terpineol (**13**) and o-Cymene (**14**) account for 7.91 % and 6.08 % of the total product. This is comparably higher than with geraniol (**3**) as the reagent and further highlights the relatively lower selectivity attainable at this reactant ratio using nerol (**4**). A selection of acyclic products formed at this reaction ratio including non-monoterpene acyclic compounds such as Linalool methyl ether, 2,6-Octadiene,1-(1-ethoxyethoxy)-3,7-dimethyl, and acyclic monoterpenes such as Beta-Ocimene and Beta-Linalool. The diversity and number of different acyclic compounds

highlights that although nerol (**4**) only forms 1.92 % of the product, its conversion to the target products is low at this ratio (40:10:0.5).

The highest content of p-Mentha-1,4(8)-diene (**7**) (57.37 %), was detected in the product of H₂O:methanol:nerol molar ratio 80:10:1. Therefore, this reactant ratio offers good conditions for the dehydration of nerol (**4**) to create a product with high selectivity to p-Mentha-1,4(8)-diene (**7**). This reactant ratio also produced the lowest D-Limonene (**8**) content (5.18 %). Although the products of geraniol (**3**) at various ratios showed a linear relation of increasing water in the reaction leads to higher D-Limonene (**8**) content in the product, this trend does not appear to apply with nerol (**4**). In fact the opposite seems to apply; the ratios with the lower water concentration such as 20:20:0.5 and 40:20:1 exhibit higher D-Limonene (**8**) content than the ratios with the higher water concentration such as 80:10:1, and 40:5:2. The γ -Terpinene (**9**) content (15.99 %) was also higher at 80:10:1 compared to the other ratios. The higher than average amount of p-Mentha-1,4(8)-diene (**7**) and γ -Terpinene (**9**) in the product of 80:10:1 resulted in the highest total cyclic compounds (91.24 %), relative to the other ratios. As a result, the total acyclic compounds at this ratio was a very low 8.76 %. Nerol (**4**) accounted for majority of the acyclic product at 4.28 %. This indicates the acyclic intermediates such as Beta-Ocimene which are common in higher proportion in the other ratios underwent transformation to cyclic compounds. These findings indicate that this reaction ratio (80:10:1) was effective in converting nerol (**4**) to highly selective cyclic monoterpene compounds.

Similar to the geraniol (**3**) products at 40:20:1, nerol (**4**) generated a product with very high selectivity at this ratio. p-Mentha-1,4(8)-diene (**7**), D-Limonene (**8**), and γ -Terpinene (**9**) collectively accounted for 82.48 % of the total product and 94.32 % of the total cyclic compounds. The largest D-Limonene (**8**) content relative to the other ratios was obtained at 40:20:1 molar ratio. The high content of these monoterpenes demonstrates that this reactant ratio offers excellent conditions for dehydration of nerol (**4**) to selectively produce cyclic monoterpenes. Also, similar to geraniol (**3**) products at 40:20:1, nerol (**4**) conversion at this ratio was the highest as negligible amounts of nerol (0.06 %) was detected. However, acyclic compounds such as Beta-Ocimene and (2E)-1-Methoxy-3,7-dimethylocta-2,6,diene (**12**) formed 3.62 % and 3.33 % of the product. Hence, although nerol (**4**) conversion was high, undesired compounds still formed.

At the H₂O:methanol:nerol molar ratio 40:5:2, p-Mentha-1,4(8)-diene (**7**), γ -Terpinene (**9**) and D-Limonene (**8**) made up majority of the products at 47.51 %, 10.99 % and 10.46 %, respectively. Like geraniol (**3**) products at 40:5:2, a higher than average amount of o-Cymene (**14**) compared to the other ratios was detected. As previously mentioned, this may be due to the improved acidic ability of water at lower concentration of supercritical methanol to catalyse the dehydrogenation of p-Mentha-1,4(8)-diene (**7**) to o-Cymene (**14**) as shown in Scheme 6.5. The total acyclic compounds at this reactant ratio was 10.90 %. Nerol (**4**) and Beta-Linalool

accounted for most of the acyclic fraction at 3.89 % and 2.51 %, respectively. Generally, higher reactant conversion is achieved with nerol (**4**) compared to geraniol (**3**), because the amount of nerol (**4**) remaining in the products at various reaction ratios ranges from 0-4.28 %. Whereas, with geraniol (**3**) it is 0-9.24 %.

6.3.5. Effect of various reaction time - Geraniol

The effect of various reaction times (1 h, 2 h, 3 h, 4 h, 5 h) at constant temperature setting (400 °C) and H₂O:Methanol:Geraniol molar ratio (40:20:1) on the reaction products of geraniol (**3**) conversion was investigated. A summary of the GCMS analysis results is provided in Table 6.4.

Table 6.4 Summary of GCMS analysis results of the geraniol reaction products at various reaction times.

Constant temperature setting (400 °C) and H₂O:Methanol:Geraniol molar ratio (40:20:1). Full GCMS data is available in Appendix 3.- Table 3 and 14 to 17.

Compound	Relative Area% at various reaction time				
	1 h	2 h	3 h	4 h	5 h
D-Limonene	19.24	17.71	37.00	13.73	15.94
p-Mentha-1,4(8)-diene	32.56	42.05	22.88	43.86	40.36
γ-Terpinene	6.88	11.43	12.66	9.96	7.78
Beta-Pinene	4.70	3.71	3.27	0.55	0.39
Alpha-Terpineol	5.03	0.15	2.82	2.92	2.56
1,3-Cyclohexadiene,1,3,5,5-tetramethyl	1.06	3.39	6.37	5.80	7.40
1,2,4,4-Tetramethylcyclopentene		0.16		0.23	0.26
1,3-Cyclopentadiene,5,5-dimethyl-1-propyl	0.16	0.27		0.24	0.30
o-Cymene	0.21	0.89	6.78	4.70	6.57
p-Mentha-3,8-diene	0.32	0.10	0.43	0.59	0.71
1,3-Cyclopentadiene,5,5-dimethyl-2-propyl		0.45	0.17	1.22	1.41
p-Menth-8-en-1-ol	0.16				
5-Caranol,(1S,3R,5S,6R)-(-)-	0.40			0.10	
2-Cyclohexene-1-methanol,2,6,6-trimethyl-	0.09				
Terpinen-4-ol	0.12			0.09	
4-Caranone,cis	0.28		0.57	0.57	0.43
2-Norbornanone,1,3,3-trimethyl				0.12	0.22
2-tert-Butyltoluene				0.82	0.73
2-Bornene			0.93		
p-Mentha-2,8-diene,(1R,4R)-(+)-			3.12		
p-Cymenene			0.10		

Total Cyclic Compounds	71.20	80.31	97.08	85.50	85.06
Beta-Ocimene	10.77	7.49		4.79	4.77
2,4,6-Octariene,2,6-dimethyl-,(E,Z)-	9.70	4.39	1.44	2.83	2.77
(2E)-1-Methoxy-3,7-dimethylocta-2,6,diene	4.86	4.32		4.13	5.06
Nerol, methyl ether		1.11			
Geraniol	2.14			1.14	0.89
Beta-Linalool	1.12	0.41		1.34	1.04
Linalool, methyl ether	0.22	1.96	0.43	0.25	0.40
2,6-Octadiene,1-(1-ethoxyethoxy)-3,7-dimethyl			1.06		
Total Acyclic Compounds	28.80	19.67	2.92	14.50	14.94
Total	100.00	99.99	100.01	100.00	100.00

The lowest total cyclic compounds (71.20 %) and the highest total acyclic compounds (28.80 %) was observed in the products of the 1 h reaction. The compounds Beta-Ocimene, 2,4,6-Octariene,2,6-dimethyl-,(E,Z)-, and (2E)-1-Methoxy-3,7-dimethylocta-2,6,diene (**12**) formed majority of the acyclic products at 10.77 %, 9.70 %, and 4.86 %, respectively. The highest proportion of Beta-Ocimene, and 2,4,6-Octariene,2,6-dimethyl-,(E,Z)-, in a product was observed after the 1 h reaction. This may suggest that these compounds are kinetically favoured. In kinetically controlled chemical reactions, the molecules of the starting material follow the route of the lower energy transition state to form the product. These reactions involve short reaction times or low temperature. The short reaction time prevents the products further converting to more thermodynamically stable products. In the case of geraniol (**3**) conversion, the 1 h reaction enabled geraniol (**3**) conversion to kinetically favoured compounds (Beta-Ocimene, 2,4,6-Octariene,2,6-dimethyl-,(E,Z)-, and (2E)-1-Methoxy-3,7-dimethylocta-2,6,diene) and prevented their conversion to the more thermodynamically stable monocyclic terpenes. Therefore, shorter reaction time is good for geraniol (**3**) conversion to a mixture of products which includes a moderate proportion of acyclic monoterpenes such as Beta-Ocimene, and 2,4,6-Octariene,2,6-dimethyl-,(E,Z)-.

With increasing time up to 3 h the total cyclic compounds increases from 71.20 %, 80.31 % to 97.08 % for 1 h, 2 h and 3 h, respectively. The compounds D-Limonene (**8**), p-Mentha-1,4(8)-diene (**7**) and γ -Terpinene (**9**) consistently make up a major proportion of the cyclic compounds and increase with increasing time; 58.68 % for 1 h, 71.19 % for 2h and 72.53 % for 3 h. This indicates that these compounds are thermodynamically stable and are favoured under thermodynamic control i.e. increased reaction times. At the same time, the kinetic products (Beta-Ocimene, 2,4,6-Octariene,2,6-dimethyl-,(E,Z)-, and (2E)-1-Methoxy-3,7-dimethylocta-2,6,diene) decrease with increasing time up to 3 h. This indicates that they can convert to the

more stable cyclic products given more time which they were unable to do when the reaction time was stopped at 1 h. The selectivity also appears to improve with increasing time up to 3 h because the number of different compounds from 1 h (19 compounds), 2 h (17 compounds), to 3 h (16 compounds) decreases. This further highlights that D-Limonene (**8**), p-Mentha-1,4(8)-diene (**7**) and γ -Terpinene (**9**) are the thermodynamically stable compounds in the geraniol (**3**) conversion reactions and the transition state compounds tend to favour converting to these cyclic monoterpenes.

Comparing the products at various reaction times, 3 h reaction time generated the peak total cyclic compound (97.08 %) and this decreases with increasing time of 4 h (85.50 %) and 5 h (85.06 %). After 4 h and 5 h reactions, D-Limonene (**8**), p-Mentha-1,4(8)-diene (**7**) and γ -Terpinene (**9**) were still the major product fractions and accounted for 67.55 % and 64.08 % of the total product, respectively. However, 4 h reaction time offered the lowest product selectivity as 21 different product compounds were detected. Similarly, after 5 h the product selectivity was low as 19 different compounds were detected. The compounds Beta-Ocimene, 2,4,6-Octatriene,2,6-dimethyl-(E,Z)-, and (2E)-1-Methoxy-3,7-dimethylocta-2,6,diene (**12**) were significantly reduced in the 3 h reaction products, but formed a total of 11.76 % and 12.60 % in the 4 h and 5 h reaction products, respectively.

6.3.6. Effect of various reaction time- Nerol

The effect of various reaction times (1 h, 2 h, 3 h, 4 h, 5 h) at constant temperature setting (400 °C) and H₂O:Methanol:Nerol molar ratio (40:20:1) on the reaction products of nerol (**4**) conversion was also examined. A summary of the GCMS analysis results is provided in Table 6.5.

Like geraniol (**3**), the lowest total cyclic compounds (70.13 %) and the highest total acyclic compounds (29.88 %) was observed in the products of the 1 h reaction. The lowest nerol (**4**) conversion was achieved after this reaction as 9.70 % of the product was nerol (**4**). The compound 2,6-Octadiene,1-(1-ethoxyethoxy)-3,7-dimethyl is a kinetic product and forms under kinetic control because the highest proportion (6.44 %) was obtained after the 1 h reaction and less of it was detected in the increased reaction times. The transformation of nerol (**4**) to cyclic monoterpenes was restricted in the 1 h reaction time compared to the longer reaction times which generated total cyclic compounds ranging from 81.87 – 93.41 %. The lowest proportion of p-Mentha-1,4(8)-diene (**7**) (13.52 %) in a nerol (**4**) reaction product was obtained after the 1 h reaction. This indicates that its formation was restricted in the short reaction time. On the other hand, an unusually high alpha-Terpineol (**13**) content was identified in the product at 18.08 %. The high proportion of alpha-Terpineol (**13**) (C₁₀H₁₈O) relative to of p-Mentha-1,4(8)-diene (**7**) (C₁₀H₁₆) may be an indication that effective dehydration of geraniol (**3**) was restricted at the short reaction time.

The 4 h reaction time generated a product with the highest content of total cyclic compounds at 93.41 %. For the 2 h and 3 h reaction time, the total cyclic compounds was very similar at 87.45 % and 86.67 %, respectively. However, the selectivity at 2 h reaction time was the highest as only 17 different compounds were detected compared to 21 at 3 h and 4 h. The p-Mentha-1,4(8)-diene (**7**) content was also relatively consistent from 2 h, 3 h and 4 h at 47.05 %, 44.95%, and 46.03 %, respectively. The compounds D-Limonene (**8**), p-Mentha-1,4(8)-diene (**7**) and γ -Terpinene (**9**) formed majority of the product at 2 h, 3 h and 4 h reaction times as they accounted for 82.48 %, 70.03 % and 71.75% of the total product, respectively. Although the nerol (**4**) content decreased with time, only the 2 h reaction achieved complete conversion as negligible amounts (0.06 %) of nerol (**4**) was detected in the products. Ultimately, the 2 h reaction time may be more ideal compared to 3 h and 4 h because of its higher product selectivity and higher conversion at shorter reaction time.

After 5 h reaction of nerol (**4**), 28 different compounds were detected in the product. Interestingly, the amount of 2-tert-Butyltoluene in the product increased with reaction time and formed a high 10.21 % of the product after 5 h reaction. 2-tert-Butyltoluene ($C_{11}H_{16}$) contains a benzene ring and possesses an extra carbon atom compared to the cyclic monoterpenes ($C_{10}H_{16}$). The high 2-tert-Butyltoluene content may indicate that 5 h reaction time facilitates the conversion of nerol (**4**) to very stable benzene ring containing compounds. Moreover, the rise in 2-tert-Butyltoluene content with increasing time highlights that this is a thermodynamic product which forms under a thermodynamically favoured reaction pathway, i.e. longer reaction time.

Table 6.5 Summary of GCMS analysis results of the nerol reaction products at various reaction times.

Constant temperature setting (400 °C) and H₂O:Methanol:Nerol molar ratio (40:20:1). Full GCMS data is available in Appendix 3. Table 9 and 18 to 21.

Compound	Relative Area% at various reaction time				
	1 h	2 h	3 h	4 h	5 h
D-Limonene	21.53	22.55	10.71	16.36	18.79
p-Mentha-1,4(8)-diene	13.52	47.05	44.95	46.03	21.44
γ-Terpinene	2.35	12.88	14.37	9.36	5.86
Beta-Pinene	1.07	2.26	2.52	0.78	1.01
Alpha-Terpineol	18.08	0.10	4.10	8.77	11.58
1,3-Cyclohexadiene,1,3,5,5-tetramethyl	1.00	1.03	3.28	1.79	0.68
1,2,4,4-Tetramethylcyclopentene		0.07	0.20	0.10	
1,3-Cyclopentadiene,5,5-dimethyl-1-propyl		0.11	0.12		
o-Cymene	6.21	1.03	3.23	3.74	5.46
p-Mentha-3,8-diene	0.36	0.13	0.96	0.23	0.37
1,3-Cyclopentadiene,5,5-dimethyl-2-propyl		0.24	0.69	0.21	
2H-Pyran,2-ethenyltetrahydro-2,6,6-trimethyl	0.91				
p-Menth-8-en-1-ol	0.33			0.17	0.24
5-Caranol,(1S,3R,5S,6R)-(-)-				0.21	
Terpinen-4-ol			0.11	0.21	
4-Caranone,cis			0.75	2.49	2.89
2-Norbornanone,1,3,3-trimethyl			0.17		
2-tert-Butyltoluene	0.72		0.52	2.49	10.21

2-Bornene					0.10
p-Cymenene	1.44				0.40
p-Menth-3-ene					0.10
p-Menthane-1,8-diol	0.39				0.22
Carvacrol					0.15
1,5,5-Trimethyl-6-methylene-cyclohexene				0.47	
Acetophenone,3'-methyl-	1.39				0.92
p-Menth-6-en-2-one,(S)-(+)-					0.36
p-Menth-1-en-3-one					0.16
Carvenone	0.12				0.30
(2,2,6-Trimethyl-bicyclo[4.1.0]hept-1-yl)-methanol					0.32
p-Mentha-2,8-diene,(1R,4R)-(+)-	0.72				0.31
Total Cyclic Compounds	70.13	87.45	86.67	93.41	81.87
Beta-Ocimene		3.62	3.67	1.62	
2,4,6-Octariene,2,6-dimethyl-,(E,Z)-		1.64	2.57		
(2E)-1-Methoxy-3,7-dimethylocta-2,6,diene	3.97	3.33	1.32	0.26	3.26
Nerol, methyl ether	2.23	2.29			1.51
Beta-Linalool	3.99	0.15	0.63	0.98	2.38
Linalool, methyl ether	3.38	1.45	0.66	1.00	2.02
2,6-Octadiene,1-(1-ethoxyethoxy)-3,7-dimethyl	6.44		2.19	1.03	4.02
Nerol	9.70	0.06	2.28	1.70	3.35
1-Methylpentanoic anhydride					1.59

Citral	0.17				
Total Acyclic Compounds	29.88	12.54	13.33	6.59	18.14
Total Compounds	100.01	99.99	100.00	100.00	100.01

6.3.7. Effect of various reaction temperature- Geraniol

N.B. Although 400 °C was the heating temperature set, the temperature and pressure inside the reactor (i.e. of the reaction mixture) reached a maximum temperature of 300 °C at the ratio of 40:20:1. This is further discussed in 6.3.9. In this section, 300 °C refers to the reaction that had 400 °C temperature setting.

The effects of varying reaction temperatures (100 °C, 150 °C, 200 °C and 300 °C) at constant time (2 h) and H₂O:Methanol:Geraniol molar ratio (40:20:1) on the conversion of geraniol (**3**) in the sub/supercritical water-methanol reaction was investigated. A summary of the GCMS analysis results is provided in Table 6.6 and Figure 6.3 which compares the relative area % of the major compounds in the geraniol products at various reaction temperatures.

Table 6.6 Summary of GCMS analysis results of the geraniol reaction products at various reaction temperatures.

Constant time (2 h) and H₂O:Methanol:Geraniol molar ratio (40:20:1). Full GCMS data is available in Appendix 3. Table 3 and 22.

Compound	Relative Area% at various reaction setting temperatures			
	100 (°C)	150 (°C)	200 (°C)	300 (°C)
D-Limonene			19.84	17.71
p-Mentha-1,4(8)-diene			24.89	42.05
γ-Terpinene			4.32	11.43
Beta-Pinene			5.49	3.71
Alpha-Terpineol			9.43	0.15
1,3-Cyclohexadiene,1,3,5,5-tetramethyl			0.47	3.39
1,2,4,4-Tetramethylcyclopentene				0.16
1,3-Cyclopentadiene,5,5-dimethyl-1-propyl				0.27
o-Cymene			0.10	0.89
p-Mentha-3,8-diene			0.12	0.10
1,3-Cyclopentadiene,5,5-dimethyl-2-propyl			0.20	0.45
2H-Pyran,2-ethenyltetrahydro-2,6,6-trimethyl			0.94	
p-Menth-8-en-1-ol			0.13	
5-Caranol,(1S,3R,5S,6R)-(-)-			0.59	

2-Cyclohexene-1-methanol,2,6,6-trimethyl-			0.07	
Terpinen-4-ol			0.16	
Total Cyclic Compounds			66.74	80.31
Beta-Ocimene			11.06	7.49
2,4,6-Octariene,2,6-dimethyl-,(E,Z)-			6.07	4.39
(2E)-1-Methoxy-3,7-dimethylocta-2,6,diene			13.13	4.32
Nerol, methyl ether				1.11
Geraniol	100.00	100.00	1.56	
Beta-Linalool			1.02	0.41
Linalool, methyl ether			0.30	1.96
(4E)-2,7-Dimethyl-4,6-octadien-2-ol			0.12	
Total Acyclic Compounds	100.00	100.00	33.26	19.67
Total	100.00	100.00	100.01	99.99

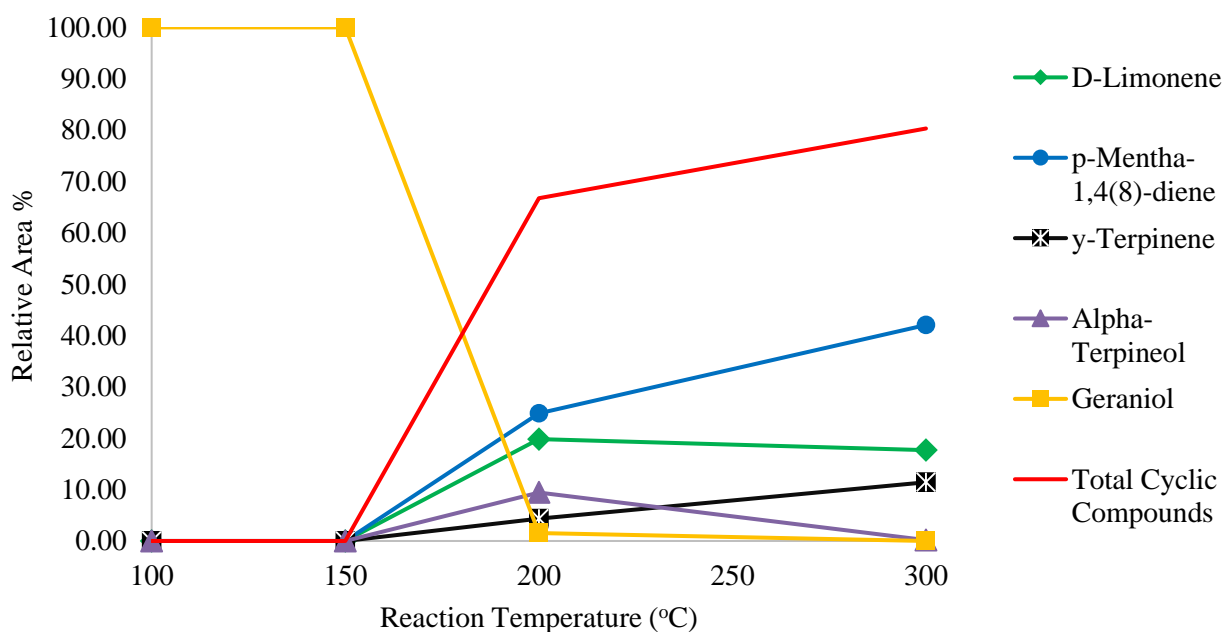


Figure 6.3 Major compounds in the geraniol reaction products at various reaction temperatures.

Constant time (2 h) and H₂O:Methanol:Geraniol molar ratio (40:20:1)

At reaction temperatures 100 °C and 150 °C no products were detected; hence the formation of terpenes did not occur at these temperatures. This indicates that the operating temperature can have a unique influence on this reaction; below certain temperatures the reaction does not take place and at higher temperatures the product distribution can greatly vary. Furthermore, the failure to generate products at 100 °C and 150 °C reaction temperatures demonstrates that at higher temperatures, water behaves like a catalyst and co-solvent with methanol, and can thus initiate the reaction and facilitate product formation. Therefore, at the lower temperatures of 100 °C and 150 °C, water and methanol do not possess these characteristics which would enable product formation.

The products of the geraniol (**3**) reaction at 200 °C contained 66.74 % cyclic compounds and 33.26 % acyclic compounds. This is a lower ratio of cyclic to acyclic components than the geraniol (**3**) reaction at 300 °C which generated 80.31 % cyclic compounds and 19.67 % acyclic compounds. This shows that lower/subcritical temperature conditions have a higher tendency towards generating a product with more acyclic compounds. This is because at the lower temperature of 200 °C, kinetic control is operative and due to the lower energy available the reactant favours conversion to kinetic products such as the acyclic compounds. Whereas at the higher temperature of 300 °C, thermodynamic control is operative and thermodynamically favoured products form such as stable cyclic monoterpene compounds.

Despite the higher tendency towards acyclic compounds at 200 °C compared to 300 °C, the compounds D-Limonene (**8**) and p-Mentha-1,4(8)-diene (**7**) formed the largest fraction of the products after the 200 °C reaction, accounting for 19.84 % and 24.89 % of the total product, respectively. However, this is comparably lower than the 300 °C reaction products. At 300 °C, the compounds D-Limonene (**8**), p-Mentha-1,4(8)-diene (**7**) and γ -Terpinene (**9**) formed a total of 71.20 % of the product and 88.64 % of the cyclic compounds. Whereas at 200 °C, a relatively lower total amount (49.04 %) of these compounds were achieved in the product. Additionally, alpha-Terpineol (**13**) formed 9.43 % of the product after 200 °C which is higher than at 300 °C which exhibited 0.15 %. The comparably higher content of alpha-Terpineol (**13**) (C₁₀H₁₈O) and lower content of D-Limonene (**8**) (C₁₀H₁₆), p-Mentha-1,4(8)-diene (**7**) (C₁₀H₁₆) and γ -Terpinene (**9**) (C₁₀H₁₆) indicates that at 200 °C the dehydration of geraniol (**3**) was less effective. This may be due to a suppressed acidic ability of subcritical water to promote dehydration reactions at this temperature. By increasing the reaction temperature from 200 °C to 300 °C, water is more dissociated and can more effectively function as an acid catalyst by promoting the dehydration of geraniol (**3**) to cyclic monoterpenes. Similarly, Anikeev et al. found raising the pressure of a mixture of supercritical ethanol-water- alpha-pinene resulted in an increase in the density of the supercritical medium in the critical region [94]. This consequently led to an increase in the H⁺ ion concentration due to the increasing degree of ionisation of water. As a result, water exhibited the properties of an acid catalyst and could therefore increase the reaction rate.

The high pressures which accompany reactions performed in supercritical solvents directly lead to increased density of the medium [92]. Consequently, this can lead to increased or decreased reaction rate. The influence of pressure on the rate of the chemical reaction is due to: a specific interaction of the solvent with the molecules of the dissolved substance, the unique properties of the supercritical solvent, and the interaction of the clusters of dissolved substances with the solvent [92]. These features ultimately result in advanced reactions under high-temperature supercritical conditions which do not occur at lower temperatures. Therefore, at higher temperature of 300 °C the supercritical methanol-water reaction has an increased reaction rate which enables more geraniol (**3**) conversion to the stable cyclic monoterpenes than at 200 °C.

After the 200 °C reaction, geraniol (**3**) conversion was still high as it made up only 1.56 % of the products. However, the 300 °C reaction temperature achieved complete conversion as no geraniol (**3**) was detected in the products. The compounds (2E)-1-Methoxy-3,7-dimethylocta-2,6,diene (**12**) and Beta-Ocimene accounted for majority of the acyclic compounds at both 200 °C and 300 °C. However, higher amount of these compounds were observed after the 200 °C reaction at 13.13 % and 11.06 % for (2E)-1-Methoxy-3,7-dimethylocta-2,6,diene (**12**) and Beta-Ocimene, respectively. These compounds only made up 4.32 % and 7.49 %, respectively of the acyclic compounds after the 300 °C reaction. At the 200 °C condition, geraniol (**3**) has a higher tendency towards the conversion to (2E)-1-Methoxy-3,7-dimethylocta-2,6,diene (**12**) than 300 °C. This may be because the conversion to (2E)-1-Methoxy-3,7-dimethylocta-2,6,diene (**12**) needs less energy than the conversion to cyclic monoterpenes as it only requires the substitution of the hydrogen on the hydroxyl group of geraniol (**3**) by a methyl group. Also, this relatively lower temperature favours the formation of kinetic products due to the lower activation energy necessary to form them compared to the thermodynamically stable cyclic monoterpenes.

A recognised feature of supercritical fluid processes is the controllable selectivity [92,102]. By comparing the reaction products of experimental conditions 200 °C and the 300 °C, it is evident that at the higher supercritical temperature, the reaction is more selective towards the formation of cyclic compounds, especially towards p-Mentha-1,4(8)-diene (**7**). After the 300 °C reaction, it accounted for 42.05 % of the product compared to 24.89 % after the 200 °C reaction. The overall product selectivity is improved after the higher 300 °C reaction because the product distribution is lower and 17 different compounds were identified of which 11 were cyclic. Whereas after the 200 °C reaction, 20 different compounds were detected and 14 were cyclic.

6.3.8. Effect of various reaction temperature- Nerol

The influence of different reaction temperatures (100 °C, 150 °C, 200 °C and 300 °C) was also examined on the conversion of nerol (**4**). A summary of the GCMS analysis results is provided in Table 6.7 and Figure 6.4 which compares the relative area % of the major compounds in the nerol products at various reaction temperatures. Like the geraniol (**3**) experiments, conversion of nerol (**4**) was very poor at 100 °C and 150 °C. This confirms that at lower reaction temperatures, water and methanol alone cannot be utilised to catalyse the reaction or promote product formation.

The reaction products after the 200 °C nerol (**4**) reaction exhibited a lower amount of cyclic compounds (78.77 %) compared to the 300 °C reaction (87.45 %). Similar to the findings after the geraniol (**3**) reaction, this indicates that at the 200 °C condition kinetic control was operative, and due to the lower energy available, nerol (**4**) had a higher tendency to converting to acyclic compounds than at 300 °C. Hence, at the higher temperature of 300 °C the energy available enables nerol (**4**) to convert to more thermodynamically stable compounds such as cyclic monoterpenes.

The 200 °C reaction product contained a substantial amount of alpha-Terpineol at (**13**) 21.14 % which is significantly higher than the 0.10 % generated after the 300 °C reaction. In fact, alpha-Terpineol (**13**) formed the third largest fraction of the 200 °C reaction product after p-Mentha-1,4(8)-diene (**7**) (25.18 %) and D-Limonene (**8**) (22.94 %). Whereas the 300 °C reaction contained a larger amount of γ -Terpinene (**9**) at 12.88 % than the 200 °C reaction product (4.04 %). This is a similar outcome as the geraniol (**3**) reaction products at various temperatures. The higher amount of alpha-Terpineol (**13**) (C₁₀H₁₈O) and the lower amount of γ -Terpinene (**9**) (C₁₀H₁₆) in the 200 °C reaction products indicates that the methanol-water mixture is less able to promote the dehydration of nerol (**4**) at the lower reaction temperature. This could be due to a decreased acidic ability of water to facilitate dehydration reactions at this temperature. At the higher reaction temperature of 300 °C, water is more dissociated and it can effectively function as an acid catalyst. This is evident in the product distribution after the 300 °C reaction as the cyclic compounds D-Limonene (**8**), p-Mentha-1,4(8)-diene (**7**) and γ -Terpinene (**9**) formed a total of 82.48 % of the product and 94.32 % of the cyclic compounds. Compared to 52.16 % of these compounds obtained after the 200 °C reaction.

The conversion was lower after the 200 °C reaction temperature as 3.31 % of nerol (**4**) was detected in the product. Whereas, a negligible amount (0.06%) was detected after the 300 °C reaction. The compounds 2,6-Octadiene,1-(1-ethoxyethoxy)-3,7-dimethyl and (2E)-1-Methoxy-3,7-dimethylocta-2,6,diene (**12**) accounted for most of the total acyclic compounds in the 200 °C reaction products; at 6.30 % and 5.16 %, respectively. The higher proportion of total acyclic compounds after the 200 °C reaction (21.25 %) compared to the 300 °C (12.54%) confirms that at the higher reaction temperature more energy is available for preferential

formation of thermodynamically stable cyclic compounds. Additionally, product selectivity can be improved by applying higher temperature as the number of different compounds in the product decreased from 19 to 17 after the 200 °C and 300 °C reactions, respectively.

Table 6.7 Summary of GCMS analysis results of the nerol reaction products at various reaction temperatures.

Constant time (2 h) and H₂O:Methanol:Nerol molar ratio (40:20:1). Full GCMS data is available in Appendix 3. Tables 9, 23, 24, 25.

Compound	Relative Area % at various reaction temperatures			
	100 (°C)	150 (°C)	200 (°C)	300 (°C)
D-Limonene	1.58	1.38	22.94	22.55
p-Mentha-1,4(8)-diene	0.49	0.39	25.18	47.05
γ-Terpinene	0.13	0.29	4.04	12.88
Beta-Pinene	0.26	0.15	2.80	2.26
Alpha-Terpineol	0.46	0.50	21.14	0.10
1,3-Cyclohexadiene,1,3,5,5-tetramethyl				1.03
1,2,4,4-Tetramethylcyclopentene				0.07
1,3-Cyclopentadiene,5,5-dimethyl-1-propyl				0.11
o-Cymene			0.06	1.03
p-Mentha-3,8-diene				0.13
1,3-Cyclopentadiene,5,5-dimethyl-2-propyl				0.24
2H-Pyran,2-ethenyltetrahydro-2,6,6-trimethyl			0.57	
p-Menth-8-en-1-ol			0.36	
5-Caranol,(1S,3R,5S,6R)-(-)-			0.71	
Terpinen-4-ol			0.39	
p-Menthane-1,8-diol			0.59	
1,5,5-Trimethyl-6-methylene-cyclohexene	0.10	0.11		
Total Cyclic Compounds	3.02	2.83	78.77	87.45
Beta-Ocimene			3.86	3.62
2,4,6-Octariene,2,6-dimethyl-,(E,Z)-(2E)-1-Methoxy-3,7-dimethylocta-2,6,diene			0.64	1.64
Nerol, methyl ether			5.16	3.33
				2.29

Geraniol				
Beta-Linalool			0.71	0.15
Linalool, methyl ether	0.15		0.95	1.45
2,6-Octadiene,1-(1-ethoxyethoxy)-3,7-dimethyl			6.30	
Nerol	96.97	97.02	3.31	0.06
Yomogi alcohol			0.14	
Methoxycitronellal			0.17	
Total Acyclic Compounds	96.97	97.17	21.25	12.54
Total	99.99	99.99	100.02	100.00

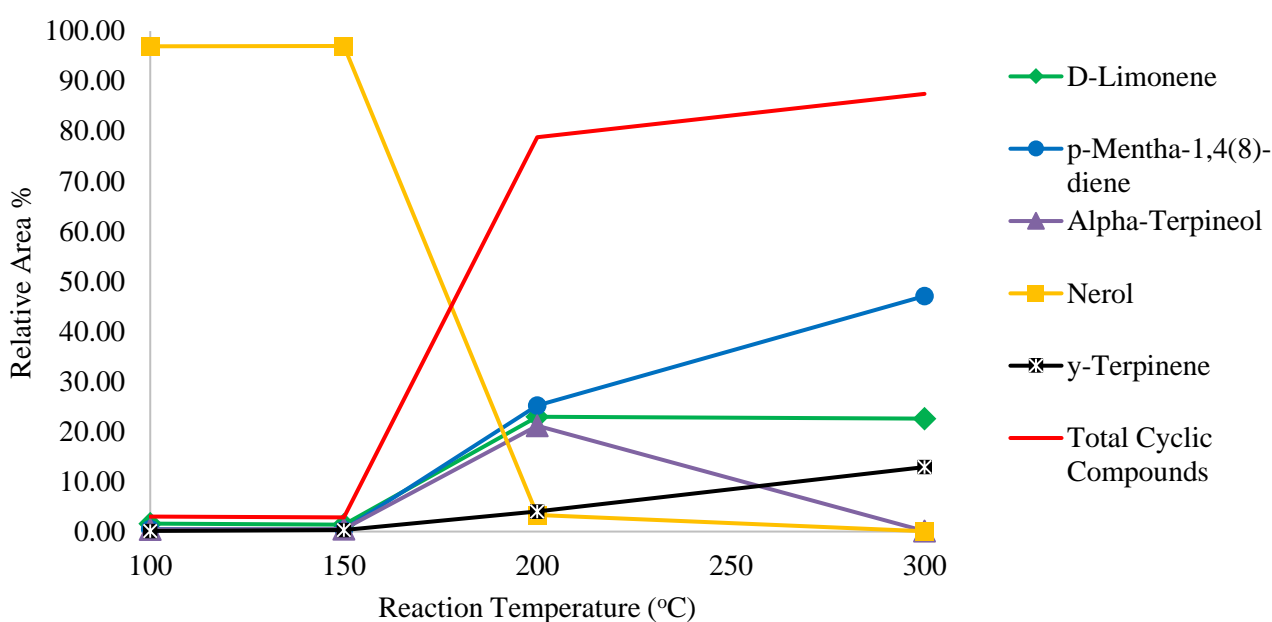


Figure 6.4 Major compounds in the nerol reaction products at various reaction temperatures. Constant time (2 h) and H₂O:Methanol:Nerol molar ratio (40:20:1)

6.3.9. Comparing the experimental reaction temperatures and pressures and the critical properties calculated by ASPEN HYSYS simulator

In order to discover if the experimental conditions achieved the critical point of the water-methanol solvent mixture, ASPEN HYSYS simulation was used. A fluid package using the Peng Robinson property method was applied to use the Critical Properties Analysis tool on ASPEN HYSYS. The critical properties were calculated by ASPEN HYSYS using the mixing rules associated with the Peng Robinson property package.

Table 6.8 includes the results of the ASPEN HYSYS calculated critical properties of various water-methanol ratios. Figure 6.5 shows the relationship between increasing concentration of water and the critical properties of the solvent mixture, using the critical data calculated using ASPEN HYSYS. Expectedly, with higher water concentration, the critical point of the water-methanol mixture increases because the critical point of water (374 °C, 221 bar) plays a greater influence.

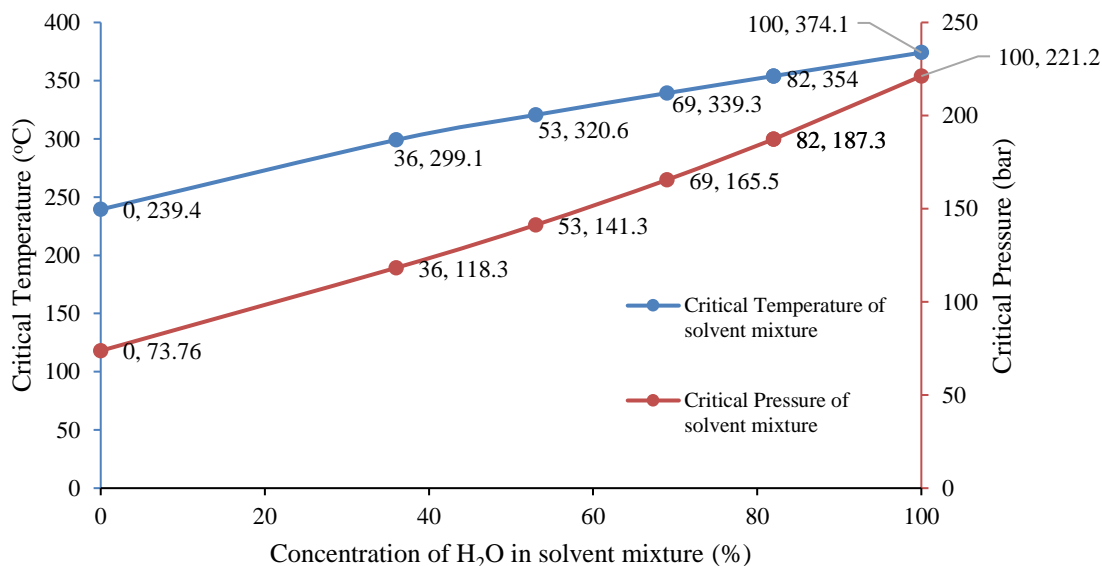


Figure 6.5 Changes in the critical properties of the solvent mixture at different concentration of H₂O.

Table 6.8 Comparing the critical properties from experiments and ASPEN HYSYS.

Experiment conditions are 400 °C heating temperature setting, 2 h reaction time and various H₂O:Methanol ratio.

H ₂ O:Methanol Molar ratio	Equivalent H ₂ O concentration (%)	ASPEN HYSYS Critical Properties		Geranyl Isovalerate experiment		Geraniol experiments		Nerol experiments	
		T _c (°C)	P _c (bar)	T max (°C)	P max (bar)	T max (°C)	P max (bar)	T max (°C)	P max (bar)
40:20	53.0	320.6	141.3	265	70	300	100	300	100
80:10	82.0	354.0	187.3			313	105	307	98
40:5	82.0	354.0	187.3			340	100	336	100
40:10	69.0	339.3	165.5			316	94	313	96
20:20	36.0	299.1	118.3			366	98	350	99
0:100	0	239.4	73.76			272	110	267	100
100:0	100	374.1	221.2			369	92		

T_c, P_c, T max and P max refers to critical temperature, critical pressure, maximum reactor content temperature and maximum reactor content pressure, respectively.

Although at the experiments with the constant heating setting temperature, 400 °C was applied, the temperature and pressure inside the reactor (i.e. of the reaction mixture) varied due to the

variation in the water, and methanol ratio. Only at the equimolar and the 0:100 water methanol ratios did the geraniol and nerol experiments surpass the critical temperature calculated by ASPEN HYSYS. All the reactions surpassed methanol critical temperature and pressure of 240 °C and 74 bar. Overall, comparing the ASPEN HYSYS calculated critical properties and the temperatures and pressures achieved in the reactions, the experimental conditions can be more appropriately described as subcritical than supercritical. Nevertheless, some interesting reactions and products were achieved under this subcritical solvent mixture. This indicates energy-intensive and resource demanding supercritical conditions are not necessary to obtain high conversion of geranyl isovalerate (a bio-oil based compound) and to generate a rich mixture of monoterpenes.

6.4. Conclusion

Pollution from the chemical industry is a major contributor to climate change and global warming. One method of reducing the negative impacts of chemical processing on the environment involves using renewable feedstocks and decreasing the reliance on fossil feedstocks. Biomass, particularly from biodegradable waste material sources, is a valuable and inexpensive raw material for chemical production which also encourages closed-loop sustainable systems. This chapter examined the use of a bio-oil based compound – geranyl isovalerate – to generate a selection of valuable compounds including methyl isovalerate (**2**) and a mixture of monoterpenes especially p-Mentha-1,4(8)-diene (**7**), D-Limonene (**8**), and γ -Terpinene (**9**).

In this novel work no catalyst was used, and subcritical water was used to perform the role of a catalyst and co-solvent with supercritical methanol. Very high geranyl isovalerate (**1**) conversions was achieved, as less than 3 % of it was detected in the products and methyl isovalerate (**2**) and the monoterpenes accounted for 97 %.

To gain further insight into the formation of the monoterpenes, in-depth investigations were carried out using the geranyl isovalerate (**1**) transesterification reaction intermediates; geraniol (**3**) and nerol (**4**). The variation in the product distribution at the different reaction ratios, temperatures and times demonstrates that the selectivity to the terpenes can be controlled by varying the reaction parameters. Additionally, the desired distribution of cyclic to acyclic products can be chosen by modifying the reaction parameters.

This non-catalytic one-pot process can be cheaper than conventional processes due to the absence of catalyst. Moreover, the efficiency of the chemical reaction is improved due to the consecutive chemical reactions in the single reactor. Transesterification of geranyl isovalerate, and dehydration of the intermediates geraniol and nerol, occur in series in the single reactor. This favourably helps to avoid time consuming and expensive separation processes and purification of the intermediate chemical compounds. On the other hand, due to the diversity

and complexity of biomass feedstock, the process of chemical production from biomass is different from established processes using fossil fuel feedstock. This can lead to higher processing cost. Further research is underway, particularly on catalysis, to reduce the processing cost of converting biomass into chemical products.

7. Thesis Conclusion and Recommendations

The PhD research project aimed to examine and improve the properties of a sample of crude bio-oil by using sub/supercritical fluid technologies. An in-depth literature review was conducted as part of the research as well as a study on an efficient phenol conversion process which can potentially be applied to whole bio-oil to enhance its properties. Additionally, the major result of the research project is the identification of a novel process of producing valuable chemical building blocks from a bio-oil compound feedstock. There is a global awareness of the environmental and energy security concerns associated with using dwindling fossil feedstock reserves to produce fuels and chemicals. Therefore, this research is important for industry as it provides insight into methods of producing renewable fuels and chemicals from bio-oil.

Chapter 4 studied the physical and chemical characteristics of crude bio-oil in detail. Additionally, it showed the different effects of blending crude bio-oil with methanol, ethanol, and isopropanol compared to bio-oil treated with supercritical methanol, ethanol, and isopropanol. Supercritical methanol treatment demonstrated the most promising outcome as it showed higher reactivity compared to ethanol or isopropanol. For example, GCMS analysis demonstrated that only supercritical methanol treatment eliminated the acids in the bio-oil; consequently, the pH increased from 2.39 in the crude bio-oil to 4.04 after the methanol reaction. This was attributed to the high esterification ability of supercritical methanol based on the significant amount of newly formed esters and the increased water in the products from esterification reactions. The research in this chapter found that although the bio-oil-alcohol blends improved certain bio-oil properties, (e.g. heating value and pH), the supercritical reactions further enhanced the bio-oil properties by promoting reactions such as esterification and hydrogenation thus further improving the physicochemical properties of the bio-oil. For future work on bio-oil upgrading, efficient solvent recovery and reuse is necessary to further optimise the process.

Due to the complex mixture of compounds in crude bio-oil, identifying the supercritical fluid region and the position of the phase boundary curves in bio-oil upgrading processes is more complicated than for pure fluid [7]. Few studies of bio-oil upgrading in supercritical fluids (SCF) have focused on the phase behaviours during the upgrading process. The term 'supercritical' is only used to indicate that the operating conditions are above the critical points of the solvents. Hence, further research on the critical properties of binary mixtures and phase behaviour during bio-oil upgrading is necessary.

Most studies of bio-oil upgrading in supercritical fluids utilise batch reactors [109]. This is to reduce the effects of other variables except temperature, pressure, and catalyst. However, batch reactors are inefficient in terms of time, energy, and cost. Thus, continuous flow reactors

should be considered to increase bio-oil production efficiency and suitability for commercialisation processes. However, the high viscosity of crude bio-oil presents a technical challenge when feeding into the continuous reactor. This can be solved with SCF addition as bio-oil treatment with SCF produces a bio-oil with lower viscosity, as well as higher yield and fuel quality [34]. Thus, there is opportunity for further research on the application of continuous reactors in bio-oil upgrading in SCFs.

Chapter 5 extended on the findings of Chapter 4 which showed the crude bio-oil contained 37.03 % phenols and even after blending and supercritical solvent treatment, minimal changes in phenol concentration in the product bio-oils were observed. Phenol in bio-oil is undesirable because it can behave like an acid; thus it can be highly reactive in bio-oil [64]. Additionally, phenols are reportedly the main cause for coke formation and catalyst deactivation during bio-oil processes [5]. Therefore, the objective was to utilise supercritical methanol and water as co-solvents and Raney-Ni catalyst to transform phenol to less reactive compounds. This in situ hydrogenation process demonstrated high phenol conversion (99.07 %) and high cyclohexanol yield (93.35 %) and selectivity (94.23 %). Raney-Ni proved to be an excellent catalyst for both methanol reforming and phenol hydrogenation. ASPEN HYSYS simulator was used to calculate the critical properties of the reactions and the findings showed the reactions did not reach the calculated critical parameters. Therefore, the experimental conditions are better referred to as subcritical than supercritical. Nevertheless, the high conversions and yields showed that the process is an economic alternative to conventional catalytic hydrogenation processes which involve precious metal supported catalysts and external molecular hydrogen. The use of model compounds instead of whole bio-oil elucidates the chemistry of bio-oil reactions by focusing on one compound rather than a complex mixture of crude bio-oil. However, this does not present an accurate depiction of the reaction with whole bio-oil, because it does not consider the effects of the mixture of compounds on the reaction. Therefore, for future research the in situ catalytic hydrogenation process can be applied to whole-bio-oil to improve its properties.

Chapter 6 discussed the findings of a novel non-catalytic one-pot synthesis of valuable compounds (methyl isovalerate and a mixture of monoterpenes) from a bio-oil based compound (geranyl isovalerate). This ester was identified in the GCMS analysis of a sample of crude bio-oil in Chapter 4. A near-critical methanol-water mixture was utilised as solvent and catalyst in the process. Very high geranyl isovalerate (**1**) conversions was achieved as less than 3 % of it was detected in the products and methyl isovalerate (**2**) and the monoterpenes accounted for 97 %. Recovering valuable compounds from waste and utilising them as starting materials for the production of valuable chemical building blocks are efforts which may enable production routes that rely less on fossil sources as feedstock. This is important because pollution from the chemical industry is a major contributor to climate change and global warming. For future research, a stronger link between waste producers and chemical

producers would enable efficient identification and utilisation of a waste (with a high concentration of the desired starting material compound, e.g. geranyl isovalerate) as a feedstock for chemical production.

Chapter 6 involved the use of bio-oil compounds to produce the chemical products. Alternatively, biomass can be directly used rather than bio-oil. For example, biomass can be converted to chemicals via one-pot reactions where enzymatic and chemical steps are conducted in series to achieve the transformation [100]. This method reduces processing cost because it prevents product isolation, does not require intermediate product recovery, reduces operating time and potentially reduces the quantity of waste produced.

Despite the advantages of SCF processes compared to conventional catalytic reactions, researchers have highlighted the weaknesses of this technology [8]. The process is energy-intensive due to the high temperature and pressure conditions necessary. For example, a supercritical methanol reaction requires temperatures and pressures above 239 °C and 8.1 MPa, respectively. This means the energy consumed to produce biofuel in a SCF process can be more than the energy provided by the biofuel. One approach to alleviate the high heating requirements is installing a double tube heat exchanger before the supercritical reactor to pre-heat the reactants by the reactor output stream. This reduces the heating and cooling requirements of the input and output streams, respectively. Researchers have found integrated heating and cooling systems reduce the energy requirements of SCF processes to levels close to conventional catalytic reactions [8].

Commercialisation of SCF processes has been limited due to the costs associated with the process. Due to the conditions of SCF reactions, expensive items are required such as high-pressure pumps, furnaces, and reactors specifically constructed of durable materials that can withstand severe conditions. To improve the economic viability of supercritical processes, researchers have proposed two-stage reactions. By using two reactors of smaller size the pumping power and heat duty requirements can be reduced compared to a single-stage reactor. Additionally, two smaller reactors in series lower the reactor construction cost. Furthermore, the extreme operating conditions of SCF reactions raise safety concerns as it could lead to severe consequences if a reactor vessel leakage was to occur. The two-stage process can be used to lower the risk related to operation and maintenance of SCF processes.

References

1. Bridgwater A V: Upgrading Fast Pyrolysis Liquids. Thermochemical Processing of Biomass Conversion into Fuels, Chemicals and Power. Brown R C. Wiley, United Kingdom; 2011, s. 157--188.
2. Holm-Nielsen J B: Introduction to biomass supply chains. Biomass supply chains for bioenergy and biorefining. Holm-Nielsen J B, Ehiازه A E. Elsevier; 2016, s. 3--13.
3. Bridgwater A V. Review of fast pyrolysis of biomass and product upgrading. Biomass and Bioenergy, 2012, 38: 68--94.
4. Demirbas A. Competitive liquid biofuels from biomass. Applied Energy, 2011, 88(1): 17--28.
5. Si Z, Zhang X, Wang C, Ma L, Dong R. An Overview on Catalytic Hydrodeoxygenation of Pyrolysis Oil and Its Model Compounds. Catalysts, 2017, 7(6): 169.
6. Jessop P G, Leitner W: Introduction. Chemical Synthesis Using Supercritical Fluids. New York: Wiley; 2008, s. 1--65.
7. Baiker A. Supercritical Fluids in Heterogeneous Catalysis. Chemical Reviews, 1999, 99(2): 453--473.
8. Tan K T, Lee K T. A review on supercritical fluids (SCF) technology in sustainable biodiesel production: Potential and challenges. Renewable and Sustainable Energy Reviews, 2011, 15(5): 2452--2456.
9. Anitescu G, Bruno T J. Fluid properties needed in supercritical transesterification of triglyceride feedstocks to biodiesel fuels for efficient and clean combustion - A review. The Journal of Supercritical Fluids, 2012, 63: 133--149.
10. Akhtar J, Aishah N, Amin S. A review on process conditions for optimum bio-oil yield in hydrothermal liquefaction of biomass. Renewable and Sustainable Energy Reviews, 2011, 15(3): 1615--1624.
11. Sohail S, Rosendahl L, Rudolf A. Hydrothermal liquefaction of biomass : A review of subcritical water technologies. Energy, 2011, 36(5): 2328--2342.
12. Brand S, Susanti R F, Kim S K, Lee H shik, Kim J, Sang B I. Supercritical ethanol as an enhanced medium for lignocellulosic biomass liquefaction: Influence of physical process parameters. Energy, 2013, 59: 173--182.
13. Guo Y, Wang S Z, Xu D H, Gong Y M, Ma H H, Tang X Y. Review of catalytic supercritical water gasification for hydrogen production from biomass. Renewable and Sustainable Energy Reviews, 2010, 14: 334--343.
14. Matsumura Y, Minowa T, Potic B, Kersten S, Prins W, Swaaij W et al. Biomass gasification in near- and super-critical water: Status and prospects. Biomass and Bioenergy, 2005, 29: 269--292.
15. Azadi P, Farnood R. Review of heterogeneous catalysts for sub- and supercritical water gasification of biomass and wastes. International Journal of Hydrogen Energy, 2011, 36(16): 9529--9541.
16. Zhang Q, Chang J, Wang T, Xu Y. Review of biomass pyrolysis oil properties and upgrading research. Energy Conversion and Management, 2007, 48(1): 87--92.
17. Perry R H, Green D W, Maloney J O red. Perry's chemical engineers' handbook. New York : McGraw-Hill, 2008, 1999.
18. Xu Y, Duan P, Wang B. Catalytic upgrading of pretreated algal oil with a two-component catalyst mixture in supercritical water. Algal Research, 2015, 9: 186--193.

19. Prajitno H, Insyani R, Park J, Ryu C, Kim J. Non-catalytic upgrading of fast pyrolysis bio-oil in supercritical ethanol and combustion behavior of the upgraded oil. *Applied Energy*, 2016, 172: 12–22.
20. Isa K M, Snape C E, Uguna C, Meredith W, Deng H. Pyrolysis oil upgrading in high conversions using sub- and supercritical water above 400°C. *Journal of Analytical and Applied Pyrolysis*, 2016, 119: 180–188.
21. Li W, Pan C, Sheng L, Liu Z, Chen P, Lou H Z X. Upgrading of high-boiling fraction of bio-oil in supercritical methanol. *Bioresource Technology*, 2011, 102(19): 9223–9228.
22. Zhang X, Chen L, Kong W, Wang T, Zhang Q, Long J, Xu Y, Ma L. Upgrading of bio-oil to boiler fuel by catalytic hydrotreatment and esterification in an efficient process. *Energy*, 2015, 84: 83–90.
23. Zhang J, Luo Z, Dang Q, Wang J, Chen W. Upgrading of bio-oil over bifunctional catalysts in supercritical monoalcohols. *Energy and Fuels*, 2012, 26(5): 2990–2995.
24. Remon J, Arauzo J, Garcia L, Arcelus-Arrillaga P, Millan M, Suelves I P J L. Bio-oil upgrading in supercritical water using Ni-Co catalysts supported on carbon nanofibres. *Fuel Processing Technology*, 2016, 154: 178–187.
25. Ahmadi S, Yuan Z, Rohani S, Xu C. Effects of nano-structured CoMo catalysts on hydrodeoxygenation of fast pyrolysis oil in supercritical ethanol. *Catalysis Today*, 2016, 269: 182–194.
26. Duan P, Savage P E. Upgrading of crude algal bio-oil in supercritical water. *Bioresource Technology*, 2011, 102: 1899–906.
27. Chen W, Luo Z, Yu C, Li G, Yang Y, Zhang H. Upgrading of bio-oil in supercritical ethanol: Catalysts screening, solvent recovery and catalyst stability study. *Journal of Supercritical Fluids*, 2014, 95: 387–393.
28. Li W, Pan C, Zhang Q, Liu Z, Peng J, Chen P, Lou H Z X. Upgrading of low-boiling fraction of bio-oil in supercritical methanol and reaction network. *Bioresource Technology*, 2011, 102(7): 4884–4889.
29. Xu X, Zhang C, Zhai Y, Liu Y, Zhang R, Tang X. Upgrading of Bio-Oil Using Supercritical 1 - Butanol over a Ru/C Heterogeneous Catalyst: Role of the Solvent. *Energy & Fuels*, 2014, 28: 4611–4621.
30. Zhang Q, Zhang L, Wang T, Xu Y, Zhang Q, Ma L et al. Upgrading of bio-oil by removing carboxylic acids in supercritical ethanol. *Energy Procedia*, 2014, 61: 1033–1036.
31. Cui H-Y, Wang J-H, Wei S-Q, Zhuo S-P, Li Z-H, Wang L-H et al. Upgrading bio-oil by esterification under supercritical CO₂ conditions. *Journal of Fuel Chemistry and Technology*, 2010, 38(386): 673–678.
32. Dang Q, Luo Z, Zhang J, Wang J, Chen W, Yang Y. Experimental study on bio-oil upgrading over Pt/SO₄²⁻/ZrO₂/SBA - 15 catalyst in supercritical ethanol. *Fuel*, 2013, 103: 683–692.
33. Oasmaa A, Czernik S. Fuel Oil Quality of Biomass Pyrolysis Oils State of the Art for the End Users. *Energy & Fuels*, 1999, 13(4): 914–921.
34. Xiu S, Shahbazi A. Bio-oil production and upgrading research: A review. *Renewable and Sustainable Energy Reviews*, 2012, 16(7): 4406–4414.
35. Arla D, Sinquin A, Palermo T, Hurtevent C, Graciaa A, Dicharry C. Influence of pH and water content on the type and stability of acidic crude oil emulsions. *Energy and Fuels*, 2007, 21(3): 1337–42.
36. Capunitan J A, Capareda S C. Characterization and separation of corn stover bio-oil by fractional distillation. *Fuel*, 2013, 112: 60–73.

37. Kim T, Oh S, Kim J, Choi I C J W. Study on the hydrodeoxygenative upgrading of crude bio-oil produced from woody biomass by fast pyrolysis. *Energy*, 2014, 68: 437--443.
38. Oh S, Hwang H, Choi H S, Choi J W. Investigation of chemical modifications of micro- and macromolecules in bio-oil during hydrodeoxygenation with Pd/C catalyst in supercritical ethanol. *Chemosphere*, 2014, 117(1): 806--814.
39. Tang Z, Lu Q, Zhang Y, Zhu X, Guo Q. One step bio-oil upgrading through hydrotreatment, esterification, and cracking. *Industrial and Engineering Chemistry Research*, 2009, 48(15): 6923--6929.
40. Duan P, Savage P E. Catalytic hydrotreatment of crude algal bio-oil in supercritical water. *Applied Catalysis B: Environmental*, 2011, 104(1--2): 136--143.
41. Bai X, Duan P, Xu Y, Zhang A, Savage P E. Hydrothermal catalytic processing of pretreated algal oil: A catalyst screening study. *Fuel*, 2014, 120: 141--149.
42. Zhang C, Duan P, Xu Y, Wang B, Wang F, Zhang L. Catalytic upgrading of duckweed biocrude in subcritical water. *Bioresource Technology*, 2014, 166: 37--44.
43. Tang Z, Zhang Y, Guo Q. Catalytic hydrocracking of pyrolytic lignin to liquid fuel in supercritical ethanol. *Industrial and Engineering Chemistry Research*, 2010, 49(5): 2040--2046.
44. Yao Q, Tang Z, Guo J H, Zhang Y, Guo Q X. Effect of Catalyst Properties on Hydrocracking of Pyrolytic Lignin to Liquid Fuel in Supercritical Ethanol. *Chinese Journal of Chemical Physics*, 2015, 28(2): 209--216.
45. Duan P, Zhang C, Wang F, Fu J, Lü X, Xu Y, Shi X. Activated carbons for the hydrothermal upgrading of crude duckweed bio-oil. *Catalysis Today*, 2016, 274: 73--81.
46. Oh S, Hwang H, Choi H S, Choi J W. The effects of noble metal catalysts on the bio-oil quality during the hydrodeoxygenative upgrading process. *Fuel*, 2015, 153: 535--543.
47. Duan P, Bai X, Xu Y, Zhang A, Wang F, Zhang L i wsp. Catalytic upgrading of crude algal oil using platinum/gamma alumina in supercritical water. *Fuel*, 2013, 109: 225--233.
48. Lopez Barreiro D, Gomez B R, Ronsse F, Hornung U, Kruse A, Prins W. Heterogeneous catalytic upgrading of biocrude oil produced by hydrothermal liquefaction of microalgae: State of the art and own experiments. *Fuel Processing Technology*, 2016, 148: 117--127.
49. Peng J, Chen P, Lou H, Zheng X. Upgrading of Bio-oil over Aluminum Silicate in Supercritical Ethanol, 2008, 317(1): 3489--3492.
50. Peng J, Chen P, Lou H, Zheng X. Catalytic upgrading of bio-oil by HZSM-5 in sub- and super-critical ethanol. *Bioresource Technology*, 2009, 100(13): 3415--3418.
51. Zhang Q, Xu Y, Li Y, Wang T, Zhang Q, Ma L, He M L K. Investigation on the esterification by using supercritical ethanol for bio-oil upgrading. *Applied Energy*, 2015, 160: 633--640.
52. Duan P, Xu Y, Wang F, Wang B, Yan W. Catalytic upgrading of pretreated algal bio-oil over zeolite catalysts in supercritical water. *Biochemical Engineering Journal*, 2015: 6--13.
53. Cheng S, Wei L, Julson J, Muthukumarappan K, Kharel P R. Upgrading pyrolysis bio-oil to hydrocarbon enriched biofuel over bifunctional Fe-Ni/HZSM-5 catalyst in supercritical methanol. *Fuel Processing Technology*, 2017, 167: 117--126.
54. Shi W, Gao Y, Song S, Zhao Y. One-pot conversion of bio-oil to diesel- and jet-fuel-range hydrocarbons in supercritical cyclohexane. *Industrial and Engineering Chemistry Research*, 2014, 53(28): 11557--11565.

55. Zhang X, Zhang Q, Wang T, Li B, Xu Y, Ma L. Efficient upgrading process for production of low quality fuel from bio-oil. *Fuel*, 2016, 179: 312--321.
56. Cheng S, Wei L, Julson J, Rabnawaz M. Upgrading pyrolysis bio-oil through hydrodeoxygenation (HDO) using non-sulfided Fe-Co/SiO₂ catalyst. *Energy Conversion and Management*, 2017, 150(June): 331--342.
57. Cheng S, Wei L, Julson J, Muthukumarappan K, Kharel P R. Upgrading pyrolysis bio-oil to biofuel over bifunctional Co-Zn/HZSM-5 catalyst in supercritical methanol. *Energy Conversion and Management*, 2017, 147: 19--28.
58. Yang T, Jie Y, Li B, Kai X, Yan Z, Li R. Catalytic hydrodeoxygenation of crude bio-oil over an unsupported bimetallic dispersed catalyst in supercritical ethanol. *Fuel Processing Technology*, 2016, 148: 19--27.
59. Jo H, Prajitno H, Zeb H, Kim J. Upgrading low-boiling-fraction fast pyrolysis bio-oil using supercritical alcohol: Understanding alcohol participation, chemical composition, and energy efficiency. *Energy Conversion and Management*, 2017, 148: 197--209.
60. Remón J, Arcelus-Arrillaga P, García L, Arauzo J. Production of gaseous and liquid bio-fuels from the upgrading of lignocellulosic bio-oil in sub- and supercritical water: Effect of operating conditions on the process. *Energy Conversion and Management*, 2016, 119: 14--36.
61. Ahmadi S, Reyhanitash E, Yuan Z, Rohani S, Xu C (Charles). Upgrading of fast pyrolysis oil via catalytic hydrodeoxygenation: Effects of type of solvents. *Renewable Energy*, 2017, 114: 376--382.
62. Xu Y, Long J, Liu Q, Li Y, Wang C, Zhang Q, Wei L, Zhang X, Qiu S, Wang T et al. In situ hydrogenation of model compounds and raw bio-oil over Raney Ni catalyst. *Energy Conversion and Management*, 2015, 89: 188--196.
63. Xiong W M, Fu Y, Zeng F X, Guo Q X. An in situ reduction approach for bio-oil hydroprocessing. *Fuel Processing Technology*, 2011, 92(8): 1599--1605.
64. Wang H, Male J, Wang Y. Recent advances in hydrotreating of pyrolysis bio-oil and its oxygen-containing model compounds. *ACS Catalysis*, 2013, 3(5): 1047--1070.
65. Boucher M E, Chaala A, Pakdel H, Roy C. Bio-oils obtained by vacuum pyrolysis of softwood bark as a liquid fuel for gas turbines Part II : Stability and ageing of bio-oil and its blends with methanol and a pyrolytic aqueous phase. *Biomass and Bioenergy*, 2000, 19: 351--361.
66. Nguyen D, Honnery D. Combustion of bio-oil ethanol blends at elevated pressure. *Fuel*, 2008, 87: 232--243.
67. Oasmaa A, Kuoppala E, Selin J F, Gust S S Y. Fast pyrolysis of forestry residue and pine 4 Improvement of the product quality by solvent addition. *Energy & Fuels*, 2004, 18(5): 1578--1583.
68. Pidasang B, Sukkasi S, Pattiya A. Effect of in-situ addition of alcohol on yields and properties of bio-oil derived from fast pyrolysis of eucalyptus bark. *Journal of Analytical and Applied Pyrolysis*, 2016, 120: 82--93.
69. Pidasang B, Udomsap P, Sukkasi S, Chollacoop N P A. Influence of alcohol addition on properties of bio-oil produced from fast pyrolysis of eucalyptus bark in a free-fall reactor. *Journal of Industrial and Engineering Chemistry*, 2013, 19: 1851--1857.
70. Krutof A, Hawboldt K. Blends of pyrolysis oil , petroleum , and other bio-based fuels : A review. *Renewable and Sustainable Energy Reviews*, 2016, 59: 406--419.
71. Weerachanchai P, Tangsathitkulchai C, Tangsathitkulchai M. Phase behaviors and fuel properties of bio-oil-diesel-alcohol blends. *World Academy of Science, Engineering and*

- Technology, 2009, 32(8): 387--393.
72. Yu F, Deng S, Chen P, Liu Y, Wan Y, Olson A, Kittelson D., Ruan R. Physical and chemical properties of bio-oils from microwave pyrolysis of corn stover. *Applied Biochemistry and Biotechnology*, 2007, 136--140(2): 957--970.
 73. Mante O D, Agblevor F A. Storage stability of biocrude oils from fast pyrolysis of poultry litter. *Waste Management*, 2012, 32(1): 67--76.
 74. Udomsap P, Yeinn Y H, Hui J T H, Yoosuk B, Yusuf S B, Sukkasi S. Towards stabilization of bio-oil by addition of antioxidants and solvents, and emulsification with conventional hydrocarbon fuels. *International Conference & Utility Exhibition on Power and Energy Systems: Issues and Prospects for Asia (ICUE)*, 2011: 1--5.
 75. Diebold J P, Czernik S. Additives to lower and stabilize the viscosity of pyrolysis oils during storage. *Energy & Fuels*, 1997, 11(10): 1081--91.
 76. Zhang X, Tang W, Zhang Q, Li Y, Chen L, Xu Y, Wang C M L. Production of hydrocarbon fuels from heavy fraction of bio-oil through hydrodeoxygenative upgrading with Ru-based catalyst. *Fuel*, 2018, 215: 825--834.
 77. Shafaghat H, Kim J M, Lee I G, Jae J, Jung S C, Park Y K. Catalytic hydrodeoxygenation of crude bio-oil in supercritical methanol using supported nickel catalysts. *Renewable Energy*, 2018: 1--8.
 78. Shakya R, Adhikari S, Mahadevan R, Hassan E B, Dempster T A. Catalytic upgrading of bio-oil produced from hydrothermal liquefaction of *Nannochloropsis* sp. *Bioresource Technology*, 2018, 252: 28--36.
 79. Zhang Z, Wang Q, Tripathi P, Pittman Jr C U. Catalytic upgrading of bio-oil using 1-octene and 1-butanol over sulfonic acid resin catalysts. *Green Chemistry*, 2011, 13: 940--9.
 80. Boundy B, Diegel S, Wright L D S. *Biomass Energy Data Book: Edition 4*. US Department of Energy, 2011: 201.
 81. Nishimura S, Ikeda N, Ebitani K. Selective hydrogenation of biomass-derived 5-hydroxymethylfurfural (HMF) to 2,5-dimethylfuran (DMF) under atmospheric hydrogen pressure over carbon supported PdAu bimetallic catalyst. *Catalysis Today*, 2014, 232: 89--98.
 82. Wang X, Liu Y L X. Hydrogenolysis of 5-hydroxymethylfurfural to 2,5-dimethylfuran over supported Pt-Co bimetallic catalysts under mild conditions. *Green Chemistry*, 2018, 20: 2894--2902.
 83. Roman-Leshkov Y, Barrett C J, Liu Z Y D J A. Production of dimethylfuran for liquid fuels from biomass-derived carbohydrates. *Nature*, 2007, 447(June): 982--986.
 84. Meng J, Moore A, Tilotta D C, Kelley S S, Adhikari S, Park S. Thermal and storage stability of bio-oil from pyrolysis of torrefied wood. *Energy and Fuels*, 2015, 29(8): 5117--5126.
 85. He Z, Xu D, Wang S, Zhang H, Jing Z. Catalytic upgrading of water-soluble biocrude from hydrothermal liquefaction of *Chlorella*. *Energy & Fuels*, 2018, 32(2): 1893--1899.
 86. Feng J, Hse C, Yang Z, Wang K, Jiang J, Xu J. Liquid phase in situ hydrodeoxygenation of biomass-derived phenolic compounds to hydrocarbons over bifunctional catalysts. *Applied Catalysis A: General*, 2017, 542(November 2016): 163--173.
 87. Fan L, Zhang Y, Liu S, Zhou N, Chen P, Cheng Y et al. Bio-oil from fast pyrolysis of lignin: Effects of process and upgrading parameters. *Bioresource Technology*, 2017, 241: 1118--1126.
 88. Li X, Xiang Y. A novel liquid system of catalytic hydrogenation. *Science in China, Series*

- B: Chemistry, 2007, 50(6): 746--753.
89. Wang Z, Zeng Y, Lin W, Song W. In-situ hydrodeoxygenation of phenol by supported Ni catalyst – explanation for catalyst performance. *International Journal of Hydrogen Energy*, 2017, 42(33): 21040--21047.
 90. Feng J, Yang Z, Hse C, Su Q, Wang K, Jiang J et al. In situ catalytic hydrogenation of model compounds and biomass-derived phenolic compounds for bio-oil upgrading. *Renewable Energy*, 2017, 105: 140--148.
 91. Gollakota A R K, Reddy M, Subramanyam M D, Kishore N. A review on the upgradation techniques of pyrolysis oil. *Renewable and Sustainable Energy Reviews*, 2016, 58: 1543--1568.
 92. Anikeev V I. Thermal transformations of some monoterpene compounds in supercritical lower alcohols. *Flavour and Fragrance Journal*, 2010, 25: 443--455.
 93. Anikeev V I. Transformations of Organic Compounds in Supercritical Fluid Solvents : From Experiments to Kinetics , Thermodynamics , Simulation , and Practical Applications. *Kinetics and Catalysis*, 2009, 50(2): 284--296.
 94. Anikeev V I, Ermakova A, Chibiryayev A M, Kozhevnikov I V. Kinetics of Thermal Conversions of Monoterpenic Compounds in Supercritical Lower Alcohols. *Kinetics and Catalysis*, 2010, 51(2): 162--193.
 95. Ikushima Y, Sato M. A one-step production of fine chemicals using supercritical water : an environmental benign application to the synthesis of monoterpene alcohol. *Chemical Engineering Science*, 2004, 59: 4895--4901.
 96. Monteiro J.L.F, Veloso C.O. Catalytic conversion of terpenes into fine chemicals, 2004, 27(February): 169--180.
 97. Rubulotta G, Quadrelli E A. Terpenes : A Valuable Family of Compounds for the Production of Fine Chemicals. *Studies in Surface Science and Catalysis*, 2019, 178: 215--229.
 98. K.A.D. Swift. Catalytic transformations of the major terpene feedstocks. *Topics in Catalysis*, 2004, 27(February): 143--155.
 99. Eisenacher M, Beschnitt S, Hölderich W. Novel route to a fruitful mixture of terpene fragrances in particular phellandrene starting from natural feedstock geraniol using weak acidic boron based catalyst. *Catalysis Communications*, 2012, 26: 214--217.
 100. Gallezot P. Catalytic routes from renewables to fine chemicals. *Catalysis Today*, 2007, 121: 76--91.
 101. Costa C, Johnstone R A W, Whittaker D. Catalysis of terpene rearrangements by zirconium phosphates and zirconium organo-substituted phosphonates. *Journal of Molecular Catalysis A: Chemical*, 1998, 129: 79--89.
 102. Yılmazoğlu E, Akgün M. p -Cymene production from orange peel oil using some metal catalyst in supercritical alcohols. *The Journal of Supercritical Fluids*, 2018, 131(127): 37--46.
 103. Ermakova A, Chibiryayev A M, Mikenin P E, Sal'nikova O I, Anikeev V I. The Influence of Water on the Isomerization of a -Pinene in a Supercritical Aqueous – Alcoholic Solvent. *Russian Journal of Physical Chemistry A*, 2008, 82(1): 62--67.
 104. Baxter R L, Laurie W A, McHale D. Transformations of monoterpenoids in aqueous acids. *Tetrahedron*, 1978, 34: 2195--2199.
 105. Otera J. Transesterification. *Chemical Reviews*, 1993, 93(4): 1449--1470.
 106. Meher L C, Sagar D V, Naik S N. Technical aspects of biodiesel production by

- transesterification — a review. *Renewable and Sustainable Energy Reviews* 10, 2006(November 2017): 248--268.
107. Ejikeme P M, Anyaogu I D, Ejikeme C L, Nwafor N P, Egbuonu C A C, Ukogu, K et al. Catalysis in Biodiesel Production by Transesterification Processes-An Insight. *E-Journal of Chemistry*, 2010, 7(4): 1120--1132.
 108. Demirbas A. Biodiesel fuels from vegetable oils via catalytic and non-catalytic supercritical alcohol transesterifications and other methods: a survey. *Energy Conversion and Management*, 2003, 44: 2093--2109.
 109. Lee H, Kim Y M, Lee I G, Jeon J K, Jung S C, Chung, Jin Do et al. Recent advances in the catalytic hydrodeoxygenation of bio-oil. *Korean Journal of Chemical Engineering*, 2016, 33(12): 1–17.

Appendix 1. GCMS results of bio-oil blending and reactions

Table 1. Chemical composition of the crude bio-oil, bio-oil-methanol/ethanol/isopropanol blends (BM1, BE1, BI1) and bio-oil-alcohol reaction products (BM2, BE2, BI2) measured using GC-MS.

Compound	Retention Time (min.)	Bio-oil		BM1		BM2		BE1		BE2		BI1		BI2	
		Area count	% of Total	Area count	% of Total	Area count	% of Total	Area count	% of Total	Area count	% of Total	Area count	% of Total	Area count	% of Total
Acids															
Propanoic acid	6.25	121223.00	0.57	69728.00	0.59			5445.20	0.56	4193.90	0.48	60613.00	0.70	73092.00	1.13
Hexanoic acid	14.57	67484.00	0.32												
Oxiraneoctanoic acid, 3-octyl-, cis-	36.17	258206.00	1.21	132419.00	1.12			1047.40	1.08			103772.00	1.19		
Acetic acid	3.85	540760.00	2.53	310665.00	2.62			2913.79	3.02	1594.71	1.83	293394.00	3.38	235738.00	3.65
Propanoic acid, 2-methyl-, anhydride	15.70									1405.43	1.61				
Propanoic acid, 2-(methoxymethoxy)-	9.08											44793.00	0.52		
Total Acids			4.63		4.33				4.66		3.92		5.79		4.78
Phenols															
Phenol	16.27	223241.00	1.05	85437.00	0.72	99,221.00	1.13	7222.80	0.75	8074.30	0.93	74284.00	0.85	75649.00	1.17
Phenol, 2-methoxy-	16.53	100300.00	4.70	438533.00	3.70	559,319.00	6.37	3738.51	3.87	4713.04	5.41	348803.00	4.01	499099.00	7.74
Phenol, 2-methyl-	17.64	236340.00	1.11	109671.00	0.92	153,992.00	1.76	8735.10	0.90	1032.48	1.18	88453.00	1.02	103585.00	1.61
Phenol, 4-methyl-	18.63	254644.00	1.19	99818.00	0.84	81,889.00	0.93	8291.90	0.86	7646.20	0.88	81985.00	0.94	67986.00	1.05

**TABLE
CONTINUED**

Compound	Retention Time (min.)	Bio-oil		BM1		BM2		BE1		BE2		BI1		BI2	
		Area count	% of Total	Area count	% of Total	Area count	% of Total	Area count	% of Total	Area count	% of Total	Area count	% of Total	Area count	% of Total
Phenols															
Phenol, 2-methoxy-4-methyl-	19.45	143600.00	6.72	664576.00	5.60	745,407.00	8.50	583522.00	6.04	631471.00	7.24	555111.00	6.39	571604.00	8.86
Phenol, 2,5-dimethyl-	19.91	316459.00	1.48	121247.00	1.02	121,207.00	1.38	96750.00	1.00	102457.00	1.18	94956.00	1.09	99170.00	1.54
Phenol, 4-ethyl-2-methoxy-	21.71	599465.00	2.81	238599.00	2.01	326,249.00	3.72	200011.00	2.07	274615.00	3.15	180409.00	2.08	285528.00	4.43
Phenol, 3-ethyl-5-methyl-	22.16	121070.00	0.57	47154.00	0.40	47,391.00	0.54	39288.00	0.41	43531.00	0.50	39509.00	0.45	47064.00	0.73
Phenol, 2-methoxy-3-(2-propenyl)-	23.83	669143.00	3.13	256368.00	2.16	169,991.00	1.94	232824.00	2.41	138616.00	1.59	237448.00	2.73	153199.00	2.37
Phenol, 2-methoxy-4-propyl-	23.92, 28.49	299320.00, 340245.00	2.99	113991.00, 134873.00	2.10	332,677.00	3.79	92232.00, 2,001,145.63.00	2.14	348170.00	3.99	94403.00, 116406.00	2.43	315177.00	4.89
2-Methoxy-4-vinylphenol	23.21	138101.00	0.65	56743.00	0.48			44925.00	0.46			40267.00	0.46		
Phenol, 2-methoxy-4-(1-propenyl)-	25.23, 26.53	502494.00, 477238.00	4.59	191387.00, 178526.00	3.12	88,218.00	1.01	156989.00, 144349.00	3.12	93669.00	1.07	154410.00, 142660.00	3.42	101051.00	1.57
Phenol, 4-(3-hydroxy-1-propenyl)-2-methoxy-	31.20	384044.00	1.80	133683.00	1.13			109460.00	1.13			125559.00	1.45		
Vanillin	27.02	797658.00	3.74	350245.00	2.95	100,922.00	1.15	283109.00	2.93	101228.00	1.16	292748.00	3.37	97024.00	1.50

**TABLE
CONTINUED**

Compound	Retention Time (min.)	Bio-oil		BM1		BM2		BE1		BE2		BI1		BI2	
		Area count	% of Total												
Phenols															
Phenol, 3-ethyl-	21.03	106616.00	0.50	83015.00	0.70	44,473.00	0.51	38202.00	0.40	41529.00	0.48	37358.00	0.43	37187.00	0.58
Total Phenols			37.03		27.85		32.73		28.49		28.76		31.12		38.04
Esters															
Geranyl isovalerate	24.60	187749.00	0.88	80535.00	0.68	87,404.00	1.00	64266.00	0.67	74694.00	0.86	63880.00	0.74	71088.00	1.10
Carbamic acid, ethyl-, methyl ester	10.09	105800.00	0.50	36333.00	0.31			57848.00	0.60			78022.00	0.90		
Oxalic acid, bis(isobutyl) ester	7.01	93474.00	0.44	40372.00	0.34			41943.00	0.43			37059.00	0.43		
1,2,3-Propanetriol, monoacetate	7.20	53093.00	0.25												
2-Furancarboxylic acid, methyl ester	12.70, 17.28	75085.00	0.35			50,566.00	0.58								
Dasycarpidan-1-methanol, acetate (ester)	37.84	281734.00	1.32	135277.00	1.14			102221.00	1.06			103719.00	1.19		
Acetic acid, 1-methylethyl ester	5.79			39416.00	0.33										
Acetic acid, 3,4-dihydroxy-3-methyl-butyl ester	21.89			72508.00	0.61										
Propanoic acid, methyl ester	2.70					272,929.00	3.11								
Carbonic acid, diethyl ester	4.92					161,758.00	1.84								
2-Butenoic acid, methyl ester, (E)-	5.23					56,533.00	0.64								
Propanoic acid, 2-hydroxy-, methyl ester, (f̄)-	5.43					100,773.00	1.15								

**TABLE
CONTINUED**

Compound	Retention Time (min.)	Bio-oil		BM1		BM2		BE1		BE2		B11		B12	
		Area count	% of Total												
Esters															
Acetic acid, methoxy-, methyl ester	5.91					51,734.00	0.59								
Propanoic acid, 2-methoxy-, methyl ester	6.27					100,874.00	1.15								
2-Pentenoic acid, methyl ester, (E)-	8.08					34,119.00	0.39								
Hexanoic acid, methyl ester	9.32					37,400.00	0.43								
Pentanoic acid, 4-oxo-, methyl ester	13.91					155,489.00	1.77								
Butanedioic acid, dimethyl ester	14.56					200,277.00	2.28								
Butanedioic acid, methyl-, dimethyl ester	15.29					151,688.00	1.73								
Benzoic acid, methyl ester	15.64					34,006.00	0.39								
Methyl 6-oxoheptanoate	20.65					35,560.00	0.41								
Octanoic acid, oct-3-en-2-yl ester	25.16					136,511.00	1.56								
Hexanoic acid, 2-ethyl-, oxybis(2,1-ethanedioxy-2,1-ethanedioyl) ester	25.47					70,725.00	0.81								
Hexanoic acid, 2-ethyl-, oxybis(2,1-ethanedioxy-2,1-ethanedioyl) ester	25.62					91,985.00	1.05								
Nonanedioic acid, dimethyl ester	28.13					129,063.00	1.47								

**TABLE
CONTINUED**

Compound	Retention Time (min.)	Bio-oil		BM1		BM2		BE1		BE2		BI1		BI2	
		Area count	% of Total												
Esters															
Benzeneacetic acid, 4-hydroxy-3-methoxy-, methyl ester	30.47					99,906.00	1.14								
Pentadecanoic acid, 13-methyl-, methyl ester	34.37					191,712.00	2.18								
10-Octadecenoic acid, methyl ester	37.83					237,147.00	2.70								
Ammonium acetate	3.89					132,930.00	1.52								
Propanoic acid, ethyl ester	3.79									293616.00	3.37				
Butanoic acid, 3-hydroxy-4-(benzyloxy)-, ethyl ester	4.62									37882.00	0.43				
Butanoic acid, ethyl ester	5.71									96699.00	1.11				
Acetic acid, ethoxy-, ethyl ester	9.97									62315.00	0.71				
Hexanoic acid, ethyl ester	11.51									52986.00	0.61				
2-Furancarboxylic acid, ethyl ester	14.95									65430.00	0.75				
Pentanoic acid, 4-oxo-, ethyl ester	16.00									169067.00	1.94				
Hexanoic acid, 5-oxo-, ethyl ester	16.86									41167.00	0.47				
Octanoic acid, ethyl ester	17.36									36577.00	0.42				
Butanedioic acid, diethyl ester	18.58									234511.00	2.69				

**TABLE
CONTINUED**

Compound	Retention Time (min.)	Bio-oil		BM1		BM2		BE1		BE2		BI1		BI2		
		Area count	% of Total	Area count	% of Total	Area count	% of Total	Area count	% of Total							
Esters																
Butanedioic acid, methyl-, diethyl ester	19.08									1415 22.00	1.62					
Pentanedioic acid, diethyl ester	21.34									9534 4.00	1.09					
5-Methyl-3-propylhexanoic acid, methyl ester	23.43									8572 3.00	0.98					
Hexadecanoic acid, ethyl ester	24.37 , 35.62									8382 0.00 , 2151 05.00	3.43			69179.00	1.07	
2,4-Dimethyl-nonanedioic acid, dimethyl ester	31.00									1316 20.00	1.51					
Ethyl Oleate	38.95									3233 95.00	3.71					
Dehydroabietic acid, trimethylsilyl ester	43.75									1729 73.00	1.98					
2,5-Dimethyl-3-hexanol acetate	19.08											35155.00	0.40			
Propanoic acid, 1-methylethyl ester	4.53													187568.0 0	2.91	
Butanoic acid, 1-methylethyl ester	6.68													56247.00	0.87	
Carbonic acid, ethyl-, methyl ester	7.89													177652.0 0	2.75	
Propanoic acid, 2-hydroxy-, 1-methylethyl ester, (2S)-	8.23														60276.00	0.93

**TABLE
CONTINUED**

Compound	Retention Time (min.)	Bio-oil		BM1		BM2		BE1		BE2		BI1		BI2	
		Area count	% of Total	Area count	% of Total	Area count	% of Total	Area count	% of Total	Area count	% of Total	Area count	% of Total	Area count	% of Total
Esters															
2-Propenoic acid, 2-methyl-, 1-methylethyl ester	8.41													36345.00	0.56
Pentanoic acid, 4-oxo-, propyl ester	16.83													103261.00	1.60
Succinic acid diisopropyl ester	20.19													97687.00	1.51
Isopropyl hexadecanoate	36.06													174101.00	2.70
Elaidic acid, isopropyl ester	39.33													254161.00	3.94
Octadecanoic acid, decyl ester	39.61													103755.00	1.61
Acetic acid, (1-methylethoxy)-, 1-methylethyl ester	12.43													51908.00	0.80
Total Esters			3.74		3.41		29.89		2.76		27.68		3.66		22.35
Ketones															
Ethanone, 1-bicyclo[2.2.1]hept-2-yl-, exo-	7.97	52350.00	0.25												
2-Cyclopenten-1-one	8.72	187533.00	0.88	254878.00	2.15	29,910.00	0.34	82897.00	0.86	29702.00	0.34	80154.00	0.92	44527.00	0.69
2-Pentanone, 4-hydroxy-4-methyl-	9.22	43470.00	0.20	37960.00	0.32	40,005.00	0.46	36353.00	0.38	33609.00	0.39	31809.00	0.37	33869.00	0.52
2-Cyclopenten-1-one, 2-methyl-	10.44	125091.00	0.59	58013.00	0.49	118,044.00	1.35	50607.00	0.52	140101.00	1.61	43017.00	0.50	119304.00	1.85

**TABLE
CONTINUED**

Compound	Retention Time (min.)	Bio-oil		BM1		BM2		BE1		BE2		BI1		BI2	
		Area count	% of Total												
Ketones															
Ethanone, 1-(2-furanyl)-	10.91	61368.00	0.29			43,353.00	0.49			32530.00	0.37			33649.00	0.52
2-Cyclopenten-1-one, 3-methyl-	13.37	127857.00	0.60	49750.00	0.42	40,345.00	0.46	42830.00	0.44	35440.00	0.41	69879.00	0.80	35789.00	0.55
2,4-Hexanedione, 5,5-dimethyl-	14.38	55589.00	0.26												
1,2-Cyclopentanedione, 3-methyl-	15.14	458702.00	2.15	196998.00	1.66	85,127.00	0.97	166950.00	1.73	77819.00	0.89	168880.00	1.94	97527.00	1.51
1,3-Cyclopentanedione, 2,4-dimethyl-	15.55	72996.00	0.34			40,290.00	0.46			37802.00	0.43			33877.00	0.53
Adrenalone	21.21	131556.00	0.62	53450.00	0.45	55,282.00	0.63	43531.00	0.45	62399.00	0.72	43136.00	0.50	51674.00	0.80
Ethanone, 1-(4-hydroxy-3-methoxyphenyl)-	28.97	685853.00	3.21	256130.00	2.16	233,913.00	2.67	208416.00	2.16	181507.00	2.08	228587.00	2.63	188433.00	2.92
2-Propanone, 1-(4-hydroxy-3-methoxyphenyl)-	30.19	391935.00	1.84	160344.00	1.35	165,465.00	1.89	132659.00	1.37	147520.00	1.69	135654.00	1.56	135895.00	2.11
2(3H)-Naphthalenone, 4,4a,5,6,7,8-hexahydro-1-methoxy-	30.87	286902.00	1.34	109689.00	0.92	91,069.00	1.04	92084.00	0.95	87309.00	1.00	93949.00	1.08	81272.00	1.26
3,12-Oleandione	41.56	239551.00	1.12	134658.00	1.13	100,652.00	1.15	91510.00	0.95	99427.00	1.14	100852.00	1.16	94088.00	1.46
4H-Pyran-4-one, 3,5-dihydroxy-2-methyl-	19.76	121620.00	0.57												
2(5H)-Furanone	13.85	260115.00	1.22	99899.00	0.84			85477.00	0.88			81477.00	0.94		

**TABLE
CONTINUED**

Compound	Retention Time (min.)	Bio-oil		BM1		BM2		BE1		BE2		BI1		BI2	
		Area count	% of Total												
Ketones															
2(5H)-Furanone, 5-methyl-	14.26	73859.00	0.35												
4-Methyl-5H-furan-2-one	18.40	197388.00	0.92	76927.00	0.65			64089.00	0.66			62802.00	0.72		
2(3H)-Furanone, 5-methyl-	12.13	138044.00	0.65	53035.00	0.45			46109.00	0.48			45077.00	0.52		
2,5-Hexanedione	12.54					37,839.00	0.43			30107.00	0.35			39563.00	0.61
2-Cyclopenten-1-one, 3,4-dimethyl-	13.78					36,399.00	0.41								
3-Penten-2-one, 3-ethyl-4-methyl-	20.25					32,709.00	0.37								
2-Butanone, 4-hydroxy-	2.54							33233.00	0.34						
2-Pentanone, 5,5-diethoxy-	17.90							101091.00	1.05						
Total Ketones			17.40		12.99		13.12		13.22		11.42		13.64		15.33
Alcohols/Ethers															
3-Pentanol, 2,4-dimethyl-	2.63	52416.00	0.25												
2-Pentanol, 4-methyl-	5.41	33733.00	0.16												
3-Heptanol, 2,4-dimethyl-	7.71	32588.00	0.15												
2-Octen-1-ol, (E)-	13.19	75109.00	0.35												
2-Propanol, 1-methoxy-	3.33	99729.00	0.47									39388.00	0.45		
Methane, dimethoxy-	3.69	72696.00	0.34	32034.00	0.27										
1,3-Dioxane	8.36	224538.00	1.05												

**TABLE
CONTINUED**

Compound	Retention Time (min.)	Bio-oil		BM1		BM2		BE1		BE2		BI1		BI2	
		Area count	% of Total	Area count	% of Total	Area count	% of Total	Area count	% of Total	Area count	% of Total	Area count	% of Total	Area count	% of Total
Alcohols/Ethers															
Methyl-(2-hydroxy-3-ethoxy-benzyl) ether	32.95	626772.00	2.93	246571.00	2.08	328,333.00	3.74	206775.00	2.14	258745.00	2.97	208169.00	2.40	238512.00	3.70
Methane, trimethoxy-	4.57, 7.33	475381.00	2.23	203641.00, 58311.00	2.21			186119.00	1.93			170493.00	1.96		
2-Furanmethanol	12.70	82442.00	0.39												
1,2-Nonadecanediol	36.71	278225.00	1.30	142812.00	1.20			113782.00	1.18						
p-Dioxane-2,3-diol				179614.00	1.51										
Benzenemethanol, 4-(phenylmethyl)-	27.28			138982.00	1.17										
Ethane, 1,1-dimethoxy-	2.23			113016.00	0.95	94,595.00	1.08								
Propane, 2,2-dimethoxy-	2.62			761960.00	6.42	207,439.00	2.36								
Propane, 1,1-dimethoxy-	3.11			57123.00	0.48	53,604.00	0.61								
Ethane, 1,1,1-trimethoxy-	8.39			131843.00	1.11										
1,1-Dimethoxyhexane	14.89			85678.00	0.72										
Propane, 1,1,3,3-tetramethoxy-	12.39			159129.00	1.34										
1,1-Dimethoxyhexane	16.73			181114.00	1.53										
2-Furanethanol, β-methoxy-(S)-	10.84			140815.00	1.19										

**TABLE
CONTINUED**

Compound	Retention Time (min.)	Bio-oil		BM1		BM2		BE1		BE2		B11		B12	
		Area count	% of Total	Area count	% of Total	Area count	% of Total	Area count	% of Total	Area count	% of Total	Area count	% of Total	Area count	% of Total
Alcohols/Ethers															
Furan, tetrahydro-2,5-dimethoxy-	7.70			168062.00	1.42										
1,2-Butanediol	7.79					32,356.00	0.37								
4-Octanol, 2,4-dimethyl-	22.79					80,660.00	0.92								
3-Methoxy-3-methyl-tetrahydropyran-2-one	14.77, 17.28					44,469.00, 39,242.00	0.95								
3,4-Dimethoxytoluene	20.13					33,569.00	0.38								
Hexane, 3-methoxy-	8.48					29,440.00	0.34								
Ethanol	3.43							3116.00	0.32						
Ethanol, 2,2-diethoxy-	10.95							9955.60	1.03						
Ethane, 1,1-diethoxy-	3.72							2372.82	2.46	5293.71	6.07				
Propane, 2,2-diethoxy-	4.19							4579.79	4.74	1425.84	1.64				
Propane, 1,1-diethoxy-	5.42							7625.70	0.79	7356.90	0.84				
Pentane, 1,1-diethoxy-	15.70							1193.12	1.23						
Heptane, 1,1-diethoxy-	21.89							1015.64	1.05						
2-Ethoxytetrahydrofuran	5.95							3835.10	0.40						

**TABLE
CONTINUED**

Compound	Retention Time (min.)	Bio-oil		BM1		BM2		BE1		BE2		BI1		BI2	
		Area count	% of Total	Area count	% of Total	Area count	% of Total	Area count	% of Total	Area count	% of Total	Area count	% of Total	Area count	% of Total
Alcohols/Ethers															
Furan, 2,5-diethoxytetrahydro-	11.46, 11.86							2775 24.00 2314 62.00	5.27						
1,3-Dioxan-5-ol	9.79									1199 34.00	1.38				
Ethane, 1-ethoxy-1-methoxy-	2.84									3030 1.00	0.35				
Tetramethoxymethane	6.82									9245 1.00	1.06				
2-Propanol, 1,1'-oxybis-	2.23											92265.00	1.06		
1-Propanol, 2-ethoxy-	4.74											241991.00	2.79		
3-Hexanol, 3,4-diethyl-,	13.01, 14.11											203595.00, 177960.00	4.39		
1,1-Diisopropoxyethane	5.80											45183.00	0.52		
2-Hexanol	11.59													34941.00	0.54
Ethanol, 2-[2-(2-propenyloxy)ethoxy]-	5.40													32590.00	0.51
Total Alcohols/Ethers			9.62		23.60		10.75		22.54		14.31		13.57		4.75
Aldehydes															
4-Hydroxy-2-methoxycinnamaldehyde	35.67	702604 .00	3.29	336538 .00	2.84			2710 43.00	2.81			294440.00	3.39		

**TABLE
CONTINUED**

Compound	Retention Time (min.)	Bio-oil		BM1		BM2		BE1		BE2		BI1		BI2	
		Area count	% of Total	Area count	% of Total	Area count	% of Total	Area count	% of Total	Area count	% of Total	Area count	% of Total	Area count	% of Total
Aldehydes															
2-Furancarboxaldehyde, 5-(hydroxymethyl)-	24.36	496300.00	2.32	182371.00	1.54			169747.00	1.76			178786.00	2.06		
Furfural	8.78	479993.00	2.25	135689.00	1.14			151081.00	1.56			145360.00	1.67		
2-Furancarboxaldehyde, 5-methyl-	12.96	150838.00	0.71	58421.00	0.49			53647.00	0.56						
2-Furaldehyde diethyl acetal	14.27							51940.00	0.54						
Total Aldehydes			8.57		6.01				7.23				7.12		
Sugar Derivatives															
β-D-Glucopyranose, 4-O-β-D-galactopyranosyl-	32.58	1032000.00	4.83	667324.00	5.62			620294.00	6.42			636530.00	7.33		
α-D-Glucopyranoside, O-α-D-glucopyranosyl-(1.fwdarw.3)-α-D-fructofuranosyl	26.46	426569.00	2.00	186803.00	1.57			146771.00	1.52			146547.00	1.69		
Total Sugar Derivatives			6.83		7.19				7.94				9.01		
Hydrocarbons															
Cyclohexene, 3-(1-methylethyl)-	16.74					26,258.00	0.30								
Others															
Maltol	17.74	128149.00	0.60	89813.00	0.76										

**TABLE
CONTINUED**

Compound	Retention Time (min.)	Bio-oil		BM1		BM2		BE1		BE2		BI1		BI2	
		Area count	% of Total	Area count	% of Total	Area count	% of Total	Area count	% of Total	Area count	% of Total	Area count	% of Total	Area count	% of Total
Others															
6,7-Epoxy pregn-4-ene-9,11,18-triol-3,20-dione, 11,18-diacetate	35.29	236649.00	1.11									84427.00	0.97		
1H-Cyclopropa[3,4]benz[1,2-e]azulene-4a,5,7b,9,9a(1aH)-pentol, 3-[(acetyloxy)methyl]-1b,4,5,7a,8,9-hexahydro-1,1,6,8-tetramethyl-, 9,9a-diacetate, [1aR-(1aà,1bá,4aá,5à,7aà,7bà,8à,9á,9aà)]-	39.35	239638.00	1.12	121430.00	1.02			89385.00	0.93			97967.00	1.13		
Butanoic acid, 1a,2,5,5a,6,9,10,10a-octahydro-5,5a-dihydroxy-4-(hydroxymethyl)-1,1,7,9-tetramethyl-11-oxo-1H-2,8a-methanocyclopenta[a]cyclopropa[e]cyclodecen-6-yl ester, [1aR-(1aà,2à,5á,5aá,6á,8aà,9á,10aà)]-	43.00, 44.90	223821.00, 258951.00	2.26	167015.00	1.41	169,908.00, 175,763.00	3.94	109641.00, 135669.00	2.54	183407.00	2.10	133678.00	1.54	158558.00	2.46
tert-Hexadecanethiol	28.72	305844.00	1.43	112072.00	0.94										

**TABLE
CONTINUED**

Compound	Retention Time (min.)	Bio-oil		BM1		BM2		BE1		BE2		B11		B12	
		Area count	% of Total	Area count	% of Total	Area count	% of Total	Area count	% of Total	Area count	% of Total	Area count	% of Total	Area count	% of Total
Others															
2-Acetyl-9-[3-deoxy- α -D-ribofuranosyl]hypoxanthine	22.59	160076.00	0.75	67564.00	0.57			5644.00	0.58			54733.00	0.63		
2-Vinyl-9-[3-deoxy- α -D-ribofuranosyl]hypoxanthine	17.82	126974.00	0.59												
Cyclopenta[d]anthracene-8,11-dione, 1,2,3,3a,4,5,6,6a,7,8,11,12-dodecahydro-3-(1-methylethyl)-12-hydroxy-	45.74, 49.16	205003.00	0.96	151294.00, 152389.00	2.56	224,414.00	2.56	1410.00, 1340.00	2.85	1402.00, 55.00	1.61	134839.00, 128464.00	3.03	135469.00	2.10
9-Octadecenoic acid, (2-phenyl-1,3-dioxolan-4-yl)methyl ester, trans-	34.57	260723.00	1.22	130611.00	1.10			1106.00, 58.00	1.15			112760.00	1.30		
Androst-5,7-dien-3-ol-17-one, acetate	42.02, 42.75, 49.87,	243281.00, 223146.00	2.18	136067.00, 139684.00	2.32	103,345.00, 265,241.00	4.20	1125.00, 1358.00, 77.00	2.57	9504.00, 8.00, 9889.00, 3.00, 1640.00, 02.00	4.11	108582.00, 106915.00	2.48	91806.00, 112065.00	3.16
Tetradecanoic acid, 3,3a,4,6a,7,8,9,10,10a,10b-decahydro-3a,10a-dihydroxy-5-(hydroxymethyl)-	40.48			129826.00	1.09										

2,10-dimethyl-3-oxobenz[e]azulen-8-yl ester, [3aR-(3aà,6aà,8à,10á,10aá,10bá)]-															
--	--	--	--	--	--	--	--	--	--	--	--	--	--	--	--

**TABLE
CONTINUED**

Compound	Retention Time (min.)	Bio-oil		BM1		BM2		BE1		BE2		BI1		BI2	
		Area count	% of Total												
Others															
Benz[e]azulene-3,8-dione, 3a,4,6a,7,9,10,10a,10b-octahydro-3a,10a-dihydroxy-5-(hydroxymethyl)-2,10-dimethyl-, (3aà,6aà,10á,10aá,10bá)-(+)-	46.52			192006.00	1.62										
Methyl 4-O-acetyl-2,3,6-tri-O-ethyl-à-d-mannopyranoside	26.70			145048.00	1.22			101077.00	1.05			107869.00	1.24		
Furan, 2,5-dimethyl-	3.36					32,174.00	0.37			54087.00	0.62			61528.00	0.95
1,3-Dioxolane, 4-ethyl-	13.64					126,671.00	1.44								
1-Oxaspiro[2.5]octane, 2,4,4-trimethyl-8-methylene-	23.29					64,305.00	0.73			53815.00	0.62			55444.00	0.86
Formamide, N-methoxy-	7.74							69908.00	0.72						
Desulphosinigrin	23.53							77143.00	0.80						
Dimethylamine	7.29									105774.00	1.21				
Bicyclo[2.2.1]heptane-2-carboxylic acid,	17.77									55052.00	0.63				

6-hydroxy-3-(hydroxymethyl)-, (1r,2-cis,3-trans,4-cis,6-trans)-															
1,2-Cyclopentanedicarboxylic acid, 4-(1,1-dimethylethyl)-, dimethyl ester, (1à,2à,4à)-	17.88									4115 7.00	0.47				
l-Gala-l-ido-octonic lactone	26.25									9393 6.00	1.08				

**TABLE
CONTINUED**

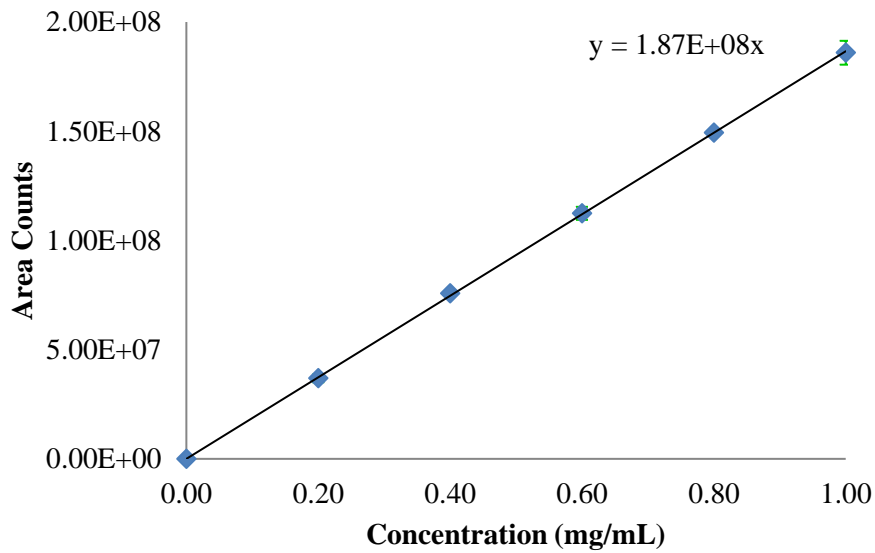
Compound	Retention Time (min.)	Bio-oil		BM1		BM2		BE1		BE2		B11		B12	
		Area count	% of Total	Area count	% of Total	Area count	% of Total	Area count	% of Total						
Others															
1,3-Dioxolane-4-methanol, 2-pentadecyl-, acetate, trans-	27.55									9700 5.00	1.11				
Furan, 2-ethyl-5-methyl-	5.14									2843 2.00	0.33				
Propanamide, N-methyl-	8.33											43951.00	0.51		
Spiro[tricyclo[4.4.0.0(5,9)]decane-10,2'-oxirane], 1-methyl-4-isopropyl-7,8-dihydroxy-, (8S)-	28.71											89556.00	1.03		
6-Isopropyl-1-oxaspiro[2.5]octane-4,5-dicarboxylic acid, dimethyl ester	33.55											81504.00	0.94		
1-Methyl-8-propyl-3,6-diazahomoadamantan-9-ol	36.64											112563.00	1.30		

4-(3,4-Dihydro-2H-quinolin-1-yl)-4-oxobutyric acid hydrazide	20.55													59877.00	0.93
1,3-Dioxolane, 4,4,5-trimethyl-2-pentadecyl-	22.73													49702.00	0.77
4-Hexenoic acid, 4-methyl-6-(fluorodimethylsilyl)-6-trimethylsilyl-	26.69													66611.00	1.03
6-Methyl-11-propenyl-5-(toluene-4-sulfonyloxy)-12,13-dioxatricyclo[7.3.1.0(1,6)]tridecane-8-carboxylic acid, methyl ester	32.05													88343.00	1.37

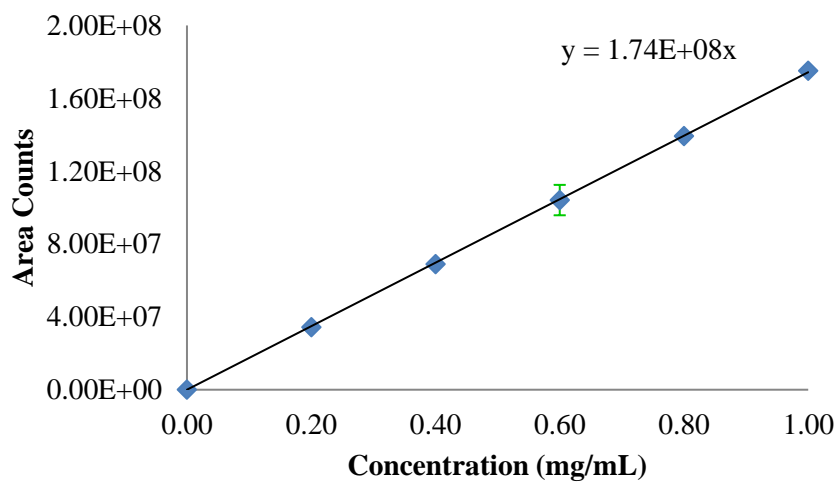
**TABLE
CONTINUED**

Compound	Retention Time (min.)	Bio-oil		BM1		BM2		BE1		BE2		BI1		BI2	
		Area count	% of Total	Area count	% of Total	Area count	% of Total	Area count	% of Total	Area count	% of Total	Area count	% of Total	Area count	% of Total
Others															
Furan, 2-methyl-	2.27													71031.00	1.10
Total Other Compounds			12.22		14.61		13.24		13.19		13.89		16.10		14.73
Total Compounds		213556 53.00	100.0 0	118655 20.00	100.0 0	8,774,2 33.00	100.0 0	9662 254.0 0	100.0 0	8716 532.0 0	100.0 0	8688964.0 0	100.00	6451325. 00	100.00

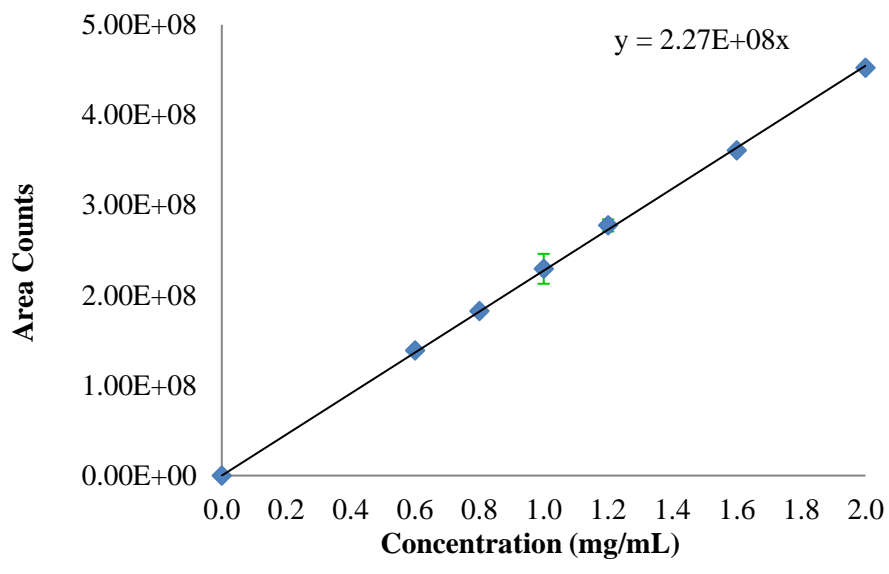
Appendix 2. Detailed results of in situ catalytic hydrogenation of phenol



Phenol calibration curve



Cyclohexanone calibration curve



Cyclohexanol calibration curve

Table 1. GCMS results of phenol conversion at various catalyst loadings

#	Catalyst loading (g)	Peak Area Count Run 1	Peak Area Count Run 2	Cx ^b 1 (mg/mL)	Cx ^b 2 (mg/mL)	Average Cx (mg/mL)	STDEV	Phenol out concentration (mg/mL)	Phenol in concentration (mg/mL)	Phenol Conversion (%)
1	0.00	100233609.16	102222431.12	0.54	0.55	0.54	0.01	48.23	48.73	1.03
2	0.21	25883757.19	23983533.84	0.14	0.13	0.13	0.01	12.03 ^c	53.48	77.50
3	0.44	9628608.99	9441496.90	0.05	0.05	0.05	0.00	4.81	60.96	92.11
4	0.61	3237414.59	3216431.51	0.02	0.02	0.02	0.00	1.54	58.21	97.36
5	0.82	1243037.78	1239904.17	0.01	0.01	0.01	0.00	0.66	59.69	98.89
6	1.03	950013.61	946534.33	0.01	0.01	0.01	0.00	0.51	54.80	99.07
7	1.01 ^a	3420263.88	3439515.32	0.02	0.02	0.02	0.00	1.67	58.21	97.13

^a Reproducibility run; ^b Cx refers to unknown concentration of analyte and was determined using the calibration curve in Chapter 5.2.3.

^c A sample calculation of *concentration out* is as follows using #2 as an example:

1. For GCMS analysis 0.11g of the product was diluted with 10.01 g MeOH therefore:

$$0.11 + 10.01 = 10.12$$

2. In terms of percentages this is:

$$1.11 \% + 98.89 \% = 100 \%$$

3. Therefore, since the peak area count with 1.11 % concentration of product gives 0.13 mg/mL concentration; then at 100 % product concentration equates to 12.03 mg/mL.

Table 2. GCMS results of cyclohexanone selectivity and yield at various catalyst loading

Catalyst loading (g)	Peak Area Count Run 1	Peak Area Count Run 2	Cx ^b 1 (mg/mL)	Cx ^b 2 (mg/mL)	Average Cx (mg/mL)	STDEV	Cyclohexanone Concentration (mg/mL)	Cyclohexanone Concentration (mol/L)	Total Product concentration (mol/L)	Cyclohexanone Selectivity (%)	Cyclohexanone Yield (%)
0.00	0.00	0.00	0.00	0.00	0.00	0.00	0.00	0.00	0.00	0.00	0.00
0.21	32301676.20	32345857.93	0.19	0.19	0.19	0.00	16.77	0.17	0.61	28.10	21.78
0.44	18349326.21	18103940.56	0.11	0.10	0.10	0.00	9.88	0.10	0.63	15.88	14.63
0.61	11595920.18	11799334.68	0.07	0.07	0.07	0.00	5.98	0.06	0.71	8.57	8.35
0.82	7579437.55	7723278.83	0.04	0.04	0.04	0.00	4.39	0.04	0.72	6.22	6.15
1.03	7041774.13	6551660.41	0.04	0.04	0.04	0.00	3.93	0.04	0.69	5.77	5.72
1.01 ^a	7747990.60	7761570.59	0.04	0.04	0.04	0.00	4.06	0.04	0.55	7.52	7.31

^a Reproducibility run

Table 3. GCMS results of cyclohexanol selectivity and yield at various catalyst loading

Catalyst loading (g)	Peak Area Count Run 1	Peak Area Count Run 2	Cx ^b 1 (mg/mL)	Cx ^b 2 (mg/mL)	Average Cx (mg/mL)	STDEV	Cyclohexanol Concentration (mg/mL)	Cyclohexanol Concentration (mol/L)	Total Product concentration (mol/L)	Cyclohexanol Selectivity (%)	Cyclohexanol Yield (%)
0.00	0.00	0.00	0.00	0.00	0.00	0.00	0.00	0.00	0.00	0.00	0.00
0.21	1082645 87.71	11191853 5.34	0.48	0.49	0.48	0.01	43.77	0.44	0.61	71.90	55.72
0.44	1257154 84.33	13128953 8.12	0.55	0.58	0.57	0.02	53.42	0.53	0.63	84.12	77.48
0.61	1622128 07.47	16992582 9.54	0.71	0.75	0.73	0.02	65.13	0.65	0.71	91.43	89.01
0.82	1549767 78.51	15220904 7.15	0.68	0.67	0.68	0.01	67.57	0.67	0.72	93.78	92.74
1.03	1468659 09.11	14844091 5.79	0.65	0.65	0.65	0.00	65.38	0.65	0.69	94.23	93.35
1.01 ^a	1269119 33.07	12693729 1.40	0.56	0.56	0.56	0.00	50.97	0.51	0.55	92.48	89.82

^a Reproducibility run

Table 4. GCMS results of phenol conversion at various reaction times

Reaction time (h)	Peak Area Count Run 1	Peak Area Count Run 2	Cx ^b 1 (mg/mL)	Cx ^b 2 (mg/mL)	Average Cx (mg/mL)	STDEV	Phenol out concentration (mg/mL)	Phenol in concentration (mg/mL)	Phenol Conversion (%)
1	57459880.49	58818497.03	0.31	0.31	0.31	0.01	28.85	57.75	50.05
2	950013.61	946534.33	0.01	0.01	0.01	0.00	0.51	54.80	99.07
3	0.00	0.00	0.00	0.00	0.00	0.00	0.00	0.00	100.00
4	1415194.70	1410178.06	0.01	0.01	0.01	0.00	0.67	47.59	98.59
5	955542.62	957489.83	0.01	0.01	0.01	0.00	0.47	53.60	99.11

Table 5. GCMS results of cyclohexanone selectivity and yield at various reaction times

Reaction time (h)	Peak Area Count Run 1	Peak Area Count Run 2	Cx 1 (mg/mL)	Cx 2 (mg/mL)	Average Cx (mg/mL)	STDEV	Cyclohexanone Concentration (mg/mL)	Cyclohexanone Concentration (mol/L)	Total Product concentration (mol/L)	Cyclohexanone Selectivity (%)	Cyclohexanone Yield (%)
1	15690738.79	15517254.84	0.09	0.09	0.09	0.00	8.32	0.08	0.34	24.61	12.32
2	7041774.13	6551660.41	0.04	0.04	0.04	0.00	3.93	0.04	0.69	5.77	5.72
3	4021017.35	3937859.76	0.02	0.02	0.02	0.00	2.10	0.02	0.56	3.79	3.79
4	3207932.83	3103161.41	0.02	0.02	0.02	0.00	1.61	0.02	0.62	2.66	2.62
5	1785929.08	1806131.39	0.01	0.01	0.01	0.00	0.96	0.01	0.60	1.64	1.63

Table 6. GCMS results of cyclohexanol selectivity and yield at various reaction times

Reaction time (h)	Peak Area Count Run 1	Peak Area Count Run 2	Cx 1 (mg/mL)	Cx 2 (mg/mL)	Average Cx (mg/mL)	STDEV	Cyclohexanol Concentration (mg/mL)	Cyclohexanol Concentration (mol/L)	Total Product concentration (mol/L)	Cyclohexanol Selectivity (%)	Cyclohexanol Yield (%)
1	63839293.07	63466460.96	0.28	0.28	0.28	0.00	26.02	0.26	0.34	75.39	37.74
2	146865909.11	148440915.79	0.65	0.65	0.65	0.00	65.38	0.65	0.69	94.23	93.35
3	135493417.57	133473833.51	0.60	0.59	0.59	0.01	54.37	0.54	0.56	96.21	96.21
4	151483113.93	155877993.55	0.67	0.69	0.68	0.01	59.98	0.60	0.62	97.34	95.97
5	145407040.89	141367263.13	0.64	0.62	0.63	0.01	58.64	0.59	0.60	98.36	97.49

Table 7. GCMS results of phenol conversion at various reaction temperatures

Reaction temperature (°C)	Peak Area Count Run 1	Peak Area Count Run 2	Cx ^b 1 (mg/mL)	Cx ^b 2 (mg/mL)	Average Cx (mg/mL)	STDEV	Phenol out concentration (mg/mL)	Phenol in concentration (mg/mL)	Phenol Conversion (%)
100	101941625.36	100625573.31	0.55	0.54	0.54	0.00	52.45	58.21	9.89
200	99919988.21	97572164.37	0.56	0.53	0.54	0.01	50.29	58.21	13.61
300	950013.61	946534.33	0.01	0.01	0.01	0.00	0.51	54.80	99.07

Table 8. GCMS results of cyclohexanone selectivity and yield at various reaction temperatures

Reaction temperature (°C)	Peak Area Count Run 1	Peak Area Count Run 2	Cx ^b 1 (mg/mL)	Cx ^b 2 (mg/mL)	Average Cx (mg/mL)	STDEV	Cyclohexanone Concentration (mg/mL)	Cyclohexanone Concentration (mol/L)	Total Product concentration (mol/L)	Cyclohexanone Selectivity (%)	Cyclohexanone Yield (%)
100	746044.53	743567.42	0.004	0.004	0.004	0.000	0.41	0.004	0.004	95.64	9.46
200	586971.15	588348.33	0.003	0.003	0.003	0.000	0.31	0.003	0.004	82.13	11.18
300	7041774.13	6551660.41	0.04	0.04	0.04	0.00	3.93	0.04	0.69	5.77	5.72

Table 9. GCMS results of cyclohexanol selectivity and yield at various reaction temperatures

Reaction temperature (°C)	Peak Area Count Run 1	Peak Area Count Run 2	Cx ^b 1 (mg/mL)	Cx ^b 2 (mg/mL)	Average Cx (mg/mL)	STDEV	Cyclohexanol Concentration (mg/mL)	Cyclohexanol Concentration (mol/L)	Total Product concentration (mol/L)	Cyclohexanol Selectivity (%)	Cyclohexanol Yield (%)
100	45108.06	45386.43	0.000	0.000	0.000	0.000	0.02	0.000	0.004	4.36	0.43
200	168515.62	172011.69	0.001	0.001	0.001	0.000	0.07	0.001	0.004	17.87	2.43
300	146865909.11	148440915.79	0.65	0.65	0.65	0.00	65.38	0.65	0.69	94.23	93.35

Table 10. GCMS results of phenol conversion at various starting material ratios

H ₂ O:MeOH:Phenol molar ratio	Peak Area Count Run 1	Peak Area Count Run 2	Cx ^b 1 (mg/mL)	Cx ^b 2 (mg/mL)	Average Cx (mg/mL)	STDEV	Phenol out concentration (mg/mL)	Phenol in concentration (mg/mL)	Phenol Conversion (%)
0:100:1	46756889.46	46742944.63	0.25	0.25	0.25	0.00	24.45	22.94	0.00
80:10:1	1221389.73	1282370.87	0.01	0.01	0.01	0.00	0.58	39.21	98.51
40:5:2	4398805.73	4391748.68	0.02	0.02	0.02	0.00	2.07	121.15	98.29
40:10:0.5	28807289.16	28852687.97	0.15	0.15	0.15	0.00	14.45	33.65	57.07
20:20:0.5	77626080.43	77526129.99	0.42	0.41	0.41	0.00	39.60	34.37	0.00
40:20:1	950013.61	946534.33	0.01	0.01	0.01	0.00	0.51	54.80	99.07

Table 11. GCMS results of cyclohexanone selectivity and yield at various starting material ratios

H ₂ O:MeOH:Phenol molar ratio	Peak Area Count Run 1	Peak Area Count Run 2	Cx ^b 1 (mg/mL)	Cx ^b 2 (mg/mL)	Average Cx (mg/mL)	STDEV	Cyclohexanone Concentration (mg/mL)	Cyclohexanone Concentration (mol/L)	Total Product concentration (mol/L)	Cyclohexanone Selectivity (%)	Cyclohexanone Yield (%)
0:100:1	0.00	0.00	0.00	0.00	0.00	0.00	0.00	0.00	0.00	0.00	0.00
80:10:1	2867963.55	2871159.03	0.02	0.02	0.02	0.00	1.44	0.01	0.27	5.38	5.30
40:5:2	11090148.29	11186156.14	0.06	0.06	0.06	0.00	5.65	0.06	0.11	52.18	51.29
40:10:0.5	6726125.61	6669746.52	0.04	0.04	0.04	0.00	3.61	0.04	0.19	18.92	10.80
20:20:0.5	2526890.16	2529150.19	0.01	0.01	0.01	0.00	1.39	0.01	0.02	0.00	0.00
40:20:1	7041774.13	6551660.41	0.04	0.04	0.04	0.00	3.93	0.04	0.69	5.77	5.72

Table 12. GCMS results of cyclohexanol selectivity and yield at various starting material ratios

H ₂ O:MeOH:Phe nol molar ratio	Peak Area Count Run 1	Peak Area Count Run 2	Cx ^b 1 (mg/mL)	Cx ^b 2 (mg/mL)	Average Cx (mg/mL)	STDE V	Cyclohexano l Concentratio n (mg/mL)	Cyclohexan ol Concentratio n (mol/L)	Total Product concentrati on (mol/L)	Cyclohexan ol Selectivity (%)	Cyclohexano l Yield (%)
0:100:1	0.00	0.00	0.00	0.00	0.00	0.00	0.00	0.00	0.00	0.00	0.00
80:10:1	66389902. 95	68082238.3 7	0.29	0.30	0.30	0.01	25.79	0.26	0.27	94.62	93.22
40:5:2	13639583. 99	13536042.9 8	0.06	0.06	0.06	0.00	5.28	0.05	0.11	47.82	47.00
40:10:0.5	38423037. 79	38010725.2 6	0.17	0.17	0.17	0.00	15.78	0.16	0.19	81.08	46.27
20:20:0.5	1156856.4 0	1153855.37	0.01	0.01	0.01	0.00	0.49	0.00	0.02	0.00	0.00
40:20:1	146865909 .11	148440915. 79	0.65	0.65	0.65	0.00	65.38	0.65	0.69	94.23	93.35

Appendix 3. GCMS results of monoterpene production

N.B. There are minor differences (< 1 min) in the retention times of the compounds in some of the samples. For GCMS results tables: 8, 15, 18, and 21 a column cooling stage was added to the GCMS method and this caused a minor shift (< 1 min) in the retention times of the compounds. The method was slightly modified as follows: the GC oven temperature was initially held at 45 °C for 2.5 min, then ramped up at 10 °C/min to 225 °C, and held at 225 °C for 0.5 min. The temperature was then decreased to 45 °C at a rate of 50 °C/min and held at 45 °C for 0.40 min. Any other differences in the retention times of the compounds are minor and mainly due to running the samples at different days/weeks/months.

Table 1. Geranyl isovalerate experiment 1 GCMS results. Each product sample was analysed by GCMS twice and an average of the relative area % of the two runs was taken.

Compound	Retention time	Average Rel.Area% TIC	Mean standard deviation ±
Methyl isovalerate	2.91	28.77	0.07
Isovaleric acid	4.61	0.47	0.10
1,3-Cyclohexadiene,1,3,5,5-tetramethyl	5.13	1.05	0.04
γ-Terpinene	5.39	0.08	0.01
γ-Terpinene	5.46	0.33	0.00
Cyclohexene,1,5,5-trimethyl-3-methylene	5.65	0.37	0.03
1,3-Cyclopentadiene,5,5-dimethyl-1-propyl	5.70	0.15	0.01
p-Mentha-2,8-diene,(1R,4R)-(+)-	5.81	0.70	0.07
D-Limonene	5.91	0.88	0.05
p-Mentha-1,4(8)-diene	6.13	0.62	0.07
Cyclohexene,1,5,5-trimethyl-3-methylene	6.36	1.57	0.27
Cyclohexene,1,5,5-trimethyl-3-methylene	6.50	4.89	0.09
γ-Terpinene	6.78	1.37	0.07
p-Mentha-1,4(8)-diene	6.96	18.03	0.79
p-Mentha-1,4(8)-diene	7.12	1.94	0.06
D-Limonene	7.17	6.77	0.16
3-Carene	7.49	2.62	0.05
γ-Terpinene	7.68	9.14	0.16
3-Isopropenyl-5-methyl-1-cyclohexene	7.91	0.47	0.01
p-Mentha-1,4(8)-diene	8.14	13.30	0.05

2,4,6-Octariene,2,6-dimethyl-,(E,Z)-	8.83	1.71	0.04
2,4,6-Octariene,2,6-dimethyl-,(E,Z)-	9.02	2.29	0.30
2,6-Octadiene,1-(1-ethoxyethoxy)-3,7-dimethyl-	10.24	0.35	0.02
Geranyl isovalerate	15.21	2.13	0.38
Total		100.01	

Table 2. Geranyl isovalerate experiment 2 GCMS results. Each product sample was analysed by GCMS twice and an average of the relative area % of the two runs was taken.

Compound	Retention time	Average Rel.Area% TIC	Mean \pm standard deviation
Methyl isovalerate	2.89	27.28	0.34
Isovaleric acid	4.41	0.82	0.60
1,3-Cyclohexadiene,1,3,5,5-tetramethyl	5.10	1.04	0.01
γ -Terpinene	5.36	0.17	0.00
γ -Terpinene	5.43	0.52	0.05
Cyclohexene,1,5,5-trimethyl-3-methylene	5.62	0.56	0.00
1,3-Cyclopentadiene,5,5-dimethyl-1-propyl	5.68	0.21	0.02
p-Mentha-2,8-diene,(1R,4R)-(+)-	5.78	1.00	0.08
D-Limonene	5.88	1.22	0.10
p-Mentha-1,4(8)-diene	6.10	1.41	0.09
Cyclohexene,1,5,5-trimethyl-3-methylene	6.32	2.06	0.12
Cyclohexene,1,5,5-trimethyl-3-methylene	6.47	4.19	0.28
γ -Terpinene	6.75	1.47	0.03
p-Mentha-1,4(8)-diene	6.92	22.55	0.22
p-Mentha-1,4(8)-diene	7.10	1.17	0.05
D-Limonene	7.14	2.74	0.11
3-Carene	7.47	1.62	0.07
γ -Terpinene	7.65	9.60	0.04
3-Isopropenyl-5-methyl-1-cyclohexene	7.87	1.31	0.01
p-Mentha-1,4(8)-diene	8.11	12.13	0.01
2,4,6-Octariene,2,6-dimethyl-,(E,Z)-	8.80	2.39	0.05
2,4,6-Octariene,2,6-dimethyl-,(E,Z)-	8.99	2.83	0.03
2,6-Octadiene,1-(1-ethoxyethoxy)-3,7-dimethyl-	10.22	0.14	0.02

Geranyl isovalerate	15.18	1.57	0.11
Total		100.00	

Table 3. Geraniol experiment 40:20:1 H₂O:Methanol:Geraniol molar ratio, constant heating setting temperature (400 °C) and time (2 h). The product sample was analysed by GCMS three times and an average of the relative area % of the three runs was taken.

Compound	Retention time	Average Rel.Area% TIC	Mean \pm standard deviation
1,2,4,4-Tetramethylcyclopentene	3.96	0.16	0.01
1,3-Cyclohexadiene,1,3,5,5-tetramethyl	4.96	0.62	0.04
p-Mentha-1,4(8)-diene	5.29	0.19	0.01
1,3-Cyclopentadiene,5,5-dimethyl-1-propyl	5.48	0.27	0.01
1,3-Cyclopentadiene,5,5-dimethyl-2-propyl	5.53	0.12	0.01
1,3-Cyclopentadiene,5,5-dimethyl-2-propyl	5.63	0.33	0.03
D-Limonene	5.73	0.80	0.04
p-Mentha-1,4(8)-diene	5.95	0.88	0.03
Alpha-Terpineneol	6.13	0.15	0.02
1,3-Cyclohexadiene,1,3,5,5-tetramethyl	6.18	0.92	0.03
Beta-Pinene	6.32	3.21	0.05
Beta-Pinene	6.40	0.50	0.02
y-Terpinene	6.60	1.70	0.04
p-Mentha-1,4(8)-diene	6.78	17.93	0.17
o-Cymene	6.95	0.89	0.03
D-Limonene	6.99	16.42	0.15
D-Limonene	7.15	0.49	0.02
Beta-Ocimene	7.31	7.49	0.05
y-Terpinene	7.50	9.64	0.08
y-Terpinene	7.69	0.10	0.01
p-Mentha-3,8-diene	7.73	0.10	0.01
p-Mentha-1,4(8)-diene	7.97	23.04	0.24
Beta-Linalool	8.25	0.41	0.03
1,3-Cyclohexadiene,1,3,5,5-tetramethyl	8.65	1.86	0.07
Linalool, methyl ether	8.69	1.96	0.04
2,4,6-Octariene,2,6-dimethyl-,(E,Z)-	8.84	4.39	0.06
Nerol, methyl ether	9.75	1.11	0.03
(2E)-1-Methoxy-3,7-dimethylocta-2,6,diene	10.08	4.32	0.12

Total		99.99	0.01
-------	--	-------	------

Table 4. Geraniol experiment 80:10:1 H₂O:Methanol:Geraniol molar ratio, constant heating setting temperature (400 °C) temperature (400 °C) and time (2 h). The product sample was analysed by GCMS three times and an average of the relative area % of the three runs was taken.

Compound	Retention time	Average Rel.Area% TIC	Mean standard deviation ±
1,2,4,4-Tetramethylcyclopentene	3.15	0.19	0.01
1,3-Cyclohexadiene,1,3,5,5-tetramethyl	4.11	1.54	0.05
1,3-Cyclopentadiene,5,5-dimethyl-2-propyl	4.63	0.22	0.01
1,3-Cyclopentadiene,5,5-dimethyl-2-propyl	4.77	0.38	0.03
D-Limonene	4.87	0.24	0.02
Cyclopentane,2-methyl-1-methylene-3-(1-methylethenyl)-	4.92	0.54	0.04
Alpha-Terpineol	5.12	1.31	0.02
1,3-Cyclohexadiene,1,3,5,5-tetramethyl	5.31	4.07	0.02
Beta-Pinene	5.49	2.54	0.03
2,6-Dimethyl-2-trans-6-octadiene	5.65	0.13	0.01
γ-Terpinene	5.74	0.51	0.04
p-Mentha-1,4(8)-diene	5.91	9.11	0.02
o-Cymene	6.08	1.16	0.09
D-Limonene	6.11	20.37	0.25
Beta-Ocimene	6.46	7.21	0.03
γ-Terpinene	6.64	4.94	0.04
p-Mentha-1,4(8)-diene	6.90	0.30	0.01
p-Mentha-1,4(8)-diene	7.08	22.74	0.15
Beta-Linalool	7.30	0.48	0.03
Beta-Linalool	7.39	2.17	0.01
2,4,6-Octariene,2,6-dimethyl-,(E,Z)-	7.80	4.03	0.06
2,4,6-Octariene,2,6-dimethyl-,(E,Z)-	8.00	1.57	0.02
4-Caranone,cis	8.29	0.16	0.01
Terpinen-4-ol	8.65	0.12	0.01
Alpha-Terpineol	8.85	2.53	0.04
(2E)-1-Methoxy-3,7-dimethylocta-2,6,diene	9.24	2.21	0.06
Geraniol	9.67	9.24	0.07
Total		100.01	

Table 5. Geraniol experiment 40:5:2 H₂O:Methanol:Geraniol molar ratio, constant heating set temperature (400 °C) and time (2 h). The product sample was analysed by GCMS three times and an average of the relative area % of the three runs was taken.

Compound	Retention time	Average Rel.Area% TIC	Mean standard deviation ±
1,2,4,4-Tetramethylcyclopentene	3.10	0.54	0.02
2-Norbornanone,1,3,3-trimethyl	3.54	0.24	0.01
1,3-Cyclohexadiene,1,3,5,5-tetramethyl	4.07	1.84	0.04
p-Mentha-1,4(8)-diene	4.33	0.15	0.01
γ-Terpinene	4.40	0.26	0.01
p-Menth-2-ene	4.51	0.10	0.01
1,3-Cyclopentadiene,5,5-dimethyl-1-propyl	4.58	0.38	0.00
1,3-Cyclopentadiene,5,5-dimethyl-2-propyl	4.63	0.17	0.02
1,3-Cyclopentadiene,5,5-dimethyl-2-propyl	4.73	1.27	0.02
D-Limonene	4.83	1.43	0.03
p-Mentha-1,4(8)-diene	5.05	2.25	0.04
1,3-Cyclohexadiene,1,3,5,5-tetramethyl	5.27	4.80	0.07
Beta-Pinene	5.44	0.50	0.08
2,4,6-Octariene,2,6-dimethyl-,(E,Z)-	5.47	0.21	0.05
γ-Terpinene	5.69	2.73	0.05
p-Mentha-1,4(8)-diene	5.89	16.64	0.31
p-Mentha-1,4(8)-diene	5.97	0.82	0.06
o-Cymene	6.05	7.22	0.36
D-Limonene	6.10	7.05	0.65
Beta-Ocimene	6.26	0.68	0.01
Beta-Ocimene	6.42	4.38	0.05
γ-Terpinene	6.60	7.02	0.10
p-Mentha-3,8-diene	6.82	0.75	0.01
p-Mentha-1,4(8)-diene	7.06	18.59	0.31
p-Mentha-1,4(8)-diene	7.17	0.27	0.01
Beta-Linalool	7.34	4.21	0.05
2,4,6-Octariene,2,6-dimethyl-,(E,Z)-	7.76	0.69	0.04
Linalool, methyl ether	7.81	1.03	0.05
Linalool, methyl ether	7.95	1.50	0.01
4-Caranone,cis	8.23	0.30	0.03
5-Caranol,(1S,3R,5S,6R)-(-)-	8.41	0.10	0.00
Terpinen-4-ol	8.58	0.10	0.00

Alpha-Terpineol	8.80	2.49	0.02
(2E)-1-Methoxy-3,7-dimethylocta-2,6,diene	9.18	2.98	0.05
Geraniol	9.48	0.03	0.00
Geraniol	9.66	5.86	0.08
2-tert-Butyltoluene	10.79	0.41	0.01
Total		100.01	

Table 6. Geraniol experiment 40:10:0.5 H₂O:Methanol:Geraniol molar ratio, constant heating set temperature (400 °C) and time (2 h). The product sample was analysed by GCMS three times and an average of the relative area % of the three runs was taken.

Compound	Retention time	Average Rel.Area% TIC	Mean \pm standard deviation
1,2,4,4-Tetramethylcyclopentene	3.14	0.20	0.02
1,3-Cyclohexadiene,1,3,5,5-tetramethyl	4.11	1.93	0.05
p-Mentha-1,4(8)-diene	4.38	0.00	0.00
y-Terpinene	4.45	0.17	0.01
1,3-Cyclopentadiene,5,5-dimethyl-2-propyl	4.62	0.52	0.02
1,3-Cyclopentadiene,5,5-dimethyl-2-propyl	4.77	0.85	0.03
D-Limonene	4.87	1.05	0.06
Alpha-Terpineol	5.10	1.10	0.01
1,3-Cyclohexadiene,1,3,5,5-tetramethyl	5.30	4.74	0.09
Beta-Pinene	5.51	1.91	0.09
y-Terpinene	5.74	1.51	0.04
p-Mentha-1,4(8)-diene	5.91	15.73	0.37
o-Cymene	6.08	2.72	0.39
D-Limonene	6.12	14.19	0.31
Beta-Ocimene	6.47	5.34	0.19
y-Terpinene	6.64	5.99	0.10
p-Mentha-1,4(8)-diene	6.89	0.55	0.04
p-Mentha-1,4(8)-diene	7.09	25.66	0.47
Beta-Linalool	7.29	0.89	0.06
Beta-Linalool	7.39	1.37	0.11
Linalool, methyl ether	7.85	2.11	0.05
2,4,6-Octariene,2,6-dimethyl-,(E,Z)-	8.02	0.53	0.03
4-Caranone,cis	8.27	0.63	0.02
Alpha-Terpineol	8.86	1.84	0.02

(2E)-1-Methoxy-3,7-dimethylocta-2,6,diene	9.25	1.79	0.12
Geraniol	9.68	6.70	0.61
		100.00	

Table 7. Geraniol experiment 20:20:0.5 H₂O:Methanol:Geraniol molar ratio, constant heating set temperature (400 °C) and time (2 h). The product sample was analysed by GCMS three times and an average of the relative area % of the three runs was taken.

Compound	Retention time	Average Rel.Area% TIC	Mean ± standard deviation
1,2,4,4-Tetramethylcyclopentene	3.14	0.12	0.01
2-Norbornanone,1,3,3-trimethyl	3.59	0.30	0.02
1,3-Cyclohexadiene,1,3,5,5-tetramethyl	4.12	1.47	0.04
γ-Terpinene	4.45	0.14	0.01
1,3-Cyclopentadiene,5,5-dimethyl-2-propyl	4.67	0.32	0.00
1,3-Cyclopentadiene,5,5-dimethyl-2-propyl	4.78	1.07	0.02
Cyclopentane,2-methyl-1-methylene-3-(1-methylethenyl)-	4.87	1.43	0.03
Alpha-Terpineol	5.12	1.23	0.03
1,3-Cyclohexadiene,1,3,5,5-tetramethyl	5.31	4.63	0.08
Beta-Pinene	5.50	0.21	0.02
p-Menth-3-ene	5.53	0.30	0.03
2,6-Dimethyl-2-trans-6-octadiene	5.64	0.38	0.01
γ-Terpinene	5.74	0.33	0.03
p-Mentha-1,4(8)-diene	5.92	2.94	0.03
D-Limonene	6.01	0.59	0.02
o-Cymene	6.07	2.73	0.32
D-Limonene	6.12	11.28	0.17
Beta-Ocimene	6.47	1.89	0.03
γ-Terpinene	6.65	0.34	0.01
p-Mentha-3,8-diene	6.88	1.71	0.04
p-Mentha-1,4(8)-diene	7.08	9.70	0.08
Beta-Linalool	7.29	0.22	0.01
Beta-Linalool	7.38	0.76	0.03
Cyclopentanol,3-isopropenyl-1,2-dimethyl-,(1R,2S,3S)-(-)-	7.63	0.36	0.01
Linalool, methyl ether	7.79	1.41	0.10

Cyclopentanol,3-isopropenyl-1,2-dimethyl-,(1R,2S,3S)-(-)-	8.08	1.23	0.02
Cyclopentanol,3-isopropenyl-1,2-dimethyl-,(1R,2S,3S)-(-)-	8.21	0.28	0.01
4-Caranone,cis	8.26	0.07	0.04
5-Caranol,(1S,3R,5S,6R)-(-)-	8.50	0.21	0.00
Terpinen-4-ol	8.61	0.27	0.00
Alpha-Terpineol	8.82	16.39	0.15
(2E)-1-Methoxy-3,7-dimethylocta-2,6,diene	9.20	29.30	0.18
Geraniol	9.49	0.03	0.00
Geraniol	9.66	5.16	0.05
2-tert-Butyltoluene	10.82	0.85	0.04
Nerol, methyl ether	11.01	0.15	0.01
5-Caranol,(1S,3R,5S,6R)-(-)-	11.25	0.21	0.01
Total		100.00	

Table 8. Geraniol experiment 100:0:1 H₂O:Methanol:Geraniol molar ratio, constant heating set temperature (400 °C) and time (2 h). The product sample was analysed by GCMS three times and an average of the relative area % of the three runs was taken.

Compound	Retention time	Average Rel.Area% TIC	Mean \pm standard deviation
1,3-Cyclohexadiene,1,3,5,5-tetramethyl	3.15	1.39	0.05
γ -Terpinene	3.38	0.21	0.01
2-Bornene	3.52	0.24	0.03
2-Bornene	3.64	1.00	0.02
p-Mentha-2,8-diene,(1R,4R)-(+)-	3.90	3.48	0.01
γ -Terpinene	4.16	1.25	0.02
p-Menth-3-ene	4.25	1.03	0.01
2H-Pyran,2-ethenyltetrahydro-2,6,6-trimethyl	4.35	0.64	0.03
1,3-Cyclohexadiene,1,3,5,5-tetramethyl	4.45	2.49	0.02
1,3-Cyclohexadiene,1,3,5,5-tetramethyl	4.61	1.68	0.03
Beta-Pinene	4.72	1.72	0.04
Beta-Pinene	4.85	1.67	0.03
p-Mentha-1,4(8)-diene	4.99	1.14	0.02
D-Limonene	5.11	17.37	0.22
D-Limonene	5.25	9.98	0.00
o-Cymene	5.55	17.58	0.03
p-Mentha-1,3,8-triene	5.67	0.15	0.01

y-Terpinene	5.81	6.84	0.22
y-Terpinene	5.98	0.18	0.02
p-Mentha-3,8-diene	6.03	0.87	0.01
p-Mentha-1,4(8)-diene	6.27	16.66	0.11
1,3-Cyclopentadiene,5,5-dimethyl-2-propyl	6.64	0.00	0.00
p-Cymenene	6.83	0.27	0.01
p-Cymenene	6.94	0.05	0.00
Linalool, methyl ether	7.00	0.01	0.00
Linalool, methyl ether	7.17	0.11	0.01
1,3-Cyclohexadiene,1,3,5,5-tetramethyl	7.20	0.88	0.01
Beta-Linalool	7.54	3.73	0.10
Linalyl 3-methylbutanoate	7.80	0.12	0.01
4-Caranone,cis	8.34	0.13	0.01
2,6-Octadiene,1-(1-ethoxyethoxy)-3,7-dimethyl	8.50	0.22	0.01
(2E)-1-Methoxy-3,7-dimethylocta-2,6,diene	8.78	0.81	0.03
Alpha-Terpineol	8.99	2.02	0.07
Geraniol	9.62	0.20	0.01
Geraniol	10.01	3.89	0.19
Total		100.00	

Table 9. Nerol experiment 40:20:1 H₂O:Methanol:Nerol molar ratio, constant heating set temperature (400 °C) and time (2 h). The product sample was analysed by GCMS three times and an average of the relative area % of the three runs was taken.

Compound	Retention time	Average Rel.Area% TIC	Mean ± standard deviation
1,2,4,4-Tetramethylcyclopentene	3.98	0.07	0.00
1,3-Cyclohexadiene,1,3,5,5-tetramethyl	4.98	0.21	0.01
p-Mentha-1,4(8)-diene	5.32	0.06	0.01
1,3-Cyclopentadiene,5,5-dimethyl-1-propyl	5.50	0.11	0.01
1,3-Cyclopentadiene,5,5-dimethyl-2-propyl	5.55	0.16	0.01
1,3-Cyclopentadiene,5,5-dimethyl-2-propyl	5.66	0.08	0.00
D-Limonene	5.75	0.35	0.02
p-Mentha-1,4(8)-diene	5.97	0.81	0.01
Alpha-Terpineol	6.14	0.10	0.00
1,3-Cyclohexadiene,1,3,5,5-tetramethyl	6.20	0.25	0.01
Beta-Pinene	6.34	2.06	0.01
Beta-Pinene	6.42	0.20	0.01
y-Terpinene	6.61	1.99	0.04

p-Mentha-1,4(8)-diene	6.80	18.36	0.19
o-Cymene	6.96	1.03	0.06
D-Limonene	7.01	21.99	0.16
D-Limonene	7.17	0.21	0.01
Beta-Ocimene	7.33	3.62	0.01
y-Terpinene	7.52	10.87	0.05
y-Terpinene	7.71	0.02	0.00
p-Mentha-3,8-diene	7.75	0.13	0.01
p-Mentha-1,4(8)-diene	7.99	27.83	0.08
Beta-Linalool	8.26	0.15	0.01
1,3-Cyclohexadiene,1,3,5,5-tetramethyl	8.67	0.57	0.02
Linalool, methyl ether	8.71	1.45	0.02
2,4,6-Octariene,2,6-dimethyl-,(E,Z)-	8.86	1.64	0.03
Nerol, methyl ether	9.75	2.29	0.08
(2E)-1-Methoxy-3,7-dimethylocta-2,6,diene	10.06	3.33	0.08
Nerol	10.22	0.06	0.01
Total		99.99	

Table 10. Nerol experiment 80:10:1 H₂O:Methanol:Nerol molar ratio, constant heating set temperature (400 °C) and time (2 h). The product sample was analysed by GCMS three times and an average of the relative area % of the three runs was taken.

Compound	Retention time	Average Rel.Area% TIC	Mean \pm standard deviation
1,2,4,4-Tetramethylcyclopentene	3.12	0.09	0.01
1,3-Cyclohexadiene,1,3,5,5-tetramethyl	4.08	0.33	0.02
1,3-Cyclopentadiene,5,5-dimethyl-2-propyl	4.63	0.33	0.01
1,3-Cyclopentadiene,5,5-dimethyl-2-propyl	4.74	0.28	0.01
D-Limonene	4.84	0.41	0.02
p-Mentha-1,4(8)-diene	5.06	2.16	0.04
1,3-Cyclohexadiene,1,3,5,5-tetramethyl	5.28	1.25	0.02
Beta-Pinene	5.48	1.18	0.03
y-Terpinene	5.70	2.46	0.03
p-Mentha-1,4(8)-diene	5.87	31.45	0.42
o-Cymene	6.05	1.31	0.59
D-Limonene	6.09	4.77	0.48
Beta-Ocimene	6.46	0.85	0.02
y-Terpinene	6.60	13.54	0.17
p-Mentha-3,8-diene	6.83	1.39	0.01

p-Mentha-1,4(8)-diene	7.05	22.58	0.08
p-Mentha-1,4(8)-diene	7.26	1.17	0.06
Beta-Linalool	7.38	0.91	0.13
Linalool, methyl ether	7.82	1.17	0.01
Linalool, methyl ether	8.00	0.56	0.04
4-Caranone,cis	8.26	0.26	0.02
Terpinen-4-ol	8.61	0.25	0.05
Alpha-Terpineol	8.81	6.04	0.21
2,6-Octadiene,1-(1-ethoxyethoxy)-3,7-dimethyl	9.13	0.86	0.03
(2E)-1-Methoxy-3,7-dimethylocta-2,6,diene	9.22	0.13	0.01
Nerol	9.28	4.28	0.36
Total		100.00	

Table 11. Nerol experiment 40:5:2 H₂O:Methanol:Nerol molar ratio, constant heating set temperature (400 °C) and time (2 h). The product sample was analysed by GCMS three times and an average of the relative area % of the three runs was taken.

Compound	Retention time	Average Rel.Area% TIC	Mean \pm standard deviation
1,2,4,4-Tetramethylcyclopentene	3.11	0.18	0.01
1,3-Cyclohexadiene,1,3,5,5-tetramethyl	4.08	0.50	0.02
γ -Terpinene	4.41	0.20	0.01
1,3-Cyclopentadiene,5,5-dimethyl-2-propyl	4.63	0.25	0.01
1,3-Cyclopentadiene,5,5-dimethyl-2-propyl	4.74	0.31	0.01
D-Limonene	4.84	0.34	0.01
p-Mentha-1,4(8)-diene	5.05	1.89	0.04
1,3-Cyclohexadiene,1,3,5,5-tetramethyl	5.28	2.22	0.03
Beta-Pinene	5.45	0.19	0.02
2,4,6-Octariene,2,6-dimethyl-,(E,Z)-	5.48	0.09	0.02
γ -Terpinene	5.69	2.32	0.05
p-Mentha-1,4(8)-diene	5.87	22.68	0.52
o-Cymene	6.03	8.65	0.74
D-Limonene	6.08	10.12	0.87
Beta-Ocimene	6.43	1.57	0.01
γ -Terpinene	6.59	8.47	0.18
p-Mentha-3,8-diene	6.82	0.59	0.01
p-Mentha-1,4(8)-diene	7.04	22.94	0.50
Beta-Linalool	7.25	0.29	0.01
Beta-Linalool	7.34	2.23	0.06

Linalool, methyl ether	7.80	1.27	0.06
Linalool, methyl ether	7.97	0.46	0.03
4-Caranone,cis	8.23	0.16	0.00
Terpinen-4-ol	8.58	0.17	0.01
Alpha-Terpineol	8.79	6.91	0.08
2,6-Octadiene,1-(1-ethoxyethoxy)-3,7-dimethyl	9.12	0.89	0.01
(2E)-1-Methoxy-3,7-dimethylocta-2,6,diene	9.19	0.22	0.03
Nerol	9.26	3.89	0.17
Total		99.99	

Table 12. Nerol experiment 40:10:0.5 H₂O:Methanol:Nerol molar ratio, constant heating set temperature (400 °C) and time (2 h). The product sample was analysed by GCMS three times and an average of the relative area % of the three runs was taken.

Compound	Retention time	Average Rel.Area% TIC	Mean standard deviation ±
1,2,4,4-Tetramethylcyclopentene	3.11	0.13	0.01
1,3-Cyclohexadiene,1,3,5,5-tetramethyl	4.07	0.50	0.01
1,3-Cyclopentadiene,5,5-dimethyl-2-propyl	4.63	0.17	0.01
1,3-Cyclopentadiene,5,5-dimethyl-2-propyl	4.73	0.35	0.01
D-Limonene	4.83	0.38	0.00
p-Mentha-1,4(8)-diene	5.05	1.90	0.01
1,3-Cyclohexadiene,1,3,5,5-tetramethyl	5.27	1.65	0.02
Beta-Pinene	5.44	0.62	0.02
2,4,6-Octariene,2,6-dimethyl-,(E,Z)-	5.48	0.10	0.01
y-Terpinene	5.68	2.28	0.00
p-Mentha-1,4(8)-diene	5.87	19.08	0.16
o-Cymene	6.03	6.08	0.38
D-Limonene	6.08	9.88	0.41
Beta-Ocimene	6.27	0.29	0.00
Beta-Ocimene	6.42	2.49	0.01
y-Terpinene	6.59	8.78	0.07
p-Mentha-3,8-diene	6.81	0.75	0.00
p-Mentha-1,4(8)-diene	7.05	20.47	0.11
p-Mentha-1,4(8)-diene	7.17	1.39	0.03
Beta-Linalool	7.33	2.49	0.04
Linalool, methyl ether	7.80	2.94	0.02
Linalool, methyl ether	7.95	0.91	0.02
p-Menth-8-en-1-ol	8.11	0.08	0.01

4-Caranone,cis	8.22	0.65	0.01
5-Caranol,(1S,3R,5S,6R)-(-)-	8.40	0.07	0.01
Terpinen-4-ol	8.57	0.16	0.01
Alpha-Terpineol	8.79	7.91	0.10
2,6-Octadiene,1-(1-ethoxyethoxy)-3,7-dimethyl	9.12	2.72	0.12
(2E)-1-Methoxy-3,7-dimethylocta-2,6,diene	9.18	1.35	0.07
Nerol	9.26	1.92	0.11
Geraniol	9.66	0.45	0.05
2-Cyclohexen-1-one, 4-ethyl-3,4-dimethyl-	9.75	0.56	0.02
Carvacrol	10.41	0.11	0.01
2-tert-Butyltoluene	10.80	0.39	0.01
		100.00	

Table 13. Nerol experiment 20:20:0.5 H₂O:Methanol:Nerol molar ratio, constant heating set temperature (400 °C) and time (2 h). The product sample was analysed by GCMS three times and an average of the relative area % of the three runs was taken.

Compound	Retention time	Average Rel.Area% TIC	Mean ± standard deviation
1,2,4,4-Tetramethylcyclopentene	3.11	0.05	0.01
2-Norbornanone,1,3,3-trimethyl	3.57	0.15	0.01
1,3-Cyclohexadiene,1,3,5,5-tetramethyl	4.08	0.70	0.02
1,3-Cyclopentadiene,5,5-dimethyl-2-propyl	4.63	0.11	0.01
1,3-Cyclopentadiene,5,5-dimethyl-2-propyl	4.74	0.28	0.01
D-Limonene	4.84	0.40	0.01
Alpha-Terpineol	4.96	0.08	0.01
Alpha-Terpineol	5.09	0.85	0.02
1,3-Cyclohexadiene,1,3,5,5-tetramethyl	5.28	1.68	0.02
Beta-Pinene	5.45	0.83	0.02
γ-Terpinene	5.70	0.78	0.02
p-Mentha-1,4(8)-diene	5.88	4.65	0.02
o-Cymene	6.04	2.06	0.11
D-Limonene	6.08	17.63	0.37
Beta-Ocimene	6.29	0.13	0.00
Beta-Ocimene	6.44	2.03	0.07
γ-Terpinene	6.61	1.40	0.03
p-Mentha-3,8-diene	6.87	1.34	0.02
p-Mentha-1,4(8)-diene	7.05	18.22	0.07

Beta-Linalool	7.26	0.14	0.01
Beta-Linalool	7.34	1.81	0.02
Cyclopentanol,3-isopropenyl-1,2-dimethyl-,(1R,2S,3S)-(-)-	7.60	0.30	0.00
Linalool, methyl ether	7.81	2.81	0.01
Cyclopentanol,3-isopropenyl-1,2-dimethyl-,(1R,2S,3S)-(-)-	8.06	0.45	0.01
p-Menth-8-en-1-ol	8.12	0.08	0.01
4-Caranone,cis	8.18	0.09	0.01
4-Caranone,cis	8.23	0.10	0.01
Linalool, methyl ether	8.29	0.08	0.01
5-Caranol,(1S,3R,5S,6R)-(-)-	8.41	0.22	0.01
Terpinen-4-ol	8.58	0.78	0.01
Alpha-Terpineol	8.80	21.00	0.04
2,6-Octadiene,1-(1-ethoxyethoxy)-3,7-dimethyl	9.12	6.90	0.12
(2E)-1-Methoxy-3,7-dimethylocta-2,6,diene	9.18	8.02	0.12
Nerol	9.26	2.12	0.04
Geraniol	9.67	0.95	0.04
2-tert-Butyltoluene	10.80	0.67	0.05
Nerol, methyl ether	10.98	0.11	0.01
		100.00	

Table 14. Geraniol experiment 1 h reaction time constant heating set temperature (400 °C) and H₂O:Methanol:Geraniol molar ratio (40:20:1). The product sample was analysed by GCMS three times and an average of the relative area % of the three runs was taken.

Compound	Retention time	Average Rel.Area% TIC	Mean ± standard deviation
1,3-Cyclohexadiene,1,3,5,5-tetramethyl	4.08	0.30	0.01
1,3-Cyclopentadiene,5,5-dimethyl-1-propyl	4.59	0.16	0.00
D-Limonene	4.84	0.68	0.01
Alpha-Terpineol	5.10	0.30	0.01
1,3-Cyclohexadiene,1,3,5,5-tetramethyl	5.28	0.76	0.01
Beta-Pinene	5.44	4.70	0.03
γ-Terpinene	5.70	1.07	0.01
p-Mentha-1,4(8)-diene	5.88	8.88	0.03
o-Cymene	6.04	0.21	0.08
D-Limonene	6.09	18.56	0.16
Beta-Ocimene	6.28	0.19	0.00

Beta-Ocimene	6.42	10.59	0.04
γ -Terpinene	6.60	5.80	0.03
p-Mentha-3,8-diene	6.81	0.32	0.01
p-Mentha-1,4(8)-diene	7.05	23.29	0.12
p-Mentha-1,4(8)-diene	7.17	0.39	0.02
Beta-Linalool	7.26	0.23	0.01
Beta-Linalool	7.35	0.89	0.02
2,4,6-Octariene,2,6-dimethyl-,(E,Z)-	7.59	0.15	0.00
2,4,6-Octariene,2,6-dimethyl-,(E,Z)-	7.76	3.60	0.07
Linalool, methyl ether	7.80	0.22	0.12
2,4,6-Octariene,2,6-dimethyl-,(E,Z)-	7.94	5.95	0.02
p-Menth-8-en-1-ol	8.13	0.16	0.01
4-Caranone,cis	8.23	0.28	0.01
5-Caranol,(1S,3R,5S,6R)-(-)-	8.42	0.40	0.01
2-Cyclohexene-1-methanol,2,6,6-trimethyl-	8.52	0.09	0.02
Terpinen-4-ol	8.59	0.12	0.02
Alpha-Terpineol	8.80	4.73	0.07
(2E)-1-Methoxy-3,7-dimethylocta-2,6,diene	9.19	4.86	0.00
Geraniol	9.66	2.14	0.09
		100.00	

Table 15. Geraniol experiment 3 h reaction time constant heating set temperature (400 °C) and H₂O:Methanol:Geraniol molar ratio (40:20:1). The product sample was analysed by GCMS three times and an average of the relative area % of the three runs was taken.

Compound	Retention time	Average Rel.Area% TIC	Mean \pm standard deviation
1,3-Cyclohexadiene,1,3,5,5-tetramethyl	3.18	1.89	0.04
2-Bornene	3.55	0.22	0.01
2-Bornene	3.66	0.71	0.03
p-Mentha-2,8-diene,(1R,4R)-(+)-	3.93	3.12	0.04
γ -Terpinene	4.18	1.13	0.02
1,3-Cyclohexadiene,1,3,5,5-tetramethyl	4.48	2.93	0.07
1,3-Cyclohexadiene,1,3,5,5-tetramethyl	4.63	0.98	0.01
Beta-Pinene	4.76	1.70	0.05
Beta-Pinene	4.88	1.57	0.03
p-Mentha-1,4(8)-diene	5.02	0.68	0.06
D-Limonene	5.12	16.18	0.19

D-Limonene	5.27	20.82	0.23
o-Cymene	5.48	0.16	0.02
o-Cymene	5.57	6.63	0.12
γ -Terpinene	5.83	11.53	0.08
p-Mentha-3,8-diene	6.06	0.43	0.04
p-Mentha-1,4(8)-diene	6.19	0.07	0.01
p-Mentha-1,4(8)-diene	6.29	22.04	0.11
p-Mentha-1,4(8)-diene	6.54	0.09	0.01
1,3-Cyclopentadiene,5,5-dimethyl-2-propyl	6.71	0.17	0.01
p-Cymene	6.91	0.10	0.01
Linalool, methyl ether	7.16	0.30	0.01
1,3-Cyclohexadiene,1,3,5,5-tetramethyl	7.26	0.57	0.03
2,4,6-Octatriene,2,6-dimethyl-,(E,Z)-	7.50	1.44	0.06
Linalool, methyl ether	7.72	0.13	0.03
4-Caranone,cis	8.39	0.57	0.06
2,6-Octadiene,1-(1-ethoxyethoxy)-3,7-dimethyl	8.55	1.06	0.11
Alpha-Terpineol	9.11	2.82	0.10
		100.01	

Table 16. Geraniol experiment 4 h reaction time constant heating set temperature (400 °C) and H₂O:Methanol:Geraniol molar ratio (40:20:1). The product sample was analysed by GCMS three times and an average of the relative area % of the three runs was taken.

Compound	Retention time	Average Rel.Area% TIC	Mean \pm standard deviation
1,2,4,4-Tetramethylcyclopentene	3.11	0.23	0.01
2-Norbornanone,1,3,3-trimethyl	3.57	0.12	0.01
1,3-Cyclohexadiene,1,3,5,5-tetramethyl	4.07	1.68	0.05
γ -Terpinene	4.41	0.22	0.00
1,3-Cyclopentadiene,5,5-dimethyl-1-propyl	4.59	0.24	0.02
1,3-Cyclopentadiene,5,5-dimethyl-2-propyl	4.63	0.08	0.01
1,3-Cyclopentadiene,5,5-dimethyl-2-propyl	4.73	1.14	0.02
D-Limonene	4.83	1.20	0.01
p-Mentha-1,4(8)-diene	5.06	1.44	0.02
1,3-Cyclohexadiene,1,3,5,5-tetramethyl	5.27	4.12	0.09
Beta-Pinene	5.46	0.29	0.04

Beta-Pinene	5.48	0.26	0.07
y-Terpinene	5.69	1.98	0.00
p-Mentha-1,4(8)-diene	5.87	18.68	0.26
o-Cymene	6.04	4.70	0.51
D-Limonene	6.09	12.53	0.56
Beta-Ocimene	6.43	4.79	0.08
y-Terpinene	6.60	7.76	0.07
p-Mentha-3,8-diene	6.83	0.59	0.03
p-Mentha-1,4(8)-diene	7.05	23.65	0.41
p-Mentha-1,4(8)-diene	7.20	0.09	0.00
Beta-Linalool	7.26	0.32	0.02
Beta-Linalool	7.36	1.02	0.04
2,4,6-Octariene,2,6-dimethyl-,(E,Z)-	7.78	0.91	0.03
Linalool, methyl ether	7.81	0.25	0.08
2,4,6-Octariene,2,6-dimethyl-,(E,Z)-	7.96	1.92	0.04
4-Caranone,cis	8.23	0.57	0.03
5-Caranol,(1S,3R,5S,6R)-(-)-	8.50	0.10	0.01
Terpinen-4-ol	8.60	0.09	0.00
Alpha-Terpineol	8.81	2.92	0.08
(2E)-1-Methoxy-3,7-dimethylocta-2,6,diene	9.19	4.13	0.08
Geraniol	9.70	1.14	0.08
2-tert-Butyltoluene	10.82	0.82	0.03
		100.00	

Table 17. Geraniol experiment 5 h reaction time constant heating set temperature (400 °C) and H₂O:Methanol:Geraniol molar ratio (40:20:1). The product sample was analysed by GCMS three times and an average of the relative area % of the three runs was taken.

Compound	Retention time	Average Rel.Area% TIC	Mean \pm standard deviation
1,2,4,4-Tetramethylcyclopentene	3.10	0.26	0.01
2-Norbornanone,1,3,3-trimethyl	3.55	0.22	0.01
1,3-Cyclohexadiene,1,3,5,5-tetramethyl	4.07	2.14	0.06
p-Mentha-1,4(8)-diene	4.33	0.00	0.00
y-Terpinene	4.41	0.23	0.01
1,3-Cyclopentadiene,5,5-dimethyl-1-propyl	4.59	0.30	0.01
1,3-Cyclopentadiene,5,5-dimethyl-2-propyl	4.63	0.05	0.01
1,3-Cyclopentadiene,5,5-dimethyl-2-propyl	4.73	1.36	0.03

D-Limonene	4.83	0.97	0.02
p-Mentha-1,4(8)-diene	5.05	1.37	0.04
1,3-Cyclohexadiene,1,3,5,5-tetramethyl	5.27	5.26	0.10
Beta-Pinene	5.45	0.39	0.05
2,4,6-Octariene,2,6-dimethyl-,(E,Z)-	5.48	0.30	0.04
y-Terpinene	5.69	1.98	0.02
p-Mentha-1,4(8)-diene	5.87	15.64	0.27
o-Cymene	6.03	6.57	0.72
D-Limonene	6.09	14.97	0.54
Beta-Ocimene	6.27	0.25	0.00
Beta-Ocimene	6.42	4.52	0.06
y-Terpinene	6.60	5.57	0.08
p-Mentha-3,8-diene	6.84	0.71	0.02
p-Mentha-1,4(8)-diene	7.05	23.15	0.47
p-Mentha-1,4(8)-diene	7.19	0.20	0.02
Beta-Linalool	7.26	0.12	0.01
Beta-Linalool	7.34	0.92	0.02
2,4,6-Octariene,2,6-dimethyl-,(E,Z)-	7.76	0.82	0.10
Linalool, methyl ether	7.80	0.40	0.02
2,4,6-Octariene,2,6-dimethyl-,(E,Z)-	7.95	1.66	0.03
4-Caranone,cis	8.23	0.43	0.02
Alpha-Terpineol	8.81	2.56	0.02
(2E)-1-Methoxy-3,7-dimethylocta-2,6,diene	9.18	5.06	0.10
Geraniol	9.67	0.89	0.03
2-tert-Butyltoluene	10.81	0.73	0.02
		100.00	

Table 18. Nerol experiment 1 h reaction time constant heating set temperature (400 °C) and H₂O:Methanol:Nerol molar ratio (40:20:1). The product sample was analysed by GCMS three times and an average of the relative area % of the three runs was taken.

Compound	Retention time	Average Rel.Area% TIC	Mean ± standard deviation
1,3-Cyclohexadiene,1,3,5,5-tetramethyl	3.16	0.33	0.00
p-Mentha-2,8-diene,(1R,4R)-(+)-	3.91	0.72	0.02
y-Terpinene	4.15	0.33	0.01
2H-Pyran,2-ethenyltetrahydro-2,6,6-trimethyl	4.36	0.91	0.04

1,3-Cyclohexadiene,1,3,5,5-tetramethyl	4.45	0.67	0.04
Beta-Pinene	4.74	0.73	0.02
Beta-Pinene	4.86	0.34	0.01
p-Mentha-1,4(8)-diene	4.99	0.12	0.01
D-Limonene	5.10	2.35	0.03
D-Limonene	5.26	19.18	0.25
o-Cymene	5.55	6.21	0.03
y-Terpinene	5.81	2.02	0.02
p-Mentha-3,8-diene	6.02	0.36	0.01
p-Mentha-1,4(8)-diene	6.13	0.20	0.00
p-Mentha-1,4(8)-diene	6.27	13.20	0.14
p-Cymene	6.69	0.09	0.01
p-Cymene	6.85	0.23	0.04
p-Cymene	6.88	1.12	0.01
Linalool, methyl ether	7.18	3.38	0.02
Beta-Linalool	7.55	3.99	0.07
p-Menth-8-en-1-ol	8.02	0.33	0.02
2,6-Octadiene,1-(1-ethoxyethoxy)-3,7-dimethyl	8.36	0.82	0.02
Nerol, methyl ether	8.42	2.23	0.05
2,6-Octadiene,1-(1-ethoxyethoxy)-3,7-dimethyl	8.50	5.62	0.07
(2E)-1-Methoxy-3,7-dimethylocta-2,6,diene	8.77	3.97	0.05
Alpha-Terpineol	8.97	18.08	0.08
Acetophenone,3'-methyl-	9.29	1.39	0.04
Nerol	9.55	0.22	0.01
Nerol	9.63	9.25	0.10
Nerol	10.23	0.22	0.05
Carvenone	10.32	0.12	0.01
Citral	10.47	0.17	0.02
2-tert-Butyltoluene	11.31	0.72	0.04
p-Menthane-1,8-diol	11.49	0.39	0.02
		100.01	

Table 19. Nerol experiment 3 h reaction time constant heating set temperature (400 °C) and H₂O:Methanol:Nerol molar ratio (40:20:1). The product sample was analysed by GCMS three times and an average of the relative area % of the three runs was taken.

Compound	Retention time	Average Rel.Area% TIC	Mean \pm standard deviation
1,2,4,4-Tetramethylcyclopentene	3.10	0.20	0.01
2-Norbornanone,1,3,3-trimethyl	3.55	0.17	0.01
1,3-Cyclohexadiene,1,3,5,5-tetramethyl	4.07	0.74	0.05
γ -Terpinene	4.40	0.11	0.00
1,3-Cyclopentadiene,5,5-dimethyl-1-propyl	4.60	0.12	0.01
1,3-Cyclopentadiene,5,5-dimethyl-2-propyl	4.63	0.13	0.01
1,3-Cyclopentadiene,5,5-dimethyl-2-propyl	4.73	0.56	0.02
D-Limonene	4.83	0.84	0.02
p-Mentha-1,4(8)-diene	5.05	2.44	0.04
1,3-Cyclohexadiene,1,3,5,5-tetramethyl	5.28	2.54	0.06
Beta-Pinene	5.45	2.52	0.03
γ -Terpinene	5.69	3.33	0.03
p-Mentha-1,4(8)-diene	5.90	19.83	0.20
o-Cymene	6.07	3.23	0.09
D-Limonene	6.12	9.72	0.64
D-Limonene	6.27	0.15	0.00
Beta-Ocimene	6.43	3.67	0.03
γ -Terpinene	6.61	10.93	0.13
p-Mentha-3,8-diene	6.82	0.96	0.00
p-Mentha-1,4(8)-diene	7.08	21.93	0.06
p-Mentha-1,4(8)-diene	7.17	0.75	0.01
Beta-Linalool	7.34	0.63	0.01
2,6-Octadiene,1-(1-ethoxyethoxy)-3,7-dimethyl	7.76	0.69	0.01
Linalool, methyl ether	7.80	0.66	0.02
2,4,6-Octariene,2,6-dimethyl-,(E,Z)-	7.94	1.88	0.04
4-Caranone,cis	8.22	0.75	0.01
Terpinen-4-ol	8.58	0.11	0.00
Alpha-Terpineol	8.80	4.10	0.04
2,6-Octadiene,1-(1-ethoxyethoxy)-3,7-dimethyl	9.12	2.19	0.04
(2E)-1-Methoxy-3,7-dimethylocta-2,6,diene	9.18	1.32	0.01
Nerol	9.27	2.28	0.03
2-tert-Butyltoluene	10.79	0.52	0.02
		100.00	

Table 20. Nerol experiment 4 h reaction time constant heating set temperature (400 °C) and H₂O:Methanol:Nerol molar ratio (40:20:1). The product sample was analysed by GCMS three times and an average of the relative area % of the three runs was taken.

Compound	Retention time	Average Rel.Area% TIC	Mean \pm standard deviation
1,2,4,4-Tetramethylcyclopentene	3.09	0.10	0.02
1,3-Cyclohexadiene,1,3,5,5-tetramethyl	4.06	0.44	0.01
1,3-Cyclopentadiene,5,5-dimethyl-2-propyl	4.72	0.21	0.01
D-Limonene	4.82	0.34	0.02
p-Mentha-1,4(8)-diene	5.04	1.09	0.01
1,3-Cyclohexadiene,1,3,5,5-tetramethyl	5.26	1.35	0.01
Beta-Pinene	5.47	0.78	0.03
y-Terpinene	5.68	1.57	0.03
p-Mentha-1,4(8)-diene	5.85	17.14	0.08
o-Cymene	6.02	3.74	0.01
D-Limonene	6.06	16.02	0.20
Beta-Ocimene	6.43	1.62	0.02
y-Terpinene	6.58	7.78	0.06
p-Mentha-3,8-diene	6.81	0.23	0.02
p-Mentha-1,4(8)-diene	7.02	26.77	0.10
p-Mentha-1,4(8)-diene	7.24	1.03	0.01
Beta-Linalool	7.35	0.98	0.06
Linalool, methyl ether	7.79	1.00	0.04
1,5,5-Trimethyl-6-methylene-cyclohexene	7.98	0.47	0.04
p-Menth-8-en-1-ol	8.12	0.17	0.01
4-Caranone,cis	8.21	2.49	0.07
5-Caranol,(1S,3R,5S,6R)-(-)-	8.47	0.21	0.03
Terpinen-4-ol	8.59	0.21	0.01
Alpha-Terpineol	8.79	8.77	0.13
2,6-Octadiene,1-(1-ethoxyethoxy)-3,7-dimethyl	9.11	1.03	0.01
(2E)-1-Methoxy-3,7-dimethylocta-2,6,diene	9.20	0.26	0.02
Nerol	9.30	1.70	0.10
2-tert-Butyltoluene	10.80	2.49	0.05
		100.00	

Table 21. Nerol experiment 5 h reaction time constant heating set temperature (400 oC) and H2O:Methanol:Nerol molar ratio (40:20:1). The product sample was analysed by GCMS three times and an average of the relative area % of the three runs was taken.

Compound	Retention time	Average Rel.Area% TIC	Mean \pm standard deviation
1,3-Cyclohexadiene,1,3,5,5-tetramethyl	3.15	0.11	0.01
2-Bornene	3.64	0.10	0.01
p-Mentha-2,8-diene,(1R,4R)-(+)-	3.90	0.31	0.01
y-Terpinene	4.15	0.33	0.00
p-Menth-3-ene	4.25	0.10	0.01
1,3-Cyclohexadiene,1,3,5,5-tetramethyl	4.44	0.42	0.01
1,3-Cyclohexadiene,1,3,5,5-tetramethyl	4.60	0.15	0.01
Beta-Pinene	4.73	0.31	0.01
Beta-Pinene	4.84	0.70	0.01
p-Mentha-1,4(8)-diene	4.98	0.59	0.01
D-Limonene	5.09	8.28	0.12
D-Limonene	5.24	10.51	0.12
o-Cymene	5.53	5.46	0.05
y-Terpinene	5.80	5.53	0.08
p-Mentha-3,8-diene	6.03	0.37	0.02
p-Mentha-1,4(8)-diene	6.08	0.11	0.01
p-Mentha-1,4(8)-diene	6.26	20.73	0.14
p-Cymene	6.84	0.21	0.02
p-Cymene	6.91	0.19	0.01
Linalool, methyl ether	7.17	2.02	0.03
Beta-Linalool	7.54	2.38	0.02
1-Methylpentanoic anhydride	7.91	1.59	0.01
p-Menth-8-en-1-ol	8.02	0.24	0.00
4-Caranone,cis	8.33	2.89	0.04
Nerol, methyl ether	8.42	1.51	0.02
2,6-Octadiene,1-(1-ethoxyethoxy)-3,7-dimethyl	8.50	4.02	0.04
(2E)-1-Methoxy-3,7-dimethylocta-2,6,diene	8.77	3.11	0.04
Alpha-Terpineol	8.97	11.58	0.12
Acetophenone,3'-methyl-	9.34	0.92	0.02
Nerol	9.50	0.37	0.01
Nerol	9.61	2.98	0.07

(2E)-1-Methoxy-3,7-dimethylocta-2,6,diene	10.01	0.15	0.00
p-Menth-6-en-2-one,(S)-(+)-	10.06	0.36	0.01
p-Menth-1-en-3-one	10.21	0.16	0.01
Carvenone	10.29	0.30	0.01
(2,2,6-Trimethyl-bicyclo[4.1.0]hept-1-yl)-methanol	10.43	0.32	0.02
2-tert-Butyltoluene	11.25	10.21	0.11
p-Menthane-1,8-diol	11.47	0.22	0.02
Carvacrol	11.59	0.15	0.01
		100.01	

Table 22. Geraniol experiment 200 °C set temperature 2 h reaction time and H₂O:Methanol:Geraniol molar ratio (40:20:1). The product sample was analysed by GCMS three times and an average of the relative area % of the three runs was taken.

Compound	Retention time	Average Rel.Area% TIC	Mean ± standard deviation
1,3-Cyclohexadiene,1,3,5,5-tetramethyl	4.13	0.14	0.01
1,3-Cyclopentadiene,5,5-dimethyl-2-propyl	4.63	0.20	0.01
D-Limonene	4.87	0.44	0.01
2H-Pyran,2-ethenyltetrahydro-2,6,6-trimethyl	5.12	0.94	0.01
1,3-Cyclohexadiene,1,3,5,5-tetramethyl	5.32	0.33	0.00
Beta-Pinene	5.47	5.49	0.08
γ-Terpinene	5.73	0.99	0.02
p-Mentha-1,4(8)-diene	5.91	4.78	0.09
o-Cymene	6.07	0.10	0.01
D-Limonene	6.11	19.39	0.31
Beta-Ocimene	6.30	0.27	0.03
Beta-Ocimene	6.45	10.79	0.02
γ-Terpinene	6.63	3.33	0.05
p-Mentha-3,8-diene	6.84	0.12	0.01
p-Mentha-1,4(8)-diene	6.91	0.15	0.01
p-Mentha-1,4(8)-diene	7.08	19.95	0.12
Beta-Linalool	7.28	0.15	0.01
Beta-Linalool	7.37	0.87	0.10
2,4,6-Octatriene,2,6-dimethyl-,(E,Z)-	7.61	0.18	0.01

2,4,6-Octariene,2,6-dimethyl-,(E,Z)-	7.78	2.83	0.08
Linalool, methyl ether	7.83	0.22	0.06
2,4,6-Octariene,2,6-dimethyl-,(E,Z)-	7.97	3.06	0.10
p-Menth-8-en-1-ol	8.14	0.13	0.02
(4E)-2,7-Dimethyl-4,6-octadien-2-ol	8.27	0.12	0.02
Linalool, methyl ether	8.31	0.08	0.01
5-Caranol,(1S,3R,5S,6R)-(-)-	8.40	0.59	0.05
2-Cyclohexene-1-methanol,2,6,6-trimethyl-	8.54	0.07	0.01
Terpinen-4-ol	8.60	0.16	0.02
Alpha-Terpineol	8.82	9.43	0.05
(2E)-1-Methoxy-3,7-dimethylocta-2,6,diene	9.20	13.13	0.05
Geraniol	9.67	1.56	0.01
		100.01	

Table 23. Nerol experiment 200 °C set temperature 2 h reaction time and H₂O:Methanol:Nerol molar ratio (40:20:1). The product sample was analysed by GCMS three times and an average of the relative area % of the three runs was taken.

Compound	Retention time	Average Rel.Area% TIC	Mean \pm standard deviation
D-Limonene	4.88	0.10	0.00
2H-Pyran,2-ethenyltetrahydro-2,6,6-trimethyl	5.11	0.57	0.01
Beta-Pinene	5.47	2.80	0.08
γ -Terpinene	5.72	0.78	0.02
p-Mentha-1,4(8)-diene	5.90	3.95	0.05
o-Cymene	6.07	0.06	0.02
D-Limonene	6.11	22.84	0.22
Beta-Ocimene	6.45	3.86	0.07
γ -Terpinene	6.62	3.26	0.05
p-Mentha-1,4(8)-diene	6.89	0.37	0.03
p-Mentha-1,4(8)-diene	7.07	20.86	0.33
Beta-Linalool	7.28	0.16	0.01
Beta-Linalool	7.37	0.55	0.04
2,4,6-Octariene,2,6-dimethyl-,(E,Z)-	7.63	0.16	0.01
2,4,6-Octariene,2,6-dimethyl-,(E,Z)-	7.78	0.48	0.05
Linalool, methyl ether	7.82	0.33	0.09
Linalool, methyl ether	7.98	0.42	0.01

p-Menth-8-en-1-ol	8.13	0.36	0.00
Linalool, methyl ether	8.30	0.20	0.02
5-Caranol,(1S,3R,5S,6R)-(-)-	8.42	0.48	0.03
Terpinen-4-ol	8.59	0.39	0.01
Alpha-Terpineol	8.81	21.14	0.52
2,6-Octadiene,1-(1-ethoxyethoxy)-3,7-dimethyl	9.13	6.30	0.41
(2E)-1-Methoxy-3,7-dimethylocta-2,6,diene	9.19	5.16	0.41
Nerol	9.27	3.31	0.12
p-Menthane-1,8-diol	10.52	0.31	0.01
Yomogi alcohol	10.63	0.14	0.02
p-Menthane-1,8-diol	10.70	0.08	0.01
p-Menthane-1,8-diol	10.81	0.21	0.01
Methoxycitronellal	11.02	0.17	0.01
5-Caranol,(1S,3R,5S,6R)-(-)-	11.14	0.13	0.01
5-Caranol,(1S,3R,5S,6R)-(-)-	11.28	0.10	0.00
		100.02	

Table 24. Nerol experiment 150 °C set temperature 2 h reaction time and H₂O:Methanol:Nerol molar ratio (40:20:1). The product sample was analysed by GCMS three times and an average of the relative area % of the three runs was taken.

Compound	Retention time	Average Rel.Area% TIC	Mean ± standard deviation
Beta-Pinene	5.54	0.15	0.01
γ-Terpinene	5.75	0.11	0.01
p-Mentha-1,4(8)-diene	5.95	0.16	0.01
D-Limonene	6.13	1.38	0.04
γ-Terpinene	6.67	0.18	0.02
p-Mentha-1,4(8)-diene	7.12	0.23	0.01
1,5,5-Trimethyl-6-methylene-cyclohexene	7.31	0.11	0.01
Linalool, methyl ether	7.86	0.15	0.01
Alpha-Terpineol	8.85	0.50	0.00
Nerol	9.34	97.02	0.07
		99.99	

Table 25. Nerol experiment 100 °C set temperature 2 h reaction time and H₂O:Methanol:Nerol molar ratio (40:20:1). The product sample was analysed by GCMS three times and an average of the relative area % of the three runs was taken.

Compound	Retention time	Average Rel.Area% TIC	Mean ± standard deviation
Beta-Pinene	5.52	0.26	0.03
γ-Terpinene	5.75	0.13	0.01
p-Mentha-1,4(8)-diene	5.94	0.19	0.02
D-Limonene	6.13	1.58	0.14
p-Mentha-1,4(8)-diene	7.11	0.30	0.02
1,5,5-Trimethyl-6-methylene-cyclohexene	7.31	0.10	0.01
Alpha-Terpineol	8.85	0.46	0.02
Nerol	9.36	96.97	0.20
		99.99	